Acta Universitatis Agriculturae Sueciae

Doctoral Thesis No. 2022:46
Faculty of Natural Resources and Agricultural Sciences

Microbial communities and nitrogen cycling functions in barrier systems for treatment of nitrogen polluted water

Maria Hellman

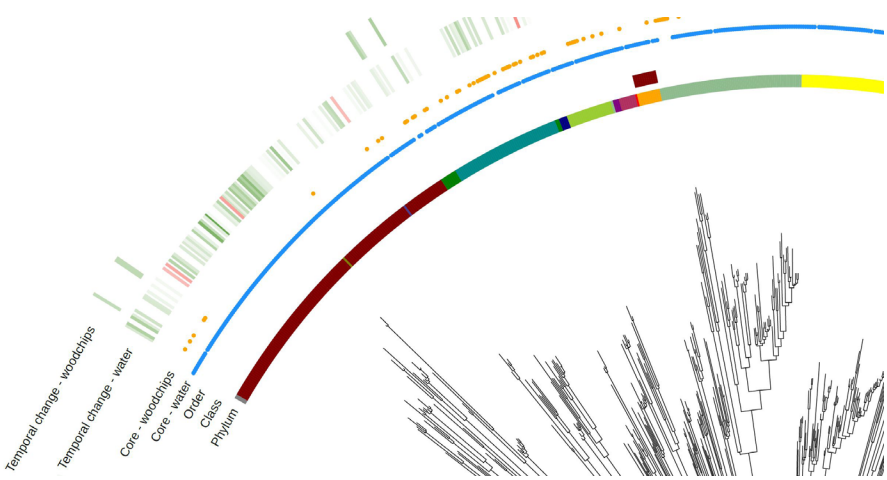

Microbial communities and nitrogen cycling functions in barrier systems for treatment of nitrogen polluted water

Maria Hellman
Faculty of Natural Resources and Agricultural Sciences
Department of Forest Mycology and Plant Pathology
Uppsala

SLU
SWEDISH UNIVERSITY OF AGRICULTURAL SCIENCES

DOCTORAL THESIS
Uppsala 2022

Acta Universitatis Agriculturae Sueciae
2022:46

Cover: Part of figure 6 in paper V, illustrating temporal and spatial patterns in the microbial community in a denitrifying bioreactor.

ISSN 1652-6880
ISBN (print version) 978-91-7760- 967-4
ISBN (electronic version) 978-91-7760- 968-1

Swedish University of Agricultural Sciences, Department of Forest Mycology and Plant Pathology, Uppsala, Sweden

Print: SLU Media-Tryck, Lund 2022

Microbial communities and nitrogen cycling functions in barrier systems for treatment of nitrogen polluted water

Abstract

Water is an increasingly threatened resource. Anthropogenic input of nitrogen (N) to surface waters causes eutrophication, and N in the groundwater can be a threat to human health, hence management measures are needed. The aim of this thesis was to evaluate two types of systems for remediating N-polluted water using permeable reactive barriers by determining N removal efficiency, possible adverse effects, and the role of the microorganisms in the systems.

Four projects evaluated denitrifying barriers, DBRs, for treatment of nitrate-polluted water originating from the use of explosives in mining industry. Woodchip DBRs were found to be suitable for remediation of this type of water. Initial leakage of nitrite, ammonium and organic carbon was observed, the emission of nitrous oxide was small. Another study used barriers based on compost or woodchips in combination with aquifer recharge to replenish groundwater using ammonium-rich treated wastewater. One out of four barriers significantly removed ammonium from the wastewater, and instead nitrate was produced. All compost-based barriers released organic carbon, replacing one pollutant with another.

The carbonaceous material in the permeable reactive barriers determined the composition of the microbial communities in the barriers; significantly different microbiomes developed depending on substrate type. Besides microorganisms capable of a range of N-transforming reactions, all barriers harboured groups of bacteria known for degrading macromolecules like cellulose. There were temporal and spatial patterns in the distribution the microorganisms, and the abundances of specific bacterial groups correlated to the chemistry in the water.

Future studies should focus on how different types of carbon affect the N-transforming processes, to maximise N-removal and minimise adverse effects.

Keywords: permeable reactive barrier, denitrifying bioreactor, woodchips, denitrification, DNRA, microbial community, N transformation processes, passive wastewater treatment, functional gene abundance, nitrous oxide

Kväveomvandlande funktioner och mikrobiella samhällen i barriärsystem för behandling av kväveförorenat vatten

Sammanfattning

Vatten är dyrbar resurs som hotas alltmer. Människan släpper ut kväve i naturen, och konsekvenserna blir övergödning och potentiellt hälsofarligt grundvatten. Därför behövs åtgärder för att minska utsläppen. Syftet med denna avhandling var att utvärdera två system för att sanera kväveförorenat vatten med hjälp av kolrika så kallade permeabla reaktiva barriärer. Barriärernas kväveavskiljande effektivitet och deras eventuella negativa miljöeffekter studerades. Rollen hos de mikroorganismer i barriärerna som utför de biokemiska reaktioner som avlägsnar kvävet undersöktes.

Denitrifierande barriärer med träflis som kolkälla användes för sanering av vatten som förorenats av nitrat vid användning av explosiva ämne i gruvindustrin. De visade sig vara lämpliga för rening av sådant vatten. Initialt observerades läckage av nitrit, ammonium och organiskt kol. Utsläppen av lustgas var små. En annan studie undersökte hur renat avloppsvatten kan användas för att skapa grundvatten genom att återfylla akvifärer. Då användes barriärer baserade på kompost alternativt träflis för att ta bort bland annat ammonium från vattnet. En av fyra barriärer reducerade mängden ammonium i vattnet, men i stället producerades nitrat. Organiskt kol lösgjordes från alla barriärer med kompost, så en förorening ersattes med en annan.

Sammansättningen av de mikrobiella samhällen som utvecklades i barriärerna styrdes av vilket kolhaltigt material som användes. Signifikant olika mikrobiom utvecklades beroende på material. Alla barriärer hyste mikroorganismer som kan utföra olika kväveomvandlande reaktioner, dessutom grupper av bakterier som är kända för att bryta ner makromolekyler som cellulosa. Det fanns tidsmässiga och rumsliga mönster i distributionen av mikroorganismerna i barriärerna, och förekomsten av specifika bakteriegrupper korrelerade med vattenkemin.

Framtida studier bör fokusera på hur olika typer av kol påverkar olika kväve-omvandlande processer, för att maximera kväveavskiljning och minimera negativa effekter.

Nyckelord: permeabel reaktiv barriär, markfilter, denitrifierande bioreaktor, träflis, denitrifikation, mikrobiellt samhälle, kväveomvandling, passiv vattenrening, abundans av funktionella gener, lustgas

Dedication

Till Mats

Contents

List of publications

This thesis is based on the work contained in the following papers, referred to by Roman numerals in the text:

I. Herbert, R., Winbjörk, H., Hellman, M., Hallin, S. (2014). Nitrogen removal and spatial distribution of denitrifier and anammox communities in a bioreactor for mine drainage treatment. Water Research, 66, pp. 350 – 360[1]. doi: 10.1016/j.watres.2014.08.038

II. **Hellman, M.**, Hubalek, V., Juhanson, J., Almstrand, R., Peura, S., Hallin, S. (2021). Substrate type determines microbial activity and community composition in bioreactors for nitrate removal by denitrification at low temperature. Science of the Total Environment, 755:143023. doi: 10.1016/j.scitotenv.2020.143023

III. Nordström, A., **Hellman, M.**, Hallin, S., Herbert, R. (2021) Microbial controls on net production of nitrous oxide in a denitrifying woodchip bioreactor. Journal of Environmental Quality, 50 (1), pp. 228 – 240[2]. doi: 10.1002/jeq2.20181

IV. **Hellman, M.**, Valhondo, C., Martínes-Landa, L., Carrera, J., Juhanson, J., Hallin, S. (2022). Nitrogen removal capacity in microbial communities developing in compost- and woodchip-based multipurpose reactive barriers for aquifer recharge with

[1] Errata: Page 358, row 10 from the end of the page, should say ‘increased’, not ‘decreased’.

[2] Errata: last words on page 231 should say ‘37 – 478 mg’, not ‘12 – 152 mg’.

wastewater. Frontiers in Microbiology, 13:877990[3]. doi: 10.3389/fmicb.2022.877990

V. **Hellman, M.[4]**, Juhanson, J.[4], Wallnäs, F., Herbert, R., Hallin, S. (2022). Spatial and temporal changes in microbial communities and greenhouse gas emissions in a denitrifying woodchip bioreactor at low water temperatures. *Manuscript.*

In addition, Maria Hellman has co-authored the following publications during the period of the thesis work:

Hallin, S., **Hellman, M.**, Choudhury, M., Ecke F. (2015). Relative importance of plant uptake and plant associated denitrification for removal of nitrogen from mine drainage in sub-arctic wetlands. Water Research, 85, pp. 377 – 383.

Hellman, M., Bonilla-Rosso, G., Widerlund, A., Juhanson, J., Hallin, S. (2019). External carbon addition for enhancing denitrification modifies bacterial community composition and affects CH_4 and N_2O production in sub-arctic mining pond sediments. Water Research, 158, pp.22 – 33.

Choudhury, M. I., Segersten, J., **Hellman, M.**, McKie, B., Hallin, S., Ecke, F. (2019). Importance of plant species for nitrogen removal using constructed floating wetlands in a cold climate. Ecological Engineering 138, pp. 126 – 132.

Norberg, L., **Hellman, M.**, Berglund, K., Hallin, S., Berglund, Ö. (2021). Methane and Nitrous Oxide Production From Agricultural Peat Soils in Relation to Drainage Level and Abiotic and Biotic Factors. Frontiers in Environmental Science 9:631112.

[3] Errata: Table 1, row woodchips, column WCB should say '49', not '-'. Heading table S3, 'Figure 3A' should say 'Figure 4A'

[4] Maria Hellman and Jaanis Juhanson contributed equally.

The contribution of Maria Hellman to the papers included in this thesis was as follows:

I. Planned and took part in the sampling. Modified the DNA extraction method for the sample type. Performed the qPCR analyses. Contributed to the writing of the manuscript.

II. Contributed to the idea and the design of the experiment. Did a major part of the monitoring, sampling, and laboratory analyses. Analysed all data with support for the initial bioinformatic analyses of the sequence data. Wrote the manuscript with support from the co-authors. Corresponding author.

III. Planned the sampling. Did nearly all molecular work on the woodchip and water samples. Contributed to the data analyses. Participated in writing of the manuscript.

IV. Did the molecular work. Analysed the data. Wrote the manuscript with support from the co-authors. Corresponding author.

V. Contributed to the idea and the design of the experiment. Did a major part of all sampling and of the chemical analyses. Did part of the molecular work in the laboratory and supervised the remaining laboratory work. Analysed all data but the sequence data. Wrote the manuscript with the other first author (equal contribution) and with support from the co-authors.

1. Introduction

Worldwide, water available for production of potable water, irrigation, and industrial use is a valuable, but increasingly threatened, resource. We need to improve how we use and manage water resources to avoid negative consequences for the environment and for human health. Several of the 17 sustainable development goals, SDGs, in the United Nations´ (UN) 2030 Agenda for Sustainable Development, directly concern water. Among them are SDG 14, *Conserve and sustainably use the oceans, seas and marine resources for sustainable development*, in which the first target is to prevent and reduce marine pollution of all kinds, including nutrient pollution. Goal number 13, *Take urgent action to combat climate change and its impacts*, includes drought, which has impact on water scarcity. In SDG 6, *Ensure availability and sustainable management of water and sanitation for all,* the indicator about safe treatment of domestic and industrial wastewater flows, is also directly related to parts of this thesis. However, the increasing population and expansion of urban areas (United Nations, 2019) together with climate change make the implementation of these goals a challenge. A variety of water management measures in agriculture, industry, and urban water handling, are required to minimise the anthropogenic impact on the environment and to provide a safe and sustainable water supply. Furthermore, a holistic view is needed, since all water is connected through the global water cycle (Fig. 1); water discharged as waste in the past becomes the valuable resource we use today.

Many different compounds can contaminate water, and in this thesis, the focus is on nitrogen (N) compounds. The N-removal technology applied in the systems studied in this thesis is based on permeable reactive barriers. A permeable reactive barrier is a construction where contaminated water is forced to flow through a solid, reactive matrix and during passage, physical,

chemical, and biological mechanisms remove contaminants. Two permeable reactive barrier techniques for water treatment were studied: 1 – cellulose-based denitrifying bioreactors for remediation of nitrate-polluted water originating from blasting operations and 2 – the addition of a reactive layer when recharging aquifers with treated municipal wastewater. The techniques share several features, for example, once established they are passive or semi-passive, they can handle large volumes of water and, relevant for this thesis, many of the processes leading to improved water quality after treatment are performed by microorganisms.

1.1 Water resources

There is not a global water shortage as such, despite the fact that there is a finite amount of water on earth. Most of the water is saline, only approximately 3 % is freshwater, out of which 79 %, is frozen or not easily available, for example hidden in underground water supplies, aquifers (olc.worldbank.org). This leaves us with less than 1 % of the Earth´s water available for use by society. The main use is food production, with 72 % of the withdrawn water used by agriculture, followed by 16 and 12 % for households and services in municipalities, and industry (United Nations, 2021).

A highly simplified depiction of the natural water cycle is presented as the leftmost section of Figure 1. Energy from the sun drives the processes by which water enters the atmosphere through evaporation from land and sea surfaces and by transpiration from the vegetation. Subsequent condensation of the water vapour in the atmosphere allows it to fall back to the surface as precipitation. Through run-off, infiltration, and percolation, the water returns to water bodies and can again be re-cycled into the atmosphere. The rightmost part of Figure 1 illustrates how water is used for food production and industrial processes, and additionally how it can be reused before being returned to the environment.

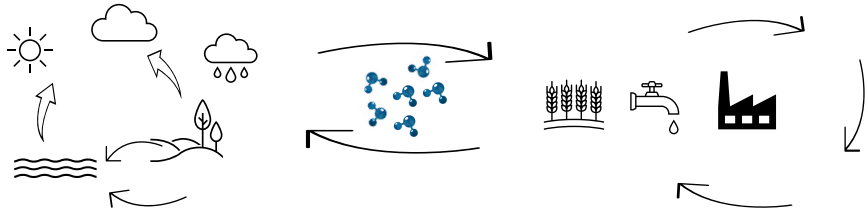

Figure 1. The water cycle. Water is withdrawn from the natural water cycle (left) and used in society (right). Before returning the water, it can be reclaimed and used several times.

Reusing the water will become increasingly important as the demand for water and the available water resources do not match geographically, and the gap between supply and demand will get bigger. In the most recent (2022) version of the UN publication World Population Prospects, it is predicted that the world population will continue to grow. The increase will be concentrated to cities, meaning that by 2050, 6.6 billion of the estimated 9.7 billion people will live in urban areas (United Nations, 2019; 2022a). Further, regions already suffering from limited water availability, for example sub-Saharan Africa, India, Pakistan, and Indonesia are among those where the population will increase the most (UN-Water, 2021; United Nations, 2019; 2022a). Local water scarcity is already a reality, and climate change and global warming will exacerbate the situation. The need for water has led to the development of a range of techniques to replenish groundwater by aquifer recharge. Resources as surface water, rainwater, and greywater can be used for this purpose, and the techniques are in use worldwide (Bekele et al., 2018).

1.2 Nitrogen as a pollutant

Nitrogen is essential for life but can at the same time be an environmental problem and a threat to human health. Globally, N originating from human activities causes eutrophication, algal blooms, and hypoxia in aquatic systems, and river basins in all continents have degraded water quality due to N pollution (Giri, 2021). In coastal ecosystems, anthropogenic inputs of N and phosphorous during the last century has been the primary cause of eutrophication and the trend might be ”the most widespread anthropogenic threat to the health of coastal ecosystems” (Malone and Newton, 2020).

Human activities have also been shown to cause elevated N concentrations in aquifers around the world, which is a threat to human health as nearly one third of the population is depending on groundwater for drinking water (Arauzo et al., 2022; United Nations, 2022b). The situation today is a legacy from decades of excessive N fertilization in agriculture around the world, and nitrate pollution of groundwaters and surface waters is now a global issue (Bijay-Singh and Craswell, 2021). In this thesis, **papers I** – **III** and **V** have direct implications for, but are not limited to, mitigating N release to watercourses in northern Sweden and the Bothnian Bay (the northernmost sub-basin of the Baltic Sea), whereas **paper IV** has implications for N pollution of groundwater.

1.2.1 Status of European waterbodies

There is a plethora of reports and data compilations describing the status of European waterbodies, for example from the European Commission (EC), the European Environment Agency (EEA) and the Baltic Marine Environment Protection Commission (aka the Helsinki Commission, HELCOM). Additionally, different approaches for assessments (European Commission, 2021) and for methods establishing threshold and background values for individual chemicals, including those for nitrate, vary between countries, making it difficult to get a complete picture of the situation.

Surface waters are characterised by their ecological and chemical status (EEA, 2018). The ecological status includes the level of eutrophication, and one of the eutrophication classification systems used, HEAT+, results in five levels from "high" to "bad" (HELCOM, 2009; Andersen et al., 2011). Input of N to the Baltic Sea sub-basins has decreased by 9 – 21 % in recent years, but the eutrophication status assessment based on data between 2011 and 2015 shows that 97 % of the surface area in the Baltic Sea is eutrophied (Fig. 2; HELCOM, 2017). Lack of data for many sections of European coasts and open seas, leave significant areas without assessment of present eutrophication status (Fig. 2; EEA 2019; European Commission, 2021). There is, however, data on the ecological status of surface water bodies (EEA, 2018) showing that Europe has regions with severely impacted rivers, lakes, and coastal areas, most likely impacting the marine environments receiving water from those water bodies.

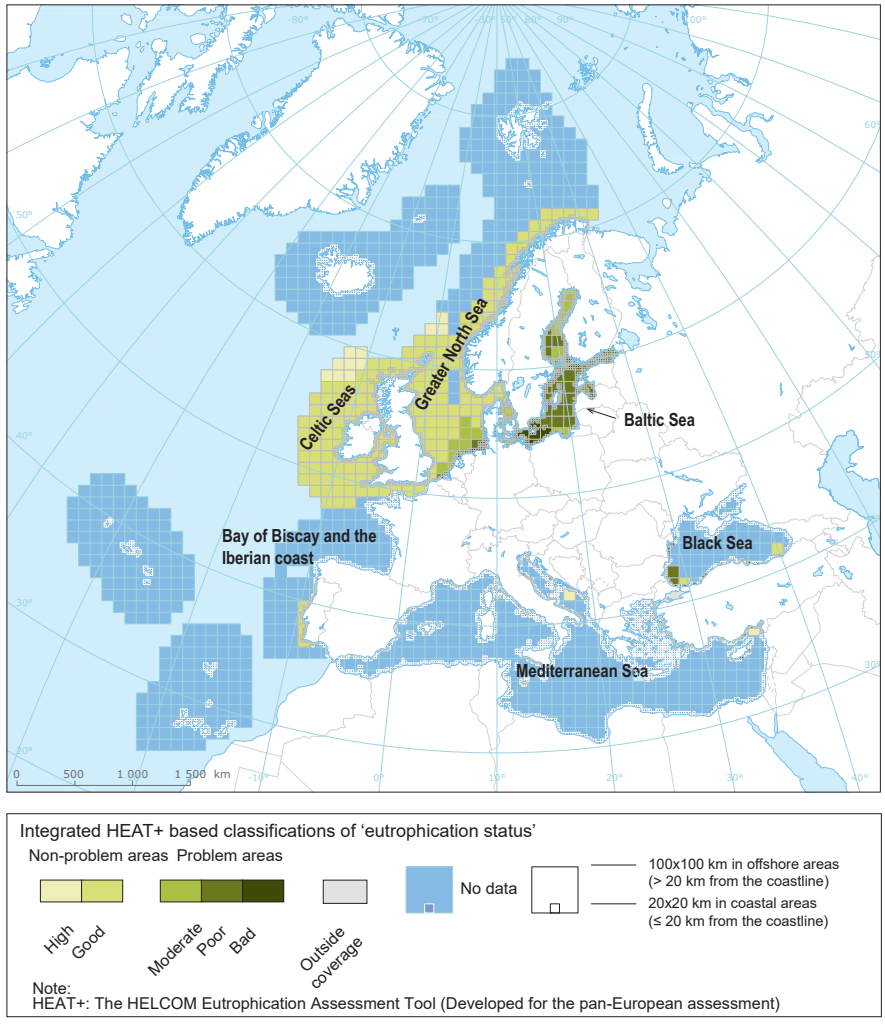

Figure 2. Eutrophication status in European waters, assessed with the HEAT+ tool. Map retrieved 2022-06-21 (www.eea.europa.eu/data-and-maps/figures/). Figure text and legend are modified for readability.

Groundwaters are not assessed according to ecological status, but according to their chemical status (EEA, 2018). The status can be "good" or "failing to achieve good" and there are regions in Europe where more than 50 % of the groundwater areas do not have the status "good" (Fig 3).

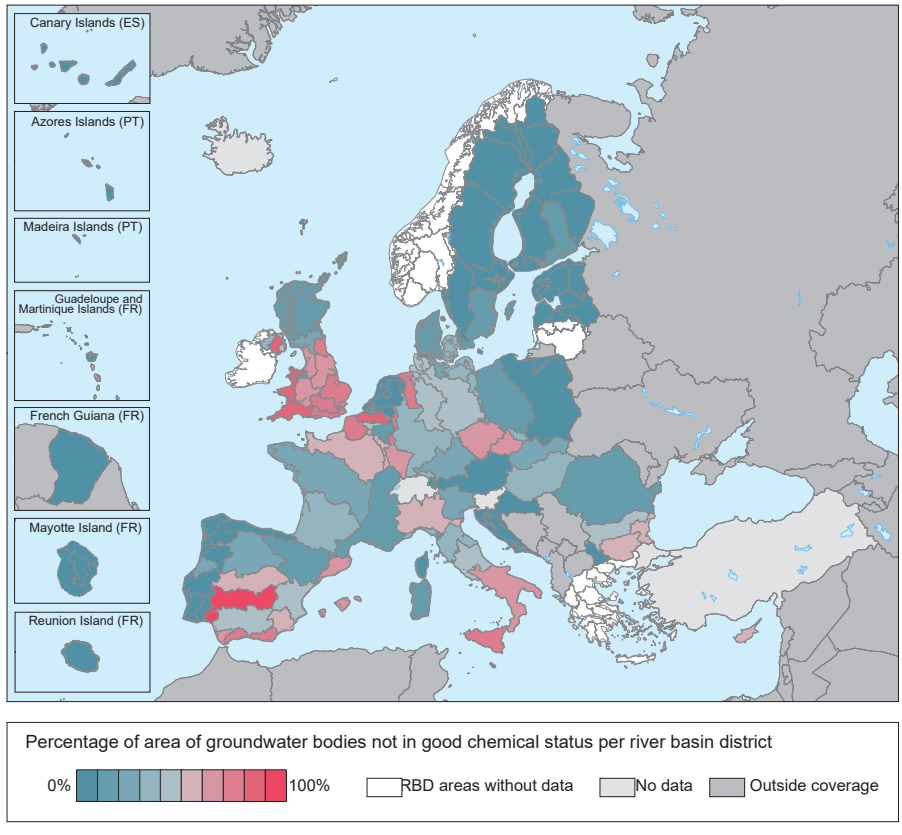

Figure 3. River basin groundwater chemical status in Europe (2015 – 2018 assessment). Map retrieved 2022-06-21 (www.eea.europa.eu/data-and-maps/figures/). Figure text and legend are modified for readability.

Overall, the proportion of groundwater body areas with poor chemical status was 25 % with an additional 31 % at risk of not achieving the status "good" in the assessment covering the time period of 2015 – 2018 (EEA, 2018). The main pollutant causing the poor chemical status was nitrate. Depending on time period assessed, 14 % – 18 % of the groundwater stations/body areas had nitrate levels exceeding 50 mg nitrate per litre, the EU standard for drinking water.

Despite efforts in mitigating the input of N to the environment, resulting in slight improvements in the ecological and chemical status of European waterbodies, the nutrient situation in European waters remains generally

poor. Measures to decrease anthropogenic N input to the environment are needed.

1.2.2 Sources of nitrogen – Europe and the Baltic Sea

Data available for Europe during the last ten years, estimates agriculture to be responsible for in average 77 % (ranging between 22 % and 99 %) of the total load of N into the environment (European Commission, 2021). Intensified fertilisation to increase food production has led to leaching of reactive N, causing high levels of nitrate in water bodies (Tilman et al., 2011). Nitrate is highly soluble in water and easily leach out from the soil if not assimilated by the crop. Background leaching from other types of terrestrial systems is another diffuse N source, while industries, wastewater treatment plants (WWTPs), and land-based recirculating aquacultures are examples of point sources of N. The relative contribution of the different N sources varies with region, here exemplified with data from the Baltic Sea. The net load of N to the Baltic Sea is dominated by diffuse background N input in the Bothnian Bay and the Bothnian Sea, and background input constitutes a considerable part of the net load also in Baltic Proper and Kattegat (Fig. 4).

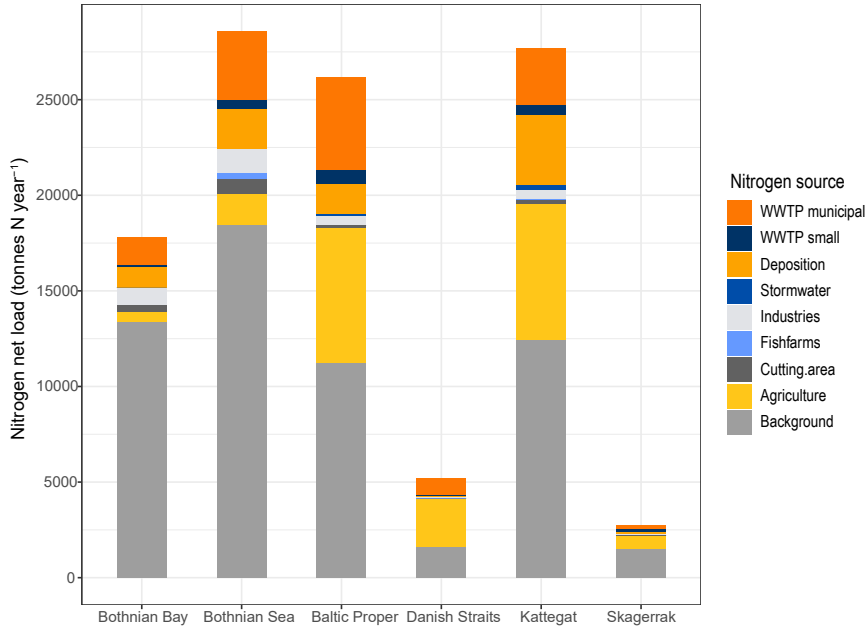

Figure 4. Sources to net load of N in the six Baltic Sea Basins 2017. WWTP = wastewater treatment plant. Figure re-drawn from the report 2019:20, The Swedish Agency for Marine and Water Management, with permission.

The anthropogenic input of N to the Baltic Sea was approximately 50 000 tonnes per year in 2017 (Fig. 4, sum of the non-background sections of the bars), unchanged from 2014 (Hansson et al., 2019). Industry and WWTPs contribute approximately 50 % in the two northernmost sub-basins of the Baltic Sea while input from agriculture dominate in the south (Fig. 4).

Another important source of N to the environment is wastewater, and during the 20th century, discharge of wastewater accounted for a high increase in the global nutrient transport of N (Preisner et al., 2021). The N in fresh domestic wastewater is mainly organic N compounds and ammonium, originating from protein metabolism in the human body. Depending on circumstances, it may be necessary to remove the N to meet specified criteria before the water is discharged. According to the EU directive 91/271 (European Commission, 1991), member states shall provide collecting systems for urban wastewater from agglomerations bigger than 2 000 population equivalents (the organic biodegradable load having a five-day

biochemical oxygen demand of 60 g of oxygen per day), and the collected water must undergo treatment.

In a conventional WWTP, this can be described as sedimentation of suspended solids to remove a fraction of the solids and reduce the organic biodegradable material (primary treatment), and a biological process to further remove solids and organic material (secondary treatment). Secondary treated wastewater is a potential water source for recharge of aquifers, but it still contains N, mainly in the form of ammonium. It also has various levels of organic micropollutants, OMPs, since the most widely used secondary treatments are not designed for removing recalcitrant carbon compounds (Loos et al., 2013; Petrie et al., 2015). If the water is to be used for aquifer recharge, the presence of N and OMPs is undesirable. If the water is to be discharged into water bodies that are or in the near future risk of being eutrophic, or is a water body intended for drinking water, it must be subjected to more stringent treatment in order to meet additional criteria regarding N and phosphorous (P) (European Commission, 1991). This requires steps specifically removing N and P (tertiary treatment, nutrient removal). Although urban wastewater treatment has improved over the last 30 – 40 years in Europe, WWTPs contribute up to 40 % of the anthropogenic N input to the Baltic Sea (Fig. 4) with large variation among the European member states. While in 2020, 69 % of the urban population in the EU were connected to WWTPs having nutrient removal, there were countries where most of the urban sewage was discharged without any treatment steps, or not even collected (eea.europa.eu). Furthermore, large rural areas with settlements having less than 2000 population equivalents are not regulated by the EU directive. In many of these areas, sewage systems do not exist, and individual or small on-site wastewater treatment solutions are used. The use of small systems is regulated in each member country, and the requirements vary substantially.

Nitrogen discharge to inland watercourses across Sweden is mainly from pulp and paper-, mining-, and metal industries, while direct N discharge to Swedish coastal waters is dominated by the pulp and paper industry (Fig. 5).

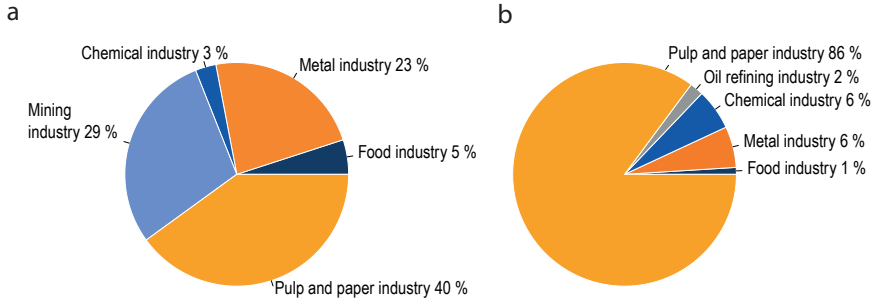

Figure 5. Distribution of N discharges from industry to Swedish waters in 2018. a) discharge to inland waters, b) discharge to coastal water. Data retrieved from Statistics Sweden (scb.se) 2022-06-02.

Until recently, blasting and the use of the explosive ANFO (Ammonium Nitrate mixed with Fuel Oil) was relatively overlooked as a N-source (**paper I**). During blasting operations in mining industries, quarries and at construction sites, not all explosives loaded in the bore holes detonate, and the ammonium nitrate is readily dissolved in the infiltrating groundwater, as is spillage during handling. Undetonated explosives are also adsorbed to the waste rock at mine sites and subsequently washed out from waste rock deposits (Nilsson and Widerlund, 2017). Yet another route for the ammonium nitrate is via the processing plants at mine sites, where it is washed out from the ore during the milling, separation, and flotation processes. The typical routes for water transport at an underground mine are depicted in Figure 6. As sublevel caving occurs below the groundwater table, the upwelling surface- and groundwater need to be removed from the mine. The water is transported to reservoirs via underground pump stations and is subsequently used in the processing plants. From the plants, the tailings slurry is pumped to a pond where the tailings are deposited. The water then flows into a clarification pond where it is retained before being recirculated to the reservoirs or being discharged to the receiving waters.

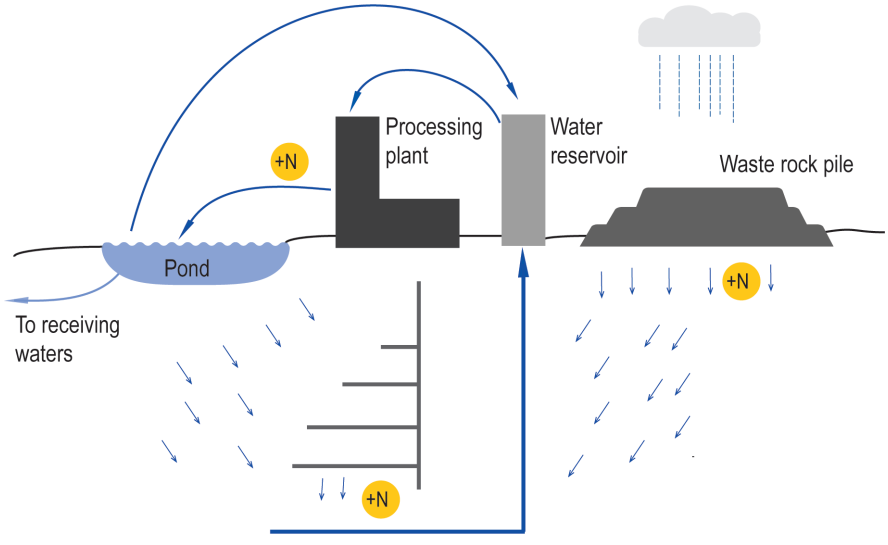

Figure 6. Water flows at a sublevel caving mine site. Points where nitrogen enters the flow paths are depicted with yellow circles.

1.3 Aim and objectives

The aim of this thesis was to investigate treatment capacity, the role of microorganisms, and possible adverse effects in systems for remediating N-polluted water using permeable reactive barriers. Ultimately, this will support improved design of such systems for different applications. Two systems were studied: cellulose-based bioreactors treating nitrate-polluted water from mining activities (**papers I – III** and **V**), and reactive barriers as a supplement to managed aquifer recharge for treating ammonium-rich effluent from a municipal wastewater treatment plant (**paper IV**).

In **paper I**, the objectives were to determine the treatment capacity of the first described cellulose-based bioreactor for nitrate-polluted mine water and to determine the abundance and distribution of denitrifying and anammox bacterial communities to determine the potential for heterotrophic and autotropic N removal processes, respectively. Additionally, we evaluated if there were preferential flow paths in the bioreactor. Since the sawdust used in **paper I** could not support N removal without acetate addition, the objectives of **paper II** were to evaluate three alternative cellulose-based bioreactor substrates for their suitability as electron donors for denitrification at low temperature in a laboratory experiment. Additional objectives were to

analyse the temporal succession of the microbial communities in the three substrates in relation the nitrate removal rates and formation of unwanted products like ammonium, nitrous oxide, and nitrite . In **papers III** and **V**, we investigated full-scale woodchip denitrifying bioreactors over two operational years treating two types of nitrate-polluted water from mining activities: water from a tailings pond and leachate from waste rock dumps, respectively. The objectives were to relate bioreactor performance to temporal and spatial changes in the overall microbial communities and genetic potential for N transformation processes affecting N removal efficiency as well as the formation of unwanted products in the water and woodchips of the bioreactors. Finally, **paper IV** focused on another application of permeable reactive barriers for treating N polluted water. The first objective was to determine the N-removal efficiency of barriers based on compost or woodchips when infiltrated with water having a high concentration of ammonium prior to aquifer recharge. Secondly, to determine the abundances of functional groups involved in N transformation processes and describe the development of the bacterial community structure in the barriers in relation to barrier performance.

2. Microbial nitrogen removal from water

Depending on the origin and type of water, dissolved N species can have different forms. Nitrogen has seven oxidation states, from +5 in nitrate to -3 in ammonia, ammonium and when bound in organic compounds. The reactions transforming N from one form to another are mediated by microorganisms, but abiotic photo- and thermochemical reactions also occur. These geochemical processes are connected in a complicated network, where many of the reactive inorganic N compounds are utilised in different pathways (Hallin et al., 2018; Kuypers et al., 2018) . In addition, N is assimilated, incorporated into biomass, by all organisms and subsequently mineralized to ammonium again during decay.

2.1 Microbial N-transforming processes

Under anoxic conditions, microorganisms can permanently remove N from water. Here, nitrite is a key compound, and the mechanism by which nitrite is reduced determines whether the N will be removed from the water or not. Nitrite can undergo denitrification or anaerobic ammonia oxidation (anammox), both leading to the formation of gaseous N compounds leaving the water. Alternatively, nitrite is reduced via dissimilatory nitrate reduction to ammonium (DNRA), leading to the formation of ammonium and the N will be retained. Since anammox involves oxidation of ammonium, the pathway removes both ammonium and nitrite. Under oxic conditions, ammonium can be removed by nitrification, but as nitrate is formed in the process, the N remains in the water. The size of the microbial communities performing specific N-transformation processes can be estimated by quantifying marker genes for the processes. Figure 7 shows which genes have been used as genetic markers in this thesis. The chemical reactions shown in sections 2.1.1

– 2.1.4 are schematic and not balanced and hydrogen and oxygen atoms are omitted if not bound to N.

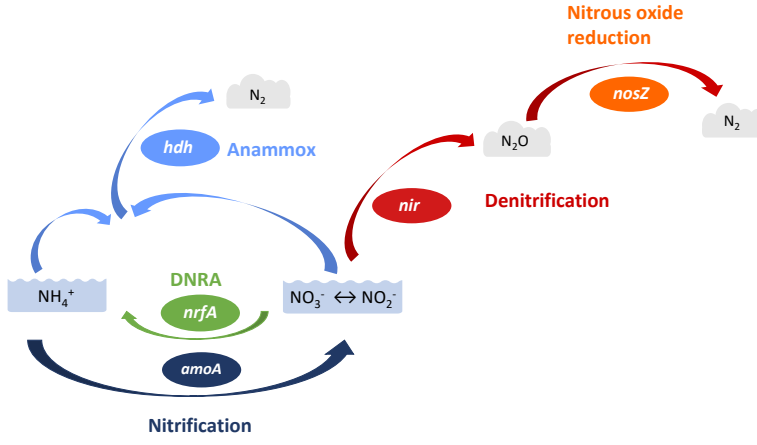

Figure 7. Schematic representation of microbial N transformation processes. Marker genes for the respective processes used for estimating the abundances of the functional microbial groups involved are indicated by italicised text. Intermediate reaction products are not shown.

2.1.1 Denitrification

Denitrification is one of the dominant biogeochemical processes involved in removal of N from terrestrial and aquatic ecosystems (Burgin and Hamilton, 2007; Devol, 2015), including its use in wastewater treatment plants. It is an anaerobic four-step pathway in which soluble nitrate is reduced to gaseous compounds:

$$NO_3^- \rightarrow NO_2^- \xrightarrow{nir} NO \rightarrow N_2O \xrightarrow{nosZ} N_2$$

Denitrifiers are found in nearly all environments that occasionally receive oxygen to some extent (Shapleigh, 2013) and there are denitrifiers in all three domains of life. Most of the cultured bacterial denitrifiers belong to the Proteobacteria (Philippot et al., 2007; Shapleigh, 2013), but there are also members in several other phyla, for example in Firmicutes and Bacteroidetes (Graf et al., 2014). In the domain Eukarya, denitrification has been described in fungi (Shoun et al., 1992; Maeda et al., 2015; Xu et al., 2019) and in

Foraminifera (Risgaard-Petersen et al., 2006; Woehle et al., 2018). Denitrification is most often used as a facultative respiratory process, producing ATP when oxygen is limiting. Since the reduction of nitrogen oxides conserves less energy than the reduction of oxygen, denitrification is most often downregulated in the presence of oxygen (Chen and Strous, 2013). The process is therefore triggered by low oxygen tension and the availability of a nitrogen oxide that can serve as electron acceptor. Most denitrifiers are heterotrophs and use organic compounds as electron donors, but some are autotrophs and use inorganic molecules as reducing agents, such as sulphur compounds or metals (Kumaraswamy et al., 2006; Herrmann et al., 2017; Xing et al., 2018). It has become clear that denitrification is modular; microorganisms harbour different sets of the genes encoding for the enzymes needed for catalysing all four steps in the reaction (Zumft 1997, Graf et al., 2014). Complete denitrification by a single organism might be the exception rather than the rule (Kuypers et al. 2018).

The second step, reduction of nitrite to nitric oxide, is the defining step for denitrification, in which an inorganic N compound is converted from a soluble to a gaseous form (Shapleigh, 2013). The reaction is catalysed by the iron- or copper-dependent nitrite reductase, encoded by *nirS* or *nirK*, respectively. The two genes are commonly used as marker genes for denitrification (Henry et al., 2004; Throbäck et al., 2004). In the last step, the reduction of nitrous oxide (N_2O) produces N_2, and the reaction is catalysed by nitrous oxide reductase, encoded by *nosZ*. The clade I and clade II *nosZ* genes are used as marker genes for the N_2O reduction (Henry et al., 2006; Jones et al., 2013).

2.1.2 Anaerobic ammonia oxidation – anammox

Anammox includes the oxidation of ammonium with nitrite as electron acceptor through a series of reactions that take place in a membrane bound structure, the anammoxosome, in anammox bacteria (Mulder et al., 1995; Dietl et al., 2015; Maalcke et al., 2016). The end products of anammox are N_2 and water:

$$NO_2^- \rightarrow NO$$

$$NO + NH_4^+ \rightarrow N_2H_2 \xrightarrow{hdh} N_2$$

Anammox is only found in five genera in the phylum Planctomycetes (Dietl et al., 2015; Jetten et al., 2015). Ecologically, it has become evident that anammox plays an important role in the oceans and in oxygen minimum zones, where it contributes substantially to nitrogen removal (Dalsgaard et el., 2005). The anammox bacteria are autotrophs and their growth is favoured by the absence of organic carbon sources (González-Cabaleiro et al., 2015). The last two decades, the process has been implemented in wastewater treatment plants (Jetten et al., 2002; Hauck et al., 2016; Weralupitiya et al., 2021). Thanks to the restricted phylogeny of anammox bacteria, it is possible to use part of the 16S rRNA gene as a molecular marker for the process (Tsushima et al., 2007; Yang et al., 2020). However, the gene *hdh*, catalysing the step converting hydrazine to N_2 is a better marker as it targets a functional gene in the anammox process (Schmid et al., 2009). Both markers have been used in the papers in this thesis.

2.1.3 Dissimilatory nitrate reduction to ammonium – DNRA

The process DNRA reduces nitrate to ammonium and can be performed by many microorganisms, including taxa within most bacterial lineages, methane-oxidising archaea, and by some diatoms and fungi (Kamp et al., 2015; Kuypers et al., 2018). DNRA is favoured by high C/N ratios and reducing conditions (Kraft et al., 2014; Hardison et al., 2015), and is for example found in soil, wetlands, peatlands, sediments, and aquaculture systems (Christensen et al., 2000; Song et al., 2014; Putz et al., 2018). Many DNRA bacteria are also fermenting (van den Berg et al., 2017).

$$NO_3^- \rightarrow NO_2^- \xrightarrow{nrfA} NH_4^+$$

The reduction of nitrite in DNRA is catalysed by the formate dependent nitrite reductase encoded by the *nrfA* gene (Einsle et al., 1999) and *nrfA* is used as marker gene for DNRA (Mohan et al., 2004; Welsh et al., 2014).

2.1.4 Nitrification

Nitrification stepwise oxidises ammonia to nitrate under oxic conditions (Caranto and Lancaster, 2017). Ammonia oxidation can be performed by either ammonia-oxidising bacteria (AOB) in the classes Beta- and Gammaproteobacteria, by ammonia-oxidising archaea (AOA) in the phylum

Thaumarchaeota, and by bacteria with capacity for complete ammonia oxidation (comammox). The *Nitrospira* within the phylum Nitrospirae is the so far only known genus to include comammox (Daims et al., 2015). The enzyme catalysing oxidation of ammonia is encoded by the *amoA* gene (Rotthauwe et al., 1997). It has been demonstrated that N_2O can be formed from hydroxylamine and during nitrifier denitrification, when ammonia oxidisers reduce nitrite, making nitrification a potential source of N_2O (Caranto et al., 2016). Nitrate is formed from nitrite by nitrite-oxidising bacteria (NOB), found among Alpha- and Gammaproteobacteria.

$$NH_3 \xrightarrow{amoA} NH_2OH \longrightarrow NO \longrightarrow NO_2^- \longrightarrow NO_3^-$$

Ammonia-oxidising organisms are ubiquitous and can be found in freshwater and marine habitats, in different types of soil, in hot springs and in wastewater treatment plants (Lehtovirta-Morley, 2018). Nitrite-oxidising bacteria are unequally distributed in the environment. *Nitrospira* is the most diverse genus and can be found in multiple habitat types, while other NOB are more restricted in their occurrence (Daims et al., 2016).

3. Cellulose-based bioreactors and reactive barriers – design aspects

3.1 Denitrifying cellulose-based bioreactors

A cellulose-based denitrifying bioreactor is a type of permeable reactive barrier. The terms denitrifying bioreactor, DBR, and bioreactor, will be used interchangeably in this text, and if needed, the reactive material will be specified. The reactive material in a cellulose-based DBR is a porous, plant-derived organic material. A DBR removes nitrate from nitrate-polluted water by converting it to N_2 during the passage through the reactive material. The reactive material is also named the substrate, since it supplies the system with organic carbon compounds that are used as electron donors when the nitrate is reduced to gaseous nitrogen compounds via denitrification by denitrifying microorganisms. In addition, the substrate serves as a surface for biofilm growth (Zhong et al., 2020). The construction can be in the form of walls, layers, compartments or beds, and which design to choose depends on if the water to be treated is diffuse or concentrated, on hydrologic conditions and of the specific site constraints (Schipper et al., 2010). Denitrifying bioreactors can be constructed and operated at relatively low cost and in the last 15 years the technique has been well established (Christianson and Schipper, 2016; Christianson et al., 2021). Today, there is good knowledge about how design parameters and environmental conditions affect the N removal efficiency and rate (Addy et al., 2016; Christianson et al., 2021) and research is ongoing on how to deal with seasonable variability in water flow or extreme flows caused by storm events (Pluer et al., 2019; Maxwell et al., 2022). There is increasing knowledge about how to avoid the production of

environmentally detrimental compounds such as greenhouse gases and ammonium.

3.1.1 Applications

The first field-scale cellulose-based denitrifying constructions were walls remediating septic tank effluents and groundwater (e.g. Robertson and Cherry, 1995; Schipper and Vojvodic-Vukovic, 2001). Today, the main application for DBRs is to treat agricultural drainage and there are several reports on field-scale bioreactors in use in areas with intense farming, for example in the U.S. (Hassanpour et al., 2017; Jang et al., 2019), New Zealand and Australia (Robertson et al., 2009; Long et al., 2011) and Europe (Jéglot et al., 2021a). In recent years, the use of DBRs have been extended to treating nitrate-rich effluent from aquaculture (Lepine et al., 2016; von Ahnen et al., 2018; Aalto et al., 2020) and treating stormwater and residential wastewater ((Lynn et al., 2015a; Lopez-Ponnada et al., 2017). With the **papers I, II, III** and **V** in this thesis, we contribute to broadening the application range for DBRs to include the mining industry, where nitrate in the process water and in leachate from waste rock dumps can be removed before discharge to recipient waters (Table 1).

Table 1. Cellulose-based bioreactors treating water from mining industry studied in this thesis. Values are approximate. Removal rate refers to per m^{-3} pore volume of the reactor.

In paper	Carbon source	Reactor volume (m^3)	Pore volume (m^3)	HRT (days)	Temperature (°C)	Water	Removal (%)	Removal rate (g N m^{-3} day^{-1})
II	wood-chips	0.54 x 10^{-3}	0.48 x 10^{-3}	6.0 – 7.2[a]	10	pond	37 – 52[a]	1.5 [a]
II	barley straw	0.54 x 10^{-3}	0.51 x 10^{-3}	1.8 – 2.2[a]	10	pond	42 – 44[a]	5.1 [a]
II	bottle sedge	0.54 x 10^{-3}	0.48 x 10^{-3}	1.7 – 1.8[a]	10	pond	46 - 51 [a]	6.4 [a]
I	saw-dust	27	5.4	0.5 – 1.2[b]	15 – 22	pond	14 – 47 [c]	NA
III	wood-chips	210	113	1 – 2.6	3 – 17	pond		9.7/ 5.5 [d]
V	wood-chips	277	201	7.5	2 – 3	leachate	80/65 [d]	6.0/ 4.2[d]

[a] after day 120
[b] depending on discharge pipe used
[c] before addition of acetate
[d] first and second full operational year, respectively

3.1.2 Nitrate removal performance

Since the first installations of DBRs in the 1990s, research has focused on how to dimension and design bioreactors to handle variations in flow and nitrate concentrations and at the same time promote a high removal efficiency. As a result, the US Department of Agriculture has issued a conservation practice standard for denitrifying bioreactors (USDA, 2020) in which it is stated how to construct a bioreactor and what considerations are needed regarding for example inflow nitrate levels, carbon source and topology of the site where the bioreactor is to be placed.

Hydraulic retention time and temperature

Hydraulic retention time (HRT) and temperature are the two most important factors determining N removal efficiency (Addy et al., 2016; Grießmeier et al., 2021). In general, longer HRTs give higher N removal efficiencies (Addy et al., 2016; Hoover et al., 2016; Martin et al., 2019; Audet et al., 2021), but

excessive HRTs are not recommended as the system becomes depleted in nitrate allowing other biogeochemical processes to take place (Lepine et al., 2016; Davis et al., 2019; Rivas et al., 2020; Audet et al., 2021). None of the studies in this thesis were designed to evaluate HRT in relation to performance, HRTs were set to meet other criteria. In **papers I** and **III**, HRTs between 12 and 60 h were chosen, retention times used in many bioreactors treating agricultural drainage. It was possible to maintain a constant and high flow since pond water was used, and there was unlimited availability of water at the two field sites. The bioreactor in **paper V** instead treated leachate from a waste rock pile. According to recommendations (USDA, 2015) the reactor was dimensioned to treat 60 % of the annually generated leachate volume. The volume of the leachate was estimated from hydrological data, but less leachate than estimated was generated. Hence, during the first operating year, there was not enough water and the system experienced longer HRTs, 7.5 days, than it was dimensioned for. In **paper II**, the flow was adjusted so that stable nitrate removal but not nitrate limited conditions would occur and that was achieved with an HRT of 6 – 7 days.

Temperature affects the N removal performance, as chemical reactions are affected by temperature, and the differences in temperature within and between the DBRs studied in this thesis could be among the factors contributing to differences in performance. The lab-scale bioreactors in **paper II** were kept at constant temperature and the field reactor in **paper V** had an underground water reservoir that kept the water at the same temperature all year around. The other bioreactors were affected by variations in ambient temperature. According to several studies, the N removal rate is approximately doubled per 10 °C in bioreactors with temperatures between 5 and 30 °C, consistent with general theories on activation energy (Addy et al., 2016; Hoover et al., 2016; Nordström and Herbert, 2017). That temperature range is reasonable in agricultural applications, but efficient N removal at lower temperatures might be needed to treat mining impacted water in cold areas. To my knowledge, no woodchip DBR operating under a permanently low temperature (< 3 °C) has been described until now (**paper V**), where we show that a high N removal efficiency is possible even at 2 – 3 °C.

Carbon source and inflow nitrate concentration

The choice of reactive material, the substrate, in a DBR is a balance between many factors since the availability of carbon is a prerequisite for

heterotrophic denitrification to take place. Woodchips have become the hallmark, for several reasons. They are cheap and easily available, have good hydraulic properties, a high enough reaction rate and can last at least a decade (Robertson et al., 2008; Cameron and Schipper, 2010; Schipper et al., 2010; Christianson et al., 2021). Initially, many of the systems described, mostly denitrifying walls, used sawdust (Robertson and Cherry, 1995; Schipper and Vojvodic-Vukovic, 2001). The pilot-scale bioreactor in **paper I** was based on sawdust, and to increase the permeability the sawdust was mixed with gravel. Schmidt and Clark (2013) showed that sawdust and woodchips are comparable in terms of reactivity, but that the ratio of organic material to sand correlated with nitrate removal. The bioreactor in **paper I** did not reach sufficient removal efficiency until an external carbon source in the form of acetate was added, and a possible explanation is that the proportion of sawdust was too low for an efficient N removal.

The role of carbon quality in DBRs has gained increased attention (Ghane et al., 2018; McGuire et al., 2021) and many other plant-derived substrates have been tested for their suitability as electron donors. Moreover, the possibility of using waste products or material available locally has been important when considering which material to choose. With that in mind, we evaluated sedge in one set of the laboratory bioreactors in **paper II**. The material has previously not been tested as an electron donor and was locally available in large quantities. We also aimed at using a substrate having higher proportions of hemicellulose and cellulose than woodchips. Hemicellulose and cellulose are the easier degradable polymers among lignin, cellulose, and hemicellulose, the three main constituents of plant fibres (Ahmad et al., 2007). Consistently with many other non-woody plant-based substrates evaluated for their nitrate removal capacity (Della Rocca et al., 2006; Greenan et al., 2006; Fowdar et al., 2015; Feyereisen et al., 2016; Pang and Wang, 2021), the sedge and barley straw bioreactors supported higher nitrate removal rates than the woodchip bioreactors. We attribute at least part of the higher removal in the sedge and straw bioreactors to the higher content of hemicellulose and cellulose in sedge and straw. Although we did not measure the concentrations of dissolved organic carbon (DOC) in the water of the bioreactors, it is likely that the more labile cellulose and hemicellulose contributed to higher DOC concentrations and hence supported the higher removal rates in the bioreactors packed with sedge and straw. Similarly, increased nitrate removal rates were observed when using the more labile

carbon source potato residues in combination with woodchips when treating aquaculture effluent (Kiani et al., 2020).

In the two systems described in this thesis where we have carbon data from the water phase, we see a relationship between carbon, performance, and age of the system. The observations agree with the findings of for example Hassanpour et al. (2017), David et al. (2016), and the meta study of Addy et al. (2016) based on 57 bioreactors. Initially, the N removal rate is high, it declines with age of the woodchip bed, and after 1 – 3 years, the removal rate stabilises. Interestingly, David et al. (2016) showed that the impact of carbon quality overruled the impact of temperature. They found no relationship between temperature and nitrate removal rate until after two years, when the load of DOC in the outlet water of the bioreactor had decreased substantially. The same relation between woodchip age, nitrate removal rate and temperature was demonstrated in a paper analysing previously published datasets (Maxwell et al., 2020). Accordingly, the woodchip DBR in **paper III** removed N at a higher rate the first year (Nordström and Herbert, 2019) and there was a strong negative correlation between the concentrations of total organic carbon and nitrate in the pore water along the distance of the reactor (Spearman´s rho = -0.94 and -0.67, $p < 0.0001$ and 0.001 the first and second operational year, respectively, Fig. 8).

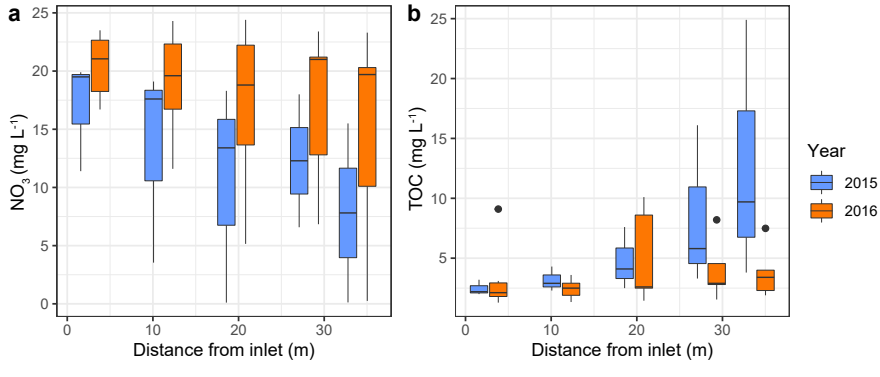

Figure 8. Nitrate (a) and total organic carbon (b) lengthwise at the bottom of the bioreactor. Based on data presented in Fig. 1 in **paper III**.

In **paper V**, the concentrations of DOC in the outlet water of the woodchip DBR were highest at start-up, fall 2018, and the highest N removal efficiency

was obtained during this period (**paper V**, Fig. S1d and a). Another factor contributing to the high N removal of the bioreactor in **paper V** during the first months is likely the high concentrations of nitrate in the incoming water. Several studies have shown that a high N load results in high removal rates (Addy et al., 2016; Nordström and Herbert, 2019; Rivas et al., 2020).

3.1.3 Adverse effects

There is a potential risk of pollution swapping, to increase one pollutant as a result of a measure introduced to reduce another, when using DBRs for nitrate removal (Hartfiel et al., 2022). Ideally, the nitrate will undergo full denitrification and be converted to N_2, but non-complete denitrification leads to the production of N_2O, and the processes DNRA retains N in the form of ammonium. Additionally, nitrite can be accumulated if the rate of nitrite production exceeds the rate of nitrite reduction.

Nitrous oxide, methane, and hydrogen sulphide production

It has been estimated that up to 10 % of the reduced nitrate leaves DBRs in the form of N_2O (Greenan et al., 2009; Healy et al., 2012; Feyereisen et al., 2016; Davis et al., 2019) and the majority of the N_2O is found dissolved in the water (Warneke et al., 2011a; Davis et al., 2019). Hydraulic retention time is one important factor controlling N_2O production (Davis et al., 2019; Audet et al., 2021; Jéglot et al., 2022), but temperature, carbon source and nitrate removal efficiency (Feyereisen et al., 2016; Nordström and Herbert, 2018; Grießmeier et al., 2021) are additional factors impacting the amount of N_2O formed. Conditions favouring N_2O production are short HRTs, low temperature, and low removal efficiency. The origin of the woodchips mattered when tested in denitrifying walls, where woodchips from hardwood produced higher N_2O fluxes (Manca et al., 2020). The bioreactors in **papers III** and **V** both emitted N_2O from the reactor surface. Comparisons on how big the contributions from nitrate-treating bioreactors are in relation to the emissions from agriculture are difficult since it is complicated to estimate the N_2O fluxes from agricultural land (Lawrence et al., 2021). However, given the size relation between agricultural land and a bioreactor, the overall contribution from DBRs is likely small. It can be further noted that covering the reactor surface with soil lowers the amount of N_2O emitted (Christianson et al., 2013a; Manca et al., 2021). Our field-scale bioreactors (**papers III** and **V**) were covered, with glacial till or till and peat, which makes it difficult to

evaluate these systems in relation to previously described ones. It might be more relevant to look at the N_2O dissolved in the water of the reactor and determine if the bioreactor produces or consumes N_2O. Both field-scale bioreactors produced N_2O the second year, but data was highly variable and during the first operational year, the bioreactor in **paper V** instead consumed N_2O.

Production of methane, also a potent greenhouse gas, can take place under reducing conditions and low levels of nitrate. Such conditions might occur at the start-up of a bioreactor due to high levels of DOC, but when methane has been detected in DBRs, it is in most cases transient (Nordström and Herbert, 2018) or in low concentrations (Warneke et al., 2011a; Jéglot et al., 2022). However, with other substrate types than woodchips, higher methane emissions have been reported (Healy et al., 2012). The bioreactor in **paper V** had neglectable fluxes of methane, and in most cases, methane was consumed, not produced.

Yet another gaseous undesired product that may form in a DBR if sulphate is present, is hydrogen sulphide, H_2S. Hydrogen sulphide is ecotoxic and can be formed if the system is anoxic and depleted of nitrate, and it has been observed in DBRs treating different types of water. Lepine et al. (2016) noted that prolonged N-limitation intensified the formation of sulphide at high DOC concentrations and temperatures around 20 °C in a reactor treating aquaculture wastewater and Rivas et al. (2020) detected the production of H_2S from its characteristic odour at low water flows in a system treating agricultural drainage. Very long retention times in a system for stormwater treatment also led to the reduction of sulphate and H_2S formation (Lynn et al., 2015). The water sampled near the outlet of the bioreactor in **paper V** had a clear smell of H_2S on some occasions the first summer when the flow was very low, and no nitrate was detected in the water.

Production of nitrite, ammonium, and leaching of dissolved organic carbon

Accumulation of nitrite in denitrifying bioreactors has been observed during the start-up phase (Warneke et al., 2011a), and the same trend was observed in all DBRs studied in this thesis. Ammonium production in the bioreactors was in general low, with concentrations in the outlet water most often < 0.5 mg N L^{-1}. The sedge- and straw-based laboratory-scale bioreactors in **paper II** though, displayed a significantly higher production of ammonium than the corresponding woodchip reactors. Ammonium levels in the outlet of both woodchip and other type of reactors are found, but have been shown to

decrease after some time (Greenan et al., 2006; Cameron and Schipper, 2010) and steady state ammonium levels of 1 – 6 mg N L^{-1} have been reported (Healy et al., 2012).

The release of dissolved organic matter from a bioreactor is an environmental risk since it can result in low oxygen levels in the receiving water bodies when the material is later degraded. The initial flush of DOC typically observed from woodchip DBRs (Hoover et al., 2016) or from reactors with a variety of other cellulose materials, decline and stabilise with time (Cameron and Schipper, 2010; Grießmeier and Gescher, 2018). And this pattern was noted also in the reactors of **papers III** and **V**.

Other concerns about DBR effluent were addressed by Lepine et al. (2021). The authors investigated the chemistry of the outflow water from bioreactors with hardwood woodchips and focused on if the water would be possible to reuse in agriculture. They concluded that the water might be possible to re-use, but that further studies are needed to ensure that a combined effect of contaminants do not cause adverse effects.

3.2 Reactive barriers as complement in Soil Aquifer Treatment

In soil aquifer treatment, (SAT), treated sewage effluent is used to produce groundwater by artificially recharging aquifers via infiltration basins in a combination of wet and dry cycles producing intermittent aerobic and anaerobic conditions in the soil under the basin. In the wet cycle, the water passes through the unsaturated zone and undergoes processes improving the water quality. The system is then allowed to dry, and the dry periods allow for aeration of the soil to renew the treatment capability of the system and when needed, maintenance of the basins. In its current form, SAT has been used for decades, especially in arid regions (Quanrud et al., 2003; Mienis and Arye, 2018), but the principle goes far back in time; it was used in Athens 2000 years ago and became common in Germany and England during the 1500s (Idelovitch and Michail, 1984). The technique is robust, cost-effective, and can remove a wide range of contaminants, including pathogens, mainly by filtration, adsorption or biological degradation or a combination of the mechanisms (Sharma and Kennedy, 2017).

The effect of SAT on DOC removal is well known; a 40 – 90 % reduction of DOC concentrations, including OMPs, has been shown in several studies

(Quanrud et al., 2003; Amy and Drewes, 2007; Suzuki et al., 2015). However, not all organic compounds are efficiently removed (Amy and Drewes, 2007; Ternes, 2007). To improve the effect of SAT, a carbon-rich reactive barrier, can be added to the system. Similar to in a DBR, the material in a reactive barrier is plant-derived and offers surfaces for biofilm growth. A layer of for example compost or woodchips releases enough DOC to the infiltrating water to generate a range of redox conditions and adds additional sorption sites, which facilitates biodegradation and retards transport of pollutants through the system. Another function of a reactive barrier is to supply labile carbon to support co-metabolic degradation of OMPs. So far, the results are promising regarding OMPs removal and lowering the number of pathogens in the treated water (Schaffer et al., 2015; Valhondo et al., 2020b; Modrzyński et al., 2021).

3.2.1 Barriers for nitrogen removal in SAT

Nitrogen removal in SAT is a function of HRT, DOC to N ratio and redox conditions (Sharma and Kennedy, 2017; Gharoon and Pagilla, 2021). It has been shown that SAT can lower concentrations of nitrate and ammonium (Sopilniak et al., 2017; Beganskas et al., 2018; Friedman et al., 2018; Grau-Martínez et al., 2018) but the effect of a reactive layer on the N-removing processes has not been well studied. When N-containing organic matter in the material is degraded and N is mineralised, it can add ammonium to the water passing through the barrier, instead of removing it. Additionally, the ammonium-producing pathway DNRA could be promoted if the C/nitrate ratio increases (Hardison et al., 2015; Putz et al., 2018). Modrzyński et al. (2021) investigated how ammonium was transformed and the N eventually removed in a column experiment with compost-based barriers treating synthetic wastewater with OMPs and a low, 2 mg L^{-1}, N as ammonium content. The ammonium was effectively removed, and nitrate was formed. Denitrification subsequently removed the nitrate, but the removal was dependent on the proportion of compost in the barrier mixtures. In addition, ammonium was re-formed in the columns having the highest proportion of compost. An increase in ammonium concentrations after SAT was observed also in the column experiments of Silver et al. (2018). The soil used for the infiltration of treated wastewater had a high organic content, and by using ^{15}N analyses the authors show that the increase in ammonium likely originated from the soil. In **paper IV**, we investigated how the addition of reactive organic

barriers affected the ability to remove N from secondary treated wastewater having high ammonium concentrations, approximately 30 – 60 mg N L^{-1}. We found that across the experimental period of nearly one year, all barriers reduced the ammonium concentrations in the infiltrated water to some degree. A sand filter was used as reference, and when normalising the ammonium removal efficiencies in the barriers to the reference, all barriers but one mixture based on compost and with vegetation, removed less ammonium than the reference. The only barrier that significantly lowered the ammonium concentrations in the water, instead increased the nitrate concentration in the water. The sand filter significantly removed DOC from the secondary effluent. In addition to the overall poor N-removal capacity in all barriers, the barriers based on compost leaked DOC to the water. This highlights the difficulties with designing multi-purpose reactive barriers, the compost-design of the barriers was also meant to facilitate degradation of OMPs, and to attenuate pathogens in the water. Some of the OMPs tested were degraded in the system but the retention of pathogens was poor (Valhondo et al., 2020).

4. Microbial communities and nitrogen cycling functions

The microbiome is the most essential component of a bioreactor. A better understanding of the microbial ecology of permeable reactive barriers for N removal will ultimately help designing systems. In 2014, when **paper I** was published, there were no more than a handful studies in the scientific literature addressing the microorganisms responsible for the N transformations leading to the removal of nitrate in cellulose-based DBRs (Long et al., 2011; Warneke et al., 2011; Andrus et al., 2014; Porter et al., 2015). Since then, the interest in understanding which microorganisms establish and sustain in a permeable reactive barrier, and what controls their activity has increased. In a recent review, 15 papers published between 2011 and 2020 addressing microbial communities in cellulose-based DBRs were summarised, (Hartfiel et al., 2022), and from 2020 until mid of 2022 several articles on this topic have been published (e.g. Jéglot et al., 2021a; Schaefer et al., 2021; Aalto et al., 2022). The microbiology in reactive barriers in combination with aquifer recharge has also gained attention the last years, yet the number of studies is still low. Barriers based on woodchips have been investigated under field and laboratory conditions (Beganskas et al., 2018; Gorski et al., 2020; Pensky et al., 2022), and the microbiology of barriers based on compost was addressed in **paper IV** and by Modrzyński et al. (2021).

To investigate the microbial communities in the bioreactors and barriers studied, we used two methods, quantitative PCR (qPCR) and Illumina sequencing of the V3 – V4 region of the 16S rRNA gene. Using qPCR, the genetic potential for a specific metabolic pathway can be quantified by targeting genes encoding for key enzymes in the pathway. The method is widely used in microbial ecology and consequently also when exploring

permeable reactive barriers (Feyereisen et al., 2016; Aalto et al., 2020; Modrzyński et al., 2021). Sequencing of the 16S rRNA variable regions gives taxonomic information and is a standard approach to determine prokaryotic community composition (Bukin et al., 2019). An alternative and complement to qPCR for determining the magnitude of different metabolic pathways, is to use metagenomic and metatranscriptomic approaches. Biases introduced by primer selection and varying PCR efficiencies can thereby be avoided. We have used qPCR to estimate the abundances of different N transformation processes in **all papers** included in this thesis. To determine the structure of the communities and the taxonomy of the community members, we used sequencing in **papers II, IV** and **V**. Except for in the first DBR, samples were collected at more than one occasion to explore temporal variability and the development of microbial communities from the start-up of reactors and up to two years of operation. We expanded to not only looking at the temporal succession of the microbial communities, but also determined if there were spatial patterns in how the microorganisms were distributed along the length and depth of reactors and barriers and, in some cases, between the solid and liquid phases of the systems. Table 2 summarises the approaches in the projects.

Table 2. Overview of the approaches and sample types used to study the microbial communities in the different papers.

In paper	Amplicon sequencing	Quantitative PCR	Substrate analysed	Water analysed	Temporal pattern	Spatial pattern
I		x	x			x
II	x	x	x		x	x[a]
III		x	x	x	x[b]	x
IV	x	x	x	x	x	x
V	x	x	x	x	x	x

[a] at the end of the experiment only
[b] in the water phase only

4.1 Spatial and temporal patterns of microbial communities – examples from papers I - V

4.1.1 Paper I

One of the objectives in **paper I** was to find out if there were preferential flow paths through the bioreactor. The design of the discharge pipes could potentially favour the water to flow faster through the middle parts and to be less mobile along the sides. The simplest way to evaluate preferential flow paths was to just look at the bioreactor material during the sampling event, when the bioreactor was excavated. In Figure 9, one of the inner dividing walls is shown. Different colours of the iron oxide deposits on the wall and in the gravel, indicate that different microorganisms had oxidised the iron. Additionally, it was clear that the sawdust in the bioreactor had been washed away from some areas, whereas others had dense patches of sawdust. All this indicates non-homogenous conditions. We hypothesised that preferential flow paths would affect the distribution of nitrate-reducing microorganisms, and for the abundances of *nirK*, this was the case. The lengthwise transects that represented the middle of the bioreactor, harboured more *nirK*-type denitrifiers than the sides of the bioreactor at the depth that was always water saturated (**paper I**, Fig. 6b). The potentially higher flow, and hence higher load of nitrate, in the middle section of the reactor, could have promoted the increase in *nirK* community size. The design of the experiment did not allow for measuring N-removal rates specifically corresponding to the transects, but as N load is one of the factors determining the N removal rate (Rivas et al., 2020), the middle section of the bioreactor likely contributed more to the overall N removal and the full reactor volume was not efficiently used. This is not ideal and makes it difficult to dimension bioreactors correctly and can reduce their life length (Christianson et al., 2013; Christianson et al., 2020), The community harbouring *nirS*-type denitrifiers displayed a different spatial pattern, as it was more abundant in the deeper, water-saturated regions of the bioreactor (**paper I**, Fig. 4). Overall, there was a higher abundance of most of the N-transforming microorganisms quantified in the deeper, water saturated layers of the bioreactor. The efficiency of the bioreactor would probably have been higher if it had been designed so that a bigger volume was water saturated.

Figure 9. Iron oxide deposits on a sheet metal inner dividing wall in the bioreactor in paper I. The photo has been modified in Photoshop. A glove positioned in the upper part of the picture, indicating size, has been replace by gravel.

4.1.2 Paper II

In contrast to the bioreactor in **paper I**, the lab-scale bioreactors in **paper II** were not meant to remove as much nitrate as possible. The design of the experiment instead aimed at exploring the development of the microbial communities in different substrates when the bioreactors were working with approximately the same removal efficiencies and never ran out of nitrate. We evaluated if the communities that developed on the substrates were different at the in- and outlet of the reactor by comparing the Shannon diversity indices and the community composition between the two positions. In general, the inlet position of the reactors had a higher diversity than the outlet position and the woodchip bioreactors always had lower diversity indices than the straw and sedge bioreactors. The spatial differences in the diversity developed with different rates in the substrate types. The succession in the woodchip columns was the fastest, the change in diversity was measurable at day 43, while it was first detected at day 181 and 216 for the sedge and straw bioreactors, respectively. All bioreactor types had high relative abundances of Alpha- and Gammaproteobacteria, and the sedge and straw bioreactors additionally harboured Actinobacteria, Bacteroidia and Fibrobacteria, contributing to the higher diversity in these reactor types. The differences in diversity were not always reflected in different genetic potentials for the N transformation reactions. For example, in the woodchip and sedge reactors, position was not a significant factor determining the size of the of nitrate-reducing community. This might be a consequence of that the bioreactors were never depleted of nitrate and therefore a high abundance

of nitrate reducers was supported throughout the reactor. In contrast to our results, bioreactors with addition of a more labile carbon source, potato residues, displayed a lower diversity compared to bioreactors with woodchip only (Kiani et al., 2020). Like in the sedge and straw bioreactors, the potato bioreactors harboured high abundances of Bacteroidota, but not a high abundance of Alpha- and Gammaproteobacteria, instead Campylobacterota and Firmicutes were abundant.

4.1.3 Papers III and V

Similar to the lab-scale bioreactors in **paper II**, Alpha- and Gammaproteobacteria, and Bacteroidia were highly abundant in the woodchip microbiome of the full-scale bioreactor in **paper V**, and these bacterial classes are frequently reported from woodchip DBRs (von Ahnen et al., 2019; Grießmeier et al., 2021; Jéglot et al., 2021a; Aalto et al. 2022). A closer look into the Gammaproteobacterial class, shows the presence of Burkholderiales in the **paper V** bioreactor. Bacteria in this order have been identified as key denitrifiers in woodchip DBRs (Grießmeier et al., 2021), and they also seem to be associated with low temperature (Jéglot et al., 2021b). As in the lab-scale bioreactors, the diversity in the woodchips, in **paper V** estimated as Faith´s PD, was higher closer to the inlet of the bioreactor (**paper V** Table S2), and the trend was similar for the Shannon index (data not shown). The composition of the microbial communities was also significantly affected by the distance from the inlet (**paper V**, Fig. 5). This contrasts with the findings of Jéglot et al. (2021a), where the diversity in the woodchips along the flow paths of three willow DBRs was analysed and presented using the Shannon index. However, this could be due to differences in the design and operation of the bioreactors. A notable distinction between the bioreactors was the age of the reactor bed, the bioreactors described by Jéglot et al. had been operating at least four years, and the one in **paper V** less than two years at the final sampling occasion. The ordination in figure 5, **paper V**, shows an overall increased similarity between the samples the second year, and the phylogenetic diversity (**paper V**, Table S2) in the water had a smaller range the second year, indicating a higher similarity between the microorganisms along the length of the reactor. Studies following the diversity of DBR microbiomes over several years are still lacking, but given the sparse existing data (Porter et al., 2015; Schaefer et al., 2022; **paper V**), and the knowledge about stabilisation in performance

after a couple of years (Addy et al., 2016), it is possible that spatial differences in community composition will decrease within the reactor. Still, since the chemical conditions along the length of the reactor will vary, different processes will be supported at different distances from the inlet.

The diversity and community composition between the woodchip- and water phases, an additional aspect of spatial patterns, in the **paper V** bioreactor were different and many taxa present in the water were not found on the woodchips. Despite the different overall community compositions, there were resemblances in the spatial patterns between the two phases, for example the occurrence of the phylum Desulfobacterota, that was present in both woodchips and water were predominantly found close to the end of the bioreactor. This phylum includes bacteria reducing sulphate and other sulphur compounds (Murphy et al., 2021; Ward et al., 2021), reactions that can occur when nitrate is depleted.

In the **paper III** bioreactor, we did not sequence the DNA from the microbial communities in the bioreactor. Instead, we quantified the genetic potential for N transformation processes and found a high degree of temporal and spatial variability. The N-cycling community structure in the pore water differed between the two years, with nitrite and dissolved N_2O as the main environmental drivers, and the abundance of *nosZ*I being the gene contributing the most to the separation of the two communities (**paper III**, Fig. 4). Spatially, the occurrences of *nirS* and *nirK* genes were strongly correlated with the woodchip and pore water samples, respectively (**paper III**, Fig. 2c).

4.1.4 Paper IV

In **paper IV**, we tested permeable reactive barriers with varying compositions to relate N-removal performance to community composition, similar to what was done in **paper II**. Here the N-polluted water was secondary treated effluent from a WWTP, and the main N compound to be removed was ammonium. Barrier samples were collected when the system experienced dry cycles, first in the beginning of the experimental period and next in the fourth dry period when the system had been running for one year (**paper IV**, Fig 1a). Within each type of barrier tested, the community composition differed between the two sampling occasions, but the diversity was similar (**paper IV**, Fig. 4, Fig. S4). One class of bacteria increasing in relative abundance in the woodchip-based barrier and in the reference sand

filter, was the nitrite oxidising Nitrospira (**paper IV**, Fig 1b), known to be important in sand filters (Fowler et al., 2018). Water for microbial analyses was collected directly after barrier passage, before the fourth dry period started. In the compost-based barriers, the Shannon and Pielou diversity indices in the water was lower than in the barriers, but the phylogenetic diversity was similar between the water and barrier in all barrier types (**paper IV**, Fig. S4).

4.2 N transformation processes in the reactor and barriers

The dominating nitrate removal pathway in cellulose-based DBRs is denitrification. This has been established in this thesis and in studies by others using a range of different methods: the water chemistry in the in- and effluent water, enrichment of the isotope ^{15}N, biochemical assays, and abundance of *nir* genes (Greenan et al., 2009; Moorman et al., 2010; Schipper et al., 2010; Nordström and Herbert, 2018; von Ahnen et al., 2019). We found genes associated with denitrification in all cellulose-based DBRs investigated, including the reactive barriers for ammonium removal. Here, denitrification is important if N is to be permanently removed. However, as denitrification is a modular pathway that can terminate with N_2O production, and DNRA produces ammonium, it is important to look at the magnitude of the latter two products and processes in relation to denitrification to avoid pollution swapping and insufficient N removal.

4.2.1 Denitrification and nitrous oxide reduction

Incomplete denitrification leads to production of N_2O. Therefore, the ratio between the genetic potential for production and consumption of N_2O, estimated as the respective abundances of the *nir* and *nosZ* genes, indicates if a system is a possible source or sink of the gas. In **paper III**, there was a positive correlation, along the length of the bioreactor, between the concentrations of N_2O in the water and the *nir*/*nosZ* ratios. Higher *nir*/*nosZ* ratios closer to the inlet, where nitrate concentrations were high, agrees with the findings that low C/nitrate ratio could lead to the promotion of microorganisms or communities with incomplete denitrification ending with N_2O (Pan et al., 2013). An increased genetic potential for N_2O production was also found in the water of the other full-scale woodchip DBR the second year, with the highest potential where nitrate was most abundant (**paper V**, Fig.

4c). For this bioreactor, dissolved N_2O could be quantified only once the second operational year, and the concentration of N_2O was higher than in the first year, while the emission of N_2O remained unchanged. The temporal pattern with increasing potential for N_2O production was not observed in the lab-scale bioreactors in **paper II**, as they developed in the opposite direction with decreasing N_2O production.

Monitoring N_2O over years, especially in relation to microbial community composition is rare. In a recent study though, describing eight DBRs of different ages, it was shown that the two youngest bioreactors acted as sinks, while the older ones were sources of N_2O (Audet et al., 2021). However, no links to differences in abundance of N-cycling genes could be detected.

4.2.2 Denitrification and DNRA

The processes denitrification and DNRA compete for nitrite and C, and based on the water chemistry and gene abundance data in **paper III**, competition between the two dissimilatory nitrite reduction processes likely occured. There was for example a negative correlation between C/nitrate and the ratio of genetic potentials for denitrification/DNRA (**paper III**, Table 1). Furthermore, C/nitrate ratios correlated positively with high ammonium concentrations (**paper III**, Table 1), and the nrfA gene abundance (Fig. 10). Altogether, this agrees with high C/nitrate ratios favouring DNRA (Putz et al., 2018). The C/nitrate conditions were not specific to year of operation or distance from inlet (Fig. 10, **paper III**), but temperature was found to affect the abundance of DNRA in the bioreactor, with more DNRA at lower temperatures, as an effect of less removal of nitrate (Nordström and Herbert, 2018). In agreement, *nrfA* increased in abundance when nitrate was in lower concentrations in the bioreactor in **paper V** (**paper V**, Fig. 2, Fig. S3). Altogether, these findings support DNRA as a possible nitrate reduction pathway in DBRs.

It has been shown that different carbon compounds specifically promote denitrification or DNRA (Carlson et al., 2020), and in **paper II** we found that the sedge and straw bioreactors harboured bigger *nrfA* communities than the woodchip reactors. The sedge and straw reactors had a notably higher relative abundance of Bacteroidia than in the corresponding woodchip reactors. Bacteroidia are known for their ability to degrade cellulose (Lapébie et al., 2019), and they have been associated with DNRA in woodchip

DBRs treating aquaculture effluents (Aalto et al., 2020). We suggest that the presence of cellulose degrading bacterial taxa together with the higher concentrations of cellulose in the substrate of these bioreactors increased the C/nitrate ratio and promoted DNRA. Nevertheless, the water chemistry in the DBRs supports that denitrification was the dominating nitrate removal pathway in all bioreactor types. After a start-up period, the risk of discharging water with high ammonium concentrations from woodchip-based DBRs seem to be small. DNRA was addressed also in **paper IV**, and as in **paper II**, the woodchip-based barrier had a smaller DNRA community than barriers based on another type of C substrate (**paper IV**, Fig. 3D). Overall, the higher C/nitrate ratio in water from the compost-based barriers (**paper IV**, Figs. 2B, D) could have contributed to DNRA and ammonium production and thereby their poor total N removal, but that is contradicted by the similarly poor performance of the woodchip-based barrier and reference.

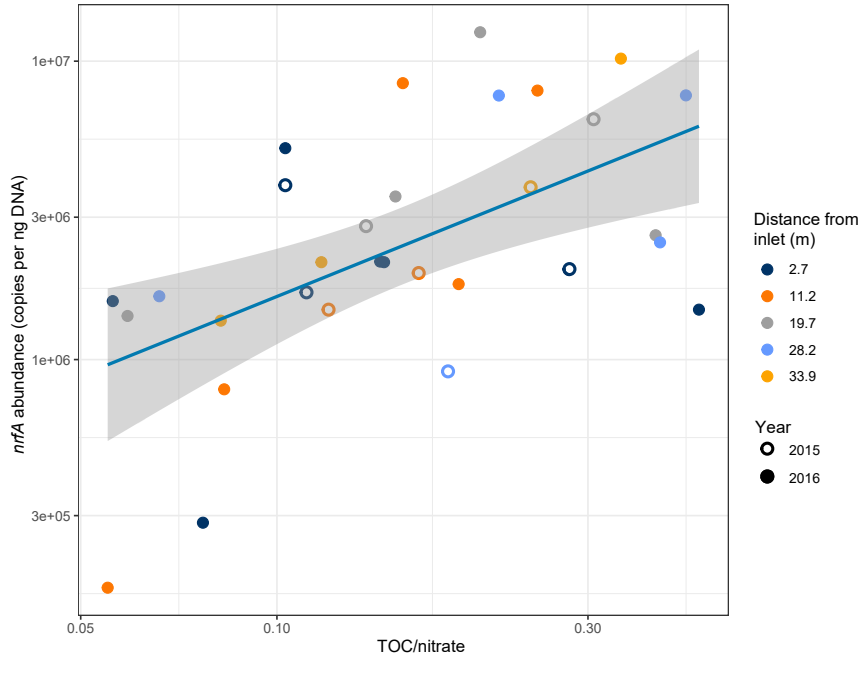

Figure 10. Relation between the total carbon/nitrate ratio and abundance of *nrfA* in the porewater of the bioreactor in paper III at different distances from the inlet of the reactor over two years of reactor operation. The shaded area represents the 95 % confidence interval.

4.2.3 Anammox

The concomitant removal of nitrite and ammonium via anammox in a permeable reactive barrier would be advantageous, as reducing power in the form of organic carbon would not be needed. The presence of anammox was analysed in the bioreactors in **papers I, II, III,** and **V**. However, since anammox is favoured by the absence of organic C, we did not expect anammox to be a significant potential N-removal pathway in the DBRs. In most papers we targeted the *hdh,* formerly known as *hzo*, using specific primers described by Schmid et al. (2008). These primers have been used to detect anammox in different environments, including wetlands, sediments, marine sediments, and moving bed bioreactors (Wittorf et al., 2016; Wu et al., 2021; Kaewyai et al., 2022; Tao et al., 2022). The gene was not detected in any of the water or woodchip samples analysed. In agreement with our findings, no expression of hydrazine oxidoreductase, the enzyme encoded by *hdh*, was detected in the bioreactors characterised by Grießmeier et al. (2017). Yet, we did find a non-neglectable genetic potential for anammox in the bioreactor in **paper I**, using taxa specific primers that have been found to have 89 – 100 % specificity for all known genera performing anammox (Yang et al., 2020). In this reactor, sawdust was used as the substrate, but it did not support denitrification well, and acetate had to be added to achieve sufficient nitrate removal. It is possible that the oligotrophic conditions in this particular reactor was more favorable for anammox compared with the other reactors and barriers. Nevertheless, if the target is not a pathway-specific gene, the question whether the organisms targeted could perform a specific function or not will always be raised. Anammox has been reported to substantially remove N from DBRs, especially if denitrification was C limited (Rambags et al., 2019). However, in the study it was not discriminated between anammox and codenitrification, why the N_2 identified with isotopic analyses also could have been a product of codenitrification.

4.2.4 Nitrification

Most of the permeable reactive barriers presented in this thesis operated under anoxic conditions, and therefore the potential for nitrification was quantified only in **paper IV** with reactive barriers treating ammonium-polluted water. Both bacterial and archaeal ammonia oxidisers were detected in the reactive barrier material. The abundance of ammonia oxidising bacteria increased over the year in the compost-based barriers with

vegetation, resulting in significantly larger ammonia oxidising communities. This was however not reflected in the ammonium removal, possibly because ammonium could have been produced in the barriers, both from mineralisation of the organic material, but also from DNRA. The one barrier that did remove ammonium, had a lower ratio of DNRA/nitrification at the end of the period, which may explain the better performance.

5. Conclusions and outlook

This thesis addressed the role of microbial communities in permeable reactive barriers for removal of N from waters with high nitrate or ammonium concentrations before discharge to recipient surface waters or when recharging aquifers to replenish groundwater reservoirs. The composition of the microbial community and the genetic potential for different N transformation processes can aid the design of permeable reactive barriers by providing insights into mechanisms that underpin N removal efficiency and production of unwanted N species in the system.

Results in this thesis show that woodchip-based DBRs are suitable for remediation of nitrate-polluted water from mining activities. Although woodchip-based bioreactors had lower nitrate removal rates than bioreactors based on other organic carbon-rich substrates, woodchip reactors are preferred due to their long life length and good hydraulic properties. According to the results in this thesis, they also have lower potential for the ammonium-generating DNRA bacterial community to develop compared to the other substrates investigated. Moreover, the results highlight the difficulties of designing multipurpose reactive barriers. The barriers treating the ammonium-rich wastewater had previously been shown to work well for other pollutants, but they had no major effect on nitrogen and the compost-based barriers released DOC.

The type of C substrate used in permeable reactive barriers determines the genetic potential for N transformation processes and composition of the microbial communities in the barrier, but not necessarily the N-removal performance. The role and importance of C substrate in the competition between denitrification and DNRA in DBRs should be further studied to understand how to achieve a high rate of denitrification while avoiding production of ammonium and leaching of DOC. To take advantage of the

higher nitrate removal rates obtained with more labile C than woodchips, woodchip DBR design could be potentially improved by replacing a fraction of the woodchips with another material, which should be investigated in future research. A reactor with mixed C substrates would likely need to be designed with the possibility of an easy replacement of the labile carbon material, as it would degrade faster than the woodchips.

The risk of pollution swapping when using DBRs and reactive barriers is under discussion, and research is ongoing. We conclude that methane emissions are negligible and that N_2O emissions from DBRs with similar design as those investigated in this thesis likely only have a minor contribution to global N_2O emissions. Nitrous oxide dissolved in the discharge water might be a problem since the N_2O can be emitted downstream if not consumed by N_2O reducers in the recipient water. To monitor N_2O from DBRs, I suggest that effort is placed on measuring N_2O concentrations in the water rather than on measuring fluxes from the bioreactor surface, at least if the bioreactor is covered with soil or peat. The release of nitrite, ammonium, and DOC at the start-up of a DBR is problematic but may be transient and should be weighed against the urgent need for mitigating N releases to the environment. Estimated over the life length of a DBR, it might be advantageous to use the technique even if the ecological footprint of a bioreactor can still be lowered. Life cycle analyses of DBRs are needed to answer the question. Also permeable reactive barriers treating ammonium polluted waters can produce greenhouse gases, although this was not investigated in this thesis.

An interesting question to address is how long-term development of microbial communities and N removal in DBRs are affected by an inoculum. When a new bioreactor is constructed, the substrate is often inoculated to support the establishment of a denitrifying community. This can be accomplished by adding material from an old bioreactor or, as in this thesis, sludge from a wastewater treatment plant or, as has been tested under laboratory conditions, pure strains of denitrifying bacteria selected for under specific conditions, for example coldness. Other organisms that could be interesting to add are cellulose and hemicellulose degraders, to support a higher rate of woodchip degradation and thereby increasing the denitrification capacity.

Finally, since DBRs can be used for multiple applications, I suggest that the conditions for introducing this technique in Sweden, as a complement to

other means mitigating nitrate pollution into the Baltic Sea, should be examined.

References

Aalto, S.L., Suurnäkki, S., von Ahnen, M., Siljanen, H.M.P., Pedersen, P.B., and Tiirola, M. (2020). Nitrate removal microbiology in woodchip bioreactors: A case-study with full-scale bioreactors treating aquaculture effluents. *Science of The Total Environment* 723**,** 138093. doi: 10.1016/j.scitotenv.2020.138093.

Aalto, S.L., Suurnäkki, S., von Ahnen, M., Tiirola, M., and Pedersen, P.B. (2022). Microbial communities in full-scale woodchip bioreactors treating aquaculture effluents. *Journal of Environmental Management* 301**,** 113852. doi: 10.1016/j.jenvman.2021.113852.

Addy, K., Gold, A.J., Christianson, L.E., David, M.B., Schipper, L.A., and Ratigan, N.A. (2016). Denitrifying Bioreactors for Nitrate Removal: A Meta-Analysis. *Journal of Environmental Quality* 45(3)**,** 873-881. doi: 10.2134/jeq2015.07.0399.

Ahmad, F., McGuire, T.M., Lee, R.S., and Becvar, E. (2007). Considerations for the Design of Organic Mulch Permeable Reactive Barriers. *Remediation-the Journal of Environmental Cleanup Costs Technologies & Techniques* 18(1)**,** 59-72. doi: 10.1002/rem.20151.

Amy, G., and Drewes, J. (2007). Soil Aquifer Treatment (SAT) as a Natural and Sustainable Wastewater Reclamation/Reuse Technology: Fate of Wastewater Effluent Organic Matter (EfOM) and Trace Organic Compounds. *Environmental Monitoring and Assessment* 129(1)**,** 19-26. doi: 10.1007/s10661-006-9421-4.

Andersen, J.H., Axe, P., Backer, H., Carstensen, J., Claussen, U., Fleming-Lehtinen, V., et al. (2011). Getting the measure of eutrophication in the Baltic Sea: towards improved assessment principles and methods. *Biogeochemistry* 106(2)**,** 137-156. doi: 10.1007/s10533-010-9508-4.

Andrus, J.M., Porter, M.D., Rodriguez, L.F., Kuehlhorn, T., Cooke, R.A., Zhang, Y., et al. (2014). Spatial variation in the bacterial and denitrifying bacterial community in a biofilter treating subsurface agricultural drainage. *Microb Ecol* 67(2)**,** 265-272. doi: 10.1007/s00248-013-0286-0.

Arauzo, M., Valladolid, M., García, G., and Andries, D.M. (2022). N and P behaviour in alluvial aquifers and in the soil solution of their catchment areas: How land use and the physical environment contribute to diffuse pollution. *Science of The Total Environment* 804**,** 150056. doi: https://doi.org/10.1016/j.scitotenv.2021.150056.

Audet, J., Jéglot, A., Elsgaard, L., Maagaard, A.L., Sørensen, S.R., Zak, D., et al. (2021). Nitrogen removal and nitrous oxide emissions from woodchip

bioreactors treating agricultural drainage waters. *Ecological Engineering* 169**,** 106328. doi: 10.1016/j.ecoleng.2021.106328.

Barbieri, M., Carrera, J., Sanchez-Vila, X., Ayora, C., Cama, J., Kock-Schulmeyer, M., et al. (2011). Microcosm experiments to control anaerobic redox conditions when studying the fate of organic micropollutants in aquifer material. *Journal of Contaminant Hydrology* 126(3-4)**,** 330-345. doi: 10.1016/j.jconhyd.2011.09.003.

Beganskas, S., Gorski, G., Weathers, T., Fisher, A.T., Schmidt, C., Saltikov, C., et al. (2018). A horizontal permeable reactive barrier stimulates nitrate removal and shifts microbial ecology during rapid infiltration for managed recharge. *Water Research* 144**,** 274-284. doi: 10.1016/j.watres.2018.07.039.

Bekele, E., Page, D., Vanderzalm, J., Kaksonen, A., and Gonzalez, D. (2018). Water Recycling via Aquifers for Sustainable Urban Water Quality Management: Current Status, Challenges and Opportunities. *Water* 10(4). doi: 10.3390/w10040457.

Bijay-Singh, and Craswell, E.T. (2021). Fertilizers and nitrate pollution of surface and ground water: an increasingly pervasive global problem. *SN Applied Sciences*. doi: 10.1007/s42452-021-04521-8

Bukin, Y.S., Galachyants, Y.P., Morozov, I.V., Bukin, S.V., Zakharenko, A.S., and Zemskaya, T.I. (2019). The effect of 16S rRNA region choice on bacterial community metabarcoding results. *Scientific Data* 6(1)**,** 190007. doi: 10.1038/sdata.2019.7.

Burgin, A.J., and Hamilton, S.K. (2007). Have we overemphasized the role of denitrification in aquatic ecosystems? A review of nitrate removal pathways. *Frontiers in Ecology and the Environment* 5(2)**,** 89-96. doi: 10.1890/1540-9295(2007)5[89:HWOTRO]2.0.CO;2.

Cameron, S.G., and Schipper, L.A. (2010). Nitrate removal and hydraulic performance of organic carbon for use in denitrification beds. *Ecological Engineering* 36(11)**,** 1588-1595. doi: 10.1016/j.ecoleng.2010.03.010.

Caranto, J.D., and Lancaster, K.M. (2017). Nitric oxide is an obligate bacterial nitrification intermediate produced by hydroxylamine oxidoreductase. *Proceedings of the National Academy of Sciences of the United States of America* 114(31)**,** 8217-8222. doi: 10.1073/pnas.1704504114.

Caranto, J.D., Vilbert, A.C., and Lancaster, K.M. (2016). Nitrosomonas europaea cytochrome P460 is a direct link between nitrification and nitrous oxide emission. *Proceedings of the National Academy of Sciences* 113(51)**,** 14704-14709. doi: 10.1073/pnas.1611051113.

Carlson, H.K., Lui, L.M., Price, M.N., Kazakov, A.E., Carr, A.V., Kuehl, J.V., et al. (2020). Selective carbon sources influence the end products of microbial nitrate respiration. *Isme Journal* 14(8)**,** 2034-2045. doi: 10.1038/s41396-020-0666-7.

Chen, J., and Strous, M. (2013). Denitrification and aerobic respiration, hybrid electron transport chains and co-evolution. *Biochimica et Biophysica Acta*

(BBA) - Bioenergetics 1827(2), 136-144. doi: 10.1016/j.bbabio.2012.10.002.

Christensen, P.B., Rysgaard, S., Sloth, N.P., Dalsgaard, T., and Schwaerter, S. (2000). Sediment mineralization, nutrient fluxes, denitrification and dissimilatory nitrate reduction to ammonium in an estuarine fjord with sea cage trout farms. *Aquatic Microbial Ecology* 21(1), 73-84.

Christianson, L., Hanly, J., Jha, N., Saggar, S., and Hedley, M. (2013a). "Denitrification bioreactor nitrous oxide emissions under fluctuating flow conditions", in: *2013 Kansas City, Missouri, July 21 - July 24, 2013.* (St. Joseph, MI: ASABE).

Christianson, L., Helmers, M., Bhandari, A., and Moorman, T. (2013b). Internal hydraulics of an agricultural drainage denitrification bioreactor. *Ecological Engineering* 52, 298-307. doi: 10.1016/j.ecoleng.2012.11.001.

Christianson, L.E., Cooke, R.A., Hay, C.H., Helmers, M.J., Feyereisen, G.W., Ranaivoson, A.Z., et al. (2021). Effectiveness of Denitrifying Bioreactors on Water Pollutant Reduction from Agricultural Areas. *Transactions of the ASABE* 64(2), 641-658. doi: 10.13031/trans.14011.

Christianson, L.E., Feyereisen, G.W., Hay, C., Tschirner, U.W., Kult, K., Wickramarathne, N.M., et al. (2020). Denitrifying Bioreactor Woodchip Recharge: Media Properties after Nine Years. *Transactions of the ASABE* 63(2), 407-416. doi: 10.13031/trans.13709.

Christianson, L.E., and Schipper, L.A. (2016). Moving Denitrifying Bioreactors beyond Proof of Concept: Introduction to the Special Section. *Journal of Environmental Quality* 45(3), 757-761. doi: 10.2134/jeq2016.01.0013.

Daims, H., Lebedeva, E.V., Pjevac, P., Han, P., Herbold, C., Albertsen, M., et al. (2015). Complete nitrification by Nitrospira bacteria. *Nature* 528(7583), 504-509. doi: 10.1038/nature16461.

Daims, H., Lücker, S., and Wagner, M. (2016). A New Perspective on Microbes Formerly Known as Nitrite-Oxidizing Bacteria. *Trends in Microbiology* 24(9), 699-712. doi: 10.1016/j.tim.2016.05.004.

Dalsgaard, T., Thamdrup, B., and Canfield, D.E. (2005). Anaerobic ammonium oxidation (anammox) in the marine environment. *Research in Microbiology* 156(4), 457-464. doi: 10.1016/j.resmic.2005.01.011.

David, M.B., Gentry, L.E., Cooke, R.A., and Herbstritt, S.M. (2016). Temperature and Substrate Control Woodchip Bioreactor Performance in Reducing Tile Nitrate Loads in East-Central Illinois. *Journal of Environmental Quality* 45(3), 822-829. doi: 10.2134/jeq2015.06.0296.

Davis, M.P., Martin, E.A., Moorman, T.B., Isenhart, T.M., and Soupir, M.L. (2019). Nitrous oxide and methane production from denitrifying woodchip bioreactors at three hydraulic residence times. *Journal of Environmental Management* 242, 290-297. doi: 10.1016/j.jenvman.2019.04.055.

Della Rocca, C., Belgiorno, V., and Meric, S. (2006). An heterotrophic/autotrophic denitrification (HAD) approach for nitrate removal from drinking water.

Process Biochemistry 41(5), 1022-1028. doi: 10.1016/j.procbio.2005.11.002.

Devol, A.H. (2015). Denitrification, Anammox, and N2 Production in Marine Sediments. *Annual Review of Marine Science* 7(1), 403-423. doi: 10.1146/annurev-marine-010213-135040.

Dietl, A., Ferousi, C., Maalcke, W.J., Menzel, A., de Vries, S., Keltjens, J.T., et al. (2015). The inner workings of the hydrazine synthase multiprotein complex. *Nature* 527(7578), 394-404. doi: 10.1038/nature15517.

EEA (2018). European Waters Assessment of status and pressures 2018. Report No 7/2018. (Luxemburg). doi: 10.2800/303664

EEA (2019). Nutrient enrichment and eutrophication in Europe's seas. Moving towards a healthy marine environment. Report No 14/2019. (Luxemburg). doi: 10.2800/092643

eea.europa.eu (2021). *Urban Wastewater Treatment in Europe* [Online]. Available: https://www.eea.europa.eu/data-and-maps/indicators/urban-waste-water-treatment/urban-waste-water-treatment-assessment-5 [Accessed 2022-07-11].

Einsle, O., Messerschmidt, A., Stach, P., Bourenkov, G.P., Bartunik, H.D., Huber, R., et al. (1999). Structure of cytochrome c nitrite reductase. *Nature* 400(6743), 476-480. doi: 10.1038/22802.

European Commission (1991). Council Directive of 21 May 1991 concerning urban waste water treatment. 91/271/EEC.

European Commission (2021). Report from the Commission to the Council and the European Parliament on the implementation of Council Directive 91/676/EEC concerning the protection of waters against pollution caused by nitrates from agricultural sources based on Member State reports for the period 2016–2019. (Brussels).

Feyereisen, G.W., Moorman, T.B., Christianson, L.E., Venterea, R.T., Coulter, J.A., and Tschirner, U.W. (2016). Performance of Agricultural Residue Media in Laboratory Denitrifying Bioreactors at Low Temperatures. *Journal of Environmental Quality* 45(3), 779-787. doi: 10.2134/jeq2015.07.0407.

Fowdar, H.S., Hatt, B.E., Breen, P., Cook, P.L.M., and Deletic, A. (2015). Evaluation of sustainable electron donors for nitrate removal in different water media. *Water Research* 85, 487-496. doi: 10.1016/j.watres.2015.08.052.

Fowler, S.J., Palomo, A., Dechesne, A., Mines, P.D., and Smets, B.F. (2018). Comammox Nitrospira are abundant ammonia oxidizers in diverse groundwater-fed rapid sand filter communities. *Environmental Microbiology* 20(3), 1002-1015. doi: 10.1111/1462-2920.14033.

Friedman, L., Mamane, H., Avisar, D., and Chandran, K. (2018). The role of influent organic carbon-to-nitrogen (COD/N) ratio in removal rates and shaping microbial ecology in soil aquifer treatment (SAT). *Water Research* 146, 197-205. doi: 10.1016/j.watres.2018.09.014.

Ghane, E., Feyereisen, G.W., Rosen, C.J., and Tschirner, U.W. (2018). Carbon Quality of Four-Year-Old Woodchips in a Denitrification Bed Treating Agricultural Drainage Water. *Transactions of the ASABE* 61(3)**,** 995-1000. doi: https://doi.org/10.13031/trans.12642.

Gharoon, N., and Pagilla, K.R. (2021). Critical review of effluent dissolved organic nitrogen removal by soil/aquifer-based treatment systems. *Chemosphere* 269. doi: 10.1016/j.chemosphere.2020.129406.

Giri, S. (2021). Water quality prospective in Twenty First Century: Status of water quality in major river basins, contemporary strategies and impediments: A review. *Environmental Pollution* 271**,** 116332. doi: 10.1016/j.envpol.2020.116332.

González-Cabaleiro, R., Ofiţeru, I.D., Lema, J.M., and Rodríguez, J. (2015). Microbial catabolic activities are naturally selected by metabolic energy harvest rate. *The ISME Journal* 9**,** 2630-2641. doi: 10.1038/ismej.2015.69.

Gorski, G., Dailey, H., Fisher, A.T., Schrad, N., and Saltikov, C. (2020). Denitrification during infiltration for managed aquifer recharge: Infiltration rate controls and microbial response. *Science of the Total Environment* 727. doi: 10.1016/j.scitotenv.2020.138642.

Graf, D.R.H., Jones, C.M., and Hallin, S. (2014). Intergenomic Comparisons Highlight Modularity of the Denitrification Pathway and Underpin the Importance of Community Structure for N2O Emissions. *Plos One* 9(12)**,** e114118. doi: 10.1371/journal.pone.0114118.

Grau-Martínez, A., Folch, A., Torrentó, C., Valhondo, C., Barba, C., Domènech, C., et al. (2018). Monitoring induced denitrification during managed aquifer recharge in an infiltration pond. *Journal of Hydrology* 561**,** 123-135. doi: 10.1016/j.jhydrol.2018.03.044.

Greenan, C.M., Moorman, T.B., Kaspar, T.C., Parkin, T.B., and Jaynes, D.B. (2006). Comparing carbon substrates for denitrification of subsurface drainage water. *Journal of Environmental Quality* 35(3)**,** 824-829. doi: 10.2134/jeq2005.0247

Greenan, C.M., Moorman, T.B., Parkin, T.B., Kaspar, T.C., and Jaynes, D.B. (2009). Denitrification in Wood Chip Bioreactors at Different Water Flows. *Journal of Environmental Quality* 38(4)**,** 1664-1671. doi: 10.2134/jeq2008.0413.

Grießmeier, V., Bremges, A., McHardy, A.C., and Gescher, J. (2017). Investigation of different nitrogen reduction routes and their key microbial players in wood chip-driven denitrification beds. *Scientific Reports* 7:17028(1). doi: 10.1038/s41598-017-17312-2.

Grießmeier, V., and Gescher, J. (2018). Influence of the Potential Carbon Sources for Field Denitrification Beds on Their Microbial Diversity and the Fate of Carbon and Nitrate. *Frontiers in Microbiology* 9:1313. doi: 10.3389/fmicb.2018.01313.

Grießmeier, V., Wienhöfer, J., Horn, H., and Gescher, J. (2021). Assessing and modeling biocatalysis in field denitrification beds reveals key influencing

factors for future constructions. *Water Research* 188**,** 116467. doi: 10.1016/j.watres.2020.116467.

Hallin, S., Philippot, L., Loffler, F.E., Sanford, R.A., and Jones, C.M. (2018). Genomics and Ecology of Novel N2O-Reducing Microorganisms. *Trends in Microbiology* 26(1)**,** 43-55. doi: 10.1016/j.tim.2017.07.003.

Hansson, K., Ejhed, H., Widén-Nilsson, E., Johnsson, H., Tengdelius Brunell, J., Gustavsson, H., Hytteborn, J. and Åkerblom, S. (2019). Näringsbelastningen på Östersjön och Västerhavet 2017. Sveriges underlag till Helcoms:s sjunde Pollution Load Compilation, Havs- och vattenmyndighetens rapport 2019:20. In Swedish.

Hardison, A.K., Algar, C.K., Giblin, A.E., and Rich, J.J. (2015). Influence of organic carbon and nitrate loading on partitioning between dissimilatory nitrate reduction to ammonium (DNRA) and N-2 production. *Geochimica Et Cosmochimica Acta* 164**,** 146-160. doi: 10.1016/j.gca.2015.04.049.

Hartfiel, L.M., Schaefer, A., Howe, A.C., and Soupir, M.L. (2022). Denitrifying bioreactor microbiome: Understanding pollution swapping and potential for improved performance. *Journal of Environmental Quality* 51(1)**,** 1-18. doi: 10.1002/jeq2.20302.

Hassanpour, B., Giri, S., Pluer, W.T., Steenhuis, T.S., and Geohring, L.D. (2017). Seasonal performance of denitrifying bioreactors in the Northeastern United States: Field trials. *Journal of Environmental Management* 202**,** 242-253. doi: 10.1016/j.jenvman.2017.06.054.

Hauck, M., Maalcke-Luesken, F.A., Jetten, M.S.M., and Huijbregts, M.A.J. (2016). Removing nitrogen from wastewater with side stream anammox: What are the trade-offs between environmental impacts? *Resources, Conservation & Recycling* 107(C)**,** 212-219. doi: 10.1016/j.resconrec.2015.

Healy, M.G., Ibrahim, T.G., Lanigan, G.J., Serrenho, A.J., and Fenton, O. (2012). Nitrate removal rate, efficiency and pollution swapping potential of different organic carbon media in laboratory denitrification bioreactors. *Ecological Engineering* 40**,** 198-209. doi: 10.1016/j.ecoleng.2011.12.010.

HELCOM (2009). Eutrophication in the Baltic Sea - an integrated thematic assessment of the effects of nutrient enrichment and eutrophication in the Baltic Sea Region, Baltic Sea Environmental Proceedings No 115B, Baltic Marine Environment Protection Commission, Helsinki, Finland. (Luxemburg).

HELCOM (2017). The integrated assessment of eutrophication - supplementary report to the first version of the 'State of the Baltic Sea' report 2017.

Henry, S., Baudoin, E., López-Gutiérrez, J.C., Martin-Laurent, F., Brauman, A., and Philippot, L. (2004). Quantification of denitrifying bacteria in soils by nirK gene targeted real-time PCR. *Journal of Microbiological Methods* 59(3)**,** 327-335. doi: 10.1016/j.mimet.2004.07.002.

Henry, S., Bru, D., Stres, B., Hallet, S., and Philippot, L. (2006). Quantitative detection of the nosZ gene, encoding nitrous oxide reductase, and comparison of the abundances of 16S rRNA, narG, nirK, and nosZ genes

in soils. *Applied and Environmental Microbiology* 72(8)**,** 5181-5189. doi: 10.1128/aem.00231-06.

Herrmann, M., Opitz, S., Harzer, R., Totsche, K.U., and Kusel, K. (2017). Attached and Suspended Denitrifier Communities in Pristine Limestone Aquifers Harbor High Fractions of Potential Autotrophs Oxidizing Reduced Iron and Sulfur Compounds. *Microbial Ecology* 74(2)**,** 264-277. doi: 10.1007/s00248-017-0950-x.

Hoover, N.L., Bhandari, A., Soupir, M.L., and Moorman, T.B. (2016). Woodchip Denitrification Bioreactors: Impact of Temperature and Hydraulic Retention Time on Nitrate Removal. *Journal of Environmental Quality* 45(3)**,** 803-812. doi: 10.2134/jeq2015.03.0161.

Idelovitch, E., and Michail, M. (1984). Soil-Aquifer Treatment: A New Approach to an Old Method of Wastewater Reuse. *Journal (Water Pollution Control Federation)* 56(8)**,** 936-943. http://www.jstor.org/stable/25042398

Jang, J., Anderson, E.L., Venterea, R.T., Sadowsky, M.J., Rosen, C.J., Feyereisen, G.W., et al. (2019). Denitrifying Bacteria Active in Woodchip Bioreactors at Low-Temperature Conditions. *Frontiers in Microbiology* 10. doi: 10.3389/fmicb.2019.00635.

Jéglot, A., Audet, J., Sørensen, S.R., Schnorr, K., Plauborg, F., and Elsgaard, L. (2021a). Microbiome Structure and Function in Woodchip Bioreactors for Nitrate Removal in Agricultural Drainage Water. *Frontiers in Microbiology* 12. doi: 10.3389/fmicb.2021.678448.

Jéglot, A., Miranda-Velez, J.F., Plauborg, F., and Elsgaard, L. (2022). Nitrate removal and environmental side-effects controlled by hydraulic residence time in woodchip bioreactors treating cold agricultural drainage water. *Environmental Technology***,** 1-10. doi: 10.1080/09593330.2022.2091482.

Jéglot, A., Sørensen, S.R., Schnorr, K.M., Plauborg, F., and Elsgaard, L. (2021b). Temperature Sensitivity and Composition of Nitrate-Reducing Microbiomes from a Full-Scale Woodchip Bioreactor Treating Agricultural Drainage Water. *Microorganisms* 9(6). doi: 10.3390/microorganisms9061331.

Jetten, M.S.M., Schmid, M., Schmidt, I., Wubben, M., van Dongen, U., Abma, W., et al. (2002). Improved nitrogen removal by application of new nitrogen-cycle bacteria. *Reviews in Environmental Science and Biotechnology* 1(1)**,** 51-63. doi: 10.1023/A:1015191724542.

Jones, C.M., Graf, D.R.H., Bru, D., Philippot, L., and Hallin, S. (2013). The unaccounted yet abundant nitrous oxide-reducing microbial community: a potential nitrous oxide sink. *Isme Journal* 7(2)**,** 417-426. doi: 10.1038/ismej.2012.125.

Kaewyai, J., Noophan, P., Lin, J.G., Munakata-Marr, J., and Figueroa, L.A. (2022). A comparison of nitrogen removal efficiencies and microbial communities between anammox and de-ammonification processes in lab-scale ASBR, and full-scale MBBR and IFAS plants. *International Biodeterioration & Biodegradation* 169. doi: 10.1016/j.ibiod.2022.105376.

Kamp, A., Hogslund, S., Risgaard-Petersen, N., and Stief, P. (2015). Nitrate Storage and Dissimilatory Nitrate Reduction by Eukaryotic Microbes. *Frontiers in Microbiology* 6:1492. doi: 10.3389/fmicb.2015.01492.

Kiani, S., Kujala, K., T. Pulkkinen, J., Aalto, S.L., Suurnäkki, S., Kiuru, T., et al. (2020). Enhanced nitrogen removal of low carbon wastewater in denitrification bioreactors by utilizing industrial waste toward circular economy. *Journal of Cleaner Production* 254**,** 119973. doi: https://doi.org/10.1016/j.jclepro.2020.119973.

Kraft, B., Tegetmeyer, H.E., Sharma, R., Klotz, M.G., Ferdelman, T.G., Hettich, R.L., et al. (2014). The environmental controls that govern the end product of bacterial nitrate respiration. *Science* 345(6197)**,** 676-679. doi: 10.1126/science.1254070.

Kumaraswamy, R., Sjollema, K., Kuenen, G., van Loosdrecht, M., and Muyzer, G. (2006). Nitrate-dependent Fe(II)EDTA (2-) oxidation by Paracoccus ferrooxidans sp nov., isolated from a denitrifying bioreactor. *Systematic and Applied Microbiology* 29(4)**,** 276-286. doi: 10.1016/j.syapm.2005.08.001.

Kuypers, M.M.M., Marchant, H.K., and Kartal, B. (2018). The microbial nitrogen-cycling network. *Nature Reviews Microbiology* 16(5)**,** 263-276. doi: 10.1038/nrmicro.2018.9.

Lapébie, P., Lombard, V., Drula, E., Terrapon, N., and Henrissat, B. (2019). Bacteroidetes use thousands of enzyme combinations to break down glycans. *Nature Communications* 10(1)**,** 2043. doi: 10.1038/s41467-019-10068-5.

Lawrence, N.C., Tenesaca, C.G., VanLoocke, A., and Hall, S.J. (2021). Nitrous oxide emissions from agricultural soils challenge climate sustainability in the US Corn Belt. *Proceedings of the National Academy of Sciences* 118(46)**,** e2112108118. doi: doi:10.1073/pnas.2112108118.

Lehtovirta-Morley, L.E. (2018). Ammonia oxidation: Ecology, physiology, biochemistry and why they must all come together. *FEMS Microbiology Letters* 365(9). doi: 10.1093/femsle/fny058.

Lepine, C., Christianson, L., Sharrer, K., and Summerfelt, S. (2016). Optimizing Hydraulic Retention Times in Denitrifying Woodchip Bioreactors Treating Recirculating Aquaculture System Wastewater. *Journal of Environmental Quality* 45(3)**,** 813-821. doi:10.2134/jeq2015.05.0242.

Lepine, C., Christianson, L., Soucek, D., McIsaac, G., and Summerfelt, S. (2021). Metal leaching and toxicity of denitrifying woodchip bioreactor outflow?Potential reuse application. *Aquacultural Engineering* 93. doi: 10.1016/j.aquaeng.2020.102129.

Long, L.M., Schipper, L.A., and Bruesewitz, D.A. (2011). Long-term nitrate removal in a denitrification wall. *Agriculture Ecosystems & Environment* 140(3-4)**,** 514-520. doi: 10.1016/j.agee.2011.02.005.

Loos, R., Carvalho, R., António, D.C., Comero, S., Locoro, G., Tavazzi, S., et al. (2013). EU-wide monitoring survey on emerging polar organic

contaminants in wastewater treatment plant effluents. *Water Research* 47(17), 6475-6487. doi: 10.1016/j.watres.2013.08.024.

Lopez-Ponnada, E.V., Lynn, T.J., Peterson, M., Ergas, S.J., and Mihelcic, J.R. (2017). Application of denitrifying wood chip bioreactors for management of residential non-point sources of nitrogen. *J Biol Eng* 11, 16. doi: 10.1186/s13036-017-0057-4.

Lynn, T.J., Yeh, D.H., and Ergas, S.J. (2015a). Performance and Longevity of Denitrifying Wood-Chip Biofilters for Stormwater Treatment: A Microcosm Study. *Environmental Engineering Science* 32(4), 321-330. doi: 10.1089/ees.2014.0358.

Lynn, T.J., Yeh, D.H., and Ergas, S.J. (2015b). Performance of Denitrifying Stormwater Biofilters Under Intermittent Conditions. *Environmental Engineering Science* 32(9), 796-805. doi: 10.1089/ees.2015.0135.

Maalcke, W.J., Reimann, J., de Vries, S., Butt, J.N., Dietl, A., Kip, N., et al. (2016). Characterization of Anammox Hydrazine Dehydrogenase, a Key N-2-producing Enzyme in the Global Nitrogen Cycle. *Journal of Biological Chemistry* 291(33), 17077-17092. doi: 10.1074/jbc.M116.735530.

Maeda, K., Spor, A., Edel-Hermann, V., Heraud, C., Breuil, M.-C., Bizouard, F., et al. (2015). N2O production, a widespread trait in fungi. *Scientific Reports* 5:9697. doi: 10.1038/srep09697

Malone, T.C., and Newton, A. (2020). The Globalization of Cultural Eutrophication in the Coastal Ocean: Causes and Consequences. *Frontiers in Marine Science* 7. doi: 10.3389/fmars.2020.00670.

Manca, F., De Rosa, D., Reading, L.P., Rowlings, D.W., Scheer, C., Layden, I., et al. (2020). Nitrate removal and greenhouse gas production of woodchip denitrification walls under a humid subtropical climate. *Ecological Engineering* 156, 105988. doi: 10.1016/j.ecoleng.2020.105988.

Manca, F., De Rosa, D., Reading, L.P., Rowlings, D.W., Scheer, C., Schipper, L.A., et al. (2021). Effect of soil cap and nitrate inflow on nitrous oxide emissions from woodchip bioreactors. *Ecological Engineering* 166, 106235. doi: 10.1016/j.ecoleng.2021.106235.

Martin, E.A., Davis, M.P., Moorman, T.B., Isenhart, T.M., and Soupir, M.L. (2019). Impact of hydraulic residence time on nitrate removal in pilot-scale woodchip bioreactors. *Journal of Environmental Management* 237, 424-432. doi: 10.1016/j.jenvman.2019.01.025.

Maxwell, B., Christianson, L., Cooke, R.A.C., Foltz, M., Wickramarathne, N., Chacon, R., et al. (2022). Nitrate Removal and Woodchip Properties across a Paired Denitrifying Bioreactor Treating Centralized Agricultural Ditch Flows. *Water* 14(1). doi: 10.3390/w14010056.

Maxwell, B.M., Díaz-García, C., Martínez-Sánchez, J.J., Birgand, F., and Álvarez-Rogel, J. (2020). Temperature sensitivity of nitrate removal in woodchip bioreactors increases with woodchip age and following drying–rewetting cycles. *Environmental Science: Water Research & Technology* 6(10), 2752-2765. doi: 10.1039/D0EW00507J.

McGuire, P.M., Dai, V.T., Walter, M.T., and Reid, M.C. (2021). Labile carbon release from oxic-anoxic cycling in woodchip bioreactors enhances nitrate removal without increasing nitrous oxide accumulation. *Environmental Science-Water Research & Technology* 7(12), 2357-2371. doi: 10.1039/d1ew00446h.

Mienis, O., and Arye, G. (2018). Long-term nitrogen behavior under treated wastewater infiltration basins in a soil-aquifer treatment (SAT) system. *Water Research* 134, 192-199. doi: 10.1016/j.watres.2018.01.069.

Modrzyński, J.J., Aamand, J., Wittorf, L., Badawi, N., Hubalek, V., Canelles, A., et al. (2021). Combined removal of organic micropollutants and ammonium in reactive barriers developed for managed aquifer recharge. *Water Research* 190. doi: 10.1016/j.watres.2020.116669.

Mohan, S.B., Schmid, M., Jetten, M., and Cole, J. (2004). Detection and widespread distribution of the nrfA gene encoding nitrite reduction to ammonia, a short circuit in the biological nitrogen cycle that competes with denitrification. *Fems Microbiology Ecology* 49(3), 433-443. doi: 10.1016/j.femsec.2004.04.012.

Moorman, T.B., Parkin, T.B., Kaspar, T.C., and Jaynes, D.B. (2010). Denitrification activity, wood loss, and N2O emissions over 9 years from a wood chip bioreactor. *Ecological Engineering* 36(11), 1567-1574. doi: 10.1016/j.ecoleng.2010.03.012.

Mulder, A., Vandegraaf, A.A., Robertson, L.A., and Kuenen, J.G. (1995). Anaerobic Ammonium Oxidation Discovered in a Denitrifying Fluidized-Bed Reactor. *FEMS Microbiology Ecology* 16(3), 177-183. doi: 10.1111/j.1574-6941.1995.tb00281.x.

Murphy, C.L., Biggerstaff, J., Eichhorn, A., Ewing, E., Shahan, R., Soriano, D., et al. (2021). Genomic characterization of three novel Desulfobacterota classes expand the metabolic and phylogenetic diversity of the phylum. *Environmental Microbiology* 23(8), 4326-4343. doi: 10.1111/1462-2920.15614.

Nilsson, L., and Widerlund, A. (2017). Tracing nitrogen cycling in mining waters using stable nitrogen isotope analysis. *Applied Geochemistry* 84, 41-51. doi: 10.1016/j.apgeochem.2017.05.025.

Nordström, A., and Herbert, R.B. (2017). Denitrification in a low-temperature bioreactor system at two different hydraulic residence times: laboratory column studies. *Environmental Technology* 38(11), 1362-1375. doi: 10.1080/09593330.2016.1228699.

Nordström, A., and Herbert, R.B. (2018). Determination of major biogeochemical processes in a denitrifying woodchip bioreactor for treating mine drainage. *Ecological Engineering* 110, 54-66. doi: 10.1016/j.ecoleng.2017.09.018.

Nordström, A., and Herbert, R.B. (2019). Identification of the temporal control on nitrate removal rate variability in a denitrifying woodchip bioreactor. *Ecological Engineering* 127, 88-95. doi: 10.1016/j.ecoleng.2018.11.015.

olc.worldbank.org *Earth's Water* [Online]. Available: https://olc.worldbank.org/sites/default/files/sco/E7B1C4DE-C187-5EDB-3EF2-897802DEA3BF/Nasa/chapter1.html [Accessed 2022-05-09].

Pan, Y., Ni, B.-J., Bond, P.L., Ye, L., and Yuan, Z. (2013). Electron competition among nitrogen oxides reduction during methanol-utilizing denitrification in wastewater treatment. *Water Research* 47(10)**,** 3273-3281. doi: 10.1016/j.watres.2013.02.054.

Pang, Y., and Wang, J. (2021). Various electron donors for biological nitrate removal: A review. *Science of The Total Environment* 794**,** 148699. doi: 10.1016/j.scitotenv.2021.148699.

Pensky, J., Fisher, A.T., Gorski, G., Schrad, N., Dailey, H., Beganskas, S., et al. (2022). Enhanced cycling of nitrogen and metals during rapid infiltration: Implications for managed recharge. *Science of The Total Environment* 838**,** 156439. doi: 10.1016/j.scitotenv.2022.156439.

Petrie, B., Barden, R., and Kasprzyk-Hordern, B. (2015). A review on emerging contaminants in wastewaters and the environment: Current knowledge, understudied areas and recommendations for future monitoring. *Water Research* 72**,** 3-27. doi: 10.1016/j.watres.2014.08.053.

Philippot, L., Hallin, S., and Schloter, M. (2007). "Ecology of denitrifying prokaryotes in agricultural soil," in *Advances in Agronomy, Vol 96,* ed. D.L. Sparks.), 249-305.

Pluer, W.T., Morris, C.K., Walter, M.T., and Geohring, L.D. (2019). Denitrifying bioreactor response during storm events. *Agricultural Water Management* 213**,** 1109-1115. doi: 10.1016/j.agwat.2018.12.004.

Porter, M.D., Andrus, J.M., Bartolerio, N.A., Rodriguez, L.F., Zhang, Y., Zilles, J.L., et al. (2015). Seasonal Patterns in Microbial Community Composition in Denitrifying Bioreactors Treating Subsurface Agricultural Drainage. *Microbial Ecology* 70(3)**,** 710-723. doi: 10.1007/s00248-015-0605-8.

Preisner, M., Neverova-Dziopak, E., and Kowalewski, Z. (2021). Mitigation of eutrophication caused by wastewater discharge: A simulation-based approach. *Ambio* 50(2)**,** 413-424. doi: 10.1007/s13280-020-01346-4.

Putz, M., Schleusner, P., Rütting, T., and Hallin, S. (2018). Relative abundance of denitrifying and DNRA bacteria and their activity determine nitrogen retention or loss in agricultural soil. *Soil Biology & Biochemistry* 123**,** 97-104. doi: 10.1016/j.soilbio.2018.05.006.

Quanrud, D.M., Hafer, J., Karpiscak, M.M., Zhang, H.M., Lansey, K.E., and Arnold, R.G. (2003). Fate of organics during soil-aquifer treatment: sustainability of removals in the field. *Water Research* 37(14)**,** 3401-3411. doi: 10.1016/s0043-1354(02)00489-x.

Rambags, F., Tanner, C.C., and Schipper, L.A. (2019). Denitrification and anammox remove nitrogen in denitrifying bioreactors. *Ecological Engineering* 138**,** 38-45. doi: https://doi.org/10.1016/j.ecoleng.2019.06.022.

Risgaard-Petersen, N., Langezaal, A.M., Ingvardsen, S., Schmid, M.C., Jetten, M.S.M., Op den Camp, H.J.M., et al. (2006). Evidence for complete

denitrification in a benthic foraminifer. *Nature* 443**,** 93. doi: 10.1038/nature05070

Rivas, A., Barkle, G., Stenger, R., Moorhead, B., and Clague, J. (2020). Nitrate removal and secondary effects of a woodchip bioreactor for the treatment of subsurface drainage with dynamic flows under pastoral agriculture. *Ecological Engineering* 148**,** 105786. doi: https://doi.org/10.1016/j.ecoleng.2020.105786.

Robertson, W.D., and Cherry, J.A. (1995). In-Situ Denitrification of Septic-System Nitrate Using Reactive Porous-Media Barriers - Field Trials *Ground Water* 33(1)**,** 99-111. doi: 10.1111/j.1745-6584.1995.tb00266.x.

Robertson, W.D., Ptacek, C.J., and Brown, S.J. (2009). Rates of Nitrate and Perchlorate Removal in a 5-Year-Old Wood Particle Reactor Treating Agricultural Drainage. *Ground Water Monitoring and Remediation* 29(2)**,** 87-94. doi: 10.1111/j.1745-6592.2009.01231.x.

Robertson, W.D., Vogan, J.L., and Lombardo, P.S. (2008). Nitrate removal rates in a 15-year-old permeable reactive barrier treating septic system nitrate. *Ground Water Monitoring and Remediation* 28(3)**,** 65-72. doi: 10.1111/j.1745-6592.2008.00205.x.

Rotthauwe, J.H., Witzel, K.P., and Liesack, W. (1997). The ammonia monooxygenase structural gene amoA as a functional marker: Molecular fine-scale analysis of natural ammonia-oxidizing populations. *Applied and Environmental Microbiology* 63(12)**,** 4704-4712. doi: 10.1128/aem.63.12.4704-4712.1997.

Schaefer, A., Lee, J., Soupir, M.L., Moorman, T.B., and Howe, A. (2022). Comparison of microbial communities in replicated woodchip bioreactors. *Journal of Environmental Quality* 51(2)**,** 205-215. doi: 10.1002/jeq2.20320.

Schaefer, A., Werning, K., Hoover, N., Tschirner, U., Feyereisen, G., Moorman, T.B., et al. (2021). Impact of flow on woodchip properties and subsidence in denitrifying bioreactors. *Agrosystems Geosciences & Environment* 4(1). doi: 10.1002/agg2.20149.

Schaffer, M., Kröger, K.F., Nödler, K., Ayora, C., Carrera, J., Hernández, M., et al. (2015). Influence of a compost layer on the attenuation of 28 selected organic micropollutants under realistic soil aquifer treatment conditions: Insights from a large scale column experiment. *Water Research* 74**,** 110-121. doi: 10.1016/j.watres.2015.02.010.

Schipper, L.A., Robertson, W.D., Gold, A.J., Jaynes, D.B., and Cameron, S.C. (2010). Denitrifying bioreactors-An approach for reducing nitrate loads to receiving waters. *Ecological Engineering* 36(11)**,** 1532-1543. doi: 10.1016/j.ecoleng.2010.04.008.

Schipper, L.A., and Vojvodic-Vukovic, M. (2001). Five years of nitrate removal, denitrification and carbon dynamics in a denitrification wall. *Water Research* 35(14)**,** 3473-3477. doi: 10.1016/s0043-1354(01)00052-5.

Schmid, M.C., Hooper, A.B., Klotz, M.G., Woebken, D., Lam, P., Kuypers, M.M.M., et al. (2008). Environmental detection of octahaem cytochrome c hydroxylamine/hydrazine oxidoreductase genes of aerobic and anaerobic ammonium-oxidizing bacteria. *Environmental Microbiology* 10(11)**,** 3140-3149. doi: 10.1111/j.1462-2920.2008.01732.x.

Schmidt, C.A., and Clark, M.W. (2013). Deciphering and modeling the physicochemical drivers of denitrification rates in bioreactors. *Ecological Engineering* 60**,** 276-288. doi: 10.1016/j.ecoleng.2013.07.041.

Shapleigh, J.P. (2013). "Denitrifying Prokaryotes," in *The Prokaryotes: Prokaryotic Physiology and Biochemistry,* eds. E. Rosenberg, E.F. DeLong, S. Lory, E. Stackebrandt & F. Thompson. (Berlin, Heidelberg: Springer Berlin Heidelberg), 405-425.

Sharma, S.K., and Kennedy, M.D. (2017). Soil aquifer treatment for wastewater treatment and reuse. *International Biodeterioration & Biodegradation* 119**,** 671-677. doi: 10.1016/j.ibiod.2016.09.013.

Shoun, H., Kim, D.H., Uchiyama, H., and Sugiyama, J. (1992). Denitrification by Fungi. *FEMS Microbiology Letters* 94(3)**,** 277-281. doi: 10.1111/j.1574-6968.1992.tb05331.x.

Silver, M., Knöller, K., Schlögl, J., Kübeck, C., and Schüth, C. (2018). Nitrogen cycling and origin of ammonium during infiltration of treated wastewater for managed aquifer recharge. *Applied Geochemistry* 97**,** 71-80. doi: 10.1016/j.apgeochem.2018.08.003.

Song, B., Lisa, J.A., and Tobias, C.R. (2014). Linking DNRA community structure and activity in a shallow lagoonal estuarine system. *Frontiers in Microbiology* 5:460. doi: 10.3389/fmicb.2014.00460.

Sopilniak, A., Elkayam, R., and Lev, O. (2017). Nitrification in a soil-aquifer treatment system: comparison of potential nitrification and concentration profiles in the vadose zone. *Environmental Science: Processes & Impacts* 19(12)**,** 1571-1582. doi: 10.1039/C7EM00402H.

Suzuki, R., Kameda, I., Takabe, Y., Nishimura, F., and Itoh, S. (2015). Removal of Dissolved Organic Matter and Disinfection By-products Formation Potential in the Upper Layer during Soil Aquifer Treatment. *Journal of Water and Environment Technology* 13(2)**,** 107-118. doi: 10.2965/jwet.2015.107.

Tao, J.Q., Zhang, Y., Zhang, T., You, Z.Y., Shah, K.J., and Kim, H. (2022). Application of Reeds as Carbon Source for Enhancing Denitrification of Low C/N Micro-Polluted Water in Vertical-Flow Constructed Wetland. *Applied Sciences-Basel* 12(13). doi: 10.3390/app12136756.

Ternes, T. (2007). The occurrence of micopollutants in the aquatic environment: a new challenge for water management. *Water Science and Technology* 55(12)**,** 327-332. doi: 10.2166/wst.2007.428.

Throbäck, I.N., Enwall, K., Jarvis, A., and Hallin, S. (2004). Reassessing PCR primers targeting nirS, nirK and nosZ genes for community surveys of

denitrifying bacteria with DGGE. *Fems Microbiology Ecology* 49(3)**,** 401-417. doi: 10.1016/j.femsec.2004.04.011.

Tilman, D., Balzer, C., Hill, J., and Befort, B.L. (2011). Global food demand and the sustainable intensification of agriculture. *Proceedings of the National Academy of Sciences* 108(50)**,** 20260-20264. doi: 10.1073/pnas.1116437108.

Tsushima, I., Kindaichi, T., and Okabe, S. (2007). Quantification of anaerobic ammonium-oxidizing bacteria in enrichment cultures by real-time PCR. *Water Research* 41(4)**,** 785-794. doi: 10.1016/j.watres.2006.11.024.

United Nations (2019). Department of Economic and Social Affairs Population Division (2019), World Urbanization Prospects: The 2018 Revision (ST/ESA/SER.A/420). New York: United Nations.

United Nations (2021). The United Nations World Water Development Report 2021: Valuing Water. Paris: UNESCO.

United Nations (2022a). Department of Economic and Social Affairs, Population Division (2022). World Population Prospects 2022: Summary of Results. UN DESA/POP/2022/TR/NO.3.

United Nations (2022b). The United Nations World Water Development Report 2022: Groundwater: Making the invisible visible. Paris: UNESCO.

UN-Water 2021: Summary Progress Update 2021 - SDG 6 - water and sanitation for all. Version: July 2021. Geneva, Switzerland.

USDA (2015). Conservation practice standard: Denitrifying bioreactor, code 605. United States Department of Agriculture.

USDA (2020). Conservation practice standard: Denitrifying bioreactor, code 605. United States Department of Agriculture.

Valhondo, C., Carrera, J., Martínez-Landa, L., Wang, J.J., Amalfitano, S., Levantesi, C., et al. (2020a). Reactive Barriers for Renaturalization of Reclaimed Water during Soil Aquifer Treatment. *Water* 12(4). doi: 10.3390/w12041012.

Valhondo, C., Martínez-Landa, L., Carrera, J., Díaz-Cruz, S.M., Amalfitano, S., and Levantesi, C. (2020b). Six artificial recharge pilot replicates to gain insight into water quality enhancement processes. *Chemosphere* 240**,** 124826. doi: 10.1016/j.chemosphere.2019.124826.

van den Berg, E.M., Elisário, M.P., Kuenen, J.G., Kleerebezem, R., and van Loosdrecht, M.C.M. (2017). Fermentative bacteria influence the competition between denitrifiers and DNRA bacteria. *Frontiers in microbiology* 8**,** 1684-1684. doi: 10.3389/fmicb.2017.01684.

von Ahnen, M., Aalto, S.L., Suurnakki, S., Tiirola, M., and Pedersen, P.B. (2019). Salinity affects nitrate removal and microbial composition of denitrifying woodchip bioreactors treating recirculating aquaculture system effluents. *Aquaculture* 504**,** 182-189. doi: 10.1016/j.aquaculture.2019.01.068.

von Ahnen, M., Pedersen, P.B., and Dalsgaard, J. (2018). Performance of full-scale woodchip bioreactors treating effluents from commercial RAS.

Aquacultural Engineering 83**,** 130-137. doi: https://doi.org/10.1016/j.aquaeng.2018.10.004.

Ward, L.M., Bertran, E., and Johnston, D.T. (2021). Expanded Genomic Sampling Refines Current Understanding of the Distribution and Evolution of Sulfur Metabolisms in the Desulfobulbales. *Frontiers in Microbiology* 12. doi: 10.3389/fmicb.2021.666052.

Warneke, S., Schipper, L.A., Bruesewitz, D.A., McDonald, I., and Cameron, S. (2011a). Rates, controls and potential adverse effects of nitrate removal in a denitrification bed. *Ecological Engineering* 37(3)**,** 511-522. doi: 10.1016/j.ecoleng.2010.12.006.

Warneke, S., Schipper, L.A., Matiasek, M.G., Scow, K.M., Cameron, S., Bruesewitz, D.A., et al. (2011b). Nitrate removal, communities of denitrifiers and adverse effects in different carbon substrates for use in denitrification beds. *Water Research* 45(17)**,** 5463-5475. doi: 10.1016/j.watres.2011.08.007.

Welsh, A., Chee-Sanford, J.C., Connor, L.M., Löffler, F.E., and Sanford, R.A. (2014). Refined NrfA Phylogeny Improves PCR-Based nrfA Gene Detection. *Applied and Environmental Microbiology* 80(7)**,** 2110-2119. doi: 10.1128/aem.03443-13.

Weralupitiya, C., Wanigatunge, R., Joseph, S., Athapattu, B.C.L., Lee, T.-H., Kumar Biswas, J., et al. (2021). Anammox bacteria in treating ammonium rich wastewater: Recent perspective and appraisal. *Bioresource Technology* 334**,** 125240. doi:10.1016/j.biortech.2021.125240.

Wittorf, L., Bonilla-Rosso, G., Jones, C.M., Bäckman, O., Hulth, S. and Hallin, S. (2016). Habitat partitioning of marine benthic denitrifier communities in response to oxygen availability. *Environmental Microbiology Reports*, 8:486-492. doi: 10.1111/1758-2229.12393

Woehle, C., Roy, A.-S., Glock, N., Wein, T., Weissenbach, J., Rosenstiel, P., et al. (2018). A Novel Eukaryotic Denitrification Pathway in Foraminifera. *Current Biology* 28(16)**,** 2536-2543.e2535. doi: 10.1016/j.cub.2018.06.027.

Wu, H.N., Bertilsson, S., Zhang, W.L., Li, Y., Hui, C.Z., Wang, H.L., et al. (2021). Integrating experiments with system-level biogeochemical modeling to understand nitrogen cycling of reservoir sediments at elevated hydrostatic pressure. *Environmental Research* 200. doi: 10.1016/j.envres.2021.111671.

Xing, W., Li, J.L., Li, D.S., Hu, J.C., Deng, S.H., Cui, Y.W., et al. (2018). Stable-Isotope Probing Reveals the Activity and Function of Autotrophic and Heterotrophic Denitrifiers in Nitrate Removal from Organic-Limited Wastewater. *Environmental Science & Technology* 52(14)**,** 7867-7875. doi: 10.1021/acs.est.8b01993.

Xu, H., Sheng, R., Xing, X., Zhang, W., Hou, H., Liu, Y., et al. (2019). Characterization of Fungal nirK-Containing Communities and N2O

Emission From Fungal Denitrification in Arable Soils. *Frontiers in Microbiology* 10. doi: 10.3389/fmicb.2019.00117.

Yang, Y.C., Li, M., Li, H., Li, X.Y., Lin, J.G., Denecke, M., et al. (2020). Specific and effective detection of anammox bacteria using PCR primers targeting the 16S rRNA gene and functional genes. *Science of the Total Environment* 734. doi: 10.1016/j.scitotenv.2020.139387.

Zhong, H., Cheng, Y., Ahmad, Z., Shao, Y., Zhang, H., Lu, Q., et al. (2020). Solid-phase denitrification for water remediation: processes, limitations, and new aspects. *Critical Reviews in Biotechnology* 40(8)**,** 1113-1130. doi: 10.1080/07388551.2020.1805720.

Zumft, W.G. (1997). Cell biology and molecular basis of denitrification. *Microbiology and Molecular Biology Reviews* 61(4)**,** 533-616.

Popular science summary

Water is a precious resource that we must protect. While it is true that more than 70 % of Earth's surface is covered by water, much of this is salt water and therefore not directly usable by humans, and most of the freshwater that exists is largely locked up in glaciers or otherwise inaccessible. This means that the amount of water we have access to is limited. For our water use to be sustainable in the long term, we need to introduce measures to increase access to water but also to reduce emissions of environmentally harmful substances.

The element nitrogen is essential for life, but in excess it can be an environmental problem and a threat to human health. Different forms of nitrogen derived from human activities cause eutrophication, algal blooms and lack of oxygen in lakes and seas; the Baltic Sea, for example, is one of the world's most eutrophicated seas. The largest emission source of nitrogen, from both Sweden and other countries around the Baltic Sea, is agriculture, followed by emissions from sewage treatment plants. Some industries also contribute to nitrogen emissions, for example the mining industry where the nitrogen comes from the use of nitrogen-based explosives. Another serious consequence of nitrogen emissions is contamination of groundwater, which is an important source of drinking water. High levels of the nitrogen compound nitrate in drinking water can be a health hazard, especially for young children, and in many parts of the world the levels of nitrate in groundwater are dangerously high.

Nitrate-contaminated water can be purified by passing the water through a so-called denitrifying bioreactor. These reactors are used in many countries to reduce the input of nitrate into the environment from various sources, such as runoff from agricultural land. This technique is relatively simple and does not require a lot of resources. The water is passed through a permeable barrier

consisting of a carbon-rich material, for example woodchips or other plant-based substances, and microorganisms in the bioreactor remove the nitrate by converting it into gaseous forms of nitrogen, optimally nitrogen gas. However, microbial transformation of nitrate can proceed through different reaction paths, and not all end with harmless nitrogen gas. One path may result in the formation of the greenhouse gas nitrous oxide, whereas the other does not remove the nitrogen from water but rather converts it into ammonium, which can also damage the environment.

This thesis investigated whether the technology of denitrifying bioreactors is also suitable for nitrate-containing water from the mining industry. The work in the thesis also analysed which of the nitrogen-converting processes takes place in the barriers, as well as their timing and location in the reactors. The results showed that woodchip denitrifying bioreactors are well suited for purifying nitrate-contaminated mine water. There were also clear patterns of which nitrogen transformations were dominant, both in time and space. The performance of the reactors was related to the extent in which different nitrate transformation processes dominated, which ultimately determined whether the nitrate was removed or converted to an unwanted nitrogen compound. The type of carbonaceous material used in the bioreactor turned out to be important for determining which microorganisms established themselves, and thus also for which processes became dominant. Similar results were also obtained in a project that analysed permeable barriers intended for use in the recharge of aquifers to increase the availability of groundwater. The type of carbonaceous material again determined which microbial communities were established and which nitrogen-transforming processes took place. The results also showed the difficulties of designing barriers aiming at removing different types of chemical compounds; these barriers had no major effect on nitrogen but worked well for other pollutants.

To design future denitrifying bioreactors so that they function with high nitrogen removal efficiency and without the production of harmful compounds, it is important to have knowledge of how the development of the microbial community in a bioreactor is affected by various factors. This thesis contributes to that knowledge. Continued research should investigate more closely how different types of carbonaceous material can be used to control the composition of the microbial community in the bioreactor. Since denitrifying bioreactors can be used for multiple applications, the conditions

for introducing this technique should be examined as a means to mitigate nitrate pollution into the Baltic Sea.

Populärvetenskaplig sammanfattning

Vatten är en dyrbar resurs som vi måste värna. Visserligen är mer än 70 % av jordens yta täckt av vatten, men saltvatten är inte direkt användbart för oss och det sötvatten som finns är till stor del bundet i glaciärer eller på annat vis otillgängligt. Det gör att den mängd vatten vi har tillgång till är begränsad. För att vår vattenanvändning ska vara långsiktigt hållbar behöver vi införa åtgärder för att öka tillgången till vatten men också för att minska utsläppen av miljöskadliga ämnen.

Grundämnet kväve är livsnödvändigt men för mycket kväve kan vara ett miljöproblem och ett hot mot människors hälsa. Olika former av kväve som härrör från mänskliga aktiviteter orsakar övergödning, algblomning och syrebrist i sjöar och hav, Östersjön är till exempel ett av världens mest övergödda hav. Den största utsläppskällan av kväve, från både Sverige och övriga länder runt Östersjön, är jordbruk, följt av utsläpp från avloppsreningsverk. En del industrier bidrar också till utsläppen, till exempel gruvindustrin, där kvävet kommer från användningen av kvävebaserade sprängämnen. En annan allvarlig följd av kväveutsläpp är att grundvattnet, som är en viktig källa till dricksvatten, blir förorenat. Höga halter av kväveföreningen nitrat i dricksvattnet kan vara en hälsofarliga, speciellt för små barn och i många delar av världen är nivåerna av nitrat i grundvattnet hälsofarligt höga.

Nitratförorenat vatten kan renas genom att vattnet leds genom en så kallad denitrifierande bioreaktor. De används i många länder för att minska nitratutsläppen till miljön, till exempel i avrinningsvatten från åkermark. Tekniken är relativt enkel och kräver inte så mycket resurser. Vattnet leds genom en genomsläpplig barriär bestående av ett kolrikt material, till exempel träflis eller annat växtbaserat material, och mikroorganismer i bioreaktorn tar bort nitratet genom att omvandla det till gasformiga

kväveföreningar, mest gynnsamt till kvävgas. Men inte alla mikrobiella omvandlingar av nitrat leder till ofarlig kvävgas, nitratet kan även följa andra reaktionsvägar. En av dessa kan sluta med att växthusgasen lustgas bildas, och en annan avlägsnar inte kvävet ur vattnet utan omvandlar nitratet till ammonium, som också orsakar skador på miljön.

Den här avhandlingen undersökte om tekniken med denitrifierande bioreaktorer också är lämplig för nitrathaltigt vatten från gruvindustrin. Arbeten i avhandlingen har även analyserat vilka av de kväveomvandlande processerna som ägde rum i barriärerna, samt när och var de försiggick. Resultaten visade att denitrifierande bioreaktorer med träflis fungerar bra för att rena gruvvatten. Det fanns också tydliga mönster av vilka kväveomvandlingar som var dominerande, både i tid och rum. Bioreaktorernas prestanda, om nitratet avlägsnades eller omvandlades till oönskade kväveföreningar, var relaterat till proportionerna mellan de olika kväveomvandlande processerna. Vilket kolhaltigt material som användes i bioreaktorn visade sig vara viktigt för vilka mikroorganismer som etablerade sig, och därmed också för vilka processer som blev dominerande. Liknande resultat erhölls också i ett projekt som analyserade genomsläppliga barriärer avsedda att användas vid påfyllning av underjordiska vattenmagasin för att öka tillgången på grundvatten. Även här avgjorde typen av kolhaltigt material vilka mikrobsamhällen som etablerades och vilka kväveomvandlande processer som ägde rum. Resultaten visade också på svårigheterna med att designa barriärer med många funktioner; dessa barriärer hade ingen större effekt på kvävet, men fungerade bra för andra föroreningar.

För att designa framtida denitrifierande bioreaktorer så de fungerar med hög kväverenande effektivitet och utan produktion av skadliga föreningar är det viktigt att ha kunskap om hur utvecklingen av mikrobsamhället i en bioreaktor påverkas av olika faktorer. Denna avhandling bidrar till den kunskapen. Fortsatt forskning bör närmare undersöka hur olika typer av kolhaltigt material kan användas för att styra sammansättningen av mikrobsamhället i bioreaktorn. Denitrifierande bioreaktorer kan användas i många tillämpningar och för att minska kväveutsläppen till Östersjön bör förutsättningarna för att införa tekniken i Sverige undersökas.

Acknowledgements

I have written this section once before. Despite additional years as a PhD student, it is as difficult as it was then. Below I will only mention a few persons by name, people who have literally contributed to the texts in this thesis. It does not mean that I am less thankful to the rest of you who have supported me in one way or another, I truly am.

My supervisors, Sara Hallin and Jaanis Juhanson, my sincerest thanks. Sara, for support to go through with year 3 and 4, even when it was tough. Jaanis, for endless help whenever needed, always with patience and in a kind way.

Roger Herbert, co-author of three of the papers in the thesis. Many thanks for being available to comment on all questions I have had about the bioreactors we have been working with. Additional co-authors of my papers: Harry Winbjörk, Valerie Hubalek, Robert Almstrand, Sari Peura, Albin Nordström, Cristina Valhondo, Lurdes Martínez-Landa, Jesús Carrera, and Felicia Wallnäs, thank you for qualified and creative contributions, making it possible to publish the papers in well recognised scientific journals.

Employees at LKAB, it has been a privilege and pleasure working with so positive, helpful, and innovative persons, many thanks.

Christopher Welch and Christopher Jones, I am deeply grateful to you for helping me by reading parts of the thesis text and coming with suggestions for improvements. In the end I did change a little here and there, all mistakes are my own.

Colleagues at Mykopat and Biocenter, thank you all for creating a nice work environment.

Finally, my family, in Uppsala and Umeå. I love you.

I

Available online at www.sciencedirect.com

ScienceDirect

journal homepage: www.elsevier.com/locate/watres

Nitrogen removal and spatial distribution of denitrifier and anammox communities in a bioreactor for mine drainage treatment

Roger B. Herbert Jr.[a,*], *Harry Winbjörk* [b], *Maria Hellman* [c], *Sara Hallin* [c]

[a] *Uppsala University, Department of Earth Sciences, Villavägen 16, SE-752 36 Uppsala, Sweden*
[b] *LKAB, SE-983 81 Malmberget, Sweden*
[c] *Swedish University of Agricultural Sciences, Department of Microbiology, Box 7025, SE-750 07 Uppsala, Sweden*

ARTICLE INFO

Article history:
Received 17 March 2014
Received in revised form
15 July 2014
Accepted 23 August 2014
Available online 4 September 2014

Keywords:
Denitrification
Residence time
nirS
nirK
nosZ
Nitrous oxide

ABSTRACT

Mine drainage water may contain high levels of nitrate (NO_3^-) due to undetonated nitrogen-based explosives. The removal of NO_3^- and nitrite (NO_2^-) in cold climates through the microbial process of denitrification was evaluated using a pilot-scale fixed-bed bioreactor (27 m^3). Surface water was diverted into the above-ground bioreactor filled with sawdust, crushed rock, and sewage sludge. At hydraulic residence times of ca.15 h and with the addition of acetate, NO_3^- and NO_2^- were removed to below detection levels at a NO_3^- removal rate of 5–10 g N m^{-3} (bioreactor material) d^{-1}. The functional groups contributing to nitrogen removal in the bioreactor were studied by quantifying *nirS* and *nirK* present in denitrifying bacteria, *nosZI* and *nosZII* genes from the nitrous oxide – reducing community, and a taxa-specific part of the16S rRNA gene for the anammox community. The abundances of *nirS* and *nirK* were almost 2 orders of magnitude greater than the anammox specific 16S rRNA gene, indicating that denitrification was the main process involved in nitrogen removal. The spatial distribution of the quantified genes was heterogeneous in the bioreactor, with trends observed in gene abundance as a function of depth, distance from the bioreactor inlet, and along specific flowpaths. There was a significant relationship between the abundance of *nirS*, *nirK*, and *nosZI* genes and depth in the bioreactor, such that the abundance of organisms containing these genes may be controlled by oxygen diffusion and substrate supply in the partially or completely water-saturated material. Among the investigated microbial functional groups, *nirS* and anammox bacterial 16S rRNA genes exhibited a systematic trend of decreasing and increasing abundance, respectively, with distance from the inlet, which suggested that the functional groups respond differently to changing environmental conditions. The greater abundance of *nirK* along central flowpaths may indicate that the bioreactor design favored preferential flow along these flowpaths, away from the sides of the bioreactor. An improved bioreactor design should consider the role of preferential flowpaths and the heterogeneous distribution of the genetic potential for denitrification, nitrous oxide reduction and anammox on bioreactor function.

* *Corresponding author*. Tel.: +46 18 471 22 66; fax: +46 18 55 11 24.
E-mail address: roger.herbert@geo.uu.se (R.B. Herbert).
http://dx.doi.org/10.1016/j.watres.2014.08.038
0043-1354/

1. Introduction

Nitrogen release from undetonated ammonium-nitrate based explosives used in mining is an environmental issue that is just beginning to be recognized (e.g. Häyrynen et al., 2008; Bailey et al., 2013). Undetonated ammonium nitrate is readily soluble in water and quickly enters into the mine drainage. The nitrogen in these waters is primarily in the form of nitrate (NO_3^-) and ammonium (NH_4^+) with lesser amounts of nitrite (NO_2^-), which is eventually discharged to the environment. In the cold climate of northern circumpolar areas, aquatic ecosystems are often nutrient-limited, and even small nitrogen loadings could impact water bodies. In addition, a significant issue is the presence of NO_2^- and the generation of ammonia (NH_3), both of which have toxic effects on aquatic ecosystems (EPA, 2009). To prevent detrimental environmental impacts, there are a number of viable approaches for removing nitrogen from mine drainage waters. For complete nitrogen removal, most of the techniques involve oxidation of reduced nitrogen species to NO_3^- followed by denitrification. This is a microbial reaction mainly involving heterotrophic denitrifying bacteria that use organic compounds ('CH_2O') as a carbon and energy source while reducing NO_3^- to nitrogen gas (N_2) under anaerobic conditions:

$$4NO_3^- + 5CH_2O \rightarrow 2N_{2(g)} + 4HCO_3^- + H_2CO_3 + 2H_2O \quad (1)$$

A low-cost solution for treating mine drainage with highly variable water flow, low organic matter content, and variable nutrient loading is a fixed-bed denitrifying bioreactor system (e.g. Schipper et al., 2010), which is a passive or semi-passive surface or subsurface structure containing a porous organic material through which water flows. During water flow through the anaerobic regions of the bioreactor, dissimilatory reduction of NO_3^- to N_2 is promoted by the denitrifier community (reaction 1). The process can also terminate with nitrous oxide (N_2O), either due to unfavorable environmental conditions (Elgood et al., 2010) or community members lacking the genetic capacity to reduce N_2O (Jones et al., 2008; Philippot et al., 2011). When designing bioreactors for treatment of nitrogen-contaminated mine drainage, it is important to consider the fraction of denitrifiers with a complete denitrification pathway to avoid emissions of the potent greenhouse and stratospheric ozone-depleting gas N_2O. Potentially, anaerobic ammonia oxidation (anammox) resulting in NO_2^- reduction by NH_4^+ and formation of N_2 (Kuenen, 2008) could also be used in bioreactors, but little is known about the role of anammox bacteria in these types of systems.

The performance of a denitrifying bioreactor system is dependent on hydraulic conditions, geochemical conditions and microbiological characteristics, all of which in turn are at least partially dependent on the composition of the organic material in the bioreactor (e.g. Warneke et al., 2011). Nevertheless, preferential flow and other site-specific conditions may lead to short hydraulic residence times and depleted reserves of labile organic carbon in the bioreactor substrate, which in turn result in lower rates of contaminant removal (cf. Cameron and Schipper, 2011; Christianson et al., 2013). When the availability of labile organic carbon limits the denitrification rate, a supplemental carbon and energy source can be fed to the bioreactor.

This study reports on the design and operation of a pilot-scale bioreactor installed at an iron ore mine in the north of Sweden for the removal of nitrogen from drainage water. In this system, NO_3^- was the primary dissolved nitrogen species. Our objectives were to determine 1) the treatment capacity of a semi-passive bioreactor under ambient conditions, and 2) the abundance and distribution of denitrifying and anammox bacteria in the bioreactor after two years of operation. As bacterial abundances cannot be easily assessed, genes that code for key enzymes in the denitrification pathway and taxa-specific genes for anammox bacteria were used as proxies for genetic potential of the functional communities. Thus, a change in gene abundance would be interpreted as growth or decay of that particular community resulting in an increased or decreased genetic potential, respectively. Our hypotheses were that 1) availability of electron donors and acceptors and 2) preferential flowpaths affected the distribution of N-reducing microorganisms and thereby reactor performance. While bioreactor systems for denitrification have been installed for treating groundwater contaminated with sewage effluents (Robertson and Cherry, 1995; Robertson et al., 2008) or agricultural drainage – impacted runoff (Christianson et al., 2013; Schipper and Vojvodic-Vukovic, 2001; Schipper et al., 2010), this is the first reported study of a semi-passive denitrification bioreactor system for treating mine drainage.

2. Materials and methods

2.1. Site description

At the Malmberget iron ore mine in northern Sweden (67°13′N, 20°42′E), operated by the mining company LKAB, nitrogen from undetonated explosives enters into the mine drainage and groundwater, which is pumped from the mine and used as process water in the ore processing and pelletization plants. After passing through a tailings impoundment and a sedimentation pond, excess process water is discharged to the Linaälven River via a spillway at levels up to 60 000 m^3 day^{-1} (LKAB, unpublished data). In addition, nitrogen compounds are adsorbed to waste rock that is removed from the mine and deposited within the catchment area; leachate from these rock dumps also contributes to nitrogen discharges from the site. For the period 2010–2011, the average concentrations of the primary nitrogen species in discharge from the sedimentation pond were 30 mg NO_3^-–N L^{-1}, 0.8 mg NH_4^+–N L^{-1}, and 0.5 mg NO_2^-–N L^{-1}. The mean annual air temperature in the vicinity of Malmberget was −1 °C for the period 1961–1990 (SMHI, 2014).

2.2. Bioreactor construction and instrumentation

The bioreactor system was designed to treat "hot spots" of nitrogen discharge, such as close to the detonation source in the mines, or down-gradient from rock waste dumps (cf. Bailey et al., 2013). Thus, only a small fraction of the discharge from the sedimentation pond was diverted to the bioreactor system at our site to simulate this type of situation.

The bioreactor system was constructed of sheet metal (steel) in autumn 2009, with dimensions 9 m (length) ×2 m

(wide) ×1.5 m (deep). The bioreactor (Fig. 1) was an open box-like container with three inner dividing walls. The first and third dividing walls extended from the upper edge down to 0.5 m from the bottom of the bioreactor, while the second inner wall extended from the bottom up to 0.5 m; the purpose of the inner dividing walls was to force the water flow below the surface of the bioreactor so as to maintain anaerobic conditions through as much of the flowpath as possible. Water was loaded into the bioreactor from the surface on the one side, and discharged from the other side through one of three possible discharge points. The discharge points consisted of two pipes situated 100 cm from the bottom of the bioreactor, two pipes situated 40 cm from the bottom of the bioreactor, and one pipe 10 cm from the base. These three discharge points are denoted as the upper, middle, and lower discharge points, respectively (Fig. 1); the middle discharge pipes were used at the start of barrier operations on June 13, 2011.

After construction, the bioreactor was placed on a level location adjacent to the regulated spillway from the sedimentation pond at the Malmberget iron ore mine. The bioreactor was filled with two different mixtures of reactive material: the first compartment, nearest the inlet, was filled with a 10:3:1 mixture (by volume) of crushed rock (8–16 mm), water – saturated sawdust, and sewage sludge, respectively, and the remaining compartments were filled with a 15:5:1 mixture that had a greater amount of crushed rock and hence a greater permeability. The sewage sludge, obtained from the Uddebo sewage treatment plant in Luleå, contained an active community of denitrifying bacteria, while the sawdust provided a long-term carbon and electron source for heterotrophic denitrification (see Herbert, 2011). The crushed rock functioned as a supporting material and prevented the organic substrate from compacting under its own weight, which would otherwise create a zone of low hydraulic conductivity at the base of the bioreactor.

Prior to filling the bioreactor structure with the reactive material, piezometers were installed for sampling pore water (Fig. 1). The piezometers take in water at a location 30–50 cm from the bottom of the bioreactor (90–110 cm below the material surface). Thermistors (Campbell Scientific® 107 temperature probe) were installed for measuring in-situ temperature and air temperature (Fig. 1) and data was continuously stored on a CR1000 data logger. The air temperature thermistor was installed in a radiation shield (Campbell Scientific® MET20) at a height of 2.5 m above the ground surface.

2.3. *Bioreactor operation, tracer test and sampling*

The bioreactor was first operated for a test period May 17 – October 10, 2010 to establish steady flow. After this, the

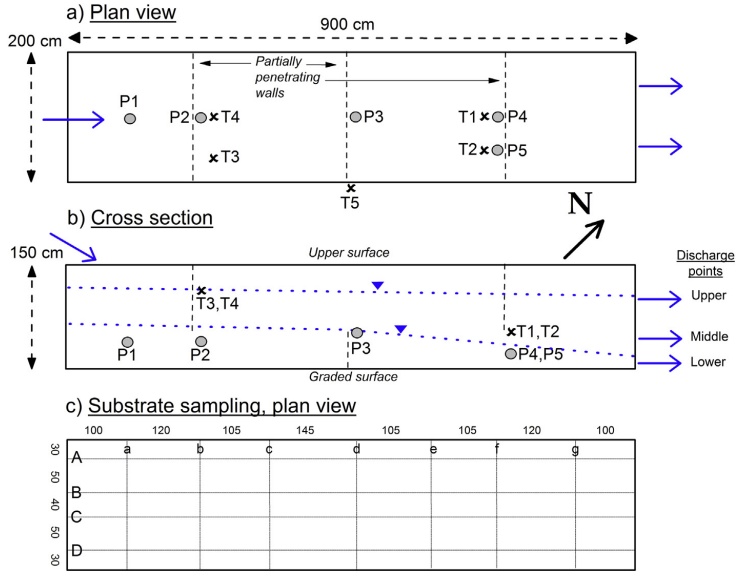

Fig. 1 – Bioreactor dimensions including location of piezometers (denoted P1 – P5) (point of water intake shown in cross-section), thermistors (denoted T1–T5), and location of reactive material sampling. (a) Bioreactor in plan view, blue arrows show locations of water inflow and outflow from bioreactor. North arrow refers to direction in plan view. (b) Bioreactor in cross section view. Dotted lines show assumed location of water level when the upper or lower discharge points were used. (c) Plan view showing location of bioreactor material samples at one depth along four transects (A–D) parallel to the direction of flow and at seven positions at increasing distance from the inlet (a–g). Numbers along edge denote distance in cm. (For interpretation of the references to colour in this figure legend, the reader is referred to the web version of this article.)

bioreactor was operated and monitored during the experimental period June 13 – September 23, 2011. During this period, a 24 h hydraulic residence time was applied; this residence time was based on the results of laboratory column experiments (Herbert and Björnström, 2009; Herbert, 2011) at 5 °C where a ca. 50% nitrate removal was achieved, and based on practical considerations (i.e. pump limitations). With this residence time as a design criteria (i.e. 24 h), a pump with regulating valve was used to maintain flow to the bioreactor at close to 3.75 L min^{-1} (5.4 m^3 d^{-1}, flow rate = total bioreactor volume × porosity/hydraulic residence time = 27 m^3 × 0.2/1 day). A porosity of 0.2 was estimated based on the measured porosity of the crushed rock (0.4) and the assumption that the sawdust and sewage sludge that fill the crushed rock pore spaces have a combined effective porosity of ca. 0.5. While both sawdust and sewage sludge generally have porosities exceeding 0.5 (cf. Horisawa et al., 1999; O'Kelly, 2004), the sawdust-sludge mixture contains a certain amount of pore space that does not participate in advective flow (Herbert, 2011), resulting in a lower effective porosity. The value of 0.5 is hence an estimated value.

From day 31 of the 2011 operational period, an acetate solution was added to the bioreactor so as to increase the supply of labile carbon and thereby increase the NO_3^- removal rate. The solution was delivered to the bioreactor surface in the first bioreactor compartment at a rate of 0.23 m^3 d^{-1}, corresponding to an organic loading rate of 4.3 g organic carbon m^{-3} d^{-1}.

Near the end of the operational period (day 95), a tracer test was conducted by rapidly adding 40 L of a concentrated NaCl solution along with the mine water at the bioreactor inlet. The purpose of this test was to determine the average hydraulic residence time of a conservative compound in the bioreactor, which would subsequently be used in the calculation of nitrate removal rates. At the time of the tracer test, the lower discharge point from the bioreactor was used. The electrical conductivity of the bioreactor discharge was measured for seven days after the start of the tracer test in order to monitor for the transport of the salt pulse through the bioreactor and to obtain a hydraulic residence time for the system.

Water sampling from the bioreactor was performed by directly collecting discharge water, or by sampling the piezometers using PVC tubing and a peristaltic pump. Samples were subsequently frozen until analysis.

After the termination of the bioreactor operations, the bioreactor material was sampled in order to determine the spatial distribution and the size of the denitrifier and anammox communities as well as of the total bacterial community. In addition, the material was sampled for the extraction of pore water for chemical analysis. Since the bioreactor started to freeze after the 2011 operational period, reactor material samples were not collected until the following year, on June 18, 2012. At the time of sampling, the bioreactor matrix was saturated from the base up to ca. 50 cm from the bottom (i.e. deeper than 90 cm below the upper surface of the bioreactor material). At this time, the bioreactor contents were emptied using a vacuum truck; the material was removed in layers so that samples could be acquired at different depths. Samples were collected using a peat corer (6 cm in diameter) at each point in a grid system as indicated in Fig. 1c. Samples were collected at the following depths below the surface of the undisturbed bioreactor material: 20–30, 60–70, 100–110 and 125–135 cm, where the latter two samples were water-saturated. In addition, samples were collected along four transects (labeled A – D, Fig. 1c), where transects B and C are presumed to lie along the predominant flowpath in the bioreactor. Samples of 50–100 mL, consisting of crushed rock and sawdust in varying proportions, were collected with dedicated, sterile plastics scoops and stored in sterile plastic bottles. Samples were stored on ice during transport and frozen until analysis. For the quantification of the microbial communities in the bioreactor, 64 samples (out of the 112 collected) distributed across all four depth horizons (12 samples at 20–30, 60–70, and 125–135 cm, and 28 at 100–110 cm) and at various distances from the inlet were analyzed.

2.4. Analyses

2.4.1. Chemical analyses of water samples

Water samples consisted of samples collected from bioreactor discharge and piezometers, as well as pore water extracted from the reactive material. Pore water from bioreactor material was extracted by first removing the crushed rock and then squeezing the samples in 60 mL syringes; samples were filtered (0.2 μm) prior to analysis.

Inorganic nitrogen compounds (NO_3^-, NO_2^-, NH_4^+), total organic carbon, and alkalinity in discharge and piezometer water samples were measured by LKAB's accredited laboratory. Alkalinity was determined by titration, NO_3^- by ion chromatography, NO_2^- by flow injection analysis, NH_4^+ by the indophenol method, and TOC by combustion followed by CO_2 detection. In a limited number of water samples from the bioreactor and in pore water extracted from the bioreactor material, nitrate was measured using an ion selective electrode (Orion™ 9707, Thermo Electron Corporation) following standard measurement procedures.

2.4.2. DNA extraction and quantitative real-time PCR

A 15 mL phosphate-buffered saline solution containing 0.05% Tween 20 was added to each bioreactor material sample (50–100 mL). The sample was extensively shaken by hand for 10 s and the liquid, including smaller particles but not the crushed rock, was transferred to a 50 ml tube. After repeating this procedure three times, the tube was left for a 3–5 min to allow the majority of the particles to settle. The water phase was decanted and filtered through a 0.22 μm Supor® membrane (Pall Corporation). The membrane was cut in two halves and DNA was extracted from one of them using the MoBio PowerWater® DNA Isolation kit following the manufacturer's instructions. The extracted DNA was quantified using a Qubit® fluorometer (Life Technologies Corporation).

Quantitative real-time PCR (qPCR) was used to determine the abundance of specific marker genes present in each of the functional bacterial communities in addition to the 16S rRNA genes in the overall bacterial community. A taxa-specific part of the16S rRNA gene was used for the anammox bacterial community, whereas the genes *nirS* and *nirK*, coding for the cytochrome-like nitrite reductase and the copper-dependent nitrite reductase, respectively, represented the denitrifying community. Nitrite reduction defines the process denitrificaton *sensu stricto* (Shapleigh, 2013) and the presence of

nirK or *nirS* indicates genetic potential for denitrification. To target *nirS* and *nirK*, we used currently available primer sets which, while not covering the extant genetic diversity of each group, still allows for a comparative analysis of the relative abundance of each in the bioreactor. This is accomplished by sampling a standard subset of each group for which denitrification functionality is verified (Penton et al., 2013) and genes coding for reduction of nitric oxide to nitrous oxide are present (Jones et al., 2008). The *nosZ*I and *nosZ*II genes, coding for the nitrous oxide reductase from clade I and II, represented the nitrous oxide reducing community; primer sets that encompass the known diversity of the *nosZ* gene were used (Jones et al., 2013), allowing for a complete assessment of the known N_2O reducing community. All amplifications were performed according to the protocols in Table S1 (see Supplementary data).

Two independent reactions were performed per gene, each in a reaction volume of 15 μL using DyNAmo Flash SYBR Green qPCR kit (Thermo Fisher Scientific Inc.), 0.1% Bovine Serum Albumin, 1.0 μM of each primer and 15 ng DNA. Standard curves were obtained by serial dilutions of linearized plasmids with cloned fragments of the specific genes. Standard curves were linear ($R^2 = 0.999$) in the range used. The amplification efficiency for 16S rRNA was 94%, whereas it was 83, 88, 90, 69 and 82% for *nirS*, *nirK*, *nosZ*I, *nosZ*II and anammox specific 16S rRNA genes, respectively. Non-template controls resulted in null or negligible values. Potential inhibition of the PCR reactions was checked by comparing amplification of a known amount of the pGEM-T plasmid (Promega) with the plasmid specific T7 and SP6 primers when added to the DNA extracts or to non-template controls. No inhibition of the amplification reactions was detected with the amount of DNA used.

2.4.3. *Statistical analysis*

For the determination of statistical significance between two sample datasets, Origin Pro 9.1 (OriginLab Corporation, Northampton, USA) was used for the application of a two sample student's *t*-test for comparing the means of both datasets.

The structure of the concatenated community of all functional groups involved in reduction of NO_3^- to N_2 among samples was analysed using non-metric multidimensional scaling (NMS). The community matrix was based on the relative gene abundances, expressed as gene copy number per ng of extracted DNA, which were compiled into a community matrix using the Bray–Curtis distance measure. Data was relativized by the column total for each gene followed by arcsine square root transformation to stabilize variance. The NMS was performed with a random starting configuration and a maximum of 200 iterations performed on 250 runs with the real data and 250 runs with randomized data to ensure that final ordination scores were significantly different from those generated from randomized data. For a solution with the lowest possible stress value, a final run using the best starting configuration from the first run was performed. Multi-Response Permutation Procedures (MRPP) were used to test whether the communities composed of the functional groups differed according to the *a priori* group depth. For the MRPP, multiple comparisons were corrected by controlling the false discovery rate according to the procedure established by Benjamini and Hochberg (1995), accepting 5% false positives. All the multivariate analyses were performed using PC-ORD version 5.10 (MjM Software, Oregon, USA).

3. Results

3.1. *Thermistor data*

Prior to the start of the 2011 operational period, the average daily core temperature in the bioreactor (thermistor T1) remained at or below 0 °C until June 5, while temperatures at thermistor T3 continuously exceeded 0 °C after April 20 (Figure S1, Supplementary Data). This temperature differential in the bioreactor was due to the solar irradiation of the southeast face of the bioreactor. After the start of water flow through the bioreactor, bioreactor temperatures generally reflect the temperature of the inflowing water from the sedimentation pond, which follows average air temperature (thermistor T5). As demonstrated by the temperature time series, the effective operational period for the bioreactor system, when the core bioreactor temperature (thermistor T1, Figure S1, Supplementary Data) was greater than 0 °C, was on the order of 5–6 months.

3.2. *Chemical analyses*

3.2.1. *Nitrate*

Inlet NO_3^- concentrations were relatively constant with a mean concentration of 30.4 mg N L^{-1} during the operational period (Fig. 2a). Outlet NO_3^- concentrations were initially in the range 16–25 mg N L^{-1}, indicating a 14–47% removal. However, the concentrations were variable, which probably reflects variations in hydraulic residence time and temperature in the bioreactor (Figure S1, Supplementary Data). After the addition of acetate on day 31, outlet NO_3^- concentrations decreased and were below the detection limit after day 57. This level persisted until after day 84, when the outlet concentration started to increase.

The decrease in NO_3^- removal after day 84 coincided with a change in the hydraulic conditions in the bioreactor system: from day 63, water started to flow over the top edge of the bioreactor system and out of the upper discharge pipes, and not only through the middle discharge pipes as intended. Therefore, outlet water was sampled from the upper discharge pipes for days 70–94. Because of the change in hydraulic conditions, the lower discharge point was used from day 95, thereby creating a greater hydraulic gradient through the bioreactor and avoiding the presumed region of low conductivity near the middle discharge pipes.

The change in the hydraulic conditions that led to water flowing over the top of the bioreactor was probably the result of a decrease in the hydraulic conductivity of the reactive material near the middle discharge pipes. The reason for the conductivity decrease is unknown, although possible explanations could be the growth of biofilm in the reactive material (cf. Seifert and Engesgaard, 2007; Seki et al., 2006; Soares et al., 1991), or the mobilization of fine-grained organic matter in the bioreactor, both of which would lead to local decreases in porosity and permeability.

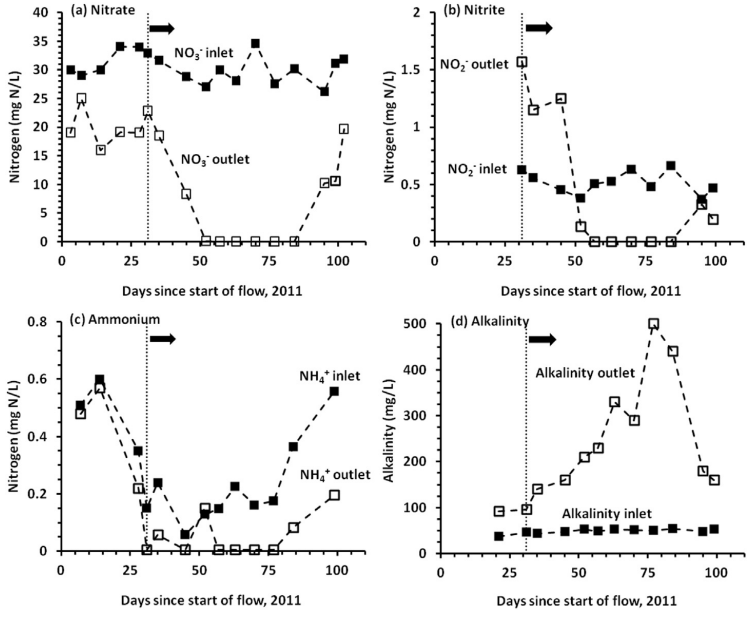

Fig. 2 – Concentrations of (a) NO_3^-, (b) NO_2^-, (c) NH_4^+, and (d) alkalinity in bioreactor inlet and outlet waters during the operational period. Dotted line and arrow mark the start of the acetate addition on day 31. Closed and open squares refer to bioreactor inlet and outlet water, respectively.

3.2.2. Nitrite, ammonium and alkalinity

Inlet NO_2^- concentrations were relatively constant with a mean level of 0.60 mg N L^1 (Fig. 2b). Outlet NO_2^- concentrations initially exceeded the mean inlet concentration by a factor of ca. 2–3, but then rapidly decreased to below detection limit after the addition of acetate with the inlet water. Similarly to NO_3^-, NO_2^- concentrations at the outlet also increased at the end of the operational period when the lower discharge point was used. The elevated NO_2^- concentrations at the beginning of the operational period were most likely attributable to the partial reduction of NO_3^- in the influent water; further reduction of NO_2^- to more reduced N species may have been limited by the availability of labile organic matter and the distribution of the denitrifying community with genes coding for nitrite reductase.

Relative to inlet NO_3^- and NO_2^- concentrations, inlet NH_4^+ concentrations exhibited greater variability (Fig. 2c), with a mean concentration of 0.28 mg N L^{-1}; the decrease in NH_4^+ concentration during the first 30 days probably reflected an increase in nitrification rate in upstream locations with increasing bioreactor temperature (see Supplementary data). At the start of the sampling period, inlet and outlet NH_4^+ concentrations were very similar. After the addition of acetate (i.e. day 31), outlet NH_4^+ concentrations were close to detection limits but this may be coincidental as NH_4^+ concentrations had started to decrease prior to the addition of acetate, perhaps due to enhanced nitrification at the surface of the bioreactor. With the exception of day 52, NH_4^+ concentrations remained low until day 84 when inlet concentrations started to increase.

Alkalinity in the bioreactor inlet water was relatively constant with a mean value of 49 mg L^{-1} HCO_3^- (Fig. 2d). After the addition of acetate, outlet alkalinity concentrations increased by up to an order of magnitude over inlet concentrations. Increases in alkalinity through the bioreactor are an indication of denitrification (reaction 1).

3.2.3. Nitrate concentrations in direction of flow

The analysis of NO_3^- in water samples from piezometers suggests that denitrification occurred along the entire flowpath, as there was a progressive decrease in nitrate concentration with distance from the inlet (Fig. 3).

3.3. *Tracer test*

Results of the tracer test on day 95 indicated an average hydraulic residence time in the bioreactor of 11 h, based on the time to maximum electrical conductivity after NaCl addition (Figure S2, Supplementary Data). At this point in time, the lower discharge point was used. Considering this measured value and the volume of bioreactor material that was water-saturated when the other discharge points were used (cf. Fig. 1), hydraulic residence times of 15 and 29 h were estimated for the middle and upper discharge points, respectively.

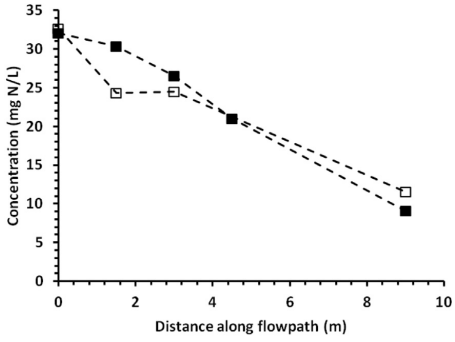

Fig. 3 – Nitrate concentration profile through the bioreactor for two sampling episodes. Profile includes samples in the sequence inlet – P1 – P2 – P3 – Outlet (see Fig. 1) and closed and open squares refer to day 45 and 95, respectively.

3.4. *Occurrence and spatial distribution of bacterial communities*

Both denitrification and anammox-related genes were detected in the bioreactor material, but the total abundance of denitrification genes *sensu stricto* (sum of *nirS* + *nirK* genes) was on average almost 2 orders of magnitude greater in abundance than the anammox specific 16S rRNA gene (Fig. 4). A trend of increasing abundances of the bacterial 16S rRNA genes and *nirS*, *nirK* and *nosZI* genes with depth was observed (Fig. 4). The abundance of the denitrification genes *nirS* and *nirK* increased the most, resulting in not only an increasing fraction of this group with increasing depth, but also a decreasing fraction of genes coding for nitrous oxide reduction in relation to denitrification. In general, there was a significant difference ($P < 0.05$) between the mean abundances of samples collected at the shallower depths (20–30 and 60–70 cm) compared with the deeper depths (100–110 and 125–135 cm) with respect to the 16S rRNA, *nirS*, *nirK*, and *nosZI* genes; the one exception was that no significant difference was found for the difference between average *nirK* gene abundance at 60–70 and 100–110 cm depth. In general, there was no significant difference ($P > 0.08$) in the samples collected at different depths in terms of the abundance of *nosZII* and anammox specific 16S rRNA genes. The concatenated community including the relative abundance of all functional groups involved in reduction of NO_3^- to N_2, either fully or partly, also indicated a separation of the bioreactor samples according to depth (Fig. 5). These differences were supported by the MRPP and were significant between all depths ($P < 0.05$), apart from the two deepest layers. The *nirS* gene contributed most to the separation.

In addition to the differences in gene abundance attributable to depth, there were observable differences in abundances along transects representing the hypothetical flowpaths A – D in Fig. 1, at a depth of 100–110 cm, which was water-saturated or close to saturation for the entire operational period (Fig. 6). The *nirS* genes decreased in abundance with distance from the inflow, although flowpath in the bioreactor (i.e. represented by transect A-D) did not appear to be important (Fig. 6a). By contrast, the abundance of *nirK* was

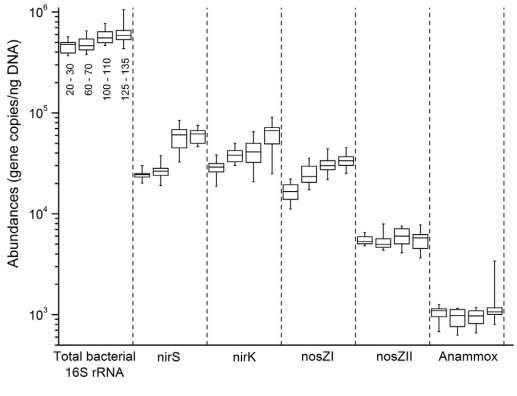

Fig. 4 – Abundances of 16S rRNA genes from the total bacterial community, *nirS* and *nirK* from denitrifying bacteria, *nosZI* and *nosZII* genes from bacteria with nitrous oxide reducing capacity, and anammox-specific16S rRNA genes in all four depths in bioreactor. Each cluster of four boxes represents the 20–30 cm ($n = 12$), 60–70 cm ($n = 12$), 100–110 cm ($n = 28$), and 125–135 cm depth ($n = 12$) in the bioreactor. Box plots indicate 25, 50 (median) and 75 percentiles and whiskers indicate 5 and 95 percentiles.

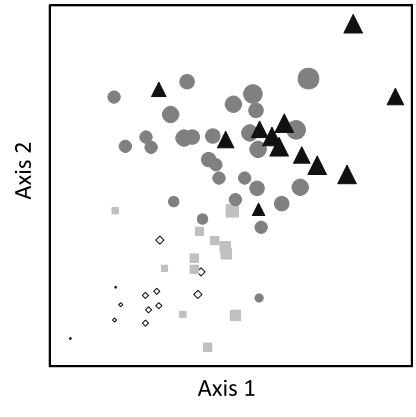

Fig. 5 – Non-metric multidimensional scaling analysis of the abundances of bacteria involved in reduction of NO_3^- to N_2 at different sampling depths in the bioreactor. The distance matrix was based on the concatenated abundances of *nirS*, *nirK*, *nosZI*, *nosZII* and anammox-specific16S rRNA genes. Symbols indicate sampling depth (◇20–30 cm, ■3 60–70 cm, ● 100–110 cm and ▲ 125–135 cm) and symbol size increases with increasing value of the size of the total denitrifying community (*nirS* + *nirK* genes) among samples. Stress value is 13.0 and the cumulative R^2 between ordination distances and distances in the original space is 0.91.

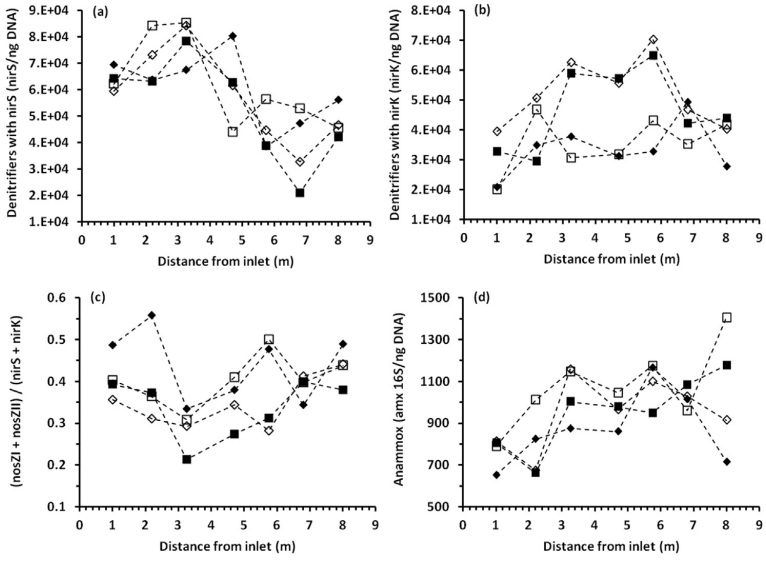

Fig. 6 – Four transects from the 100–110 cm depth depicting a) abundance of *nirS* genes, b) abundance of *nirK* genes, c) ratio of *nos* and *nir* genes (*nosZI* + *nosZII*)/(*nirS* + *nirK*), and d) abundance of anammox-specific16S rRNA genes, as a function of distance from inlet in the bioreactor. Symbols represent the four transects in the bioreactor according to Fig. 1: ◆ transect A, ◊ transect B, ■ transect C, □ transect D.

greater along the middle transects (i.e. B and C) and in the central regions of the bioreactor (positions c, d, e; Fig. 1c) than along the sides of the bioreactor (Fig. 6b). A comparison of the potential for nitrous oxide reduction relative to denitrification [(*nosZI* + *nosZII*)/(*nirS* + *nirK*), Fig. 6c] indicates a somewhat greater genetic potential for nitrous oxide reduction near the bioreactor inlet and outlet, relative to the central regions. The average abundance of anammox specific 16S rRNA genes increased slightly with distance from the inlet (Fig. 6d). There were no observable trends in the overall bacterial 16S rRNA gene copy numbers along the transects (data not shown).

4. Discussion

The chemical analyses of water samples collected from the bioreactor indicated that NO_3^- was removed in the bioreactor, but an effective NO_3^- and NO_2^- removal (>95%) was not achieved until after the addition of acetate. This suggests that denitrification and not anammox was the main process involved in nitrogen removal in the bioreactor. This is supported both by the increase in alkalinity and the detection of *nirS* and *nirK* genes at high numbers in the bioreactor material. The latter shows that growth conditions during the operational period had favored denitrifiers in the system. Compared to wastewater treatment plants designed for nitrogen removal, the number of denitrification genes were in the same range (Gabarro et al., 2013; Kim et al., 2011; Thomsen et al., 2007), but in relation to natural systems like soil, wetlands or other aquatic systems, the abundance relative to the total bacterial 16S rRNA gene copy numbers was 10–200 times higher in the bioreactor (e.g. García-Lledó et al., 2011; Hallin et al., 2009; Lyautey et al., 2013). Nevertheless, the concomitant removal of NO_2^- and NH_4^+ during days 57–77 suggests that anammox bacteria were also involved in overall nitrogen reduction, although the relatively lower abundance of genes specific for anammox bacteria in the bioreactor material compared to denitrification genes supports denitrification as the dominating process in the bioreactor during operation.

The nitrate transects through the bioreactor express a near-linear decrease in NO_3^- concentrations with distance (≈transport time), suggesting that denitrification occurred in the entire reactor and was following a zero-order rate law. A concentration-independent rate is expected for microbial processes that follow Monod kinetics and when substrate concentration (i.e. NO_3^-, acetate) is not limiting the reaction rate (Appelo and Postma, 2005). Assuming zero-order kinetics, NO_3^- removal rates for the bioreactor system were calculated as the difference between the inlet and outlet NO_3^- concentrations divided by the hydraulic residence time and multiplied by the estimated material porosity (0.2; conversion factor for liters water to liters bioreactor material). Nitrate removal rates for the period before the addition of acetate ranged 1.3–4.8 g N m^{-3} (bioreactor material) d^{-1} at a mean daily bioreactor temperature of 18 °C ± 2.5 °C, and were 5–10 g N m^{-3} d^{-1} after the addition of acetate (average daily bioreactor temperature 16 °C). Schipper et al. (2010) and Warneke et al. (2011) reported NO_3^- removal rates in denitrifying bioreactors (without additional carbon sources) to generally lie in the range 0.6–10 g N m^{-3} d^{-1} at similar temperatures; the higher end of these rates are derived from bioreactors with relatively reactive organic materials (e.g.

maize cobs, wheat straw) or with longer hydraulic residence times (e.g. Elgood et al., 2010; Greenan et al., 2009; Robertson et al., 2008). These results highlight the importance of selecting an appropriate hydraulic residence time and sufficiently reactive material in order to meet the treatment goals of the bioreactor.

A clear trend was observed with depth of an increasing abundance of specific genes characteristic of the denitrifier community (i.e. *nirS*, *nirK*, *nosZ*) and of the total bacterial community. The increase in *nirS* + *nirK* abundance is supported by a significant ($P < 0.05$) decrease in pore water NO_3^- concentrations from the 60–70 cm to the 125–135 cm depths. The increase in the abundance of denitrifying bacteria may coincide with an increase in NO_3^- removal rate with depth, as Warneke et al. (2011) has demonstrated a correlation between NO_3^- removal rate and both the abundance of *nirS* + *nirK* genes and carbon availability in bioreactors. In our bioreactor, proliferation of denitrifying bacteria was likely supported by the degree of water saturation, which would have limited oxygen availability in the deeper layers (i.e. bottom two sampling horizons. Therefore, it is expected that O_2 competed with NO_3^- as a terminal electron acceptor in the oxidation of the organic substrate in the upper horizons. If this assumption is valid, oxygen diffusion and substrate supply affected the depth distribution of denitrification potential in the bioreactor. It is apparent that the entire bioreactor cross-section was not effectively exploited for NO_3^- removal in this study, such that regions of lower water saturation were associated with a lower abundance of *nirS* and *nirK* genes, proxies for the abundance of the denitrifier community. Similar findings have been reported by Andrus et al. (2014), where increased depth and continuous water saturation in a bioreactor were linked to a more homogeneous microbial community structure, a lower exposure to O_2, and a greater availability of organic carbon.

The abundance of microbial communities capable of denitrification and anammox varied with distance from the bioreactor inlet. The abundance of *nirS* decreased with distance from the inlet while the greatest *nirK* abundance occurred in the central region of the bioreactor. This agrees with previous studies suggesting that *nirS* and *nirK* type denitrifiers have different niche preferences (Jones and Hallin, 2010), which would explain why they would respond differently to changing environmental conditions, as reported by others (Desnues et al., 2007; Enwall et al., 2010; Santoro et al., 2006; Smith and Ogram, 2008; Yuan et al., 2012). Since NO_3^- concentrations decreased to below detection limits in the outlet during the second half of the operational period, *nirS* abundance may have reflected substrate availability. Indeed, other studies (Enwall et al., 2010; Philippot et al., 2009) have reported that *nirS* rather than *nirK* abundance is more often correlated or more strongly correlated to denitrification activity in soil. In bioreactor systems, Warneke et al. (2011) noted a correlation between *nirS* + *nirK* abundance and NO_3^- removal rate, but with an increasing predominance of *nirS* with increasing temperature. In contrast to the patterns observed for specific genes characteristic of the denitrifier community, 16S rRNA gene copy numbers representing anammox bacterial communities showed a slight increase in abundance with distance from the inlet, suggesting that conditions may be more conducive for anammox (e.g. higher NO_2^- concentrations) closer to the outlet. The accumulation of NO_2^- in the bioreactor outlet in the absence of acetate as an electron donor may have been indicative of this spatial distribution in NO_2^- reduction potential.

The spatial development of the denitrifier community in the bioreactor material is ultimately tied to the hydraulic conditions in the system, in terms of water saturation, hydraulic residence times, and flowpaths. As depicted in Fig. 1, mobile water discharged from the bioreactor through either two pipes (upper and middle discharge points) or from one pipe (lower discharge point). The bioreactor design hence favored the development of preferential flow, away from the sides of the bioreactor, with regions of immobile water along the sides and in the corners. The occurrence of large volumes of immobile water has been associated with poor bioreactor performance in other studies (e.g. Christianson et al., 2013). Although there is currently insufficient data to explain the variability in *nirK* abundance along different flowpaths, it may be attributed to the continuous renewal of electron donors and acceptors (i.e. acetate and NO_3^- or NO_2^-, respectively) along the central flowpaths where preferential flow is occurring, and substrate limitation along the sides of the bioreactor where there is a higher fraction of immobile water. A similar situation has been observed in a constructed wetland (Kjellin et al., 2007), where the hydraulic residence time explained the potential denitrification rates along different flowpaths. Lower denitrification rates at longer residence times were likely linked to the limited supply of nitrate from the water to the sediments.

The fraction of genes coding for nitrous oxide reduction (sum of *nosZ*I and *nosZ*II) in relation to those for denitrification (sum of *nirS* and *nirK* amplified from respiratory denitrifiers with capacity to reduce nitric oxide to nitrous oxide) was on average 39.6 ± 9.7%. This indicates that the genetic potential for nitrous oxide *production* by denitrifiers was greater than the potential for nitrous oxide *reduction* in the bioreactor. However, this number needs to be interpreted with caution since the *nosZ*II clade could have been underestimated due to the lower amplification efficiency compared with the *nosZ*I and *nir* genes. It has previously been shown that *nosZ*I and II are found in equal abundance in a range of different environments (Jones et al., 2013) and if that would be the case in the bioreactor, *nir* genes would be more abundant than *nos*. In agreement with our results, the *nosZ* abundance in wetlands and soils is often lower than that of the denitrification genes *nirS* and *nirK* (García-Lledó et al., 2011; Henry et al., 2006; Hallin et al., 2009; Philippot et al., 2009). Similar results were reported by Warneke et al. (2011) for bioreactors, who further showed that the *nosZ*/(*nirS* + *nirK*) ratio decreased with increasing temperature. Interestingly, genetic potential for nitrous oxide reduction increased with depth when *nosZ*I were considered, whereas *nosZ*II showed no depth-related pattern. These results indicate that organisms belonging to one of the two different *nosZ* clades are not necessarily influenced by the same environmental conditions. The fact that *nosZ*II dominates among non-denitrifying nitrous oxide -reducing bacteria (Jones et al., 2013; Sanford et al., 2012) suggests that organisms capable of nitrous oxide reduction as part of the

denitrification process (mainly those harboring *nosZI*) are favored under denitrifying conditions, i.e. the prevailing condition in the deeper layer of the bioreactor. In relative terms, there was a tendency for a higher fraction of overall genetic potential for nitrous oxide reduction in relation to denitrification in the upper sampling horizon compared with the lower, but there were no differences along flowpaths or with distance from inlet. Overall, our results suggest that the emission of nitrous oxide from the bioreactor may be linked to bioreactor performance.

5. Conclusions

The results of this study indicated that a bioreactor system could successfully remove NO_3^- at concentrations of ca. 30 mg N L^{-1} to below detection levels, at hydraulic residence times of ~15 h, with the addition of acetate as an external carbon and energy source for heterotrophic denitrifying bacteria. The concomitant removal of NO_2^- and NH_4^+ in the bioreactor, along with the detection of genes that code for anammox activity, suggested that anammox processes may be a pathway for NO_2^- and NH_4^+ removal, although denitrification was the dominating nitrogen removal process. In light of these findings, the importance of the anammox pathway for the treatment of nitrogen-contaminated mine drainage should be further investigated.

There was a significant relationship between the abundance of *nirS, nirK*, and *nosZI* genes and depth, which is likely controlled by oxygen diffusion and substrate supply in the partially or completely water-saturated material. In terms of lateral spatial distribution, the abundance of genes coding for nitrite reduction (*nirS* + *nirK*) and the potential for nitrous oxide production varied with distance from the bioreactor inlet and, in the case of *nirK*, varied with different flowpaths. This spatial variability is likely linked to the hydraulic conditions of the system (e.g. water saturation, hydraulic residence times, flowpaths) and to the continuous renewal of electron donors and acceptors. The findings imply that an overall, greater genetic potential for nitrite reduction and nitrous oxide reduction could have developed in the bioreactor if water-saturated conditions had been maintained at all depths, and preferential flow had been avoided.

The knowledge of preferential flowpaths and the heterogeneous distribution of the denitrifying community should be considered in an improved bioreactor design, yielding a greater NO_3^- and NO_2^- removal. For example, to prevent preferential flow, the treated water should be allowed to discharge over the entire width of a bioreactor. In terms of the heterogeneous distribution of *nirS* and *nirK*, it needs to be investigated if this is due primarily to variations in the flow field and water saturation, or if other factors such as pore water chemistry or competition with other functional groups should be considered. Furthermore, research on the design and performance of bioreactors needs to consider the effect of operational procedures and supported processes on net emissions of nitrous oxide, so that nitrogen removal systems do not simply transfer the problems of eutrophication and toxicity to emissions of a potent greenhouse gas.

Acknowledgements

This project was financed by VINNOVA, The Swedish Innovation Agency, through the project "Nitrogen release from mining areas – Environmental effects and natural nitrogen removal in recipients" and by LKAB. Considerable assistance has been provided by LKAB in supporting field work and providing chemical analyses at the Malmberget site. Thanks are extended to Benjamin Reynolds and Louis Sennett Shanley for their assistance with the field work and DNA extractions, respectively. The comments of two anonymous reviewers are gratefully acknowledged for their time and effort in reviewing the manuscript.

Appendix A. Supplementary data

Supplementary data related to this article can be found at http://dx.doi.org/10.1016/j.watres.2014.08.038.

REFERENCES

Andrus, J.M., Porter, M.D., Rodriguez, L.F., Kuehlhorn, T., Cooke, R.A.C., Zhang, Y., Kent, A.D., Zilles, J.L., 2014. Spatial variation in the bacteria and denitrifying bacterial community in a biofilter treating subsurface agricultural drainage. Microb. Ecol. 67, 265–272.

Appelo, C.A.J., Postma, D., 2005. Geochemistry, Groundwater and Pollution, second ed. A.A. Balkema Publishers, New York.

Bailey, B.L., Smith, L.J.D., Blowes, D.W., Ptacek, C.J., Smith, L., Sego, D.C., 2013. The Diavik waste rock project: persistence of contaminants from blasting agents in waste rock effluent. Appl. Geochem 36, 256–270.

Benjamini, Y., Hochberg, Y., 1995. Controlling the false discovery rate: a practical and powerful approach to multiple testing. J. R. Stat. Soc. Ser. B (Methodol.) 57, 289–300.

Cameron, S.G., Schipper, L.A., 2011. Evaluation of passive solar heating and alternative flow regimes on nitrate removal in denitrification beds. Ecol. Eng. 37, 1195–2104.

Christianson, L., Helmers, M., Bhandari, A., Moorman, T., 2013. Internal hydraulics of an agricultural drainage denitrification bioreactor. Ecol. Eng. 52, 298–307.

Desnues, C., Michotey, V.D., Wieland, A., Zhizang, C., Fourçans, A., Duran, R., Bonin, P.C., 2007. Seasonal and diel distributions of denitrifying and bacterial communities in a hypersaline microbial mat (Camargue, France). Water Res. 41, 3407–3419.

Elgood, Z., Robertson, W.D., Schiff, S.L., Elgood, R., 2010. Nitrate removal and greenhouse gas production in a stream-bed denitrifying bioreactor. Ecol. Eng. 36, 1575–1580.

Enwall, K., Throbäck, I.N., Stenberg, M., Söderström, M., Hallin, S., 2010. Soil resources influence spatial patterns of denitrifying communities at scales compatible with land management. Appl. Environ. Microbiol. 76, 2243–2250.

EPA, 2009. Draft 2009 Update Aquatic Life Ambient Water Quality Criteria for Ammonia – Freshwater. Report EPA-822-D-09-001. United States Environmental Protection Agency, Washington, DC.

Gabarro, J., Hernandez-del Amo, E., Gich, F., Ruscalleda, M., Balaguer, M.D., Colprim, J., 2013. Nitrous oxide reduction genetic potential from the microbial community of an

intermittently aerated partial nitritation SBR treating mature landfill leachate. Water Res. 47, 7066–7077.
García-Lledó, A., Vilar-Sanz, A., Trias, R., Hallin, S., Bañeras, L., 2011. Genetic potential for N_2O emissions from the sediment of a free water surface constructed wetland. Water Res. 45, 5621–5632.
Greenan, C.M., Moorman, T.B., Parkin, T.B., Kaspar, T.C., Jaynes, D.B., 2009. Denitrification in wood chip bioreactors at different water flows. J. Environ. Qual. 38, 1664–1671.
Hallin, S., Jones, C.M., Schloter, M., Philippot, L., 2009. Relationship between N-cycling communities and ecosystem functioning in a 50-year-old fertilization experiment. ISME J. 3, 597–605.
Henry, S., Bru, D., Stres, B., Hallet, S., Philippot, L., 2006. Quantitative detection of the *nosZ* gene, encoding nitrous oxide reductase, and comparison of the abundances of 16S rRNA, *narG*, *nirK*, and *nosZ* genes in soils. Appl. Environ. Microbiol. 72, 5181–5189.
Herbert, R.B., 2011. Implications of non-equilibrium transport in heterogeneous reactive barrier systems: evidence from laboratory denitrification experiments. J. Contam. Hydrol. 123, 30–39.
Herbert, R., Björnström, J., 2009. Barrier system for the treatment of nitrogen effluents from the Malmberget iron mine. In: Proceedings, Securing the Future and 8th ICARD, June 22 – 26, 2009, Skellefteå, Sweden.
Horisawa, S., Sunagawa, M., Tamai, Y., Matsuoka, Y., Miura, T., Terazawa, M., 1999. Biodegradation of nonlignocellulosic substances II: physical and chemical properties of sawdust before and after use as artificial soil. J. Wood Sci. 45, 492–497.
Häyrynen, K., Langwaldt, J., Pongracz, E., Väisänen, V., Mänttäri, M., Keiski, R.L., 2008. Separation of nutrients from mine water by reverse osmosis for subsequent biological treatment. Miner. Eng. 21, 2–9.
Jones, C.M., Stres, B., Rosenquist, M., Hallin, S., 2008. Evolutionary history of denitrification as assessed by phylogenetic analysis of nitrite, nitric oxide and nitrous oxide respiratory enzymes. Mol. Biol. Evol. 25, 1955–1966.
Jones, C.M., Hallin, S., 2010. Ecological and evolutionary factors underlying global and local assembly of denitrifier communities. ISME J. 4, 633–641.
Jones, C.M., Graf, D., Bru, D., Philippot, L., Hallin, S., 2013. The unaccounted yet abundant nitrous oxide reducing microbial community – a potential nitrous oxide sink. ISME J. 7, 417–426.
Kim, Y.M., Cho, H.U., Lee, D.S., Park, D., Park, J.M., 2011. Influence of operational parameters on nitrogen removal efficiency and microbial communities in a full-scale activated sludge process. Water Res. 45, 5785–5795.
Kjellin, J., Hallin, S., Wörman, A., 2007. Spatial variations in denitrification activity in wetland sediments explained by hydrology and denitrifying community structure. Water Res. 41, 4710–4720.
Kuenen, J.G., 2008. Anammox bacteria: from discovery to application. Nat. Rev. Microbiol. 6, 320–326.
Leutey, E., Hallin, S., Teissier, S., Iribar, A., Compin, A., Philippot, L., Garabetian, F., 2013. Abundance, activity and structure of denitrifier communities in phototrophic river biofilms (River Garonne, France). Hydrobiologia 716, 177–187.
O'Kelly, B.C., 2004. Geotechnical aspects of sewage sludge monofills. Munic. Eng. 157, 193–197.
Penton, C.R., Johnson, T.A., Quensen, J.F., Iwau, S., Cole, J.R., Tiedje, J.M., 2013. Functional genes to assess nitrogen cycling and aromatic hydrocarbon degradation: primers and processing matter. Front. Microbiol. 4 article 279.
Philippot, L., Cuhel, J., Saby, N.P.A., Chèneby, D., Chronáková, A., Bru, D., et al., 2009. Mapping field-scale spatial patterns of size and activity of the denitrifier community. Environ. Microbiol. 11, 1518–1526.
Philippot, L., Andert, J., Jones, C.M., Hallin, S., 2011. Importance of denitrifiers lacking the genes encoding the nitrous oxide reductase for N_2O emissions from soil. Glob. Change Biol. 17, 1497–1504.
Robertson, W.D., Cherry, J.A., 1995. In situ denitrification of septic-system nitrate using reactive porous media barriers: field trials. Ground Water 33, 99–111.
Robertson, W.D., Vogan, J.L., Lombardo, P.S., 2008. Nitrate removal rates in a 15-year-old permeable reactive barrier treating septic system nitrate. Ground Water Monit. Remed 28, 65–72.
Sanford, R., Wagner, D.D., Wu, Q., Chee-Sanford, J.C., Thomas, S.H., Cruz-García, C., et al., 2012. Unexpected nondenitrifier nitrous oxide reductase gene diversity and abundance in soils. Proc. Nat. Acad. Sci. USA 109, 19709–19714.
Santoro, A.E., Boehm, A.B., Francis, C.A., 2006. Denitrifier community composition along a nitrate and salinity gradient in a coastal aquifer. Appl. Environ. Microbiol. 72, 2102–2109.
Shapleigh, J., 2013. Denitrifying prokaryotes. In: Rosenberg, E., DeLong, E., Lory, S., Stackebrandt, E., Thompson, F. (Eds.), The Prokaryotes. Springer Berlin Heidelberg, pp. 405–425.
Schipper, L.A., Robertson, W.D., Gold, A.J., Jaynes, D.B., Cameron, S.C., 2010. Review: denitrifying bioreactors – an approach for reducing nitrate loads to receiving waters. Ecol. Eng. 36, 1532–1543.
Schipper, L.A., Vojvodic-Vukovic, M., 2001. Five years of nitrate removal, denitrification and carbon dynamics in a denitrification wall. Water Res. 35, 3473–3477.
Seifert, D., Engesgaard, P., 2007. Use of tracer tests to investigate changes in flow and transport properties due to bioclogging of porous media. J. Contam. Hydrol. 93, 58–71.
Seki, K., Thullner, M., Hanada, J., Miyazaki, T., 2006. Moderate bioclogging leading to preferential flow paths in biobarriers. Ground Water Monit. Remed. 26, 68–76.
Smith, J.M., Ogram, A., 2008. Genetic and functional variation in denitrifier populations along a short-term restoration chronosequence. Appl. Environ. Microbiol. 74, 5615–5620.
Soares, M.I.M., Braester, C., Belkin, S., Abeliovich, A., 1991. Denitrification in laboratory sand columns: carbon regime, gas accumulation and hydraulic properties. Water Res. 25, 325–332.
SMHI, 2014. Swedish Meteorological and Hydrological Institute. Website. www.smhi.se/klimatdata/meteorologi/temperatur (in Swedish).
Thomsen, T.R., Kong, Y., Nielsen, P.H., 2007. Ecophysiology of abundant denitrifying bacteria in activated sludge. FEMS Microbiol. Ecol. 60, 370–382.
Warneke, S., Schipper, L.A., Matiasek, M.G., Scow, K.M., Cameron, S., Bruesewitz, D.A., McDonald, I.R., 2011. Nitrate removal, communities of denitrifiers and adverse effects in different carbon substrates for use in denitrification beds. Water Res. 45, 5463–5475.
Yuan, Q., Liu, P., Lu, Y., 2012. Differential responses of *nirK*- and *nirS*-carrying bacteria to denitrifying conditions in the anoxic rice field soil. Environ. Microbiol. Rep. 4, 113–122.

Supplementary data to

Nitrogen removal and spatial distribution of denitrifier and anammox community abundances in pilot-scale bioreactor for mine drainage treatment

Roger B. Herbert Jr.[1*], Harry Winbjörk[2], Maria Hellman[3], Sara Hallin[3]

[1] Uppsala University, Department of Earth Sciences, Villavägen 16, SE-752 36 Uppsala, Sweden. (*corresponding author)

roger.herbert@geo.uu.se, Telephone: +46 18 471 22 66

[2] LKAB, SE-983 81 Malmberget, Sweden

[3]Swedish University of Agricultural Sciences, Department of Microbiology, Box 7025, SE-750 07 Uppsala, Sweden

Table S1. PCR primers and thermal cycling conditions used for quantification of different genes

Genes and primers	Primer sequences (5' – 3')	Primer references	Thermal conditions[a]
16S rRNA:			(95°C, 7 min) x 1
341F	CCT ACG GGA GGC AGC AG	Lopez-Gutierrez et al., 2004	(95°C, 15 s; 60°C, 30 s; 72°C, 30 s; 80°C, 30 s) x 40
534R	ATT ACC GCG GCT GCT GGC A		(95°C, 15 s;(60 to 95° C, 10 s, increment 0.5°)), x 1
***nirK*:**			(95°C, 7 min) x 1
nirK 876	ATY GGC GGV CAY GGC GA	Henry et al., 2004	(95°C, 15 s; (63°C – 58°C, -1°/cycle), 30 s; 72°C, 30 s) x 6;
nirK R3Cu	GCC TCG ATC AGG TTR TGG TT		(95°C, 15 s; 58°C, 30 s; 72°C, 30 s; 80°C, 30 s) x 35
			(95°C, 15 s;(60 to 95° C, 10 s, increment 0.5°)), x 1
***nirS*:**			(95°C, 7 min) x 1
nirSCd3aFm	AAC GYS AAG GAR ACS GG	Throbäck et al., 2004	(95°C, 15 s; (65°C – 60°C, -1°/cycle), 30 s; 72°C, 30 s) x 6;
nirSR3cdm	GAS TTC GGR TGS GTC TTS AYG AA		(95°C, 15 s; 60°C, 30 s; 72°C, 30 s; 80°C, 30 s) x 35
			(95°C, 15 s;(60 to 95° C, 10 s, increment 0.5°)), x 1
***nosZ*I:**			(95°C, 7 min) x 1
nosZ2F	CGC RAC GGC AAS AAG GTS MSS GT	Henry et al., 2006	(95°C, 15 s; (65°C – 60°C, -1°/cycle), 30 s; 72°C, 30 s) x 6;
nosZ2R	CAK RTG CAK SGC RTG GCA GAA		(95°C, 15 s; 60°C, 30 s; 72°C, 30 s; 80°C, 30 s) x 35
			(95°C, 15 s;(60 to 95° C, 10 s, increment 0.5°)), x 1
***nosZ*II:**			(95°C, 7 min) x 1
nosZII-F	CTIGGICCIYTKCAYAC	Jones et al., 2013	(95°C, 15 s; 54°C, 30 s; 72°C, 30 s; 80°C, 30 s) x 40
nosZII-R	GCIGARCARAAITCBGTRC		(95°C, 15 s;(60 to 95° C, 10 s, increment 0.5°)), x 1
amx 16S (anammox):			(95°C, 7 min) x 1
			(95°C, 15 s; 60°C, 30 s; 72°C, 30 s; 80°C, 30 s) x 35
AMX 818 F	ATG GGC ACT MRG TAG AGG GGT TT	Tsushima et al., 2007	(95°C, 15 s;(60 to 95° C, 10 s, increment 0.5°)), x 1
AMX 1066 R	AAC GTC TCA CGA CAC GAG CTG		

[a] Fluorescent signal was aquired at 80°C.

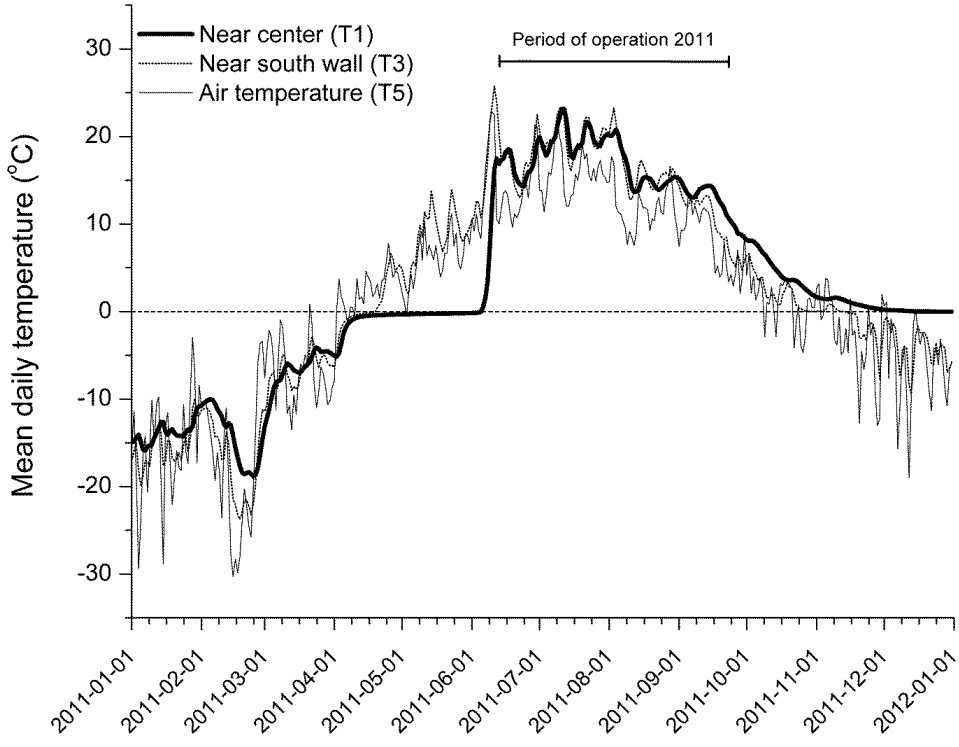

Figure S1: Average daily temperatures in bioreactor (thermistors T1, T3) and in air (thermistor T5). Period of operation is indicated.

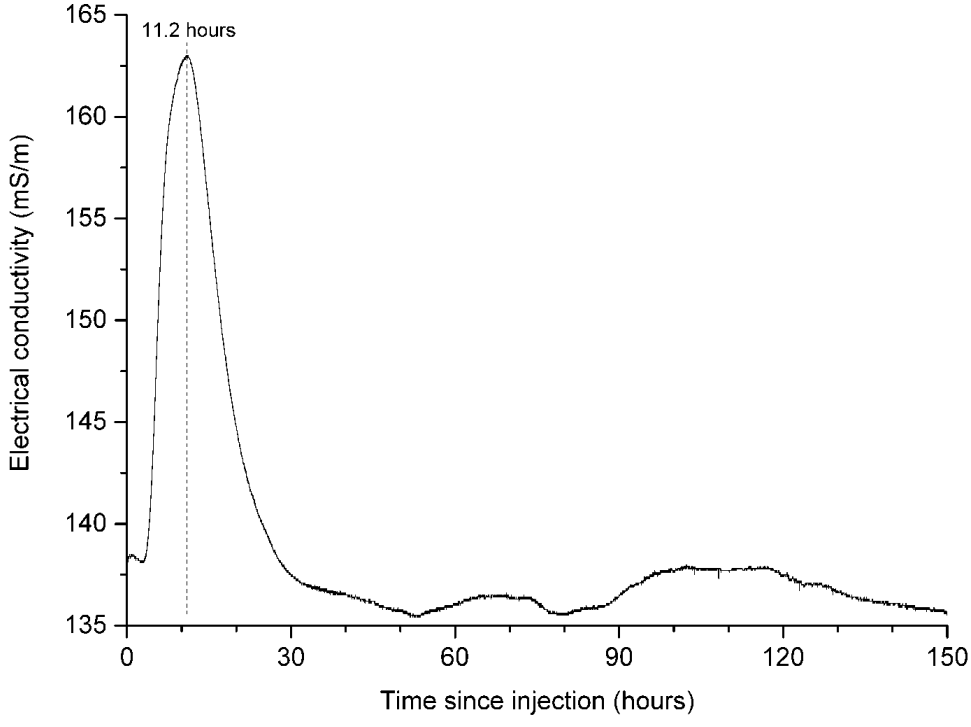

Figure S2: Electrical conductivity variations in lower bioreactor discharge point as a result of tracer test initiated on day 95 (time = 0).

References

Henry S., Baudouin, E., López-Gutiérrez, J.C., Martin-Laurent, F., Brauman, A., Philippot, L. 2004. Quantification of denitrifying bacteria in soils by *nirK* gene targeted real-time PCR. *J Microbiol Methods* 59, 327-335. Corrigendum in *J Microbiol Methods* 61 (2), 289-290.

Henry S., Bru D., Stres B., Hallet S., Philippot, L. 2006. Quantitative detection of the *nosZ* gene, encoding nitrous oxide reductase, and comparison of the abundances of 16S rRNA, *narG*, *nirK*, and *nosZ* genes in soils. *Appl Environ Microbiol* 72, 5181-5189.

Jones, C.M., Graf, D., Bru, D., Philippot, L. and Hallin, S. 2013. The unaccounted yet abundant nitrous oxide reducing microbial community - a potential nitrous oxide sink. *ISMEJ* 7, 417-426.

Lopez-Gutierrez J.C., Henry S., Hallet S., Martin-Laurent F., Catrou, G., Philippot L. 2004. Quantification of a novel group of nitrate-reducing bacteria in the environment by real-time PCR. *J Microbiol Methods* 57, 399-407.

Throbäck N., Enwall K., Jarvis A., Hallin, S. 2004. Reassessing PCR primers targeting *nirS*, *nirK* and *nosZ* genes for community surveys of denitrifying bacteria with DGGE. *FEMS Microbiol Ecol* 49, 401-417.

Tsushima, I., Kindaichi, T., Okabe, S. 2007. Quantification of anaerobic ammonium-oxidizing bacteria in enrichment cultures by real-time PCR. *Water Research* 41, 785-794.

II

Science of the Total Environment 755 (2021) 143023

Contents lists available at ScienceDirect

Science of the Total Environment

journal homepage: www.elsevier.com/locate/scitotenv

Substrate type determines microbial activity and community composition in bioreactors for nitrate removal by denitrification at low temperature

Maria Hellman *, Valerie Hubalek, Jaanis Juhanson, Robert Almstrand [1], Sari Peura, Sara Hallin

Swedish University of Agricultural Sciences, Department of Forest Mycology and Plant Pathology, Box 7026, 75007 Uppsala, Sweden

HIGHLIGHTS

- Sedge and straw bioreactors removed nitrate at higher rates than woodchip reactors.
- Denitrification was the dominant nitrate reduction process, but potential for DNRA.
- Distinct bacterial communities developed in the lignocellulosic substrates.
- The potential for N_2O reduction increased with time in all tested substrates.

GRAPHICAL ABSTRACT

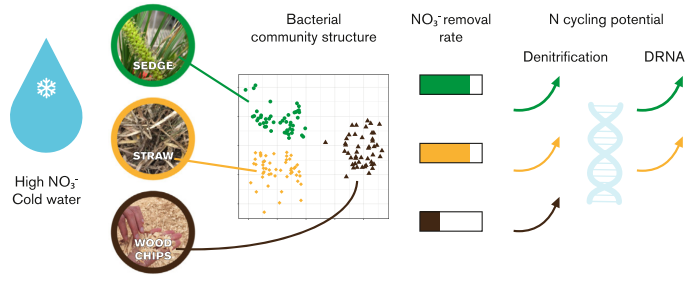

ARTICLE INFO

Article history:
Received 30 June 2020
Received in revised form 8 October 2020
Accepted 8 October 2020
Available online 19 October 2020

Editor: Frederic Coulon

Keywords:
Denitrifying woodchip reactor
DNRA
Nitrous oxide
Wastewater treatment

ABSTRACT

High levels of nitrogen originating from blasting operations, for example at mining sites or quarries, risk contaminating water bodies through leaching from waste rock dumps. Woodchip bioreactors can be a simple and cost-effective way of reducing nitrate concentrations in the leachate. In this study we investigated how bottle sedge, barley straw, and pine woodchips used as electron donors for denitrification influenced microbial community composition and nitrate removal in lab-scale bioreactors during 270 days. The reactors were operated to ensure that nitrate was never limiting and to achieve similar nitrate removal (%). Distinct bacterial communities developed due to the different substrates, as determined by sequencing of the 16S rRNA gene. Sedge and straw reactors shared more taxa with each other than with woodchips and throughout the experimental period, sedge and straw were more diverse than woodchips. Cellulose degrading bacteria like Fibrobacteres and Verrucomicrobia were detected in the substrates after 100–150 days of operation. Nitrate removal rates were highest in the sedge and straw reactors. After initial fluctuations, these reactors removed 5.1–6.3 g N m^{-3} water day^{-1}, which was 3.3–4.4 times more than in the woodchip reactors. This corresponded to 48%, 42%, and 44% nitrate removal for the sedge, straw, and woodchip reactors respectively. The functional communities were characterized by quantitative PCR and denitrification was the major nitrate removing process based on genetic potential and water chemistry, although sedge and straw developed a capacity for ammonification. Gene ratios suggested that denitrification was initially incomplete and terminating with nitrous oxide. An increase in abundances of nitrous oxide reducing capacity in all substrate types towards the end increased the potential for less emissions of the greenhouse gas nitrous oxide.

* Corresponding author.
E-mail addresses: Maria.Hellman@slu.se (M. Hellman), Valerie.Hubalek@slu.se (V. Hubalek), Jaanis.Juhanson@slu.se (J. Juhanson), Robert.Almstrand@havochvatten.se (R. Almstrand), Sari.Peura@slu.se (S. Peura), Sara.Hallin@slu.se (S. Hallin).
[1] Present address: "Swedish Agency for Marine and Water Management", Box 11930, 40439 Gothenburg, Sweden.

https://doi.org/10.1016/j.scitotenv.2020.143023

1. Introduction

Nitrogen (N) contamination of water bodies due to N-rich leachates or run-off water is a major environmental problem worldwide resulting in eutrophication and toxic levels of nitrite and ammonia for aquatic organisms (Camargo and Alonso, 2006). During the last decade, woodchip bioreactors have established as a cheap and sustainable way of treating nitrate leaching from agricultural soils and greenhouses (Christianson and Schipper, 2016; Fatehi-Pouladi et al., 2019), recirculating aquaculture systems (Aalto et al., 2020; von Ahnen et al., 2019), and from stormwater runoff (Ashoori et al., 2019). In these bioreactors, denitrifying microorganisms reduce nitrate to gaseous compounds, ultimately to N_2, using the carbon (C) in the woodchip as electron donors (Schipper et al., 2010). The technology could also be adapted for treating N originating from undetonated explosives and spillage during handling at blasting operations, for example in quarries, at mining sites, and during road construction, which is increasingly being acknowledged as an environmental issue (Bailey et al., 2013). Ammonium nitrate fuel oil is the most commonly used explosive (Forsyth et al., 1995) and the ammonium nitrate is easily washed out from rock deposits, and eventually ends up in waterbodies. Denitrifying bioreactors using woodchips or sawdust for treating nitrate contaminated mine water has been evaluated in pilot-scale reactors (Herbert Jr et al., 2014; Nordström and Herbert, 2018), but more effort is needed regarding the design to obtain high nitrate removal rates at low temperatures for use at northern latitudes, and without introducing nonwanted side effects, such as production of ammonium or nitrous oxide.

The hydraulic retention time (HRT) in the bioreactor is an important factor determining removal efficiency (Addy et al., 2016). For example, Hoover et al. (2016) showed a positive linear relationship between HRT and percent nitrate removed in woodchip columns. However, HRTs exceeding the needed reaction time will result in depletion of nitrate, allowing for more reduced conditions that can lead to undesired processes like sulfate reduction and formation of methane. Another important factor determining N removal is temperature (Hoover et al., 2016), but few studies have been conducted at 15 °C or lower (Jang et al., 2019). In the northern hemisphere were many mines are situated, even the mean summer temperature can be lower than that, challenging the application of cellulose-based denitrifying reactors for treatment of mine drainage. Further, different cellulose-based substrate types give different removal rates (Greenan et al., 2006) and C quality indicators of the solid substrate, e.g. hemicellulose content, have been studied to optimize nitrate removal (Schmidt and Clark, 2013). There is an increasing interest in the link between nitrate removal and microbial community composition in woodchip or other cellulose-based substrate bioreactors treating different types of wastewater (e.g. Aalto et al., 2020; Grießmeier et al., 2017; Hathaway et al., 2015; Herbert Jr et al., 2014; Jang et al., 2019; Kiani et al., 2020; Porter et al., 2015). Better knowledge about which microorganisms are associated with specific substrates in these types of bioreactors could help explaining differences in removal rates or why some substrates favor unwanted reactions, for example the N retaining pathway dissimilatory nitrate reduction to ammonium (DNRA) or production of the potent greenhouse gas nitrous oxide (N_2O) (e.g. Fowdar et al., 2015; Warneke et al., 2011).

The aim was to evaluate the effect of different solid substrates on nitrate removal rates and unwanted nitrogen transformation processes and to determine the development of the bacterial communities and the functional groups involved in denitrification, DNRA, and N_2O reduction when treating nitrate rich mining water at 10 °C, which is the mean summer temperature in Northern Sweden. The abundance of DNRA bacteria and N_2O reducers give information on the genetic potential for different nitrate reduction pathways in the reactors that would result in either removal or retention of N, and N_2O production or reduction. We specifically compared the substrates pine woodchips, barley straw, and bottle sedge, *Carex rostrata*, using lab-scale bioreactors, which were continuously fed with water from a clarification pond at a mine site in Sweden for 270 days. Bottle sedge was chosen because it is a common plant in wetlands in areas surrounding mining ponds in northern Sweden. It can grow to dense stands and is hence locally available at a low cost. To our knowledge sedge has not been tested as substrate in cellulose-based denitrifying bioreactors. Barley straw is also available locally and woodchips was chosen as the benchmark.

2. Material and methods

2.1. Substrates and water used in lab-scale bioreactors

Bottle sedge plants were dug up in April 2016 from a wetland area, barley straw was obtained from a farm, and pine woodchips from a lumberyard; all close to Uppsala, Sweden. The sedge plants were cultivated in 12 L plastic containers in tap water supplemented with potassium nitrate to a final concentration of 25 mg N L^{-1} four weeks in a growth cabinet under 12/12 h light/dark conditions at 25 °C and outdoors for additional three weeks at ambient conditions. The sedge biomass was cut with a scissor and left to dry at room temperature for two days. All substrate types were prepared to obtain two size fractions. The smaller sized material was packed into mesh bags, 0.300 g fresh weight per 25×25 mm bag and the bigger sized fraction was used for the bulk material of the bioreactor bed. The woodchips were sieved to obtain the two fractions, diameter 2–4 mm/length 12–20 mm and diameter 12–13 mm/length 30–40 mm. The sedge and straw were cut into 15–20 mm pieces (small size fraction) with a scissor. To ensure equal distribution of the sedge plant parts when preparing the reactors and mesh bags, the material was divided into green shoots (75% of total dry weight), dry/previous season shoots (15%) and fruit/male flowers (10%) before mixing. Water content in the substrates was determined by drying over night at 105 °C.

In the experiment, nitrate contaminated water from the clarification pond at the LKAB mining site in Kiruna, Sweden was used. The water was collected in 25 L plastic containers and shipped to Uppsala by road transport. Upon arrival, the water was frozen until use. Two batches of water from separate sampling occasions were used, with the second batch used at the very end of the experiment, days 260–270. The concentrations of nitrate, nitrite and ammonium were 22.3 ± 3.0, 0.48 ± 0.22 and 0.19 ± 0.17 mg N L^{-1} for the first batch and 32.9 ± 1.0, 0.61 ± 0.01 and 0.72 ± 0.16 mg N L^{-1} for the second respectively. The dissolved organic content (DOC) of the water was 3.6 ± 0.18 and 3.7 ± 0.18 mg L^{-1}respectively.

The substrate bulk material and mesh bags to be used in the reactors were wetted in sterile distilled water for 30 h at 10 °C. After pouring off excess water, the substrates were inoculated with sludge collected from the return activated sludge flow from the secondary clarifier at the Kungsängen municipal wastewater treatment plant in Uppsala. Inoculation was done by combining substrate, sludge and pond water in sealable plastic bags to a concentration of 0.06% dry sludge per dry mass substrate. The bags were agitated (150 rpm) over night at 10 °C.

2.2. Experimental bioreactors

The reactors were prepared in glass columns, inner diameter 48 mm, length 300 mm (Kontes Brand Chromaflex ® chromatography columns, Kimble-Chase, New Jersey, USA) with three replicate columns for each substrate type. The content of the plastic bags, i.e. sludge-inoculated substrate and pond water, was put in the columns. The mesh bags were placed in the bottom and in the top, 10 per position, to allow sampling of the substrate during the experimental period without destroying the bulk of the column. Pond water was added to completely fill the columns at the start of the experiment. As the effective porosity of the substrates were unknown, the total water volume (V_{tot}) of each column was calculated as the sum of the water content of the fresh weight material,

the distilled water soaked into the material, and the volume of added water (pond water and sludge slurry). The porosities of the packed beds, calculated as the total water volume divided by column volume, were 0.89 ± 0.017, 0.95 ± 0.007, and 0.88 ± 0.012 for the sedge, straw, and woodchip reactors respectively. A schematic drawing describing the experimental setup and detailed information on the weights and volumes are given in Supplementary Fig. S1.

During the experimental period of 270 days, the reactors were incubated in the dark at 10 °C. Pond water was continuously pumped from a 25 L container through the reactors in bottom-to-top direction using peristaltic pumps (Ismatec IPC 4- and 12 channel pumps, Cole-Parmer Instrument Company LLC, Illinois USA) and separate tubings (Tygon® 3350, inner diameter 1.42 mm) for each reactor. The inlet water container was replaced approximately every two weeks. Flows were initially set to 80 μL min^{-1} giving a theoretical hydraulic retention time (THRT) of 4.2–4.5 days (Table S1). Higher nitrate removal rates when starting cellulose-based denitrifying bioreactors are caused by a combination of the HRT and an initial flush of labile carbon (e.g. Abusallout and Hua, 2017; Hassanpour et al., 2017). After 3 weeks, the flows were regularly adjusted to reach a similar removal efficiency in the reactors, hence flow rates and THRT (Eq. 1) differed in reactors with different substrates. Across the remaining period of experiment, this resulted in THRTs of 1.5–1.8, 1.2–2.2, and 5.2–7.2 days for the sedge, straw and woodchip reactors, respectively (Table S1). After ca. 120 days, nitrate removal stabilized at approximately 45% and flow adjustment was only performed once more after that (Fig. 1a; Table S1). THRT was calculated based on the total water volume and flow rate (Q):

$$\mathrm{THRT} = \frac{V_{tot}}{Q} \tag{1}$$

With this set-up we ensured that the microbial communities were never nitrate limited, thereby also avoiding reduced conditions. Further, by allowing for the optimal reaction time for each substrate at a given removal effiency, the substrates could be compared on an equal basis in terms of the absolute nitrate removal capacity and microbial communities involved.

2.3. Sampling and analyses of reactor water and substrate

The outlet water of the reactors was sampled weekly for nitrate and biweekly for nitrite and ammonium. After adjusting flow rates, one void volume or more was allowed to pass the reactors before sampling. The compounds were analyzed using a Hach Lange DR 3900 spectrophotometer (Hach Lange, Loveland, Colorado 80539, USA) with appropriate kits. The sampling was done via a 0.2 μm syringe filter into bottles overnight. Removal rates (v) and nitrate removal efficiency (ε) were calculated based on the concentrations (C) and THRT (Hassanpour et al., 2017):

$$v = \frac{(C_{in} - C_{out})}{THRT} \tag{2}$$

$$\varepsilon = \frac{(C_{in} - C_{out})}{C_{in}} \tag{3}$$

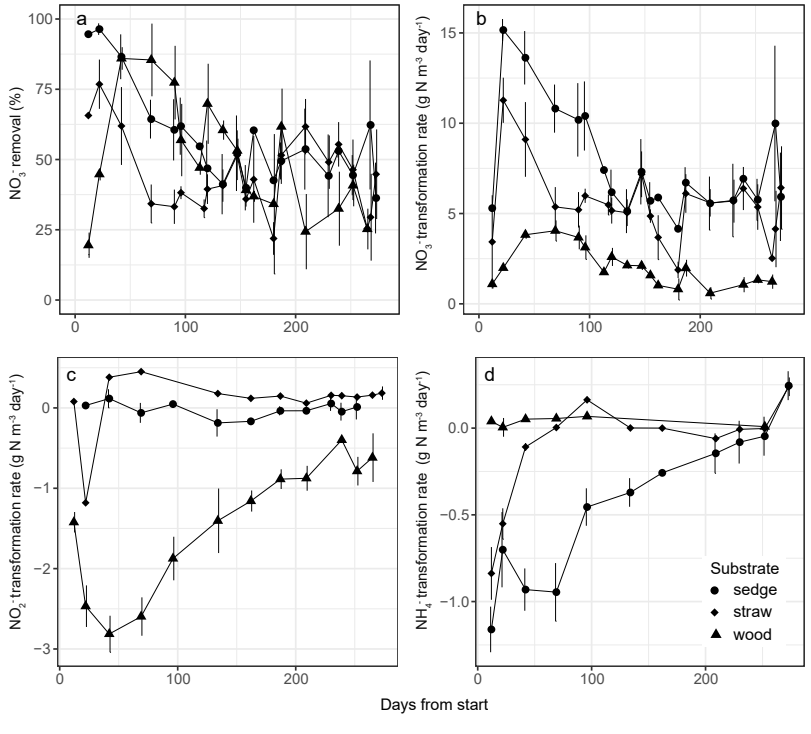

Fig. 1. Nitrogen removal and transformation rates in the reactor substrate types during the experimental period. (a) nitrate removal, (b) nitrate transformation rate, (c) nitrite transformation rate, (d) ammonium transformation rate. Positive values indicate removal and negative values indicate production of the respective nitrogen species (mean ± SD, n = 1 – 3). Substrate types are indicated with shapes.

With intervals between 4 and 8 weeks, the reactors were opened and one mesh bag from the top and one from the bottom were removed from each reactor. To fill the space of the sampled bags, they were replaced by new, sterile bags with the same substrate. The open reactors were handled under a constant flow of nitrogen gas to prevent aeration. At the end of the experiment, the bulk material of each reactor was divided into three equal parts representing the inlet, middle and outlet. Mesh bags and bulk material were kept frozen until freeze dried and further analyzed.

2.4. DNA extractions and quantitative PCR

Prior to DNA extraction, freeze dried substrate was milled for 20 s at a frequency of 30 beats/s (Laarmann, LMLW-320/2). DNA was extracted from 0.2 g using the DNeasy Power Soil kit (Qiagen GmbH, Hilden, Germany) following the manufacturer's instructions.

Quantitative PCR was used to estimate the 16S rRNA gene abundance (Muyzer et al., 1993) as a proxy of the size of the total bacterial community. The genetic potential for denitrification was determined as the abundances of the functional genes *nirS* (Throbäck et al., 2004) and *nirK* (Henry et al., 2004), nitrous oxide reduction potential as *nosZ*I (Henry et al., 2006) and *nosZ*II (Jones et al., 2013), anammox using *hdh* (Schmid et al., 2008), and DNRA using *nrfA* (Mohan et al., 2004; Welsh et al., 2014). Each reaction contained 1 ng template DNA, iQ SYBR Green Supermix (BioRad, CA, USA), 0.1% Bovine Serum Albumin (BSA), and primer concentrations of 0.5–0.8 μM in a total volume of 15 μL. The PCR reactions were run twice in separate runs using the BioRad CFX Connect Real-Time System. Thermal cycling conditions, primer sequences, and concentrations are available in Supplementary Table S2. Standard curves were obtained using serial dilutions of linearized plasmids containing fragments of the respective genes. Prior to gene quantifications, potential PCR inhibition was tested for all samples, by spiking the DNA extracts with a known amount of the pGEM-T plasmid (Promega, WI, USA) and then amplifying it with plasmid specific T7 and SP6 primers in the presence of 1 ng of DNA or water. The threshold values for quantification in controls with water were not significantly different from those with DNA, indicating no inhibition of the PCR reaction.

2.5. Sequencing of bacterial and archaeal 16S rRNA genes and sequence processing

To determine the diversity and composition of the bacterial and archaeal communities in the reactors, the V3-V4 region of the 16S ribosomal RNA gene was sequenced using the primer pair pro341F and pro805R (Takahashi et al., 2014). The preparations of amplicons were as described in Conthe et al. (2018) with the following modifications: purification steps were done using Sera-Mag™ magnetic beads (GE Healthcare, Illinois, USA), BSA concentration was 1 μg μL^{-1}, 15% of the purified amplicons from the first PCR reaction was used as template for the second reaction, and the primer concentration was 0.2 μM in the second reaction. Sequencing was performed on an Illumina MiSeq instrument using the 2 × 250 bp chemistry. The raw sequence dataset is available under BioProject accession number PRJNA639955.

The 16S rRNA gene sequences were trimmed using mothur (Schloss et al., 2009) following Kozich et al. (2013) with the exception that the clustering into OTUs was done using VSEARCH (Rognes et al., 2016) as implemented in mothur. In short, all sequences longer than 500 bases, shorter than 440 bases, and those with ambiguous bases or homopolymers longer than 8 bases were removed. Further, chimeras were removed, and sequences were cleaned for PCR and sequencing errors by clustering together all sequences with maximum of 4 bases difference. For OTU classification, the SILVA database version 132 (Yilmaz et al., 2014) was used. Finally, all samples were rarefied prior to further analysis to the smallest sample size, resulting in 2,884,050 sequences (19,227 per sample) corresponding to 135,514 OTUs. Of these, 3359 OTUs had 10 or more sequences.

2.6. Carbon analyses of the substrate

The total C content in the starting material of the three substrates was determined by isotope analyses (SLU Stable Isotope Laboratory, Umeå, Sweden). The lignocellulosic polymers hemicellulose, cellulose, and lignin were quantified as mass loss after sequential neutral detergent-acid digestion (Vansoest et al., 1991) at the Department of Animal Husbandry and Management Laboratory, SLU Uppsala, Sweden.

2.7. Sequence data handling and statistical analyses

Handling of sequence data and statistical analyses were carried out in R, versions 3.5.0 and 3.6.1 (R Core Team, 2016). PHYLOSEQ (McMurdie and Holmes, 2013) was used to process data, VEGAN (Oksanen et al., 2018) was applied for the alpha diversity indices Shannon, Pielou, and Inverse Simpson, and for non-metric multidimensional scaling (NMDS) using Bray–Curtis dissimilarity matrices to visualize community patterns. Differences in community structure were analyzed by permutational multivariate analysis of variance (PERMANOVA) using the function 'adonis'.

The effects of time and substrate on alpha-diversity, gene abundances, nitrate removal efficiency, rate of nitrate removal, and on ammonium dynamics were analyzed using a linear mixed model (the 'lme' function in NLME). The model accounted for the interaction between substrate effect and time. The autocorrelation in the error term was modeled by an AR(1) process (Pinheiro et al., 2018). For alpha-diversity and for gene abundances, the three substrates were analyzed separately and the position of the sampled bag (i.e. top or bottom of a column) was included as a fixed factor. Sampling occasions that did not have at least one observation per substrate type and variable as well as those connected to problems with the pumps were excluded from the data set. For nitrate removal rate and efficiency, 15 time points were analyzed, whereas ammonium, that was measured less frequently, included five time points. In the model for alpha-diversity and gene abundances 5–7 time points each with 3–6 observations were included. For models where the interaction term between the variables were significant, pairwise comparisons between means at the same time points and Tukey's method for *p*-value adjustments, were made (EMMEANS, Lenth, 2018). Gene abundance data was log-transformed before analyses to meet normality and variance requirements. The total C, hemicellulose, cellulose, and lignin data were analyzed using Student's *t*-test for comparison between two groups and Tukey's HSD test for multiple groups, $\alpha = 0.05$.

3. Results and discussion

3.1. Bioreactor performance

Nitrate removal was achieved in all reactors (Fig. 1). Initially, the flow rates were similar in all reactors, resulting in different nitrate removal (%) and nitrate removal rates among the substrates, with the highest removal and removal rates in sedge followed by straw and woodchips (Fig. 1a, b, Table S1). After three weeks, the flow rates were adjusted to avoid nitrate limitation and reach similar nitrate removal efficiencies and thereby different THRTs (Table S1). From day 96 and onwards, nitrate removal (Fig. 1a, Table S1) did not differ significantly (all *p*-values > 0.05) between substrates when making pairwise comparisons at each timepoint, with the exception of at day 209 where wood had a lower removal than straw ($p = 0.02$). The removal rates were significantly affected by substrate type and time, and their interaction ($p < 0.05$; Table 1). The sedge had higher removal rates than woodchip at all sampling occasions, with the exception of day 180, where there were no differences between any of the substrates (Fig. 1b, all *p*-values ≤ 0.03). After approximately four months, the removal rates stabilized, and there were no differences between the sedge and the straw reactors (day 120 ff. all *p*-values > 0.43). The average nitrate removal rates from day 120 were 6.4 ± 2.1, 5.1 ± 1.7, and

Table 1
Two-way analysis of variance on the effects of substrate type and time on nitrate removal rate and efficiency, on ammonium accumulation rates in the water and on gene abundances in the solid substrates.

Variable	Time period	Substrate		Time		Substrate × Time	
	days	F	p	F	p	F	p
Nitrate removal rate	22–120	66.24	0.0001	38.39	<0.0001	15.15	<0.0001
Nitrate removal rate	120–252	23.90	0.0014	33.78	<0.0001	7.52	<0.0001
Nitrate removal efficiency	22–120	18.20	0.0028	15.18	<0.0001	12.28	<0.0001
Nitrate removal efficiency	120–252	0.08	0.9228	6.02	<0.0001	4.73	<0.0001
Ammonium accumulation	22–252	63.16	0.0001	75.75	<0.0001	38.94	<0.0001

1.5 ± 0.7 g N m^{-3} water day^{-1} for the sedge, straw, and woodchip reactors respectively. The differences in nitrate removal rates were reflected by the differences in labile carbon content in the substrates. As expected, the sedge and straw had significantly lower total C, cellulose, and lignin content, but a higher content of hemicellulose compared to the woodchips ($p < 0.05$; Table S3). The nitrate removal rates in the woodchip reactors were lower than rates reported for 27 laboratory woodchip reactors in a meta study (Addy et al., 2016), although direct comparisons between studies are hampered by different study designs, ways of reporting results, and type of woodchips. Pine woodchips are not commonly used, instead birch (Šereš et al., 2019; Kiani et al., 2020), poplar (Grießmeier and Gescher, 2018; von Ahnen et al., 2019), mixes of species (Ashoori et al., 2019; Aalto et al., 2020) or woodchips in combination with e.g. gravel or biochar (Šereš et al., 2019; Kiani et al., 2020) have been recently investigated, but all types of woodchips tested support nitrate reduction. Both barley and wheat straw have been tested in small-scale denitrifying bioreactors treating synthetic water resembling agricultural drainage or groundwater and the overall pattern is similar to in the present study; straw reactors remove nitrate at higher rates than woodchip reactors, independent of the origin of the influent water (Feyereisen et al., 2016; Healy et al., 2012; Warneke et al., 2011). From a practical perspective, the higher removal rates for the straw and sedge are advantageous when reactor volumes are limited, for example at a road construction site. From a sustainability perspective, the choice of substrate should also be guided by local availability.

The release of nitrite in the outlet water of the wood and sedge reactors, and of ammonium, primarily from the sedge reactors, indicated that nitrate was not always efficiently converted to gaseous N compounds (Fig. 1c and d). However, ammonium and nitrite were analyzed less frequently than nitrate, and outlet concentrations were often below detection level (0.015 mg N L^{-1}), preventing the application of the statistical model to the nitrite data. In contrast with the other substrates, nitrite was released from the woodchip columns during the entire period, with the highest effluent concentrations in the beginning, 2.2 ± 0.65 g N m-3 day^{-1} (mean ± SD days 12–42) (Fig. 1c). In agreement, nitrite leaching during the startup period of woodchip-based denitrifying reactors has previously been observed (von Ahnen et al., 2019; Nordström and Herbert, 2018), although transient nitrite accumulation has also been described for other solid substrates (Fowdar et al., 2015). We speculate that this could be due to an initial imbalance between nitrate reducers, a feature common among a large number of bacterial species, and denitrifiers. Regarding ammonium, substrate type and time, as well as the interaction between the two, were significant factors affecting the dynamics ($p < 0.001$; Table 1). However, when analyzed separately, ammonium removal in the woodchip reactors was not time dependent ($p = 0.18$) and corresponded to a removal rate of 0.040 ± 0.03 g N m^{-3} day^{-1}, whereas the straw reactors released ammonium during the first ten weeks and the sedge reactors continued to release ammonium almost until the end of the experiment. In agreement, ammonium in the outlet water of denitrifying bioreactors with labile carbon substrates have been demonstrated by e.g. Warneke et al. (2011) and Greenan et al. (2006). Production of ammonium can be the result of decomposition of the substrates, but can also originate from DNRA, known to be favored by high C/NO_3^- ratios (Kraft et al., 2014; Putz et al., 2018; Song et al., 2014; van den Berg et al., 2015), and as a consequence, nitrogen removal becomes less efficient. It was recently shown that different carbon compounds influence the end products of nitrate respiration by specifically promoting denitrification or DNRA (Carlson et al., 2020). Nevertheless, the water chemistry indicate that denitrification was the dominating nitrate reduction process in all reactor types in the present study.

3.2. Microbial community development

During the experiment, a specific microbial community developed in each substrate type (PERMANOVA, $p \leq 0.001$; Fig. 2a) with different levels of alpha diversity (Shannon's diversity index, Inverse Simpson index, and Pielou's evenness; Figs. 2b and S2). The sedge reactors displayed the highest diversity followed by straw and in both cases, diversity increased over time ($p < 0.001$; Figs. 2b and S2). This was not the case in woodchips ($p > 0.09$), which also had the lowest diversity (Figs. 2b and S2). The position in the column, in- or outlet, mattered depending on substrate and diversity index (Table S4) and Shannon's diversity was always significantly higher at the inlet from day 97 in woodchips (all p-values ≤ 0.033), from day 181 in straw (all p-values ≤ 0.047) and from day 216 in sedge (all p-values ≤ 0.013). Higher Shannon's diversity of microbial communities than those in the present study have been reported in reactors using other types of woodchips and operated at higher temperatures, e.g. in Grießmeier and Gescher (2018) and in Kiani et al. (2020).

The inoculum sludge was dominated by Acidimicrobiia, Bacteroidia and Gammaproteobacteria, but the bioreactors had a different community structure and composition already at the first sampling date (Figs. 2a and 3), suggesting that the choice of inoculum might be subordinate for the final outcome. The bacterial communities in the straw and sedge reactors were more similar to each other than to the community in the woodchip reactors (Fig. 2a). The taxonomic compositions between the reactor types likely reflected not only the lignocellulosic composition in the solid substrates (Table S3), but a combination of substrate, hydraulic retention time and chemical properties in the reactor water as a result of the microbial activity. Thus, the development of the different communities in the three reactor types should have underpinned the performance of the reactors, by being directly involved in nitrogen transformations, but more importantly when considering the overall community, by controlling decomposition of the substrates that feed denitrification. Therefore, the distributions of the 50 most abundant OTUs from each of the substrates at day 270 were analyzed further to determine how the microbial communities had developed once community changes and nitrate reduction had reached steady state (Figs. 1, S3a and b). All substrates were in the end dominated by Alpha- and Gammaproteobacteria, together with Bacteroidia (Figs. 3, S3), similar to what was found in other woodchip reactors in recent studies (von Ahnen et al., 2019; Kiani et al., 2020). Within each substrate, there were no spatial differences in community composition in the reactors (inlet, mid and outlet bulk samples, PERMANOVA, $p > 0.3$, day 270). Woodchips had the highest number of unique OTUs (36) while straw and sedge had fewer (24 and 20 unique taxa respectively). Only six of the 50 most abundant OTUs were found in all substrates, the

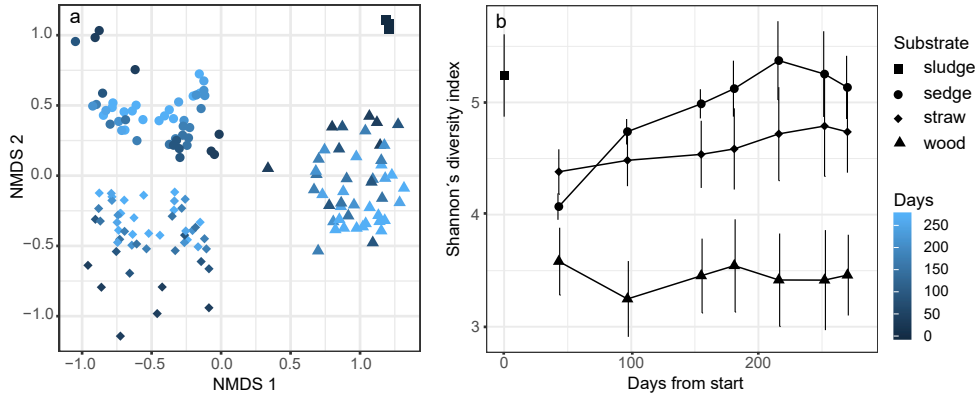

Fig. 2. Bacterial community structure and diversity in the inoculum sludge and in the reactor substrate types during the experimental period. For each of the reactors, inlet and outlet samples are included. Additionally, at day 270 bulk samples are included. (a) Non-metric multidimensional scaling based on Bray-Curtis distances of the bacterial communities. Stress value = 0.17. (b) Shannon's diversity index (mean ± SD, n = 6, day 270 n = 15). Substrate types and inoculum sludge are indicated with shapes and time with color.

majority belonging to Betaproteobacteriales, dominating all reactors at the end of the experiment. Shared families were e.g. *Burkholderiaceae*, *Sphingobacteriaceae*, *Rhizobiaceae* and *Caulobacteriaceae*. Members of *Caulobacteriaceae* are able to degrade all three lignocellulosic polymers detected in our reactors, especially lignin (Wilhelm et al., 2019). In fact, the woodchip reactors, having a higher lignin content than the other two substrates (Table S3), had a higher proportion of Caulobacterales than straw and sedge (Fig. S3). Another group separating woodchips from sedge and straw was class Bacteroidia, in woodchips represented only by Sphingobacteriales, genus *Arcticibacter*,

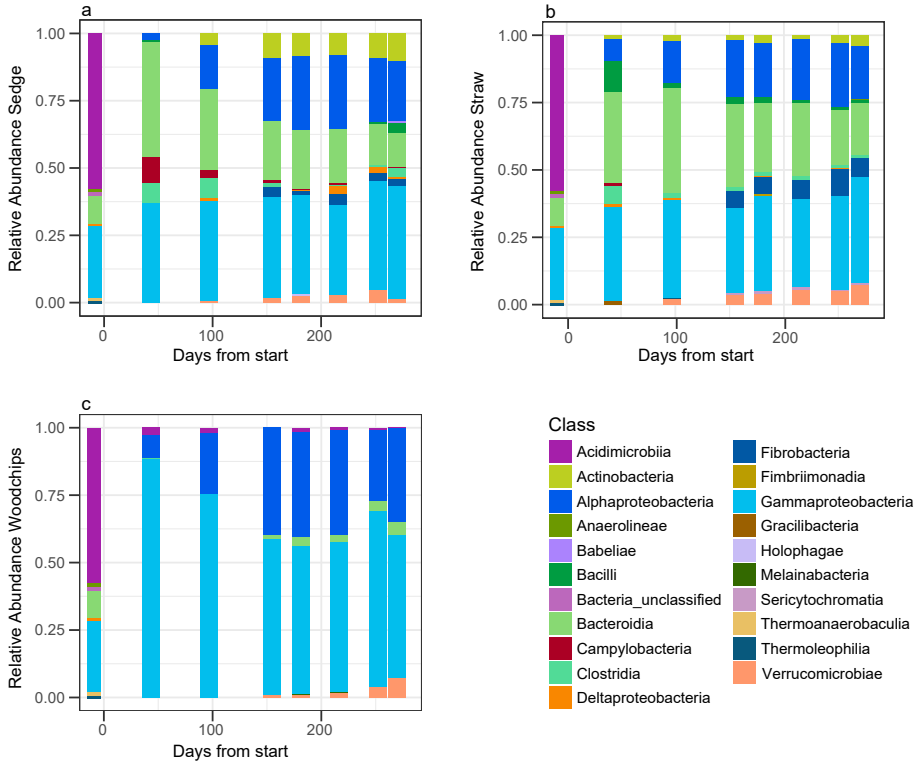

Fig. 3. Taxonomic composition of the bacterial communities in the reactor substrate types during the experimental period and in the inoculum sludge (bar before day 0). (a) sedge, (b) straw, (c) woodchips (mean, n = 3 for sludge, n = 6 for substrates days 43 – 252 and n = 15 for substrates day 270). Relative abundance at class level, taxa contributing more than 1 % in each sample type are included.

whereas in sedge and straw, other orders were also found (Figs. 3, S3). All of these are well known for their ability to degrade cellulose and they are often found in habitats where wood is degraded. *Flavobacterium*, a large genus widely distributed in aquatic habitats, with a preference for cool to cold environments (Bernardet and Bowman, 2006) were unique to the straw and sedge reactors. The genus includes denitrifying species (Bernardet and Bowman, 2006) and has been detected in groundwater and systems for management of high nitrate strength water with low C content, like in our experiment (Hou et al., 2019; Zhu et al., 2019) as well as in denitrifying woodchip reactors operated at temperatures below 15 °C (Jang et al., 2019). Straw and sedge reactors also shared one dominant OTU assigned to family *Fibrobacteraceae*, a group found in the gut of e.g. ruminants and termites (Rosenberg, 2014). Further, Verrucomicrobia were detected in all substrate types after 3–4 months of operation. Both Fibrobacteres and Verrucomicrobia are associated with anaerobic degradation of cellulose (Bao et al., 2019) and Grießmeier and Gescher (2018) found these phyla in woodchip reactors. In agreement with our results, Verrucomicrobia was deteted only after a period of operation also in the work of von Ahnen et al. (2019). Many of the unique woodchip taxa belonged to either *Sphingomonadaceae*, *Luteolibacter* or *Rhodanobacter* from orders Sphingomonadales, Verrucomicrobia and Xanthomonadales respectively. *Sphingomonadaceae* has been identified in other woodchip-based systems for treating nitrate rich water and the family was among the ten most common taxa in a reactive barrier treating nitrate rich ground water (Hiller et al., 2015).

The 16S rRNA gene abundance, a proxy for the size of the total bacterial community, differed only slightly between woodchip and the other two reactor types, with less bacteria in woodchips initially (days 43 and 97, Tukey's HSD test) (Fig. 4f). In the sedge reactors, the abundance of the total bacterial community decreased significantly over time (Table 2) but the small difference in total community size likely had minor effects on reactor performance in relation to the effects of community composition. The position (in- or outlet of the reactor) of the sampled substrate was also significant for the 16S rRNA gene abundance in these reactors (Table 2).

3.3. Functional groups involved in nitrate reduction

To decipher to which extent functional nitrogen transforming groups established in the reactors, the abundances of key players were quantified since this information is not possible to obtain from the sequence data (Fig. 4, Table 2). Anammox, quantified by the abundance of *hdh*, could not be detected in any of the reactors. Since anammox is an autotrophic process (Jetten et al., 2009), it was not expected to be a significant removal pathway in the reactors where organic C was available for the more competitive denitrifiers and DNRA bacteria that we detected. In line with the nitrate removal activity, the absolute abundances of *nirS* and *nirK* genes, indicating genetic potential for denitrification, was higher in the sedge and straw reactors compared to woodchip, and also increased over time in the sedge and straw reactors (Fig. 4a and b, Table 2). This indicates a strong selection for bacteria involved in nitrate reduction by denitrification, which agrees with other studies (e.g. Warneke et al., 2011). However, the abundance of the *nrfA* gene, indicative of DNRA bacteria, also increased in the sedge and straw reactors, but remained constantly low in those with woodchips (Fig. 4e). The increase in *nrfA* abundance coincided with the release of ammonium from the reactors (Fig. 1d). Thus, substrate type did not only affect the genetic potential for denitrification, but also controlled the potential for the two nitrate reduction pathways differently, which was reflected in the nitrate removal rates.

Denitrifiers with *nirK* type nitrite reductase increased in all reactor types, whereas the *nirS* type increased only in the straw and sedge reactors. (Fig. 4a and b). This suggests that different denitrifying communities developed since *nirK* and *nirS* are most often mutually exclusive in denitrifying bacteria (Graf et al., 2014). The dominance of *nirK* to *nirS* abundance in all substrates are in contrast to ratios reported in reactors with other substrates (von Ahnen et al., 2019; Fatehi-Pouladi et al.,

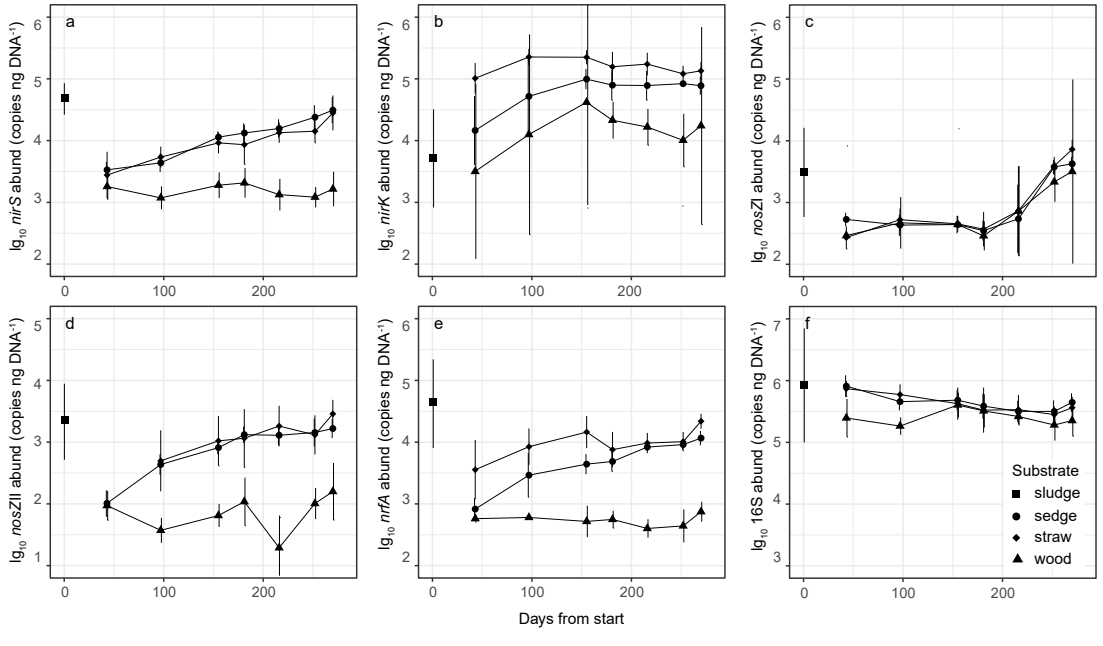

Fig. 4. Gene abundances in the reactor substrate types during the experimental period and in the inoculum sludge. (a) *nirS*, (b) *nirK*, (c) *nosZ*I, (d) *nosZ*II, (e) *nrfA*, (f) 16S rRNA gene (mean ± SD, n = 2 – 6). Note the different scales. Substrate types and inoculum sludge are indicated with shapes.

Table 2
Two-way analysis of variance on the effects of position and time on gene abundances in the solid substrates.

	Position		Time		Position × Time	
Variable	F	*p*	F	*p*	F	*p*
Sedge						
16S rRNA gene	15.65	0.001	4.76	0.002	0.81	0.574
nirS	2.41	0.132	9.28	<0.0001	1.88	0.123
nirK	0.20	0.657	1.49	0.219	1.18	0.346
*nosZ*I	5.02	0.034	48.64	<0.0001	7.50	0.0001
*nosZ*II	1.50	0.232	16.25	<0.0001	0.89	0.514
nrfA	2.18	0.154	3.14	0.028	1.11	0.387
Straw						
16S rRNA gene	14.85	0.001	4.73	0.002	3.03	0.021
nirS	4.92	0.035	10.42	<0.0001	0.70	0.649
nirK	1.11	0.302	3.60	0.009	1.63	0.176
*nosZ*I	10.84	0.003	30.01	<0.0001	3.63	0.009
*nosZ*II	9.32	0.006	2.04	0.118	0.33	0.887
nrfA	12.70	0.001	5.84	0.001	1.39	0.254
Wood						
16S rRNA gene	0.56	0.462	1.38	0.261	0.27	0.948
nirS	1.64	0.211	1.32	0.282	1.75	0.149
nirK	0.18	0.674	3.75	0.010	0.50	0.798
*nosZ*I	1.63	0.214	10.91	<0.0001	5.81	0.001
*nosZ*II	5.40	0.031	1.79	0.152	0.75	0.615
nrfA	0.15	0.708	1.25	0.356	2.14	0.158

2019). Regarding the N_2O reduction capacity, the pattern for *nosZ*I was the same in all reactors, and the abundance of this gene increased during the second half of the experimental period (Fig. 4c, $p < 0.03$ in all substrates). By contrast, *nosZ*II abundance remained at the same level from day 181 (Fig. 4d, $p = 0.63$; 0.05; 0.87 for sedge, straw and wood respectively), and was always lower in abundance than *nosZ*I. In agreement with our results, Feyereisen et al. (2016) found lower *nosZ*II abundance in a woodchip reactor compared to one with straw. The *nosZ*I gene is typically found in denitrifiers, whereas *nosZ*II is dominating in non-denitrifying N_2O reducers (Graf et al., 2014). The constantly low abundance of *nosZ*I in relation to *nir* genes in all reactor types implies that denitrification during the first six months was not complete, which would lead to emissions of N_2O (Fig. 5). However, the sum of *nosZ* genes (*nosZ*I and *nosZ*II) in relation to the sum of *nir* genes (*nirK* and *nirS*), increased over time ($p < 0.012$ for all substrates), reflecting an increasing capacity of the system to reduce N_2O. Only a minor part of the nitrate removed from denitrifying reactors is actually estimated to end up as N_2O (Greenan et al., 2009; Healy et al., 2012; Aalto et al., 2020). Emissions of N_2O have been reported from both laboratory and field reactors, and where time series data is available, the emissions seem to be higher during the start-up phase (Healy et al., 2012; Nordström and Herbert, 2017). This fits with our observations of the dynamics of the *nir* and *nosZ* functional groups, which offers an underlying mechanism as an increased *nosZ* to *nir* ratio, increase the potential for N_2O produced during denitrification to be further reduced to N_2.

4. Conclusions

The study shows that an indigenous wetland plant, bottle sedge, has at least the same potential as straw for nitrate removal via a denitrifying bioreactor at 10 °C. Both substrates supported high removal rates, allowing for shorter THRTs. Distinct bacterial communities developed in the three substrate types and the abundances of functional genes indicates that denitrification was not complete in the beginning of the experiment when flow rates were not optimized in relation to reaction time. Nitrous oxide concentrations in the water were not measured, but an increased genetic potential for N_2O reduction developed after six months. Future studies should determine DOC in the reactor water to shed light on its importance for the competition for nitrate between the processes DNRA and denitrification. Altogether, our work adds to the understanding of the microbial processes underlying the performance of denitrifying cellulose-based bioreactors.

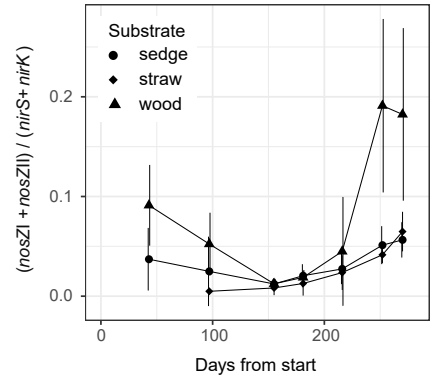

Fig. 5. Genetic potential for N_2O reduction (sum of *nosZ* gene abundances) in relation to the potential for denitrification (sum of *nir* gene abundances) in the reactor substrate types during the experimental period and in the inoculum sludge (mean ± SD, n = 2 – 6). Substrate types and sludge are indicated with shapes.

CRediT authorship contribution statement

Maria Hellman: Methodology, Investigation, Formal analysis, Writing – original draft. **Valerie Hubalek:** Investigation, Formal analysis. **Jaanis Juhanson:** Investigation, Formal analysis. **Robert Almstrand:** Methodology, Investigation. **Sari Peura:** Formal analysis. **Sara Hallin:** Methodology, Writing – original draft.

Declaration of competing interest

The authors declare that they have no known competing financial interests or personal relationships that could have appeared to influence the work reported in this paper.

Acknowledgements

This study was financed by VINNOVA (The Swedish Innovation Agency), LKAB and Boliden Minerals AB through the project "miNing" (grant numbers: 2013-03325 and 2014-01134) and by the Water Joint Programming Initiative (JPI) through the project ACWAPUR (ACcelerated Water PURification during artificial recharge of aquifers, partially funded by The Swedish Research Council Formas (grant 2016-00007). We are grateful to Joel Segersten and Johan Jonasson for help with collecting bottle sedge and water for the setup and operation of the reactors. We thank the Centre for Statistics at SLU for advice on how to handle time-series data in the statistical model.

Appendix A. Supplementary data

Supplementary data to this article can be found online at https://doi.org/10.1016/j.scitotenv.2020.143023.

References

Aalto, S.L., Suurnäkki, S., von Ahnen, M., Siljanen, H.M.P., Bovbjerg Pedersen, P., Tiirola, M., 2020. Nitrate removal microbiology in woodchip bioreactors, a case-study with full-scale bioreactors treating aquaculture effluents. Sci. Total Environ. 723, 138093.

Abusallout, I., Hua, G.H., 2017. Characterization of dissolved organic carbon leached from a woodchip bioreactor. Chemosphere 183, 36–43.

Addy, K., Gold, A.J., Christianson, L.E., David, M.B., Schipper, L.A., Ratigan, N.A., 2016. Denitrifying bioreactors for nitrate removal: a meta-analysis. J. Environ. Qual. 45, 873–881.

von Ahnen, M., Aalto, S.L., Suurnakki, S., Tiirola, M., Pedersen, P.B., 2019. Salinity affects nitrate removal and microbial composition of denitrifying woodchip bioreactors treating recirculating aquaculture system effluents. Aquaculture 504, 182–189.

Ashoori, N., Teixido, M., Spahr, S., LeFevre, G.H., Sedlak, D.L., Luthy, R.G., 2019. Evaluation of pilot-scale biochar-amended woodchip bioreactors to remove nitrate, metals, and trace organic contaminants from urban stormwater runoff. Water Res. 154, 1–11.

Bailey, B.L., Smith, L.J.D., Blowes, D.W., Ptacek, C.J., Smith, L., Sego, D.C., 2013. The Diavik waste rock project: persistence of contaminants from blasting agents in waste rock effluent. Appl. Geochem. 36, 256–270.

Bao, Y.Y., Dolfing, J., Wang, B.Z., Chen, R.R., Huang, M.S., Li, Z.P., Lin, X.G., Feng, Y.Z., 2019. Bacterial communities involved directly or indirectly in the anaerobic degradation of cellulose. Biol. Fertil. Soils 55, 201–211.

van den Berg, E.M., van Dongen, U., Abbas, B., van Loosdrecht, M.C.M., 2015. Enrichment of DNRA bacteria in a continuous culture. ISME J. 9, 2153–2161.

Bernardet, J.F., Bowman, J.P., 2006. The genus Flavobacterium. In: Dworkin, M., Falkow, S., Rosenberg, E., Schleifer, K.H., Stackebrandt, E. (Eds.), The Prokaryotes. Springer, New York.

Camargo, J.A., Alonso, Á., 2006. Ecological and toxicological effects of inorganic nitrogen pollution in aquatic ecosystems: a global assessment. Environ. Int. 32, 831–849.

Carlson, H.K., Lui, L.M., Price, M.N., Kazakov, A.E., Carr, A.V., Kuehl, J.V., Owens, T.K., Nielsen, T., Arkin, A.P., Deutschbauer, A.M., 2020. Selective carbon sources influence the end products of microbial nitrate respiration. ISME J. 14, 2034–2045.

Christianson, L.E., Schipper, L.A., 2016. Moving denitrifying bioreactors beyond proof of concept: introduction to the special section. J. Environ. Qual. 45, 757–761.

Conthe, M., Wittorf, L., Kuenen, J.G., Kleerebezem, R., van Loosdrecht, M.C.M., Hallin, S., 2018. Life on N_2O: deciphering the ecophysiology of N_2O respiring bacterial communities in a continuous culture. ISME J. 12, 1142–1153.

Fatehi-Pouladi, S., Anderson, B.C., Wootton, B., Button, M., Bissegger, S., Rozema, L., Weber, K.P., 2019. Interstitial water microbial communities as an indicator of microbial denitrifying capacity in wood-chip bioreactors. Sci. Total Environ. 655, 720–729.

Feyereisen, G.W., Moorman, T.B., Christianson, L.E., Venterea, R.T., Coulter, J.A., Tschirner, U.W., 2016. Performance of agricultural residue media in laboratory denitrifying bioreactors at low temperatures. J. Environ. Qual. 45, 779–787.

Forsyth, B., Cameron, A., Miller, S., 1995. Explosives and water quality. Proceedings of Sudbury '95 Mining and the Environment, pp. 795–803.

Fowdar, H.S., Hatt, B.E., Breen, P., Cook, P.L.M., Deletic, A., 2015. Evaluation of sustainable electron donors for nitrate removal in different water media. Water Res. 85, 487–496.

Graf, D.R.H., Jones, C.M., Hallin, S., 2014. Intergenomic comparisons highlight modularity of the denitrification pathway and underpin the importance of community structure for N_2O emissions. PLoS One 9, e114118.

Greenan, C.M., Moorman, T.B., Kaspar, T.C., Parkin, T.B., Jaynes, D.B., 2006. Comparing carbon substrates for denitrification of subsurface drainage water. J. Environ. Qual. 35, 824–829.

Greenan, C.M., Moorman, T.B., Parkin, T.B., Kaspar, T.C., Jaynes, D.B., 2009. Denitrification in wood chip bioreactors at different water flows. J. Environ. Qual. 38, 1664–1671.

Grießmeier, V., Gescher, J., 2018. Influence of the potential carbon sources for field denitrification beds on their microbial diversity and the fate of carbon and nitrate. Front. Microbiol. 9, 1313.

Grießmeier, V., Bremges, A., McHardy, A.C., Gescher, J., 2017. Investigation of different nitrogen reduction routes and their key microbial players in wood chip-driven denitrification beds. Sci. Rep. 7, 170281.

Hassanpour, B., Giri, S., Pluer, W.T., Steenhuis, T.S., Geohring, L.D., 2017. Seasonal performance of denitrifying bioreactors in the Northeastern United States, field trials. J. Environ. Manag. 202, 242–253.

Hathaway, S.K., Porter, M.D., Rodríguez, L.F., Kent, A.D., Zilles, J.L., 2015. Impact of the contemporary environment on denitrifying bacterial communities. Ecol. Eng. 82, 469–473.

Healy, M.G., Ibrahim, T.G., Lanigan, G.J., Serrenho, A.J., Fenton, O., 2012. Nitrate removal rate, efficiency and pollution swapping potential of different organic carbon media in laboratory denitrification bioreactors. Ecol. Eng. 40, 198–209.

Henry, S., Baudoin, E., López-Gutiérrez, J.C., Martin-Laurent, F., Brauman, A., Philippot, L., 2004. Quantification of denitrifying bacteria in soils by *nirK* gene targeted real-time PCR. J. Microbiol. Methods 59, 327–335.

Henry, S., Bru, D., Stres, B., Hallet, S., Philippot, L., 2006. Quantitative detection of the nosZ gene, encoding nitrous oxide reductase, and comparison of the abundances of 16S rRNA, narG, nirK, and nosZ genes in soils. Appl. Environ. Microbiol. 72, 5181–5189.

Herbert Jr., R.B., Winbjörk, H., Hellman, M., Hallin, S., 2014. Nitrogen removal and spatial distribution of denitrifier and anammox communities in a bioreactor for mine drainage treatment. Water Res. 66, 350–360.

Hiller, K.A., Foreman, K.H., Weisman, D., Bowen, J.L., 2015. Permeable reactive barriers designed to mitigate eutrophication alter bacterial community composition and aquifer redox conditions. Appl. Environ. Microbiol. 81, 7114–7124.

Hoover, N.L., Bhandari, A., Soupir, M.L., Moorman, T.B., 2016. Woodchip denitrification bioreactors, impact of temperature and hydraulic retention time on nitrate removal. J. Environ. Qual. 453, 803–812.

Hou, T.T., Chen, N., Tong, S., Li, B., He, Q.C., Feng, C.P., 2019. Enhancement of rice bran as carbon and microbial sources on the nitrate removal from groundwater. Biochem. Eng. J. 148, 185–194.

Jang, J., Anderson, E.L., Venterea, R.T., Sadowsky, M.J., Rosen, C.J., Feyereisen, G.W., Ishii, S., 2019. Denitrifying bacteria active in woodchip bioreactors at low-temperature conditions. Front. Microbiol. 10, 635.

Jetten, M.S.M., van Niftrik, L., Strous, M., Kartal, B., Keltjens, J.T., Op den Camp, H.J.M., 2009. Biochemistry and molecular biology of anammox bacteria. Crit. Rev. Biochem. Mol. Biol. 44, 65–84.

Jones, C.M., Graf, D.R.H., Bru, D., Philippot, L., Hallin, S., 2013. The unaccounted yet abundant nitrous oxide-reducing microbial community: a potential nitrous oxide sink. ISME J. 7, 417–426.

Kiani, S., Kujala, K., Pulkkinen, J.T., Aalto, S.L., Suurnäkki, S., Kiuru, T., Tiirola, M., Kløve, B., Ronkanen, A.-K., 2020. Enhanced nitrogen removal of low carbon wastewater in denitrification bioreactors by utilizing industrial waste toward circular economy. J. Clean. Prod. 254, 119973.

Kozich, J.J., Westcott, S.L., Baxter, N.T., Highlander, S.K., Schloss, P.D., 2013. Development of a dual-index sequencing strategy and curation pipeline for analyzing amplicon sequence data on the MiSeq Illumina sequencing platform. Appl. Environ. Microbiol. 79, 5112–5120.

Kraft, B., Tegetmeyer, H.E., Sharma, R., Klotz, M.G., Ferdelman, T.G., Hettich, R.L., Geelhoed, J.S., Strous, M., 2014. The environmental controls that govern the end product of bacterial nitrate respiration. Science 345, 676–679.

Lenth, R., 2018. emmeans: Estimated Marginal Means, aka Least-Squares Means. https://CRAN.R-project.org/package=emmeans.

McMurdie, P.J., Holmes, S., 2013. Phyloseq: an R Package for reproducible interactive analysis and graphics of microbiome census data. PLoS One 8, e61217.

Mohan, S.B., Schmid, M., Jetten, M., Cole, J., 2004. Detection and widespread distribution of the nrfA gene encoding nitrite reduction to ammonia, a short circuit in the biological nitrogen cycle that competes with denitrification. FEMS Microbiol. Ecol. 49, 433–443.

Muyzer, G., Dewaal, E.C., Uitterlinden, A.G., 1993. Profiling of complex Micrombial populations by denaturing gradient gel-electroforesis analysis of polymerase chain reaction-apmlified genes coding for 16S ribosomal RNA. Appl. Environ. Microbiol. 59, 695–700.

Nordström, A., Herbert, R.B., 2017. Denitrification in a low-temperature bioreactor system at two different hydraulic residence times: laboratory column studies. Environ. Technol. 38, 1362–1375.

Nordström, A., Herbert, R.B., 2018. Determination of major biogeochemical processes in a denitrifying woodchip bioreactor for treating mine drainage. Ecol. Eng. 110, 54–66.

Oksanen, J., Blanchet, F.G., Friendly, M., Kindt, R., Legendre, P., McGlinn, D., Minchin, P.R., O'Hara, R.B., Simpson, G.L., Solymos, P., Stevens, M.H.H., Szoecs, E., Wagner, H., 2018. vegan: Community Ecology Package. https://CRAN.R-project.org/package=vegan.

Pinheiro, J., Bates, D., DebRoy, S., Sarkar, D., R Core Team, 2018. nlme: Linear and Nonlinear Mixed Effects Models. https://CRAN.R-project.org/package=nlme.

Porter, M.D., Andrus, J.M., Bartolerio, N.A., Rodriguez, L.F., Zhang, Y., Zilles, J.L., Kent, A.D., 2015. Seasonal patterns in microbial community composition in denitrifying cioreactors treating subsurface agricultural drainage. Microb. Ecol. 7, 710–723.

Putz, M., Schleusner, P., Rütting, T., Hallin, S., 2018. Relative abundance of denitrifying and DNRA bacteria and their activity determine nitrogen retention or loss in agricultural soil. Soil Biol. Biochem. 123, 97–104.

R Core Team, 2016. R: A Language and Environment for Statistical Computing. R Foundation for Statistical Computings.

Rognes, T., Flouri, T., Nichols, B., Quince, C., Mahe, F., 2016. VSEARCH: a versatile open source tool for metagenomics. Peerj 4.

Rosenberg, E., 2014. The phylum Fibrobacteres. In: Rosenberg, E., DeLong, E.F., Lory, S., Stackebrandt, E., Thompson, F. (Eds.), The Prokaryotes: Other Major Lineages of Bacteria and the Archaea. Springer Berlin Heidelberg, Berlin, Heidelberg, pp. 641–642.

Schipper, L.A., Robertson, W.D., Gold, A.J., Jaynes, D.B., Cameron, S.C., 2010. Denitrifying bioreactors—an approach for reducing nitrate loads to receiving waters. Ecol. Eng. 36, 1532–1543.

Schloss, P.D., Westcott, S.L., Ryabin, T., Hall, J.R., Hartmann, M., Hollister, E.B., Lesniewski, R.A., Oakley, B.B., Parks, D.H., Robinson, C.J., Sahl, J.W., Stres, B., Thallinger, G.G., Van Horn, D.J., Weber, C.F., 2009. Introducing mothur: open-source, platform-independent, community-supported software for describing and comparing microbial communities. Appl. Environ. Microbiol. 75, 7537–7541.

Schmid, M.C., Hooper, A.B., Klotz, M.G., Woebken, D., Lam, P., Kuypers, M.M.M., Pommerening-Roeser, A., op den Camp, H.J.M., Jetten, M.S.M., 2008. Environmental detection of octahaem cytochrome c hydroxylamine/hydrazine oxidoreductase genes of aerobic and anaerobic ammonium-oxidizing bacteria. Environ. Microbiol. 10, 3140–3149.

Schmidt, C.A., Clark, M.W., 2013. Deciphering and modeling the physicochemical drivers of denitrification rates in bioreactors. Ecol. Eng. 60, 276–288.

Šereš, M., Mocová, K.A., Moradi, J., Kriška, M., Kočí, V., Hnátková, T., 2019. The impact of woodchip-gravel mixture on the efficiency and toxicity of denitrification bioreactors. Sci. Total Environ. 647, 888–894.

Song, B., Lisa, J.A., Tobias, C.R., 2014. Linking DNRA community structure and activity in a shallow lagoonal estuarine system. Front. Microbiol. 5, 460.

Takahashi, S., Tomita, J., Nishioka, K., Hisada, T., Nishijima, M., 2014. Development of a prokaryotic universal primer for simultaneous analysis of bacteria and archaea using next-generation sequencing. PLoS One 9, e105592.

Throbäck, I.N., Enwall, K., Jarvis, A., Hallin, S., 2004. Reassessing PCR primers targeting nirS, nirK and nosZ genes for community surveys of denitrifying bacteria with DGGE. FEMS Microbiol. Ecol. 49, 401–417.

Vansoest, P.J., Robertson, J.B., Lewis, B.A., 1991. Methods for dietary fiber, neutral detergent fiber, and nonstarch polysaccharides in relation to animal nutrition. J. Dairy Sci. 74, 3583–3597.

Warneke, S., Schipper, L.A., Bruesewitz, D.A., McDonald, I., Cameron, S., 2011. Rates, controls and potential adverse effects of nitrate removal in a denitrification bed. Ecol. Eng. 37, 511–522.

Welsh, A., Chee-Sanford, J.C., Connor, L.M., Löffler, F.E., Sanford, R.A., 2014. Refined NrfA phylogeny improves PCR-based nrfA gene detection. Appl. Environ. Microbiol. 80, 2110–2119.

Wilhelm, R.C., Singh, R., Eltis, L.D., Mohn, W.W., 2019. Bacterial contributions to delignification and lignocellulose degradation in forest soils with metagenomic and quantitative stable isotope probing. ISME J. 13, 413–429.

Yilmaz, P., Parfrey, L.W., Yarza, P., Gerken, J., Pruesse, E., Quast, C., Schweer, T., Peplies, J., Ludwig, W., Glockner, F.O., 2014. The SILVA and "All-species Living Tree Project (LTP)" taxonomic frameworks. Nucleic Acids Res. 42, D643–D648.

Zhu, A.P., Chen, J.Y., Gao, L., Shimizu, Y., Liang, D.M., Yi, M., Cao, L.X., 2019. Combined microbial and isotopic signature approach to identify nitrate sources and transformation processes in groundwater. Chemosphere 228, 721–734.

Supplementary material

Substrate type determines microbial activity and community composition in bioreactors for nitrate removal by denitrification at low temperature

Maria Hellman[a,*], Valerie Hubalek[a], Jaanis Juhanson[a], Robert Almstrand[a,1], Sari Peura[a], Sara Hallin[a]

[a]Swedish University of Agricultural Sciences, Department of Forest Mycology and Plant Pathology, Box 7026, 75007 Uppsala, Sweden

[1]Present address: "Swedish Agency for Marine and Water Management", Box 11930, 40439 Gothenburg, Sweden

Figures

Tables

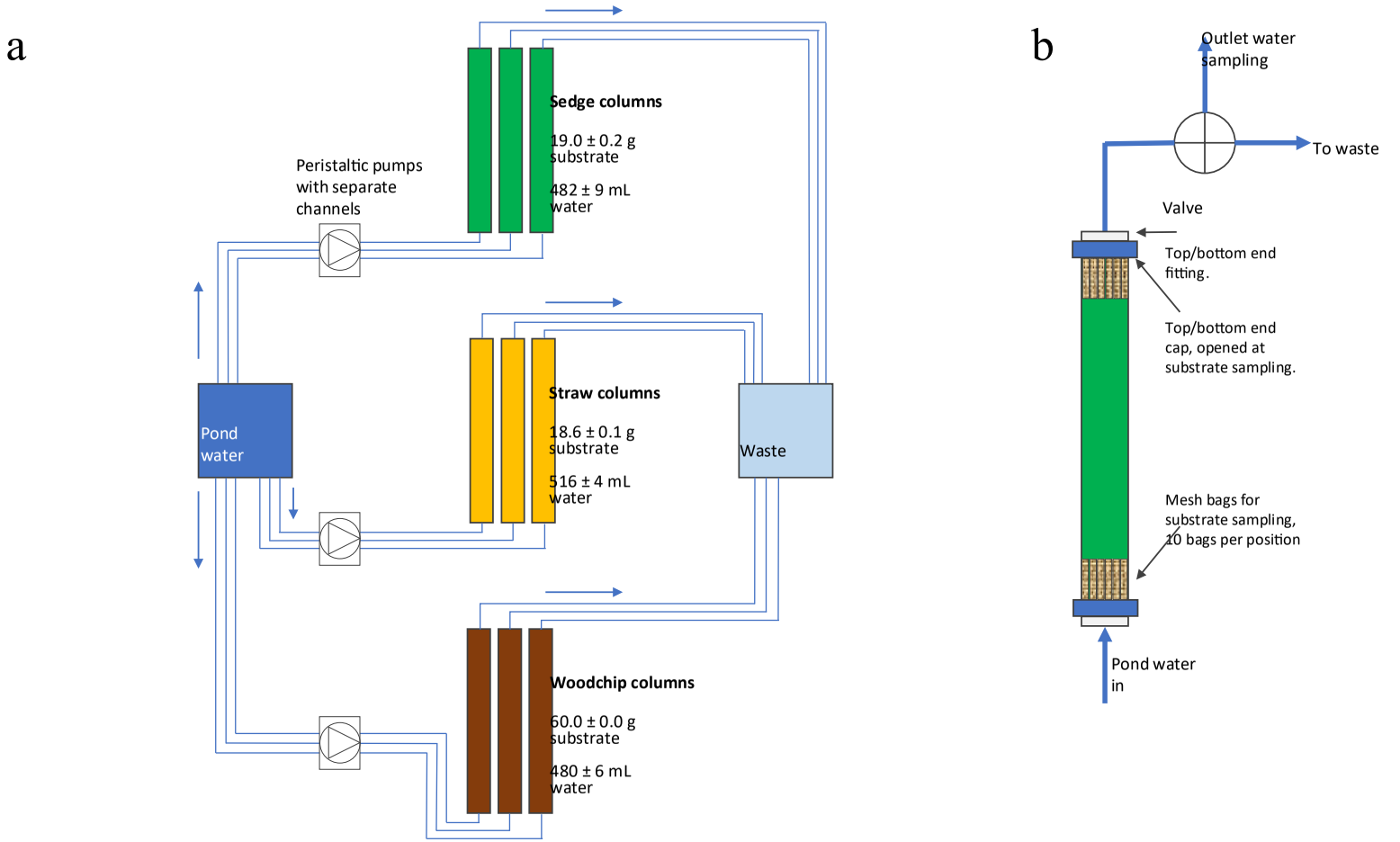

Figure S1. Experimental setup. (a) Schematic drawing showing connections between water reservoir (”Pond water”), pumps, columns, and waste reservoir. Amounts of substrate and water in the columns are indicated. (b) Detailed drawing of one column showing where substrate and water samples were taken.

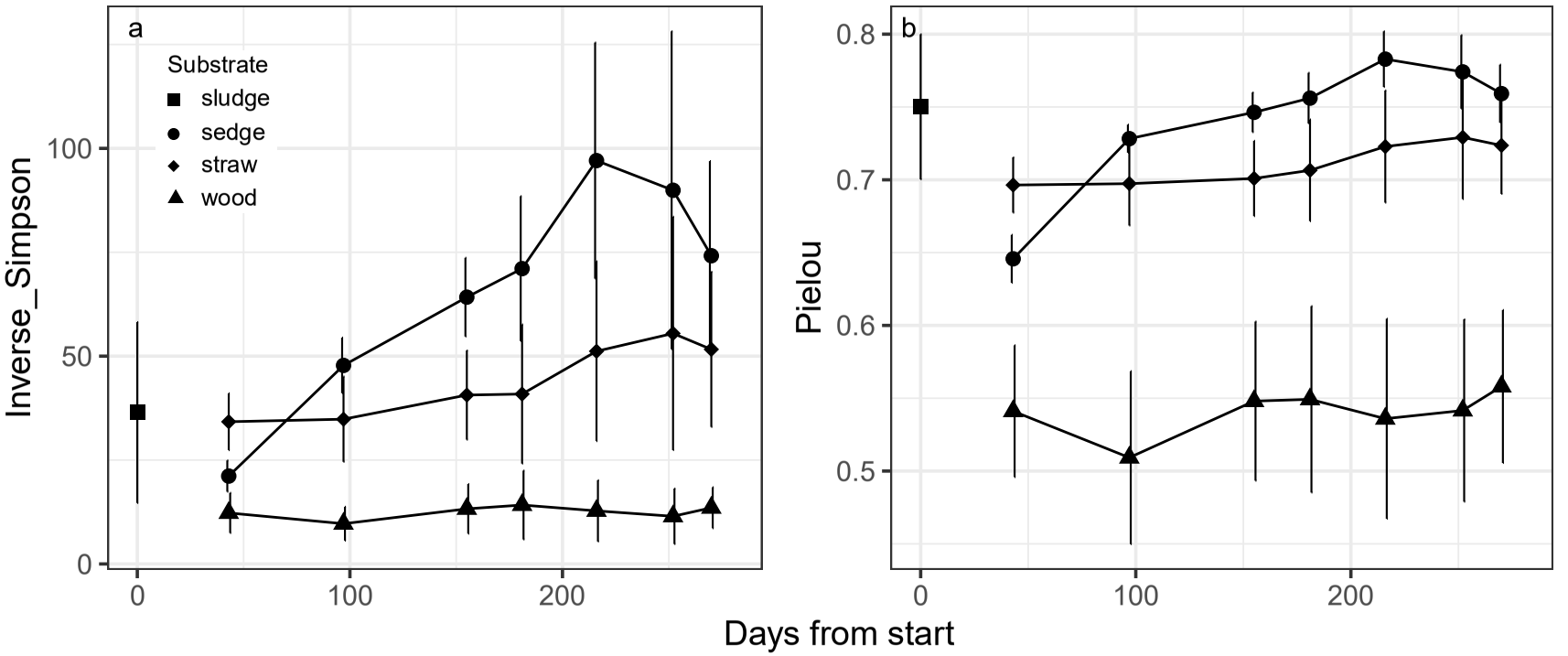

Figure S2. Bacterial alpha-diversity in the inoculum sludge and in the reactor substrate types during the experimental period. For each of the reactors, inlet and outlet samples are included. Additionally, at day 270 bulk samples are included. (a) Inverse Simpson index. (b) Pielou´s evenness. Substrate types and sludge are indicated with symbols. Mean, n=6, day 270 n= 15.

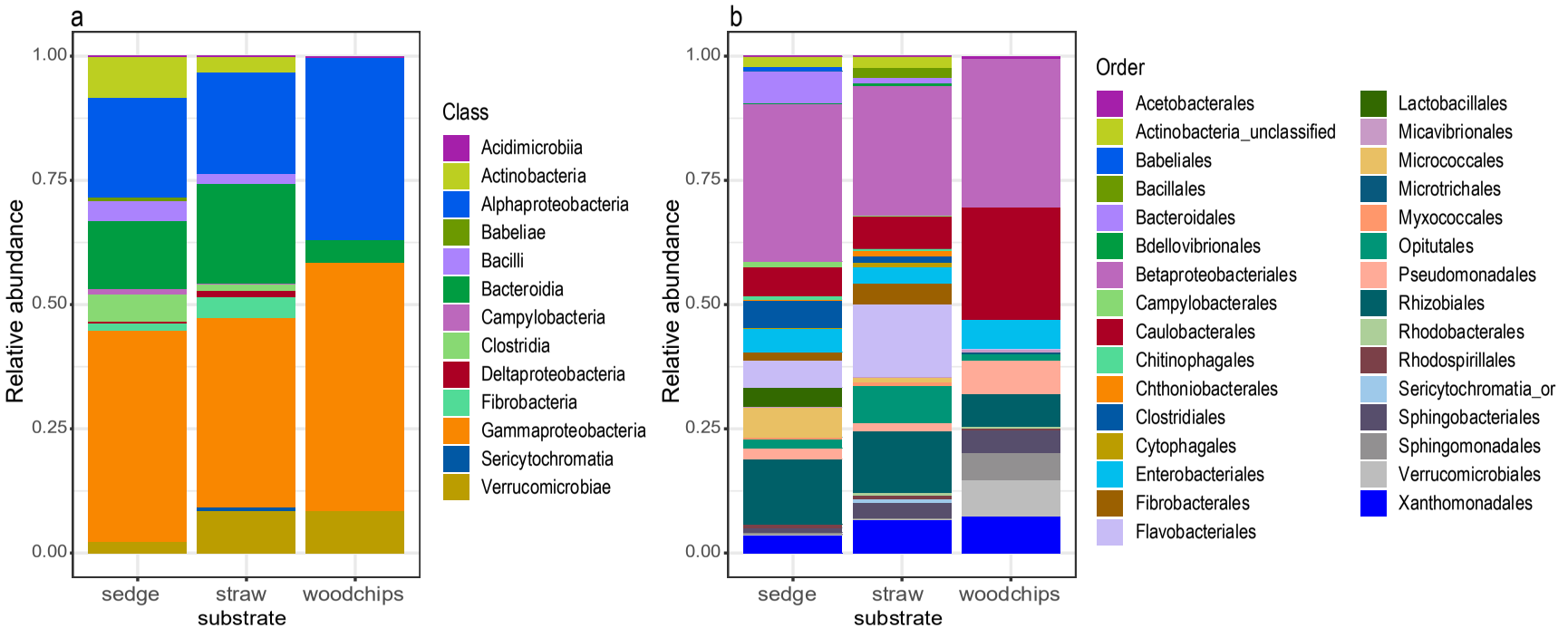

Figure S3. Taxonomic composition of the bacterial communities in the reactors at day 270 based on relative abundances of the 50 most abundant OTU:s per substrate type in the bulk samples (mean, n=9, 9, 8 for sedge, straw and woodchips respectively). (a) class level, (b) order level.

Table S1. Theoretical hydraulic residence times and N removal efficiency in the reactors.

		Sedge		Straw		Wood	
Period	N[a]	THRT	removal	THRT	removal	THRT	removal
days		days	%	days	%	days	%
5 – 21[a]	3	4.2 ± 0.1	95 ± 0.35	4.5 ± 0.0	66 ± 50	4.2 ± 0.1	20 ± 4.5
22 - 112	15	1.5 ± 0.0	74 ± 17	1.6 ± 0.0	49 ± 19	5.2 ± 0.3	70 ± 19
113 - 119	1–3	1.7 ± 0.0	55 ± NA[b]	1.2 ± 0.1	33 ± 3.2	6.0 ± 0.2	47 ± 2.5
120 - 179	13–15	1.7 ± 0.0	46 ± 11	1.8 ± 0.1	42 ± 9.2	6.0 ± 0.2	52 ± 14
180 - 270	18–24	1.8 ± 0.1	51 ± 13	2.2 ± 0.5	44 ± 16	7.2 ± 0.4	37 ± 18

[a] number of observations for calculating removal efficiency.
[b] no data for the time period.

Table S2. Primers, amplification efficiency and thermal cycling conditions for quantification of marker genes

Gene Primer names	Sequences (5'-3')	Final primer concentration (μM)	Amplification efficiency (%)	Thermal cycling protocol[a]
16S rRNA 341F 534R	CCT ACG GGA GGC AGC AG ATT ACC GCG GCT GCT GGC A	0.50	99	(95°C, 15 s; 60°C, 30 s; 72°C, 30 s; 80°C, 30 s) x 35
nirK 876F R3Cu	ATYGGCGGVCAYGGCGA GCCTCGATCAGRTTGTGGTT	0.25	88	(95°C, 15 s;(63°C – 58°C, -1°/cycle), 30 s; 72°C, 30 s) x 6 (95°C, 15 s; 58°C, 30 s; 72°C, 30 s; 80°C, 30 s) x 35
nirS cd3aFm R3cdm	AACGYSAAGGARACSGG GASTTCGGRTGSGTCTTSAYGAA	0.80	93	(95°C, 15 s;(65°C – 60°C, -1°/cycle), 30 s; 72°C, 30 s) x 6 (95°C, 15 s; 60°C, 30 s; 72°C, 30 s; 80°C, 30 s) x 35
***nosZ*I** 1840F 2090R	CGC RAC GGC AAS AAG GTS MSS GT CAK RTG CAK SGC RTG GCA GAA	0.50	84	(95°C, 15 s;(65°C – 60°C, -1°/cycle), 30 s; 72°C, 30 s) x6 (95°C, 15 s; 60°C, 30 s; 72°C, 30 s; 80°C, 30 s) x 35
***nosZ*II** nosZII-F nosZII-R	CTI GGI CCI YTK CAY AC GCI GAR CAR AAI TCB GTR C	0.80	100	(95°C, 15 s; 54°C, 30 s; 72°C, 30 s; 80°C, 30 s) x 40
nrfA nrfAF2aw nrfAR1	CARTGYCAYGTBGARTA TWNGGCATRTGRCARTC	0.50	93	(95°C, 15 s; 57°C, 30 s; 72°C, 30 s; 80°C, 30 s) x 35
***hzo* (i.e. *hdh*)** hzocl1 F1 hzocl1 R2	TGYAAGACYTGYCAYTGG ACTCCAGATRTGCTGACC	0.80	101	(95°C, 15 s; 52.5°C, 30 s; 72°C, 30 s; 80°C, 30 s) x 35

[a]All protocols started with 7 min at 95°C. All protocols ended with a melt curve: (95°C, 15 s;(60 to 95° C, 10 s, increment 0.5°)). Flourescent signal was aquired at 80°C.

Table S3. Carbon content in the reactor substrate types at start of the experiment (% dry weight; mean ± SD, n=3)

Substrate	Total C[a]	Hemicellulose[a]	Cellulose[a]	Lignin[a]
Woodchip	49.99^{A} ± 0.16	15.7^{B} ± 0.40	50.3^{A} ± 0.36	21.3^{A} ± 2.32
Barely straw	45.73^{B} ± 0.13	30.9^{A} ± 0.25	36.73^{B} ± 1.51	4.35^{B} ± 0.43
Carex	45.13^{B} ± 0.13	31.7^{A} ± 0.65	27.10^{C} ± 0.53	3.54^{B} ± 0.58

[a]Different capital letters within the same column denotes Tukey´s honest significant difference ($p<0.01$) between the substrate types.

Table S4. Two-way analysis of variance on the effects of position and time on alpha diversity indices of the microbial communities in the solid substrates.

Variable	Position		Time		Position x Time	
	F	P	F	P	F	P
Shannon index						
Woodchips	68.10	0.0012	1.84	0.1400	1.40	0.2597
Straw	7.41	0.0528	15.67	<0.0001	9.32	<0.0001
Sedge	20.56	0.0105	67.42	<0.0001	4.72	0.0032
Pielou index						
Woodchips	58.63	0.0016	2.12	0.0946	1.33	0.2892
Straw	3.54	0.1332	11.25	<0.0001	10.50	<0.0001
Sedge	1.96	0.2344	68.22	<0.0001	4.19	0.0058
Inverse Simpson						
Woodchips	34.42	0.0042	1.42	0.2545	1.15	0.3711
Straw	5.21	0.0846	10.96	<0.0001	6.16	0.0005
Sedge	16.61	<0.0001	20.84	<0.0001	4.01	0.0073

III

Received: 10 September 2019 | Accepted: 19 November 2020

DOI: 10.1002/jeq2.20181

Journal of Environmental Quality

TECHNICAL REPORTS

Bioremediation and Biodegradation

Microbial controls on net production of nitrous oxide in a denitrifying woodchip bioreactor

Albin Nordström[1] | **Maria Hellman**[2] | **Sara Hallin**[2] | **Roger B. Herbert**[1]

[1] Dep. of Earth Sciences, Uppsala Univ., Villavägen 16, Uppsala SE-752 36, Sweden

[2] Dep. of Forest Mycology and Plant, Pathology, Swedish Univ. of Agricultural Sciences, Box 7026, Uppsala SE-750 07, Sweden

Correspondence
Roger B. Herbert, Dep. of Earth Sciences, Uppsala Univ., Villavägen 16, SE-752 36, Uppsala, Sweden.
Email: roger.herbert@geo.uu.se

Assigned to Associate Editor Michelle Soupir.

Funding information
VINNOVA, Grant/Award Number: 2014-011334; Luossavaara-Kiirunavaara Aktiebolag (LKAB)

Abstract

Denitrifying woodchip bioreactors are potential low-cost technologies for the removal of nitrate (NO_3^-) in water through denitrification. However, if environmental conditions do not support microbial communities performing complete denitrification, other N transformation processes will occur, resulting in the export of nitrite (NO_2^-), nitrous oxide (N_2O), or ammonium (NH_4^+). To identify the factors controlling the relative accumulation of NO_2^-, N_2O, and/or NH_4^+ in denitrifying woodchip bioreactors, porewater samples were collected over two operational years from a denitrifying woodchip bioreactor designed for removing NO_3^- from mine water. Woodchip samples were collected at the end of the operational period. Changes in the abundances of functional genes involved in denitrification, N_2O reduction, and dissimilatory NO_3^- reduction to NH_4^+ were correlated with porewater chemistry and temperature. Temporal changes in the abundance of the denitrification gene *nirS* were significantly correlated with increases in porewater N_2O concentrations and indicated the preferential selection of incomplete denitrifying pathways ending with N_2O. Temperature and the total organic carbon/NO_3^- ratio were strongly correlated with NH_4^+ concentrations and inversely correlated with the ratio between denitrification genes and the genes indicative of ammonification (Σ*nir*/*nrfA*), suggesting an environmental control on NO_3^- transformations. Overall, our results for a denitrifying woodchip bioreactor operated at hydraulic residence times of 1.0–2.6 d demonstrate the temporal development in the microbial community and indicate an increased potential for N_2O emissions with time from the denitrifying woodchip bioreactor.

1 | INTRODUCTION

Denitrifying fixed-bed bioreactors are low-cost technologies for the removal of nitrate (NO_3^-) from water, which passes through an organic porous material, supplying electrons for the reduction of NO_3^- to nitrogen gas (N_2) (Schipper, Robertson, Gold, Jaynes, & Cameron, 2010). Woodchips are typically used due to their high permeability, moderate reactivity, and capability of providing a carbon (C) and energy source for denitrification (Cameron & Schipper, 2010; Robertson, 2010; Schipper et al., 2010). However, the release of other nitrogen (N) species (nitrite [NO_2^-], nitric oxide [NO], and the greenhouse gas nitrous oxide [N_2O]) from intermediate steps during denitrification is a potential drawback of

Abbreviations: DNRA, dissimilatory NO_3^- reduction to ammonium; DWB, denitrifying woodchip bioreactor; HRT, hydraulic residence time; NMDS, nonmetric multidimensional scaling; PCR, polymerase chain reaction; qPCR, quantitative polymerase chain reaction; TOC, total organic carbon.

denitrifying woodchip bioreactors (DWBs) (Davis, Martin, Moorman, Isenhart, & Soupir, 2019; Feyereisen et al., 2016). Up to 10% of the reduced NO_3^- is exported as N_2O from DWBs (Davis et al., 2019; Elgood, Robertson, Schiff, & Elgood, 2010; Feyereisen et al., 2016; Greenan, Moorman, Kaspar, Patkin, & Jaynes, 2006; Warneke et al., 2011b). The release of these compounds is affected by temperature, NO_3^- concentration, dissolved oxygen concentration (Elgood et al., 2010; Grießmeier, Bremges, McHardy, & Gescher, 2017), and the functional communities involved in the production or reduction of these compounds (Warneke et al., 2011b).

Denitrifiers compete with bacteria performing dissimilatory NO_3^- reduction to ammonium (NH_4^+) (DNRA) for NO_3^-, and the outcome of this competition determines if NO_3^- is removed as a gaseous N species or is converted to aqueous NH_4^+, thereby affecting the overall N removal capacity of the DWB. The availability of organic C in relation to NO_3^- (C/NO_3^- ratio) has been shown to control this competition, with high C/NO_3^- ratios favoring DNRA (Kraft et al., 2014; Van Den Berg, Van Dongen, Abbas, & Van Loosdrecht, 2015; Yoon, Cruz-García, Sanford, Ritalahti, & Löffler, 2015) and low ratios favoring denitrification, which includes an increased risk for the net production of N_2O (Pan, Ni, Bond, Ye, & Yuan, 2013). This is not only because more N_2O is produced during denitrification than DNRA but also because denitrification can terminate with N_2O under NO_3^-–rich conditions (Felgate et al., 2012). For some denitrifiers, N_2O is always the end product because they do not have the genetic repertoire needed to further reduce N_2O to N_2 and because they, as well as nondenitrifying N_2O reducers, also affect the net N_2O emissions (Graf, Jones, & Hallin, 2014; Hallin, Philippot, Löffler, Sanford, & Jones, 2018; Jones et al., 2014). In DWBs, C availability is controlled by woodchip degradation, and the relative availability of different C substrates may change throughout DWB operations (Grießmeier & Gescher, 2018; Grießmeier et al., 2017; Nordström & Herbert, 2018). It can therefore be expected that differences in relative abundances of the functional groups involved in the different N transforming processes develop over time during DWB operation. The proportion between these functional groups ultimately controls the export of N species from DWBs, but little is known about the temporal development of the N-transforming community and the associated temporal changes in the production of NO_2^-, N_2O, and NH_4^+ in DWBs.

In this study, temporal and spatial changes of the abundances of functional groups performing denitrification and DNRA in the porewater were studied with the objectives to relate these patterns with changes in the concentrations of NO_2^-, N_2O, and NH_4^+ in the porewater and overall reactor performance in a previously described DWB (Nordström & Herbert, 2018). We hypothesized that temporal and spatial changes in the genetic potential for denitrification and DNRA, determined as abundances of functional genes in denitrifying and DNRA bacteria, control concentrations of NO_2^-, N_2O, and NH_4^+ and that their abundances are a consequence of changes in C/NO_3^- ratios. Because the porewater community is more easily sampled for temporal studies than the woodchip-associated community, we primarily monitored the development of the N-reducing community in the porewater. However, for the last sampling episode, we compared the spatial distribution of the abundance of denitrifying and DNRA bacteria in the woodchip matrix with their spatial distribution in porewater.

Core Ideas

- A high degree of spatial and temporal variability for functional gene abundances was noted in porewater.
- Temperature dependence was exhibited especially for the gene *nrfA*.
- N_2O production correlated with *nirS* abundance and Σ*nir*/Σ*nosZ* ratio.
- TOC/NO_3^- ratio positively correlated with *nrfA* abundance and NH_4^+ concentration.
- A truncated denitrification pathway was promoted with time in the bioreactor.

2 | MATERIALS AND METHODS

2.1 | Study site and DWB system

The subsurface DWB described by Nordström and Herbert (2018) was constructed at the Kiruna iron ore mine, northern Sweden (67°51′ N, 20°13 ′E), with the purpose to reduce NO_3^- concentrations in mine and process water originating from the use of ammonium nitrate–based explosives. For this study, samples from the inlet, outlet, and five porewater sampling points along the bottom centerline of the DWB were used (Supplemental Figure S1).

The DWB was filled with decorticated pine woodchips. To increase the initial abundance of denitrifying microorganisms, digested sewage sludge mixed with water was added while the DWB was filled with woodchips. The center areas of the DWB were capped by glacial till (Supplemental Figure S1) with the intention to restrict oxygen diffusion into the DWB.

Mine drainage from the clarification pond at the mine site was pumped to the DWB, where it entered through a perforated drainage pipe near the surface of the DWB and extending across its width. The hydraulic residence time (HRT) of the DWB was adjusted several times during the operational periods by changing the pump discharge

(Supplemental Table S1), with 2.6 d being the most common HRT (varying between 1 and 2.6 d). The choice of HRT was based on a previous laboratory-scale experiment where relatively long HRTs at low temperature provided nearly complete removal of NO_3^- (Nordström & Herbert, 2017). The DWB was operated for two consecutive field seasons: 22 June to 21 Nov. 2015 (Days 0–151) and 9 May to 21 Oct. 2016 (Days 322–490), referred to as the first and second operational year, respectively.

2.2 | DWB sampling

2.2.1 | Water sampling

Porewater, inlet water, and outlet water were sampled once a month (referred to as "profile sampling") to analyze water chemistry (Nordström & Herbert, 2018). Briefly, a peristaltic pump was used for porewater sampling, and the first ∼2 L of water was discarded prior to sample collection to ensure a representative sample. Inlet and outlet water was grab-sampled. For analyses of microbial communities involved in N transformation processes, water sampled on Days 57, 85, 113, 365, 400, 428, 456, and 477 was filtered using Sterivex filter units, with 0.22-μm Millipore Express polyethersulfone membranes, attached to 60-ml syringes. Inlet water samples from Days 57 and 85 were discarded because of technical problems during sampling. Between 540 and 1,680 ml of water (average, 990 ml) was required to saturate the Sterivex filter units. The syringes were rinsed in sample water three times prior to filtration, and new polyvinyl chloride plastic tubing for the peristaltic pump was used for each sample. The Sterivex filter units were stored on ice for ∼6 h following collection and frozen at −20 ˚C until DNA extraction.

Denitrifying woodchip bioreactor porewater temperature was obtained from thermistors attached to porewater sampling points at the base of the DWB.

2.2.2 | Woodchips and sewage sludge media

Sewage sludge samples used as inoculum were collected in sterile 50-ml plastic tubes at the time of DWB construction and frozen at −20 ˚C until analysis. Woodchips were sampled following the termination of DWB operations (Day 490). The sampling focused on the deepest regions of the DWB because a previous DWB study indicated a significantly greater abundance of 16S rRNA, *nirS*, *nirK*, and *nosZI* genes at the greatest depths in a DWB (Herbert, Winbjörk, Hellman, & Hallin, 2014). Water was drained from the DWB, and traverse trenches were excavated at 2.7, 11.2, 19.7, 28.2, and 33.9 m from the inlet (Supplemental Figure S1). Woodchip samples were collected along a center line at bottom depth (corresponding to the five porewater sampling points) and at 0.4 m above the bottom. Samples were also collected at depths of 11.2, 19.7, and 28.2 m at ±1.35 m from the center line and 0.4 m above bottom (i.e., the deepest possible depth due to the trapezoidal shape of the reactor). At the inlet and outlet, woodchip samples were collected from the surface of the bioreactor. All samples were collected in triplicate. The samples were stored in sterile 50-ml plastic tubes and placed on ice for ∼6 h following collection, frozen at −10 ˚C for 4 d, and stored at −20 ˚C until DNA extraction.

2.3 | Analyses

2.3.1 | Chemical analyses of water samples

We used porewater chemistry data from Nordström and Herbert (2018). Dissolved N_2O concentrations were determined via headspace equilibrium and analyzed at the Swedish University of Agricultural Sciences in Uppsala. The dissolved N_2O concentrations reported in this study differ from those reported in Nordström and Herbert (2018) because errors were identified in the latter study regarding the calculation of dissolved N_2O from headspace concentrations. See Nordström and Herbert (2018) for additional details on analytical methods.

2.3.2 | DNA extraction and quantitative real-time polymerase chain reaction

DNA from the Sterivex filter units was extracted using the MoBio PowerWater Sterivex DNA kit following the manufacturer's instructions, including incubation at 90 ˚C (Mobio Laboratories Inc., 2018). For DNA extraction from the woodchips (4 g) and sewage sludge (0.2 g), the DNeasy PowerMax Soil Kit was used according to the manufacturer's instructions (Qiagen GmbH). Both the woodchips and digested sewage sludge were freeze-dried prior DNA extraction.

Real-time quantitative polymerase chain reaction (qPCR) was used to determine the abundances of functional genes specific for the denitrification, N_2O reduction, DNRA, and anammox pathways and used as proxies for the communities performing these reactions. Primers for *nirS* (Throbäck, Enwall, Jarvis, & Hallin, 2004) and *nirK* (Hallin & Lindgren, 1999; Henry et al., 2004) were used for the denitrifiers, *nosZ*I (Henry, Bru, Stres, Hallet, & Philippot, 2006) and *nosZ*II (Jones, Graf, Bru, Philippot, & Hallin, 2013) for the N_2O reducers, *hdh* (Schmid et al., 2008) for anammox bacteria, and *nrfA* (Mohan, Schmid, Jetten, & Cole, 2004; Welsh, Chee-Sanford, Connor, Löffler, & Sanford, 2014) for the DNRA communities. These primers, especially the ones

for *nir* and *nrfA*, do not cover the extant diversity of each gene (e.g., Bonilla-Rosso, Wittorf, Jones, & Hallin, 2016; Cannon, Sanford, Connor, Yang, & Chee-Sanford, 2019), which results in an underestimation of the absolute abundances. However, they allow for a comparative analysis of the relative abundance across samples by sampling a standard subset of each functional group for which functionality is verified (Penton et al., 2013).

The 16S rRNA gene (Muyzer, Dewaal, & Uitterlinden, 1993) was used as a proxy for the abundance of the total bacterial community. Each 15-µl qPCR reaction contained 2–5 ng (water samples) or 0.1–0.3 ng (woodchip samples) of DNA, 0.25–2 µM of each primer, 15 µg bovine serum albumin, and 1x iQ SYBR Green Supermix (BioRad Laboratories). Two independent quantifications per gene were performed using the BioRad CFX Real-Time System (BioRad Laboratories). Potential PCR inhibition in the samples was tested by spiking each sample with the pGEM-T plasmid (Promega Co.) and amplifying it using plasmid-specific primers. Amplification was compared between samples and nonsample (water control) reactions, and no inhibition was present in the samples with the amounts of DNA extract used. Cycling protocols and primer concentrations are described in the supporting information (Supplemental Table S2).

2.3.3 | Statistical analysis and parameter estimation

Differences in the abundances of all functional genes and the 16S rRNA genes between porewater (including outlet samples), inlet water, woodchips, and sewage sludge were tested using Dunn's test, which is appropriate for groups with unequal numbers of observations (Zar, 2010), in R package 'FSA' (Dinno, 2017), which performs a Kruskal–Wallis test (normality could not be assumed based on a Shapiro–Wilks test; Supplemental Table S3) followed by pairwise comparisons. Corrections for multiple comparisons were done by false discovery rate (Benjamini & Hochberg, 1995). For comparisons between two groups, Wilcoxon rank sum tests were used.

Nonmetric multidimensional scaling (NMDS; using the R package 'vegan' [Oksanen et al., 2018]) was used to illustrate the structural differences in the concatenated N reducing communities (i.e., based on all functional genes) between samples from the porewater (including outlet samples), inlet water, woodchips, and the inoculum (digested sewage sludge). The abundances of the studied marker genes from each individual sample in the DWB were assumed to represent a specific N-reducing community. Gene abundances were square-root transformed and submitted to Wisconsin double standardization. Then, a community matrix with Bray–Curtis dissimilarities was created and the NMDS was run with a maximum of 250 iterations.

We compared the similarity between the N reducing community in the porewater samples with those in the three potential sources: the inlet water, the woodchip media, and the inoculant sewage sludge. Community matrices based on Bray–Curtis dissimilarities were generated for each sample source using the same procedure as described above and compared using a permuted ($n = 999$) analysis of similarity (*anosim*; R-package 'vegan') (Oksanen et al., 2018).

To identify the selective pressures for changes in NO_2^-, N_2O, and NH_4^+ concentrations in the DWB, we first tested the correlation between porewater pH, temperature, and solute concentrations (NO_3^-, NO_2^-, N_2O, NH_4^+, total organic C [TOC]) with the N reducing community structure in the porewater samples using a permuted ($n = 999$) correlation test (*envift*; R-package 'vegan') (Oksanen et al., 2018). Further, a Spearman's rank correlation analysis with permutation (10,000) tests (R-package 'coin') (Hothurn, Hornik, van de Wiel, & Zeileis, 2006) was used to correlate N species in the porewater with individual gene abundances and abundance ratios.

3 | RESULTS

3.1 | Porewater chemistry

The NO_3^-–N, NO_2^-–N, NH_4^+–N, N_2O–N, and TOC concentrations as well as the C/NO_3^- ratio (calculated from TOC and NO_3^-–N concentrations) are presented as a function of time, temperature, and position in the DWB (Figure 1). Nitrate concentrations consistently decreased along the DWB flowpath throughout the operational period (Figure 1a), with the lowest concentrations observed during the warmer periods (Days 1–85, 365–428). Nitrogen removal rates ranged from 0.14 to 37.5 g N m^{-3} (DWB volume) d^{-1} and have been previously shown to have a temperature dependence (Nordström & Herbert, 2019). Nitrite concentrations (Figure 1b) were observed up to 11 mg L^{-1} in the first half of the DWB during the first operational year but were below 1 mg L^{-1} in the DWB effluent with the exception of first week of operations. Similarly, NH_4^+–N concentrations were elevated throughout the DWB during the first operational year (Figure 1c) but remained relatively constant at <0.5 mg L^{-1} during the second operational year. Nitrous oxide (Figure 1d) varied irregularly with sampling position and time but with a tendency for higher concentrations in the first half of the DWB during the summer months (Days 400 and 428). Nitrous oxide production rates, determined from the difference in inlet and outlet N_2O–N concentrations, ranged from ~0 to 3.7 mg N_2O–N m^{-3} d^{-1}; this can be compared with a production in the range of 12–152 mg

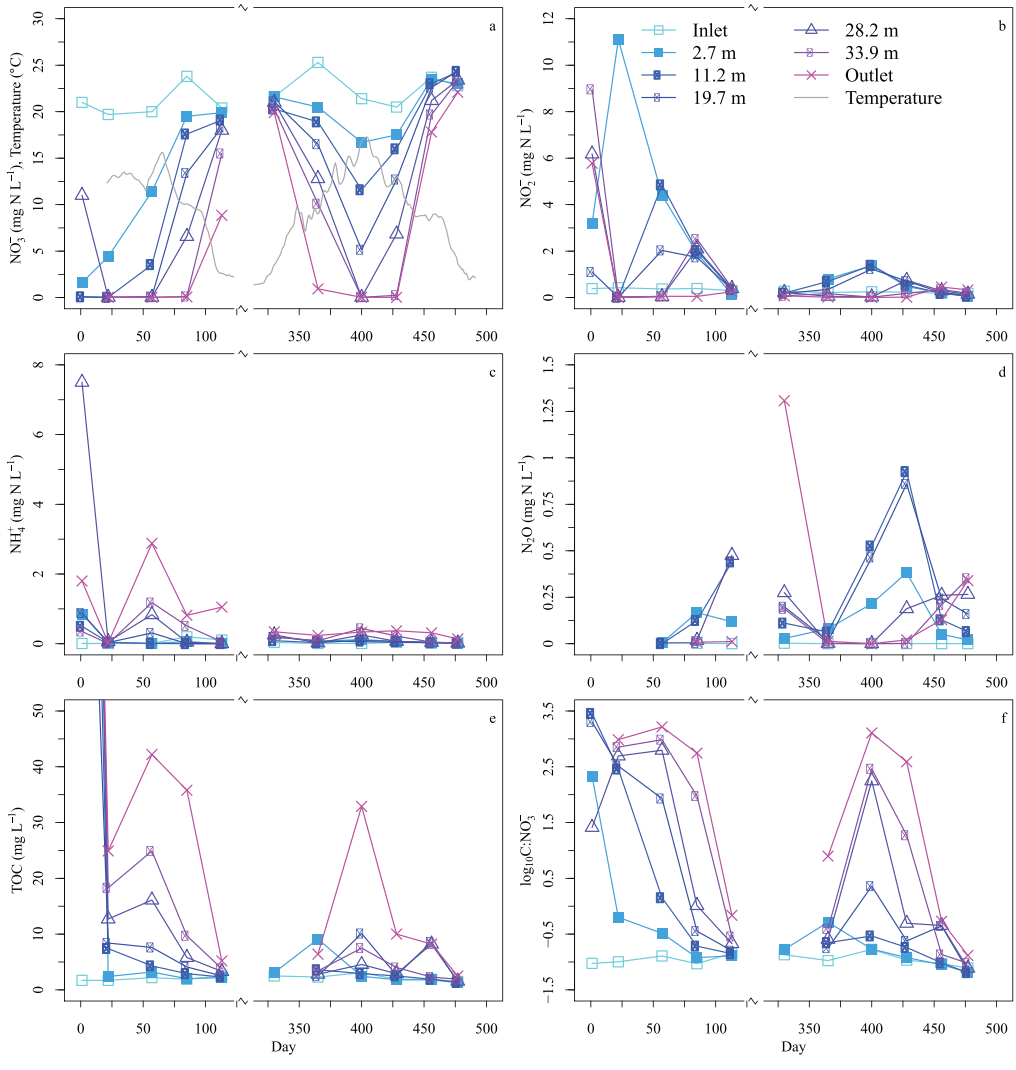

FIGURE 1 Porewater chemistry in the bioreactor. Concentrations of (a) NO_3^-–N, (b) NO_2^-–N, (c) NH_4^+–N, (d) N_2O–N, (e) total organic C (TOC), and (f) log TOC/NO_3^-–N ratio as a function of time and position in the bioreactor. Position refers to distance from bioreactor inlet. On Day 1, TOC concentrations were 138–244 mg L^{-1} (inlet excluded).

N_2O–N m^{-3} d^{-1} for DWB's with much shorter HRTs (2–16 h) and composed of hardwood woodchips (Davis et al., 2019). As demonstrated in the porewater data, the average concentrations and concentration ranges of denitrification products (i.e., NO_2^-–N, N_2O–N) when combined from all positions were significantly different between the first and second operational year (Supplemental Figure S2).

Total organic C concentrations generally decreased during the first operational year and remained <10 mg L^{-1} during the second year (with the exception of one sample; Figure 1e). The resultant TOC/NO_3^- ratio (Figure 1f) exhibited increasing values with travel distance through the DWB and during the summer months, reflecting primarily the variations in NO_3–N concentration.

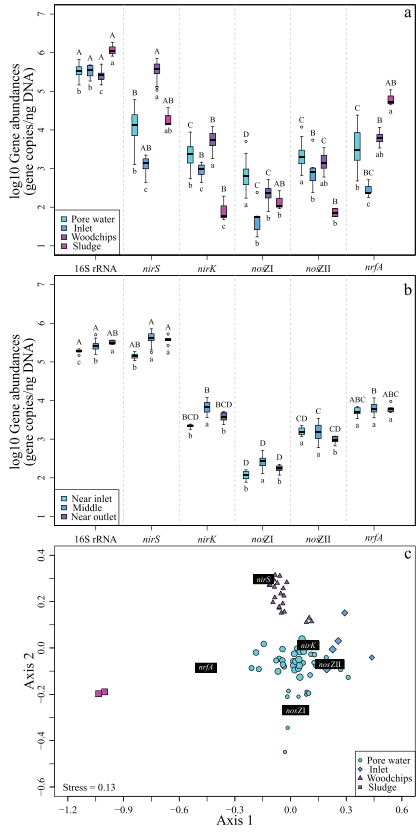

FIGURE 2 Abundances of the 16S rRNA gene and the functional genes *nirS*, *nirK*, *nosZ*I, *nosZ*II, and *nrfA* in bioreactor samples. (a) Gene abundances in porewater (n = 47–54), inlet water (n = 7), woodchips corresponding to the porewater sampling points and outlet (n = 18), and digested sewage sludge used as inoculum (n = 2–3) across the two operational years. Based on Dunn's test ($p < .05$), uppercase letters indicate differences in gene abundances within sample type, and lowercase letters indicate differences in gene abundance compared with the respective gene abundance in other sample sources. (b) Gene abundances in woodchip samples from 0 m (bottom) and 0.4 m above bottom in the bioreactor, with data from the two depths combined. "Near inlet" (n = 6) and "Near outlet" (n = 6) indicate samples from 2.7 and 33.9 m from the inlet, along the center line (see Supplemental Figure S1); "Middle" (n = 36) indicates samples from 11.2, 19.7, and 28.2 m from inlet, at both depths along the centerline and at 0.4 m depth along the sides of the reactor (±1.35 m from centerline). Based on Dunn's test ($p < .05$), uppercase letters indicate differences in gene abundances within each position, and lowercase letters indicate differences in gene abundance compared with the respective gene abundance in other positions. In (a) and (b), empty circles are outliers and lines through boxes signifies median. (c) Nonmetric multidimensional scaling ordination based on Bray–Curtis dissimilarities for the abundances of the functional genes in porewater, inlet water, woodchips (from bottom centerline, inlet, and outlet), and digested sewage sludge used as inoculum. For water samples, increasing symbol sizes imply later sampling dates. Gene names in black boxes denote species scores

3.2 | Gene abundances and N-reducing community structure

The abundances of the total bacterial community and genes coding for the different N reducing pathways differed among sample types, but the *hdh* gene coding for anammox was not detected in any of the samples (Figure 2a). An assessment of the difference between woodchip samples collected at different depths indicated that there was not a significant difference ($p < .05$, one-sided Wilcoxon test) in the abundances of the 16S rRNA genes and the functional genes between the two sampling depths, with the exception of *nirS*. For *nirS*, there were significantly lower abundances at the bottom compared with 0.4 m above ($p < .01$) (data not shown). Regardless, woodchip samples from these two sample depths are considered together for the rest of this study.

There were significant differences in the abundances of the 16S rRNA and functional genes between the porewater, inlet water, woodchips, and digested sewage sludge (Figure 2a; Supplemental Table S4). The sample source with the highest abundance of functional genes differed depending on the gene, although gene abundances in the inlet water were most often the lowest among the different sample sources (Figure 2a). For the different genes and sample sources, *nirS* was most abundant in the woodchips and sludge, whereas *nrfA* in sludge had the greatest abundance. Among the woodchip samples, the 16S rRNA and *nirS* abundance varied the most along the flowpath from inlet to outlet and the *nrfA* abundance did not vary (Figure 2b). *nirK* and *nosZ*I displayed the same pattern with the highest abundances in the middle section of the reactor, whereas *nirS* and *nosZ*II had contrasting patterns, with *nirS* lower at the inlet and *nosZ*II lower at the outlet.

The NMDS analysis (Figure 2c) showed that *nirS*-type denitrifiers were indicative of the N-reducing community structure in the woodchip media. By contrast, *nosZ*I and *nosZ*II involved in N_2O reduction were relatively more enriched in the porewater and inlet water samples in comparison to the woodchip media (Figure 2c), and *nrfA* (DNRA) characterized the N-reducing community in the digested sewage sludge.

Despite differences in absolute abundances, the distribution of gene abundances relative to each other in the porewater was comparable with that in the woodchip media (*nirS* > *nrfA* ≥ *nirK* > *nosZ*II > *nosZ*I) (Figure 2a). However, when comparing the N-cycling community in porewater at Day 477 and woodchip samples from Day 490, there was a significant difference between these two sample pools (R = .87; p = .001), demonstrating that these two matrices represent different sampling environments.

3.3 | Temporal changes in the N-reducing community and associated biogeochemical changes in the porewater

We observed differences in gene abundances between the operational years and along the flowpath of the DWB (Figure 3). In general, there was a significant increase in gene abundance between the corresponding periods in the first and second operational year with respect to *nirS*, *nirK*, *nosZ*II, and *nrfA*, whereas the total bacterial community remained approximately the same and *nosZ*I decreased significantly (Supplemental Figures S2 and S3). However, the opposite changes in *nosZ*I and *nosZ*II abundances more or less canceled out the total change in potential N_2O reduction capacity between years. The structure of the N reducing community in the porewater also changed over time and differed between the two operational years, as shown with NMDS (Figure 4), and the change was significantly associated with changes in porewater concentrations of NO_3^-–N ($R^2 = .34$; $p = .001$), NO_2^-–N ($R^2 = .30$; $p = .003$), N_2O–N ($R^2 = .17$; $p = .022$), NH_4^+–N ($R^2 = .14$; $p = .040$), TOC ($R^2 = .28$; $p = .003$), DWB temperature ($R^2 = 0.46$; $p = .001$; see also Figure 2), and TOC/NO_3^- ratio ($R^2 = .3627$; $p = .001$) but not with porewater pH ($R^2 = .01$; $p = .901$). The differences in the structure of the N reducing community between years were mainly split in relation to axis 1 (Figure 4), corresponding to changes in the porewater concentrations of NO_2^-–N and N_2O–N. Although there was no significant difference in the TOC/NO_3^- ratio between the two operational years (Supplemental Figure S2), the NMDS demonstrates that the TOC/NO_3^- ratio is likely controlled by DWB temperature (Figure 4).

Because the gene abundance data from the first operational year were limited to three sampling dates, it was not possible to make conclusive interpretations of temporal trends during the first year. The investigation of temporal changes over an operational year was hence restricted to data from the second year. During this period, gene copies representing the total bacterial community (Figure 3a) decreased in abundance by approximately 50%. Maximum gene abundances were observed during the summer months (Days 400 and 428) for *nirS* and *nrfA* and to a certain extent *nirK*, whereas *nosZ*II abundance decreased and *nosZ*I was relatively constant over this period (see Figure 3a–f). Indeed, abundances of *nrfA* closely followed porewater temperature variations during the second year, with the greatest covariation existing for sampling points towards the outlet (Figure 3f). The abundances of *nirS* also followed porewater temperature variations, but the peak in abundance appeared to lag behind the temperature maximum (Figure 3b). However, contrary to *nrfA*, *nirS* abundance peaked at locations in the first half of the DWB and increased nearest the outlet toward the end of the sampling period.

Among the investigated genes coding for NO_2^- reductases in denitrifiers (i.e., *nirS*, *nirK*), the abundance of *nirS* consistently exceeded that of *nirK* in the porewater (Figure 3b,c). The *nirS*/*nirK* ratio attained a maximum value at locations close to the inlet and during the summer months (data not shown). Relative to *nrfA*, the abundance of *nirS* + *nirK* was consistently greater during the two operational years (Figure 3g), with the exception of Day 400 near the outlet where *nrfA* > *nirS* + *nirK*. The abundance of *nirS* and *nirK* genes was also greatly in excess of the sum of the genes coding for N_2O reductase (i.e., *nosZ*I, *nosZ*II; Figure 3h).

Correlation analyses using data from the second year indicated that significant correlations ($r_s > |0.6|$; $p < .05$) existed among geochemical parameters and between geochemical parameters and gene abundances (Table 1). For example, N_2O correlated positively with NO_2^- and negatively with pH. Both NO_2^- and N_2O correlated with *nirS* and the Σ*nir*/Σ*nos* ratio. The dominance of *nirS* over *nirK* was positively correlated with NO_2^-, NO_3^-, and N_2O. The TOC/NO_3^- ratio correlated with *nirK*, *nrfA*, NH_4^+, and temperature, and *nrfA* was positively correlated with temperature, NH_4^+, and TOC and negatively correlated with NO_3^-. The ratio (*nirS* + *nirK*)/*nrfA* correlated positively with NO_3^-–N and negatively with TOC/NO_3^-.

4 | DISCUSSION

The higher abundance of functional genes involved in the denitrification pathway compared with DNRA and the absence of anammox in both the porewater and woodchip media agrees with denitrification being the major pathway for NO_3^- reduction and N removal in the DWB studied here (Nordström & Herbert, 2018) as well as in DWBs in general (Schipper et al., 2010). Based on gene abundance data, the structures of the N-reducing communities in the woodchips, sludge, inlet water, and the porewater were significantly different from one another in many instances. The original intention of inoculating with digested sewage sludge was to promote the rapid development of a denitrifying community in the woodchip material. However, the sludge also provided a high-abundance source of organisms with the *nrfA* gene (i.e., genetic capacity for DNRA, an undesired side-reaction in a denitrifying bioreactor). The gene abundances determined in the woodchip samples on Day 490 likely reflect the accumulated contribution from the sludge inoculant, the original community in the woodchips (not analyzed), the inlet water, and the temporal changes of the community in response to selective pressures. However, development of the N-reducing community is mainly determined by the type of substrate used in reactors (Hellman et al., 2020) and, as shown in Figure 4, the porewater TOC concentration, the TOC/NO_3^- ratio, and DWB temperature.

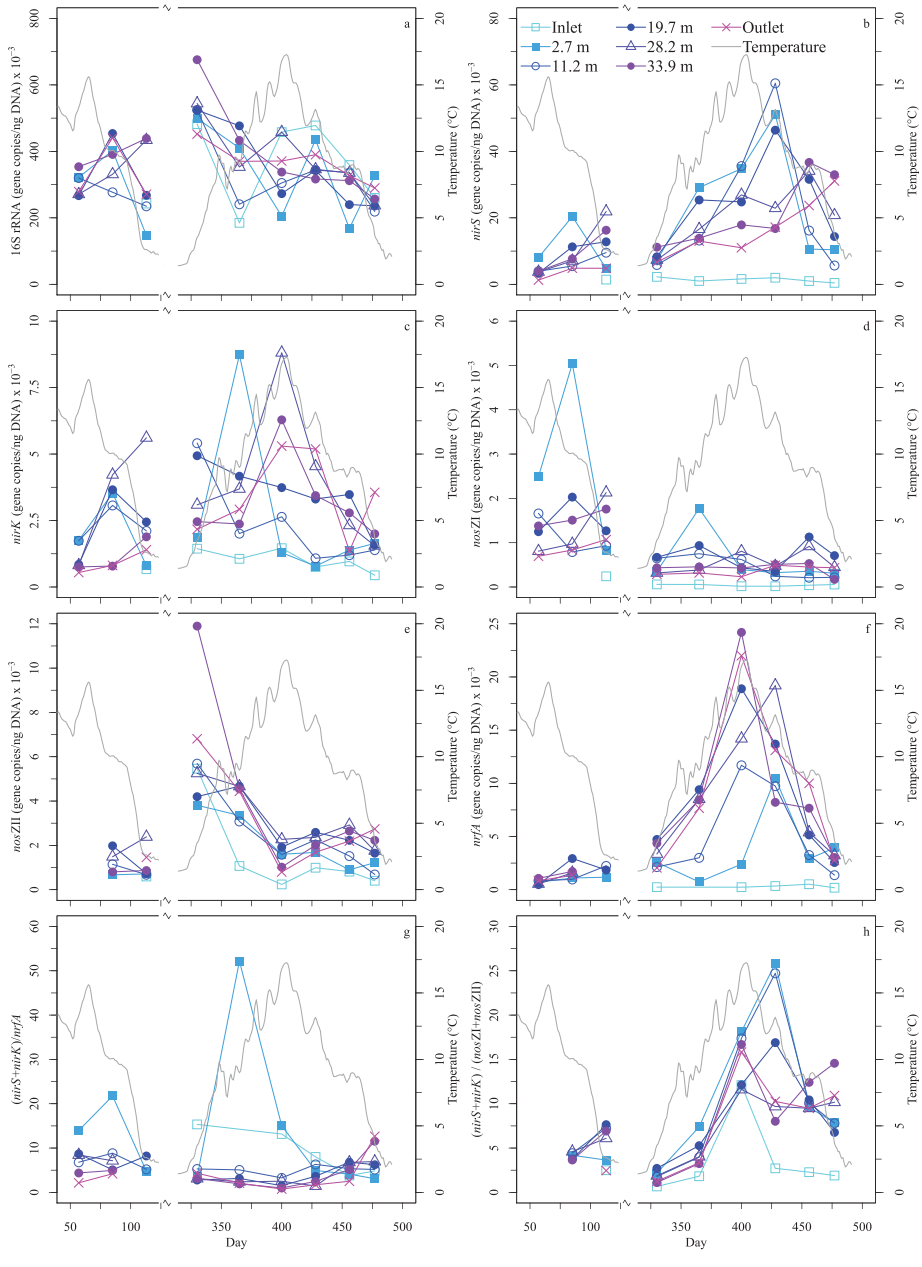

FIGURE 3 Gene abundances (a–f) and gene abundance ratios (g and h) as a function of time since start of denitrifying woodchip bioreactor operations and as a function of distance from the inlet. Abundances of (a) 16S rRNA genes and functional genes (b) *nirS*, (c) *nirK*, (d) *nosZ*I, (e) *nosZ*II, and (f) *nrfA*. Ratios (g) (*nirS* + *nirK*)/*nrfA* (h) and (*nirS* + *nirK*)/(*nosZ*I+*nosZ*II). Bioreactor temperature is plotted on secondary *y* axis. The *x* axis corresponds to day of porewater sampling (Days 57, 85, 113, 330, 365, 400, 428, 456, and 477)

TABLE 1 Spearman's rank correlation between chemistry, temperature, gene abundances, and ratios of different gene abundances in the porewater (bioreactor centerline)

	NO_3–N	NO_2–N	N_2O–N	NH_4–N	TOC	TOC/NO_3^-	pH	Temperature	*nirS*	*nirK*	*nosZ*I	*nosZ*II	*nrfA*
NO_3–N	–			−.8***	−.67***	−.85***	−.44*	−.86***					−.8***
NO_2–N		–	.7***						.62***				
N_2O–N			–			−.38*	−.66***		.71*	−.42*			
NH_4–N				–	.64***	.79***	.49*			.47*			.56*
TOC					–	.93***	.56*	.55*		.65***	.4*		.49*
TOC/NO_3^-						–	.6*	.69***		.69***			.65***
pH							–			.52*			
Temperature								–	.26*			−.05*	.70***
nirS									–				.18*
nirK										–	.43*		.45*
nosZI											–		
nosZII												–	
nrfA													–
nirS/*nirK*	.46*	.58*	.8*	−.33*	−.41*	−.5*	−.59*	−.23*	.61***	−.75***	−.15*	−.03*	−.21*
nosZII/*nosZI*	−.13*	.09*	.17*	−.03*	−.19*	−.13*	.06*	−.05*	.14*	−.23*	−.49*	.45*	.13*
Σ*nir*/*nrfA*	.75***	.37*	.55*	−.49*	−.43*	−.61***	−.51*	−.52*		−.45*			−.78***
Σ*nir*/Σ*nosZ*	−.19*	.29*	.53*	.23*	−.01*	.05*	−.52*	.44*	.67***	−.09*	−.27*	−.42*	.38*

Note. Only data from second operational year used. Empty cells indicate not significant. TOC, total organic C.

*Significant at the .05 probability level.

***Significant at the .001 probability level.

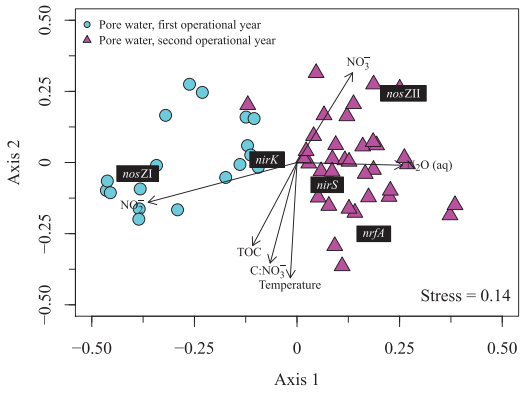

FIGURE 4 Nonmetric multidimensional scaling ordination based on Bray–Curtis dissimilarities for the abundance of the functional genes *nirS*, *nirK*, *nosZ*I, *nosZ*II, and *nrfA* in porewater samples. Arrows show significant correlations ($p < .05$) between the N cycling community structure across samples and porewater chemistry. Gene names in black boxes denote species scores. TOC, total organic C

The surface-bound N reducing community associated with the woodchips and containing *nirS*, *nirK*, and *nosZ*I increased in abundance from the bioreactor inlet to the middle of the DWB (Figure 2b), suggesting that environmental conditions promoting the growth of organisms with *nirS*, *nirK*, and *nosZ*I were better in the central region of the DWB compared with conditions closer to the inlet. A similar spatial development in gene abundance was observed in the porewater on Day 477, just prior to woodchip sampling (i.e., *nirS* and *nirK* gene abundances increased through bioreactor). Because temperature did not vary greatly within the bioreactor for any given date (data not shown), the increase in *nirS* and *nirK* gene abundances along the bioreactor flowpath was likely controlled by the relatively low concentration of organic C, elevated concentrations of NO_3^- and NO_2^-, and consequently the low TOC/NO_3^- ratio (Figure 1f). These results are contrary to our previous study (Herbert et al., 2014) that indicated a decrease in *nirS* abundance in a sawdust DWB with distance from the bioreactor inlet; however, this system (Herbert et al., 2014) was NO_3^- limited in regions further from the inlet but was not C limited (i.e., high TOC/NO_3^- ratio).

Based on the porewater samples (Figures 2 and 3), we clearly detected a shift in the structure of the N reducing community over time, as characterized by the change in the relative abundances of functional groups (Figure 3; Supplemental Figure S2). The increased abundance of the capacity for NO_2^- reduction relative to N_2O reduction during the second operational year suggests a preferential selection of *nirS*-type denitrifiers with a truncated denitrifying pathway terminating with N_2O. Dissolved N_2O porewater concentrations were most strongly correlated (Table 1) with pH and the type of NO_2^- reductase (positively with *nirS* and *nirS*/*nirK* ratio and negatively with *nirK*; c.f. Barrett et al., 2016; Jones et al., 2014) and also with the relative abundance of NO_2^- reducers to N_2O reducers (Σ*nir*/Σ*nosZ*). Furthermore, the abundances of *nirS* and *nirK* (and also *nrfA*) during the second operational year (Figure 3) demonstrated a clear temperature dependence, whereas abundances of *nosZ*I and *nosZ*II appeared to be independent of temperature, which led to a correlation between temperature and Σ*nir*/Σ*nosZ* (Table 1). Warneke, Schipper, Bruesewitz, McDonald, and Cameron (2011a) showed that an increased abundance of NO_2^- reducers over N_2O reducers at higher temperatures, including a relative enrichment in *nirS*-type to *nirK*-type denitrifiers, was associated with increased N_2O emissions in denitrifying bioreactors. Our observations imply an increased genetic potential for the production of N_2O from DWBs over time and with increasing temperature at HRTs of 1–2.6 d. In addition, the genetic potential for N_2O production was spatially variable within the bioreactor, implying a geochemical control (e.g., TOC/NO_3^-, see below) as well. These implications are important contributions to our general understanding of greenhouse gas emissions from DWBs over longer time scales because they indicate the importance of understanding the temporal development of these systems.

The preferential promotion of denitrifiers with a denitrification pathway terminating with N_2O may have been an effect of the increased competition for electron donors. The simulations by Nordström and Herbert (2018) suggested a decrease in the export of acetate from the DWB studied here with time from start-up, which is consistent with the observations of other studies (Grießmeier & Gescher, 2018; Grießmeier et al., 2017). When there is competition for available organic C by denitrifiers capable of complete denitrification, electrons are preferentially directed to the NO_2^- reductase rather than the N_2O reductase (Pan et al., 2013). This suggests that low TOC/NO_3^- ratios could lead to the preferential promotion of microorganisms with denitrification pathways truncated to N_2O, in this case *nirS* denitrifiers. This was supported in this study by the negative correlation between TOC/NO_3^- ratio and the *nirS*/*nirK* ratio and its positive correlation with *nirK* abundances. Promotion of organisms lacking the *nosZ* gene is also supported by the spatially dependent relationship between N_2O concentrations and Σ*nir*/Σ*nosZ* (Figures 1d and 3h). Further, clade II *nosZ* is frequently associated with nondenitrifying bacteria that do not have the genetic makeup needed for N_2O production (Graf et al., 2014; Jones et al., 2014). The disproportional abundance of *nos* and *nir* genes suggests that the denitrification pathway is split among community members. This decoupling of the intermediate steps of denitrification onto several populations would reduce intraorganism competition (Lilja & Johnson, 2016; Pan et al., 2013). Such decoupling and metabolic specialization among truncated denitrifiers and N_2O reducers has been inferred from

metagenomes in tidal sediments and grassland soils (Diamond et al., 2019; Marchant et al., 2018).

The abundance of *nrfA* genes detected in the porewater suggests DNRA bacteria may be competing for NO_3^- with the denitrifiers (Figures 2a and 3f). The genetic potential for NO_2^- reduction relative to DNRA (i.e., Σ*nir*/*nrfA*) was negatively correlated with the TOC/NO_3^- ratio (Table 1), in agreement with studies showing that DNRA is favored by high C/N ratios (e.g., Kraft et al., 2014). Both temperature and the TOC/NO_3^- ratio had an important control on *nrfA* abundance (Figure 3f) and hence NH_4^+–N concentrations, as indicated by significant correlations between these parameters (Table 1). However, the NH_4^+ concentrations were overall low, suggesting limited importance of this unwanted process. Interestingly, many DNRA bacteria are also fermenting (Muyzer & Stams, 2008; Van Den Berg, Elisário, Kuenen, Kleerebezem, & van Loosdrecht, 2017), and hence the DNRA bacteria may also contribute to fermentation and thereby support denitrification despite being competitors for NO_3^-.

5 | CONCLUSIONS

Denitrification was the major pathway for NO_3^- reduction and N removal in the DWB over two operational years at HRTs of 1–2.6 d but was associated with an increased genetic potential for N_2O production with time. We conclude that pH and temporal and spatial changes in the relative abundance of different denitrifier genotypes, indicated by abundances of genes involved in different steps in the denitrification pathway, controlled porewater concentrations of N_2O. Bioreactor temperature and TOC/NO_3^- ratio had a strong control on the occurrence of bacteria capable of NO_2^- reduction and those capable of DNRA (preferring high TOC/NO_3^-). A spatially variable community, likely dominated by *nirS*-type denitrifiers with a truncated pathway terminating with N_2O, developed over time in the DWB, where the supply of electron donors from substrate decomposition may be a controlling parameter on community development. Considering the significant differences in DWB chemistry and functional gene abundance between the two operational years, this study highlights the importance of distinguishing between initial variations during a start-up period, which may be extensive in length, and the long-term performance of a DWB.

ACKNOWLEDGMENTS

This work was supported by the Luossavaara-Kiirunavaara Aktiebolag (LKAB) and VINNOVA, The Swedish Innovation Agency, under Grant 2014–011334. The authors thank Christopher Jones, Carlos Palacin-Lizarbe, and Robert Almstrand for help related to the use of Sterivex filter units. The authors thank the anonymous reviewers for all their comments and advice.

CONFLICT OF INTEREST

There are no conflicts of interest.

ORCID

Albin Nordström https://orcid.org/0000-0002-0311-8368
Roger B. Herbert https://orcid.org/0000-0002-7561-757X

REFERENCES

Barrett, M., Khalil, M. I., Jahangir, M. M. R., Lee, C., Cardenas, L. M., Collins, G., … O'Flaherty, V. O. (2016). Carbon amendment and soil depth affect the distribution and abundance of denitrifiers in agricultural soils. *Environmental Science and Pollution Research*, *23*, 7899–7910. https://doi.org/10.1007/s11356-015-6030-1

Benjamini, Y., & Hochberg, Y. (1995). Controlling the false discovery rate: A practical and powerful approach to multiple testing. *Journal of the Royal Statistical Society Series B-Methodological*, *57*(1), 289–300.

Bonilla-Rosso, G., Wittorf, L., Jones, C. M., & Hallin, S. (2016). Design and evaluation of primers targeting genes encoding NO-forming nitrite reductases: Implications for ecological inference of denitrifying communities. *Scientific Reports*, *6*, 39208. https://doi.org/10.1038/srep39208

Cameron, S. G., & Schipper, L. A. (2010). Nitrate removal and hydraulic performance of organic carbon for use in denitrification beds. *Ecological Engineering*, *36*(11), 1588–1595. https://doi.org/10.1016/j.ecoleng.2010.03.010

Cannon, J., Sanford, R. A., Connor, L., Yang, W. H., & Chee-Sanford, J. (2019). Optimization of PCR primers to detect phylogenetically diverse nrfA genes associated with nitrite ammonification. *Journal of Microbiological Methods*, *160*, 49–59. https://doi.org/10.1016/j.mimet.2019.03.020

Davis, M. P., Martin, E. A., Moorman, T. B., Isenhart, T. M., & Soupir, M. L. (2019). Nitrous oxide and methane production from denitrifying woodchip bioreactors at three hydraulic residence times. *Journal of Environmental Management*, *242*, 290–297. https://doi.org/10.1016/j.jenvman.2019.04.055

Diamond, S., Andeer, P. F., Li, Z., Crits-Christoph, A., Burstein, D., Anantharaman, K., … Banfield, J. F. (2019). Mediterranean grassland soil C-N compound turnover is dependent on rainfall and depth, and is mediated by genomically divergent microorganisms. *Nature Microbiology*, *4*(8), 1356–1367. https://doi.org/10.1038/s41564-019-0449-y

Dinno, A. (2017). Dunn.test: Dunn's test of multiple comparisons using rank sums. R package version 1.3.5. Retrieved from https://CRAN.R-project.org/package=dunn.test

Elgood, Z., Robertson, W. D., Schiff, S. L., & Elgood, R. (2010). Nitrate removal and greenhouse has production in a stream-bed denitrifying bioreactor. *Ecological Engineering*, *36*(11), 1575–1580. https://doi.org/10.1016/j.ecoleng.2010.03.011

Felgate, H., Giannopoulos, G., Sullivan, M. J., Gates, A. J., Clarke, T. A., Baggs, E., … Richardson, D. J. (2012). The impact of copper, nitrate and carbon status on the emission of nitrous oxide by two species of bacteria with biochemically distinct denitrification pathways. *Environmental Microbiology*, *14*(7), 1788–1800. https://doi.org/10.1111/j.1462-2920.2012.02789.x

Feyereisen, G. W., Moorman, T. B., Christianson, L. E., Venterea, R. T., Coulter, J. A., & Tschirner, U. W. (2016). Performance of agricultural residue media in laboratory denitrifying bioreactors at low

temperatures. *Journal of Environmental Quality*, *45*(3), 779–787. https://doi.org/10.2134/jeq2015.07.0407

Graf, D. R. H., Jones, C. M., & Hallin, S. (2014). Intergenomic comparisons highlight modularity of the denitrification pathway and underpin the importance of community structure for N_2O emissions. *PLOS ONE*, *9*(12), e114118. https://doi.org/10.1371/journal.pone.0114118

Greenan, C. M., Moorman, T. B., Kaspar, T. C., Patkin, T. B., & Jaynes, D. B. (2006). Comparing carbon substrates for denitrification of subsurface drainage water. *Journal of Environmental Quality*, *35*, 824–829. https://doi.org/10.2134/jeq2005.0247

Grießmeier, V., Bremges, A., McHardy, A. C., & Gescher, J. (2017). Investigation of different nitrogen reduction routes and their key microbial players in wood chip-driven denitrification beds. *Scientific Reports*, *7*, 17028. https://doi.org/10.1038/s41598-017-17312-2

Grießmeier, V., & Gescher, J. (2018). Influence of the potential carbon sources for field denitrification beds on their microbial diversity and the fate of carbon and nitrate. *Frontiers in Microbiology*, *9*, 1313. https://doi.org/10.3389/fmicb.2018.01313

Hallin, S., & Lindgren, P.-E. (1999). PCR detection of genes encoding nitrite reductase in denitrifying bacteria. *Applied and Environmental Microbiology*, *65*(4), 1652–1657.

Hallin, S., Philippot, L., Löffler, F. E., Sanford, R. A., & Jones, C. M. (2018). Genomics and ecology of novel N_2O-reducing microorganisms. *Trends in Microbiology*, *26*(1), 43–55. https://doi.org/10.1016/j.tim.2017.07.003

Hellman, M., Hubalek, V., Juhanson, J., Almstrand, R., Peura, S., & Hallin, S. (2020). Substrate type determines microbial activity and community composition in bioreactors for nitrate removal by denitrification at low temperature. *Science of the Total Environment*. https://doi.org/10.1016/j.scitotenv.2020.143023.

Henry, S., Baudoin, E., López-Gutiérrez, J. C., Martin-Laruent, F., Brauman, A., & Philippot, L. (2004). Quantification of denitrifying bacteria in soils by *nirK* gene targeted real-time PCR. *Journal of Microbiological Methods*, *59*(3), 327–335. https://doi.org/10.1016/j.mimet.2004.07.002

Henry, S., Bru, D., Stres, B., Hallet, S., & Philippot, L. (2006). Quantitative Ddetection of the *nosZ* gene, encoding nitrous oxide reductase, and comparison of the abundances of 16S rRNA, *narG*, *nirK*, and *nosZ* genes in soils. *Applied and Environmental Microbiology*, *72*(8), 5181–5189. https://doi.org/10.1128/AEM.00231-06

Herbert, R. B., Winbjörk, H., Hellman, M., & Hallin, S. (2014). Nitrogen removal and spatial distribution of denitrifier and anammox communities in a bioreactor for mine drainage treatment. *Water Research*, *66*, 350–360. https://doi.org/10.1016/j.watres.2014.08.038

Hothurn, T., Hornik, K., van de Wiel, M. A., & Zeileis, A. (2006). A lego system for conditional inference. *American Statistician*, *60*(3), 257–263. https://doi.org/10.1198/000313006

Jones, C. M., Graf, D. R. H., Bru, D., Philippot, L., & Hallin, S. (2013). The unaccounted yet abundant nitrous oxide-reducing microbial community: A potential nitrous oxide sink. *ISME Journal*, *7*(2), 417–426. https://doi.org/10.1038/ismej.2012.125

Jones, C. M., Spor, A., Brennan, F. P., Breuil, M. C., Bru, D., Lemanceau, P., … Philippot, L. (2014). Recently identified microbial guild mediates soil N_2O sink capacity. *Nature Climate Change*, *4*, 801–805. https://doi.org/10.1038/NCLIMATE2301

Kraft, B., Tegetmeyer, H. E., Sharma, R., Klotz, M. G., Ferdelman, T. G., Hettich, R. L., … Strous, M. (2014). Nitrogen cycling: The environmental controls that govern the end product of bacterial nitrate respiration. *Science*, *345*(6197), 676–679. https://doi.org/10.1126/science.1254070

Lilja, E. E., & Johnson, D. R. (2016). Segregating metabolic processes into different microbial cells accelerates the consumption of inhibitory substrates. *The ISME Journal*, *10*, 1568–1578. https://doi.org/10.1038/ismej.2015.243

Marchant, H. K., Tegetmeyer, H. E., Ahmerkamp, S., Holtappels, M., Lavik, G., Graf, J., … Kuypers, M. M. M. (2018). Metabolic specialization of denitrifiers in permeable sediments controls N_2O emissions. *Environmental Microbiology*, *20*, 4486–4502. https://doi.org/10.1111/1462-2920.14385

MoBio Laboratories Inc. (2018). *PowerWater® Sterivex™ DNA Isolation Kit instruction manual*. Retrieved from https://www.qiagen.com/us/resources/resourcedetail?id=86fe0107-d78b-4a0d-b5fd-3c2cb414a749&lang=en

Mohan, S. B., Schmid, M., Jetten, M., & Cole, J. (2004). Detection and widespread distribution of the nrfA gene encoding nitrite reduction to ammonia, a short circuit in the biological nitrogen cycle that competes with denitrification. *FEMS Microbiology Ecology*, *49*(3), 433–443. https://doi.org/10.1016/j.femsec.2004.04.012

Muyzer, G., Dewaal, E. C., & Uitterlinden, A. G. (1993). Profiling of complex microbial populations by denaturing gradient gel electrophoresis analysis of polymerase chain reaction-amplified genes coding for 16S rRNA. *Applied and Environmental Microbiology*, *59*(3), 695–700.

Muyzer, G., & Stams, A. J. M. (2008). The ecology and biotechnology of sulphate-reducing bacteria. *Nature Reviews Microbiology*, *6*(6), 441–454. https://doi.org/10.1038/nrmicro1892

Nordström, A., & Herbert, R. B. (2017). Denitrification in a low-temperature bioreactor system at two different hydraulic residence times: Laboratory column studies. *Environmental Technology*, *38*, 1362–1375. https://doi.org/10.1080/09593330.2016.1228699

Nordström, A., & Herbert, R. B. (2018). Determination of major biogeochemical processes in a denitrifying woodchip bioreactor for treating mine drainage. *Ecological Engineering*, *110*, 54–66. https://doi.org/10.1016/j.ecoleng.2017.09.018

Nordström, A., & Herbert, R. B. (2019). Identification of the temporal control on nitrate removal rate variability in a denitrifying woodchip bioreactor. *Ecological Engineering*, *127*, 88–95. https://doi.org/10.1016/j.ecoleng.2018.11.015

Oksanen, J., Guillaume Blanchet, F., Friendly, M., Kindt, R., Legendre, P., McGlinn, D., … Wagner, H. (2018). vegan: Community ecology package. R package version 2.5-2. Retrieved from https://CRAN.R-project.org/package=vegan

Penton, C. R., Johnson, T. A., Quensen III J. F., Iwai, S., Cole, J. R., & Tiedje, J. M. (2013). Functional genes to assess nitrogen cycling and aromatic hydrocarbon degradation: Primers and processing matter. *Frontiers in Microbiology*, *4*, 279. https://doi.org/10.3389/fmicb.2013.00279

Pan, Y., Ni, B. J., Bond, P. L., Ye, L., & Yuan, Z. (2013). Electron competition among nitrogen oxides reduction during methanol-utilizing denitrification in wastewater treatment. *Water Research*, *47*(10), 3273–3281. https://doi.org/10.1016/j.watres.2013.02.054

Robertson, W. D. (2010). Nitrate removal rates in woodchip media of varying age. *Ecological Engineering*, *36*(11), 1581–1587. https://doi.org/10.1016/j.ecoleng.2010.01.008

Schipper, L. A., Robertson, W. D., Gold, A. J., Jaynes, D. B., & Cameron, S. C. (2010). Denitrifying bioreactors: An approach for reducing

nitrate loads to receiving waters. *Ecological Engineering*, *36*(11), 1532–1543. https://doi.org10.1016/j.ecoleng.2010.04.008

Schmid, M. C., Hooper, A. B., Klotz, M. G., Woebken, D., Lam, P., Kuypers, M. M. M., … Jetten, M. S. M. (2008). Environmental detection of octahaem cytochrome c hydroxylamine/hydrazine oxidoreductase genes of aerobic and anaerobic ammonium-oxidizing bacteria. *Environmental Microbiology*, *10*(11), 31–40–3149. https://doi.org/10.1111/j.1462-2920.2008.01732.x

Throbäck, I. N., Enwall, K., Jarvis, A., & Hallin, S. (2004). Reassessing PCR primers targeting nirS, nirK and nosZ genes for community surveys of denitrifying bacteria with DGGE. *FEMS Microbiology Ecology*, *49*(3), 401–417. https://doi.org/10.1016/j.femsec.2004.04.011

Van Den Berg, E. M., Elisário, M. P., Kuenen, J. G., Kleerebezem, R., & van Loosdrecht, M. C. M. (2017). Fermentative bacteria influence the competition between denitrifiers and DNRA bacteria. *Frontiers in Microbiology*, *8*, 1684. https://doi.org/10.3389/fmicb.2017.01684

Van Den Berg, E. M., Van Dongen, U., Abbas, B., & Van Loosdrecht, M. C. (2015). Enrichment of DNRA bacteria in a continuous culture. *The ISME Journal*, *9*, 2153–2161. https://doi.org/10.1038/ismej.2015.26

Warneke, S., Schipper, L. A., Bruesewitz, D. A., McDonald, I., & Cameron, S. (2011a). Rates, controls and potential adverse effects of nitrate removal in a denitrification bed. *Ecological Engineering*, *37*(3), 511–522. https://doi.org/10.1016/j.ecoleng.2010.12.006

Warneke, S., Schipper, L. A., Matiasek, M. G., Scow, K. M., Cameron, S., Bruesewitz, D. A., & McDonald, I. R. (2011b). Nitrate removal, communities of denitrifiers and adverse effects in different carbon substrates for use in denitrification beds. *Water Research*, *45*(17), 5463–5475. https://doi.org/10.1016/j.watres.2011.08.007

Welsh, A., Chee-Sanford, J. C., Connor, L. M., Löffler, F. E., & Sanford, R. A. (2014). Refined NrfA phylogeny improves PCR-Based *nrfA* gene detection. *Applied and Environmental Microbiology*, *80*(7), 2110–2119. https://doi.org/10.1128/AEM.03443-13

Yoon, S., Cruz-García, C., Sanford, R., Ritalahti, K. M., & Löffler, F. E. (2015). Denitrification versus respiratory ammonification: Environmental controls of two competing dissimilatory NO_3/NO_2 reduction pathways in *Shewanella loihica* strain PV-4. *The ISME Journal*, *9*, 1093–1104. https://doi.org/10.1038/ismej.2014.201

Zar, J. H. (2010). *Biostatistical analysis* (5th ed.). Upper Saddle River, NJ: Pearson Prentice Hall.

SUPPORTING INFORMATION

Additional supporting information may be found online in the Supporting Information section at the end of the article.

How to cite this article: Nordström A, Hellman M, Hallin S, Herbert RB. Microbial controls on net production of nitrous oxide in a denitrifying woodchip bioreactor. *J. Environ. Qual*. 2021;50:228–240. https://doi.org/10.1002/jeq2.20181

Supporting information for

Microbial Controls on Net Production of Nitrous Oxide in a Denitrifying Woodchip Bioreactor

Albin Nordström[†], Maria Hellman[‡], Sara Hallin[‡], Roger B. Herbert[†,*]

[†]*Uppsala University, Department of Earth Sciences, Villavägen 16, SE-752 36, Uppsala, Sweden. *corresponding author (roger.herbert@geo.uu.se)*

[‡]*Swedish University of Agricultural Sciences, Department of Forest Mycology and Plant Pathology, Box 7026, SE-750 07, Uppsala, Sweden*

The supporting information includes (3 figures, 5 tables, 7 pages)

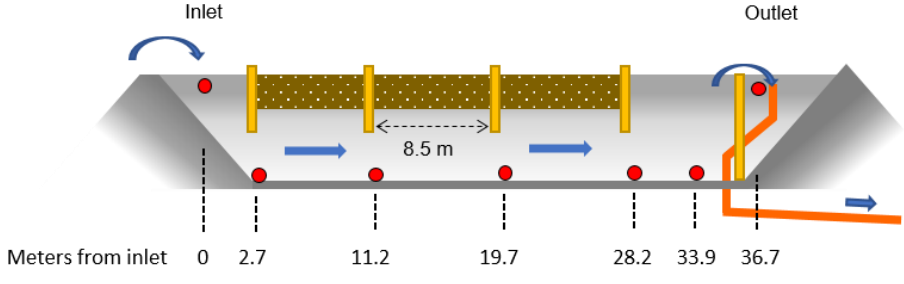

Fig. A.1. Cross-section of the denitrifying woodchip bioreactor (DWB) showing positions of the sampling points (red circles) for the inlet, outlet, and porewater along centerline.

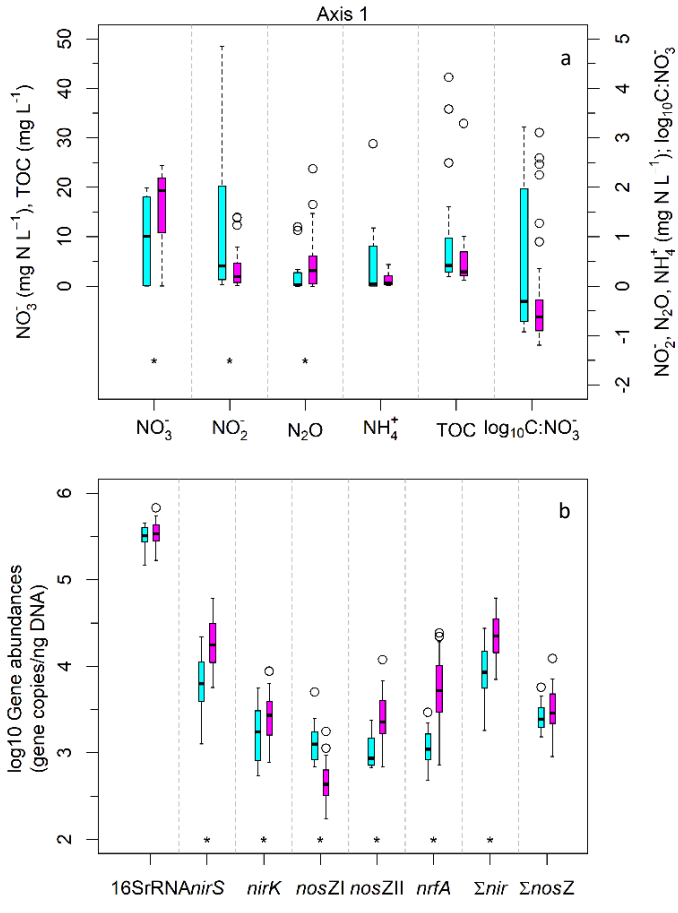

Figure A.2 a) Differences in porewater concentrations of NO_3^-, NO_2^-, N_2O, NH_4^+, and TOC, and b) functional gene abundances between the first (cyan, left) and second (magenta, right) operational years. Data include all porewater sampling locations. Lines through boxes signifies median, empty circles are outliers, and stars (*) indicate significant ($p<0.05$) differences between the two operational years based on a two-sided Wilcox test for significance. Note different scales on y-axes in panel a.

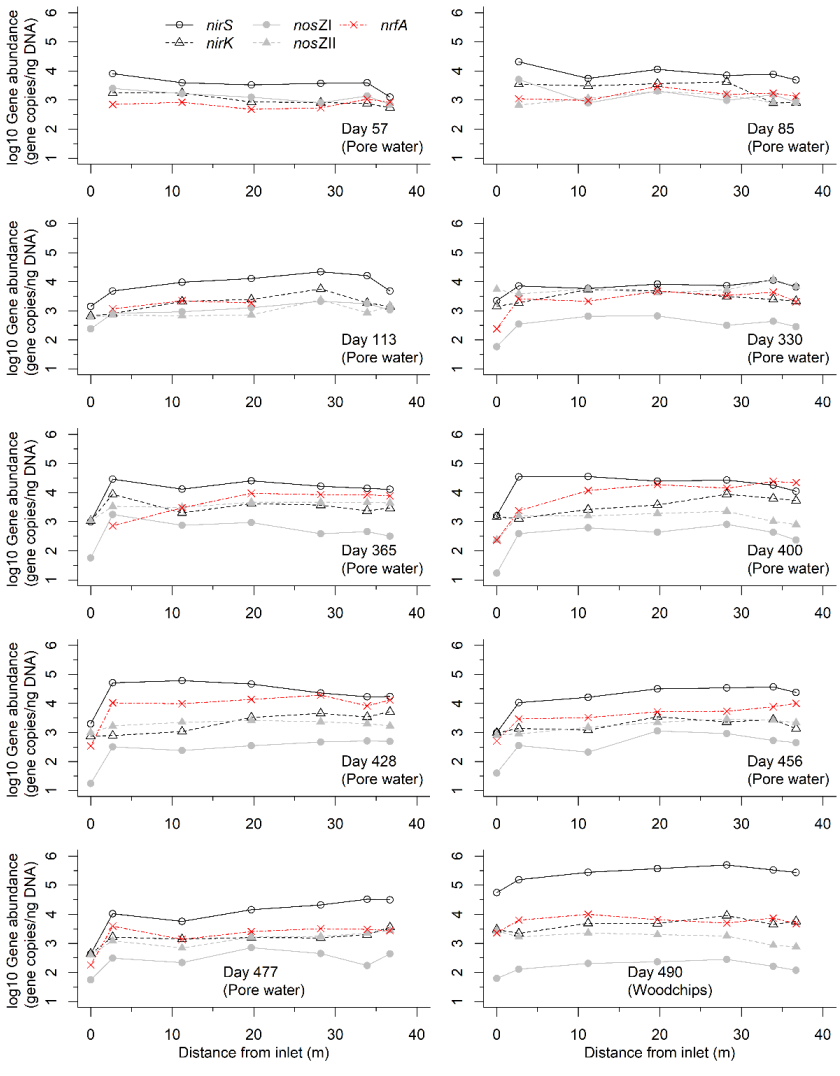

Fig. A.3 The variation in the abundances of functional genes *nirS*, *nirK*, *nos*ZI, *nos*ZII, and *nrfA* between the inlet (0 m) and the outlet (36.7 m) in the DWB at the time of porewater sampling (days 57, 85, 113, 330, 365, 400, 428, 456, and 477), and at the time of woodchip sampling (day 490). Note log-scale on y-axes. Functional gene abundances shown for woodchip samples are the average of three replicates, where samples at 0 m and 36.7 m are obtained 2.1 m above base and remaining samples are collected along the centerline at the base of the bioreactor.

Table A.1. Theoretical hydraulic residence times (HRT) calculated by dividing the estimated pore volume with the pump flow rate (Q).

Days	Q [m^3 day^{-1}]	Theoretical HRT [days]
0–45	43.2	2.6
46–52	0	No flow – Pump malfunction
53–151	59.4	1.9
152–321	0	No flow – winter intermission
322–370	43.2	2.6
371–428	48.9	2.3
429–490	109.6	1

Table A.2. Primers and reaction conditions for qPCR.

Gene	Primer pair	Primer sequence	Final conc	Melting		Annealing		Elongation		Data acquisition		Cycles[a]
	Forw/Rev	5´- 3´	(µM)	T (°C)	t (s)	T (°C)	t (s)	T (°C)	t (s)	T (°C)	t (s)	
16S rRNA	341F	CCTACGGGAGGCAGCAG	0.50	95	15	60	30	72	20	78	5	35
	534R	ATTACCGCGGCTGCTGGCA	0.50									
nirS	Cd3aFm	AACGYSAAGGARACSGG	0.80	95	15	65-60[b]	30	72	35	80	5	35
	R3cdm	GASTTCGGRTGSGTCTTSAYGAA	0.80									
nirK	F1aCu	ATCATGGTSCTGCCGCG	0.25	95	15	63-58[b]	30	72	35	80	5	45
	1040R	GCCTCGATCAGRTTRTGGTT	0.25									
*nosZ*I	1840F	CGCRACGGCAASAAGGTSMSSGT	0.50	95	15	65-60[b]	30	72	35	80	5	40
	2090R	CAKRTGCAKSGCRTGGCAGAA	0.50									
*nosZ*II	nosZIIF	CTIGGICCIYTKCAYAC	2.00	95	15	54	30	72	45	80	5	40
	nosZIIR	GCIGARCARAAITCBGTRC	2.00									
hdh	hzocl1F1	TGYAAGACYTGYCAYTGG	0.80	95	15	52.5	30	72	30	77	10	35
	hzocl1	ACTCCAGATRTGCTGACC	0.80									
nrfA	nrfAF2aw	CARTGYCAYGTBGARTA	0.50	95	15	57-52[b]	30	72	20	80	10	45
	nrfAR1	TWNGGCATRTGRCARTC	0.50									

a - Protocols start with an activation step, 95 °C for 5 minutes and are finished with a melt curve, 15 s at 95 °C followed by 65-95 °C in 0.5 °C increments for 5 s.
b - 1 °C decrease per cycle the first six cycles.

Table A.3. Shapiro-Wilk test of normality for the abundances of the 16S rRNA gene and functional genes (*nirS*, *nirK*, *nosZ*I, *nosZ*II, *nrfA*) in the porewater, influent water, and sewage sludge, respectively.

Gene	Source	Shapiro-Wilk	
		W	p-value
16S rRNA	Porewater	0.97	0.20
	Influent water	0.88	0.21
	Woodchips	0.94	0.22
	Sewage sludge	0.93	0.47
nirS	Porewater	0.89	<0.01
	Influent water	0.97	0.92
	Woodchips	0.98	0.84
	Sewage sludge	0.76	0.01
nirK	Porewater	0.88	<0.01
	Influent water	0.94	0.62
	Woodchips	0.90	0.04
	Sewage sludge	0.82	0.16
*nos*ZI	Porewater	0.69	<0.01
	Influent water	0.65	<0.01
	Woodchips	0.96	0.44
	Sewage sludge	0.83	0.18
*nos*ZII	Porewater	0.77	<0.01
	Influent water	0.61	<0.01
	Woodchips	0.94	0.22
	[a]Sewage sludge	n.a.	n.a.
nrfA	Porewater	0.80	<0.01
	Influent water	0.88	0.31
	Woodchips	0.97	0.67
	Sewage sludge	0.84	0.20

[a]*nos*ZII only quantifiable in two out of three samples (Shapiro-Wilk requires three measurements)

Table A.4. Kruskal-Wallis test for differences in the 16S rRNA and functional gene abundances in the porewater, influent water, woodchips, and sewage sludge.

Gene	Kruskal-Wallis		
	χ^2	df[a]	p-value
16S rRNA	20.98	3	<0.01
nirS	56.83	3	<0.01
nirK	32.96	3	<0.01
*nos*ZI	53.58	3	<0.01
*nos*ZII	13.23	3	<0.01
nrfA	23.79	3	<0.01

[a]df = degrees of freedom

Table A.5. Kruskal-Wallis test for differences in the 16S rRNA and functional gene abundances in the woodchip media at three different positions (near inlet, n=6; middle, n = 36; near outlet, n = 6).

Gene	Kruskal-Wallis		
	χ^2	df[a]	p-value
16S rRNA	13.75	2	<0.01
nirS	15.85	2	<0.01
nirK	23.37	2	<0.01
*nos*ZI	20.69	2	<0.01
*nos*ZII	7.23	2	0.03
nrfA	2.18	2	0.34

[a]df = degrees of freedom

IV

frontiers | Frontiers in Microbiology

ORIGINAL RESEARCH
published: 24 May 2022
doi: 10.3389/fmicb.2022.877990

Nitrogen Removal Capacity of Microbial Communities Developing in Compost- and Woodchip-Based Multipurpose Reactive Barriers for Aquifer Recharge With Wastewater

Maria Hellman[1], Cristina Valhondo[2,3], Lurdes Martínez-Landa[3,4], Jesús Carrera[2,3], Jaanis Juhanson[1] and Sara Hallin[1]*

[1] Department of Forest Mycology and Plant Pathology, Swedish University of Agricultural Sciences, Uppsala, Sweden, [2] Institute of Environmental Assessment and Water Research (IDAEA), CSIC, Barcelona, Spain, [3] Associate Unit, Hydrogeology Group (UPC-CSIC), Barcelona, Spain, [4] Department of Civil and Environmental Engineering, Universitat Politècnica de Catalunya (UPC), Barcelona, Spain

OPEN ACCESS

Edited by:
Sofia I. A. Pereira, Escola Superior de Biotecnologia - Universidade Católica Portuguesa, Portugal

Reviewed by:
Katharina Kujala, University of Oulu, Finland
Terry Gentry, Texas A&M University, United States

****Correspondence:***
Maria Hellman
maria.hellman@slu.se

Specialty section:
This article was submitted to Systems Microbiology, a section of the journal Frontiers in Microbiology

Received: *17 February 2022*
Accepted: *21 April 2022*
Published: *24 May 2022*

Citation:
Hellman M, Valhondo C, Martínez-Landa L, Carrera J, Juhanson J and Hallin S (2022) Nitrogen Removal Capacity of Microbial Communities Developing in Compost- and Woodchip-Based Multipurpose Reactive Barriers for Aquifer Recharge With Wastewater. Front. Microbiol. 13:877990. doi: 10.3389/fmicb.2022.877990

Global water supplies are threatened by climate changes and the expansion of urban areas, which have led to an increasing interest in nature-based solutions for water reuse and reclamation. Reclaimed water is a possible resource for recharging aquifers, and the addition of an organic reactive barrier has been proposed to improve the removal of pollutants. There has been a large focus on organic pollutants, but less is known about multifunctional barriers, that is, how barriers also remove nutrients that threaten groundwater ecosystems. Herein, we investigated how compost- and woodchip-based barriers affect nitrogen (N) removal in a pilot soil aquifer treatment facility designed for removing nutrients and recalcitrant compounds by investigating the composition of microbial communities and their capacity for N transformations. Secondary-treated, ammonium-rich wastewater was infiltrated through the barriers, and the changes in the concentration of ammonium, nitrate, and dissolved organic carbon (DOC) were measured after passage through the barrier during 1 year of operation. The development and composition of the microbial community in the barriers were examined, and potential N-transforming processes in the barriers were quantified by determining the abundance of key functional genes using quantitative PCR. Only one barrier, based on compost, significantly decreased the ammonium concentration in the infiltrated water. However, the reduction of reactive N in the barriers was moderate (between 21 and 37%), and there were no differences between the barrier types. All the barriers were after 1 year dominated by members of Alphaproteobacteria, Gammaproteobacteria, and Actinobacteria, although the community composition differed between the barriers. Bacterial classes belonging to the phylum Chloroflexi showed an increased relative abundance in the compost-based barriers. In contrast to the increased genetic potential for nitrification in the compost-based barriers, the woodchip-based barrier demonstrated higher genetic potentials for denitrification, nitrous oxide reduction, and dissimilatory reduction of nitrate to ammonium. The barriers have previously been shown

to display a high capacity to degrade recalcitrant pollutants, but in this study, we show that most barriers performed poorly in terms of N removal and those based on compost also leaked DOC, highlighting the difficulties in designing barriers that satisfactorily meet several purposes.

Keywords: water reuse, wastewater, nature-based solutions, soil aquifer treatment, reactive barriers, nitrogen removal, N-transforming microorganisms

INTRODUCTION

Climate change with altered precipitation patterns, an increasing human population and expansion of urban areas threaten sustainable drinking water supplies globally (Wheeler and von Braun, 2013). A continuous decline in the long-term groundwater level is becoming increasingly problematic due to over-drafting, and freshwater supplies can be limited in densely urbanized areas. More than 50% of the world's population lives in urban areas, and by 2050 it is expected to increase to 68% (United Nations [UN], 2018). Thus, there are increasing demands for transforming urban water solutions, including water reuse and reclamation, to close the urban water cycle (Valhondo and Carrera, 2019). Nature-based solutions are gaining interest, and one option is the application of managed aquifer recharge (MAR), a low-cost technology that is used for increasing groundwater resources and enhancing recharged water quality (Bekele et al., 2018; Silver et al., 2018). The effluent coming from wastewater treatment plants is a possible water resource for this purpose (Page et al., 2018). However, treated wastewater contains various contaminants, such as pharmaceuticals, personal care products, pesticides, pathogens, and nutrients, that have not been eliminated in the wastewater treatment plant (Loos et al., 2013; Petrie et al., 2015) and which affect the water quality and threaten the integrity of groundwater ecosystems.

The implementation of reactive barriers in MAR systems has been proposed to increase the removal of contaminants (Valhondo et al., 2014). A reactive barrier is a layer of carbon-rich material, for example, compost or woodchips, through which water percolates. This offers a range of redox conditions and adds sorption sites that facilitate biodegradation and retard the transport of pollutants through the system (Valhondo et al., 2018), but the efficiency and capacity to remove environmentally harmful pollutants are uncertain and will depend on the type of barrier, pollutant (Modrzyński et al., 2021), and the operation of the system. The addition of reactive barriers has shown promising results for the removal of organic micropollutants and for reducing the number of pathogens in the treated water (Schaffer et al., 2015; Valhondo et al., 2020a; Modrzyński et al., 2021). With respect to nitrogen (N) removal, reactive barriers can also support denitrification for the removal of nitrate ions (Beganskas et al., 2018; Grau-Martínez et al., 2018). However, the fate of N when ammonium-rich treated sewage water is used with compost as a reactive layer has not yet been well addressed and may even counteract the desired N removal (Modrzyński et al., 2021). Compost might add ammonium to the system by the mineralization of N-containing organic matter in the compost. Further, the introduction of compost will supply carbon (C) for co-metabolic degradation of pollutants, but could also increase the C to N ratio, which may further promote dissimilatory nitrate reduction to ammonium (DNRA), thereby retaining N in the system (Putz et al., 2018). Overall, the effects of compost addition on N removal are unclear and open the question regarding which microbial communities develop when ammonium-rich water percolates through the barrier.

Our aim was to evaluate compost- and woodchip-based reactive barriers for their ability to remove N when infiltrated with ammonium-rich treated sewage water and determine the microbial communities developing in these barriers, including the pathways underpinning N-transforming processes. We used a pilot facility representing the MAR technique soil aquifer treatment (SAT) with infiltration basins supplemented with compost- and woodchip-based barriers and an infiltration basin with only a sand filter (control) (Valhondo et al., 2020b). The basins were operated under alternating dry and wet cycles (Bouwer et al., 2008; Sharma and Kennedy, 2017), but with very long wet periods (**Supplementary Figure 2**). Nitrogen removal was studied together with the diversity and composition of the microbial communities developing during the first year of operation. The prevalence of the microbial N-transformation pathways nitrification, denitrification, nitrous oxide reduction, and DNRA was estimated by quantifying the abundance of key genes involved in N-transformation processes. We hypothesized that (1) the microbial communities developing in the barriers would affect the N-removal capacity by changing the genetic potentials for the various N-transforming processes, and (2) the compost-based barriers would develop the most diverse microbial communities, followed by the woodchip and the control barriers, because of the larger redox range offered in the compost-based barrier and the additional sorption sites for contaminants in both compost- and woodchip-based barriers.

MATERIALS AND METHODS

System Description

The pilot aquifer recharge facility located at a wastewater treatment plant (WWTP) in the vicinity of Girona, Spain, has been described in detail previously (Valhondo et al., 2020b). The facility has reactive barriers constructed using compost- or woodchip-based materials for the infiltration of secondary effluent from the WWTP and a reference system with sand only. The compost used was based on garden waste, and the woodchips were from pine wood. The barriers were 110 cm deep, including a 10 cm top layer of fine sand, and the infiltration area was 3.6 m^2. All except one of the barriers had vegetation

with mixed plant species that were established naturally. In this study, we evaluated one woodchip-based barrier (WCB), three compost-based barriers varying in the proportions of sand, compost, clay, and presence of vegetation (CB1-, CB1, and CB2), and the reference (Ref) for their ability to reduce reactive N (ammonium and nitrate) and dissolved organic compounds (DOC) in the secondary-treated effluent water from the plant (**Table 1**). The purpose of clay was to provide sorption sites for cationic compounds. The concentrations of reactive N and DOC in the influent water to the barriers were determined on several occasions using the methods described in Valhondo et al. (2020b). The average influent ammonium ($n = 31$), nitrate ($n = 29$), and DOC ($n = 12$) concentrations were 57.4, 0.44, and 15.3 mg L^{-1}, respectively (**Supplementary Table 1** and **Supplementary Figure 1**). The oxygen level in the influent water was 3.76 mg L^{-1} (SD = 2.23, $n = 28$) and pH was 7.6 (SD = 0.22, $n = 30$; **Supplementary Table 1**). The pilot plant was operated in wet and dry cycles with four recharge periods of 27–123 days and three intermittent dry periods of 13–38 days (**Figure 1A**). The average inflow rate was 1 L min^{-1}, corresponding to a recharge rate of 0.40 m day^{-1}. To facilitate uniform infiltration, the influent was distributed through a 7 m long tubing, perforated every 20–25 cm, covering the recharge area.

TABLE 1 | Barrier composition (% volume).

	CB1-	CB1	CB2	WCB	Ref
Vegetation	No	Yes	Yes	Yes	Yes
Sand	49	49	60	49	100
Compost	49	49	40	–	–
Woodchips	–	–	–	–	–
Clay	2	2	2	2	–

Sampling of Water and Barrier Material

Water samples were taken from piezometers installed in a 20-cm thick layer of gravel under each of the reactive barriers (**Figure 1B**). Samples for chemical characterization were collected at eight time points during the wet periods (**Figure 1A**). Water for microbial analyses was collected in the middle of the last wet cycle, that is, after 45 wet days (10–11 December 2018). For this purpose, 80–150 ml of infiltrated water per barrier was filtered through a Sterivex® polyethersulfone filter unit (0.22 μm pore size), and the filters were kept at −20°C until further analysis. In the following text, the term "water" refers to the water after passage through the barriers unless stated otherwise. Barrier material was collected during the dry periods by digging with a small spade 7 or 8 days after the first wet cycle (8–9 February 2018, initial sampling) and 6 days after the fourth wet cycle (14 January 2019, final sampling). Four depths were sampled: the top sand and at 27, 37, and 47 cm depth from the top of the upper sand layer (**Figure 1B**). During the last sampling, it was only possible to collect the top sand and the 27-cm layer of the reference, since the sand fell into the hole while digging. The samples were kept at −20°C until further analysis.

Chemical Analyses of Water and Barrier Material and Calculation of N Removal

Dissolved organic carbon in the water was analyzed using a TOC-VCSH analyzer (Shimadzu, Kyoto, Japan) after filtration (0.22 μm) and acidification, ammonium (NH_4^+) concentration was analyzed using an ORION Ion Selective Electrode (ISE, Thermo Fisher Scientific, Waltham, MA, United States), and nitrate (NO_3^-) concentration was determined by ion chromatography as previously described (Valhondo et al., 2020b).

The amount of reactive N removed (percent) was calculated per barrier and date ($n = 1$) as:

$$N_{removed} = 100 \times (\text{total } N_{in} - \text{total } N_{out})/\text{total } N_{in} \text{ where}$$

$$\text{total } N_{in} = (NO_3^- + NH_4^+) \text{ in inflow water (mg N } L^{-1}) \text{ and}$$

$$\text{total } N_{out} = (NO_3^- + NH_4^+) \text{ in water after barrier passage (mg N } L^{-1}).$$

Dry weight was calculated by the amount of weight lost after drying overnight at 105°C. Organic matter content in the barrier samples was determined by weight lost after combustion. The pH of the barrier samples was measured in a sample: water slurry (1:2.5 weight/weight) after incubating for 1 h on a rotary shaker (200 rpm), followed by 1.5 h for the settling of solids in the dark.

Molecular Methods

Sample Preparations and DNA Extraction

For the water samples, the filters were detached from the Sterivex® cartridges and cut into halves. For each sample, one of the halves was cut into 8–10 pieces and transferred to a microcentrifuge tube. For the barrier material, approximately 0.4 g was used for the DNA extraction. The samples collected from the woodchip barrier were first sieved, and the size fractions > 2 mm were ground in a ball mill (Laarmann LMLW-320/2, Roermond, the Netherlands) using two steel balls (20 mm diameter) for maximum of six 10 second pulses at a frequency of 30 s^{-1}. Before weighing the woodchip material for the extraction, the <2 mm and the milled > 2 mm fractions were thoroughly mixed in the same weight/weight ratio as before the sieving process. DNA was extracted from all samples using the Qiagen PowerSoil kit according to the manufacturer's instructions, with a slight modification in the cell lysis step, where Precellys tissue homogenizer (set at 5,500 rpm for 30 s) was used. The extracted DNA was quantified using the Qubit fluorometer (Thermo Fisher Scientific, Waltham, MA, United States).

Quantitative PCR

To estimate the genetic potential for carrying out different N-transformation processes, the abundances of functional genes were determined by performing quantitative real-time PCR (qPCR) as described in Modrzyński et al. (2021), using 2 ng of template in each reaction. The abundances of *nirS* and *nirK* genes were used as proxies for the denitrifying community (Henry et al., 2004; Throbäck et al., 2004), *nosZ*I and *nosZ*II for the nitrous oxide-reducing community (Henry et al., 2006;

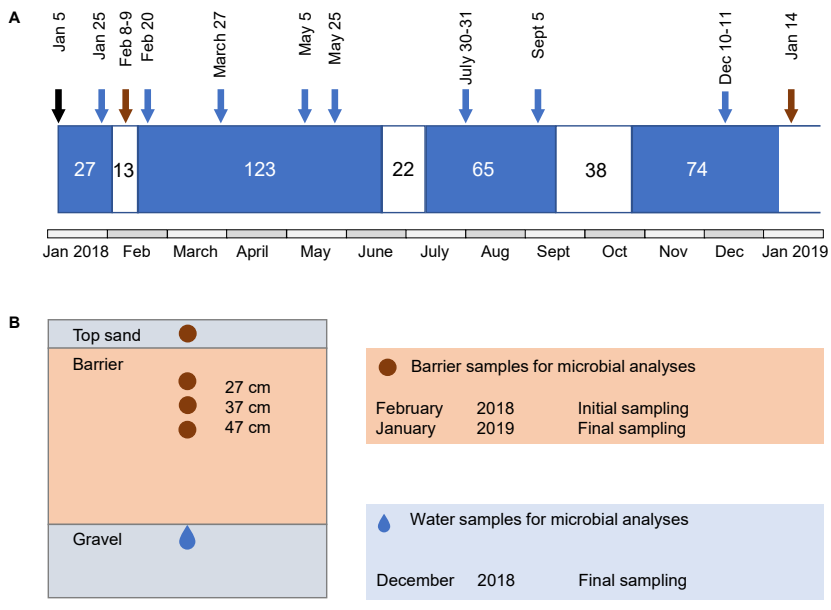

FIGURE 1 | Schematic illustration of the operational periods of the system, sampling time points, and sampling locations. **(A)** Length of wet (blue) and dry periods (white) and time points for water and barrier sampling. Sampling of barrier samples is indicated by brown arrows and water samples after barrier passage are indicated with blue arrows. The black arrow indicates the date of the first wet cycle. Microbial community analysis in water samples was only performed for the last sampling occasion. **(B)** Cross-section of the side view of barrier compartment, showing regions from where samples for characterization of microbial communities were taken. Brown area indicates barrier and gray areas indicate sand and gravel.

Jones et al., 2013), *nrfA* for the DNRA performing community (Mohan et al., 2004; Welsh et al., 2014), and *amoA* (bacterial and archaeal) for the ammonia-oxidizing communities (Rotthauwe et al., 1997; Tourna et al., 2008). Primer sequences, reaction conditions, and thermal cycling protocols are summarized in **Supplementary Table 2**.

Sequencing and Bioinformatic Analyses of 16S rRNA Genes

To determine the diversity and composition of the microbial communities in the water and barrier samples, the V3–V4 region of the bacterial and archaeal 16S ribosomal RNA genes was amplified using the primer pair of pro341F and pro805R (Takahashi et al., 2014) as previously described (Hellman et al., 2019), with the slight modifications that the first PCR was performed in 25 μl of the reaction mixture and that purification steps were carried out using Sera-Mag™ magnetic beads (GE Healthcare, Chicago, IL, United States). Sequencing was performed on an Illumina® MiSeq instrument using the 2 × 250 bp chemistry. The raw sequence dataset is available in the NCBI sequence read archive (SRA) under BioProject accession number PRJNA773712.

The sequences were processed as described in Hellman et al. (2019). Briefly, the trimmed and merged sequences were quality-filtered using a maximum expected error = 1, dereplicated using a minimum unique size = 2, clustered at 97% identity, and chimera-checked using VSEARCH (Rognes et al., 2016). Singleton operational taxonomic units (OTUs) were removed, and representative OTUs were classified using the non-redundant reference database SILVA version 132 (Yilmaz et al., 2014). A phylogenetic tree was constructed based on the aligned nucleotide sequences of representative OTUs using FastTree (Price et al., 2009) and the Jukes-Cantor and CAT model (Jukes and Cantor, 1969). Sequences representing chloroplasts and mitochondria were identified from the tree and removed. One sample (a barrier sample from CB2, February 2018) had only 94 sequences and was excluded from the analyses. The resulting dataset had 1,276,515 sequences, corresponding to 9,862 OTUs. The dataset was divided into separate sets for water and barrier samples (5 and 37 samples, respectively) and rarefied to the smallest sample size (20,364 counts per sample and 3,757 OTUs for water and 7,479 counts per sample and 7,634 OTUs for barrier). To partition OTUs identified as frequent members of the community from less frequent OTUs, a dispersion index (the ratio of the variance to the mean abundance, multiplied by the occurrence) was calculated for each OTU and used to model whether the OTUs followed a Poisson distribution. Theory predicts that rare OTU abundances are randomly (Poisson) distributed across sites and follow a log-series distribution,

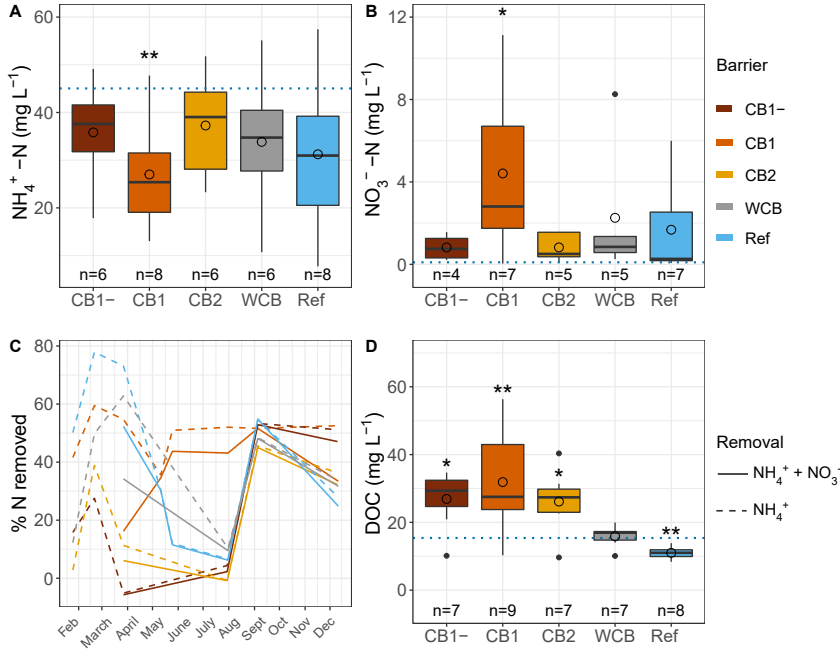

FIGURE 2 | Water chemistry after passage through the reactive barriers and reference across all time points. **(A)** Ammonium concentration, **(B)** nitrate concentration, **(C)** removal of total reactive nitrogen and ammonium over time, and **(D)** concentration of dissolved organic carbon. Inflow concentrations are indicated with dotted lines in panels **(A,B,D)** (mean values over the year, $n = 31$, 29, and 12 for ammonium, nitrate, and dissolved organic carbon, respectively). Box limits represent the inter-quartile range with median values represented by the center line and mean values by circles. Whiskers represent values ≤ 1.5 times the upper and lower quartiles, while points indicate values outside this range. The number of samples per barrier is indicated below the boxes. Stars denote if the mean value is significantly different from the mean inflow value (*t*-test, $^*p < 0.05$, $^{**}p < 0.01$).

whereas frequently occurring OTU abundances are non-randomly distributed (Magurran and Henderson, 2003). OTUs occurring at a frequency above the 2.5% confidence limit of the Chi^2 distribution were retained in the dataset (Saghaï et al., 2021). If not stated specifically, these frequently distributed communities are those analyzed and discussed in the following text. Analysis of the sequence data was carried out in R, version 4.0.3 (R Development Core Team, 2016).

Statistical Analyses

"Phyloseq" (McMurdie and Holmes, 2013) was used to estimate Shannon entropy (H′). Pielou's evenness index (J) was calculated from the Shannon entropy as $J = H'/\ln(S)$, where S is the total number of taxa in a sample, across all the samples in the dataset. Phylogenetic diversity (Faith's PD) (Faith, 1992) was estimated using the function estimate_pd in package "btools" (Battaglia, 2021). "Phyloseq" was also used for non-metric multidimensional scaling (NMDS) using Bray–Curtis dissimilarity matrices to visualize community patterns. The "vegan" (Oksanen et al., 2018) function envfit was used to correlate chemical and taxonomical data with the community structure and the function adonis to test differences in the community structures by permutational multivariate analysis of variance (PERMANOVA, using nperm = 999). Pairwise testing after significant PERMANOVAs was done using function pairwise.perm.manova from the package "RVAideMemoire" (Hervé, 2020; 999 permutations and *p*-value adjustment with "false discovery rate"). The alpha diversity estimates were done using non-rarefied data, and all other analyses were done using rarefied data. Student's *t*-test (assuming unequal variances and two-sided, if not indicated else) was used when comparing two groups, and Tukey's honest significance test (HSD test) was used when comparing three or more groups ($\alpha = 0.05$). Gene abundance data were log-transformed before statistical testing. Statistical analyses were carried out in R, version 4.0.3 (R Development Core Team, 2016).

RESULTS

Water Chemistry and N Removal

Regardless of the barrier composition, ammonium concentrations were generally reduced and nitrate concentrations

were increased after passage through the barrier, albeit significantly only in the CB1 with vegetation in the barrier (**Figures 2A,B**). CB1 showed the highest removal of ammonium from mid-May and throughout the experimental period, and despite the production of nitrate, the removal of reactive N was more than 40% during summer (**Figure 2C**). From 23 May to 29 August, the concentration of dissolved oxygen was lower than observed during the rest of the year (15.1 ± 5.3 and 50.1 ± 19.7%, respectively, mean ± SD, *t*-test, $p < 0.001$), which coincided with lower ammonium removal. The high and similar N removal capacity in all the barriers at the beginning of September might be caused by the of high dissolved oxygen concentration in the inflow water at that time (**Supplementary Table 1**). When normalizing ammonium removal to the removal capacity of the reference, CB1 had a 2.3 times higher capacity, but CB1-, CB2, and WCB removed less, 0.39, 0.39 and 0.70 times the reference, respectively (mean values of ratios of % reactive N removal, $n = 4$–8). Over the year, the amount of reactive N removed was moderate, with an average of 29% across all the barriers (including the reference, which showed a 29% removal), and there were no differences between the barriers (HSD test, **Supplementary Figure 2**). The DOC concentration increased in the water after passing through the compost barriers, but was found to be reduced in the reference and unaffected in the WCB groups (**Figure 2D**).

Genetic Potential for N-Transformation Processes

Gene abundances in the barrier material are shown separately for the top sand and the actual barrier layers in **Supplementary Figure 3**. The abundances in the top sand were lower than those in the reactive layer of all the compost barriers. With few exceptions, the gene abundances in the compost and woodchip barriers were higher after the fourth wet cycle compared to those observed after the first wet cycle, whereas the reference displayed increases only for *nirS* and *nosZ*I. The potential for ammonia oxidation (the sum of archaeal and bacterial *amoA* gene abundances), increased in the two compost barriers having vegetation (**Figure 3A**; one-sided *t*-test, top sand excluded, $p < 0.05$). In the woodchip barrier, there was an increase in the genetic potential for denitrification (sum of *nir* genes), nitrous oxide reduction (sum of *nosZ* genes), and DNRA (*nrfA*) (**Figures 2B–D**; one-sided *t*-test, top sand excluded, $p < 0.05$). Possible changes in the reference could not be tested statistically due to missing samples at the final sampling stage. A week into the first dry cycle, all processes but nitrification had a higher genetic potential in the compost barriers than in the WCB and reference (**Figures 3A–D**; HSD test). In the end, a week into the fourth dry cycle, denitrification and nitrous oxide reduction potentials were similar among all the treatments, while nitrification potential remained higher in the CB barriers than in the WCB barrier, reference excluded (**Figures 3A–C**; HSD test). The ratio between DNRA and nitrification [*nrfA*/(bacterial *amoA* + archaeal *amoA*)] was significantly lower at the end of the experiment in the vegetated CB1 barrier (not shown, *t*-test $p = 0.025$).

The genetic potentials of the N-transforming processes in the water were determined during the fourth wet cycle. Gene abundances involved in nitrous oxide reduction, DNRA, and denitrification (*nirK*) were higher in the water collected from the woodchip barrier when compared to water collected from the reference and compost barriers. The other gene abundances in the water showed no specific pattern (**Supplementary Table 1**).

Diversity and Community Structure

The phylogenetic diversity (Faith's PD) initially differed between CB2 and WCB samples, but after 1 year, there were no significant differences among the barriers (**Supplementary Figure 4A**; HSD test). Shannon's entropy and Pielou's evenness showed the same pattern (**Supplementary Figures 4B,C**; HSD test). Differences in the structure of microbial community between samples were mainly driven by barrier composition and sampling occasion (PERMANOVA, $p = 0.001$ and 0.003, respectively; **Figure 4A**). Two groups could be distinguished: one group included the compost barriers and the other included WCB and reference (pairwise comparisons after PERMANOVA, $p > 0.16$ within groups and $p < 0.007$ between the two groups). The top sand in the compost barriers was, however, more similar to the WCB and reference samples than to the deeper layers of compost barriers (**Figure 4A**). Actinobacteria, Alphaproteobacteria, and Gammaproteobacteria dominated the barrier samples both at the beginning and the end of the experimental period (**Figure 4B**). In total, 77 classes (36 phyla) were represented in the barriers, and most of them were significantly correlated with the community structure (**Supplementary Table 3**). Higher abundances of Gammaproteobacteria were correlated with the end point samples (**Figures 4A,B**), but most of the bacterial classes correlating to the separation of community structure were strongly associated ($r^2 > 0.7$) with the compost barriers (**Figure 4A** and **Supplementary Table 3**). Nitrospira was the second most abundant class present in the reference at the final sampling stage (**Figure 4B**). Organic carbon content and pH also correlated with the separation of the communities; organic carbon correlated with the compost barriers and samples from start, and pH with the deeper layers in the WCB (**Supplementary Table 3**; $p = 0.019$ and 0.011, respectively).

All gene abundances correlated positively with the compost barrier communities. Differences in the correlations with start and end communities were seen for *nir* genes, where *nirK* and *nirS* correlated with those from start and end, respectively. Also, *nosZ*I correlated with end samples, whereas *nosZ*II showed no pattern with sampling occasion (**Supplementary Table 3**).

Although the water samples were also dominated by Actinobacteria and Gammaproteobacteria (**Supplementary Figure 5**), the water and barrier samples had distinctly different bacterial communities (PERMANOVA, $p = 0.001$) at the end of the experimental period. Other highly represented classes in the water samples were Bacteroidia, Campylobacteria, and Clostridia. The water from the WCB also had a high occurrence of Desulfobulbia and Desulfuromonadia, classes not found in the water sampled from the other barriers or in the barrier samples (**Supplementary Figure 5**). The water from the WCB had the highest diversity and evenness, as indicated by Shannon's and

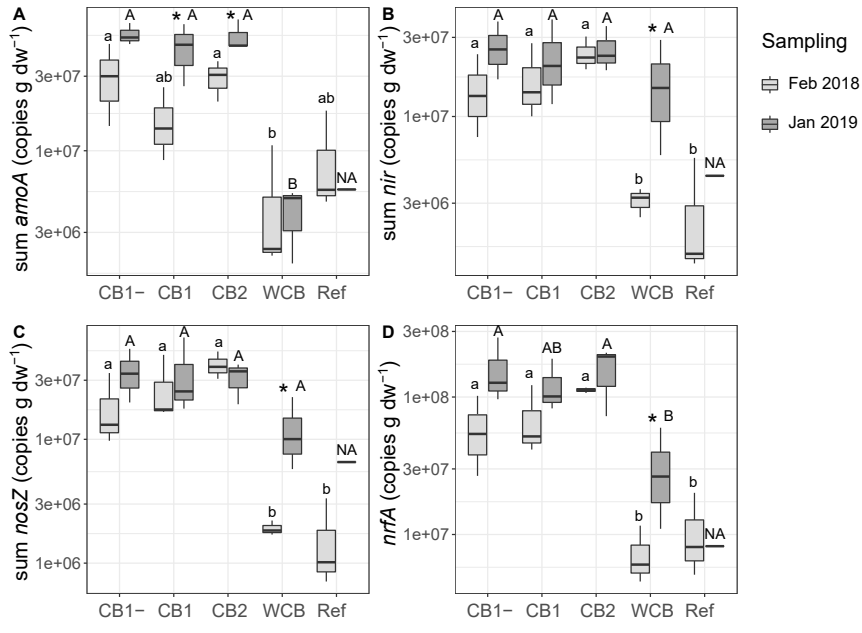

FIGURE 3 | Genetic potential for **(A)** ammonia oxidation, **(B)** denitrification, **(C)** nitrous oxide reduction, and **(D)** DNRA in the barrier materials and reference with top sand excluded across all depths based on the sum of functional groups for each process. Box limits represent the inter-quartile range with median values represented by the center line and whiskers represent values ≤ 1.5 times the upper and lower quartiles. For each barrier, stars denote if the mean values of the final abundances are significantly higher than the initial abundances (one-sided *t*-test, $^*p < 0.05$, $n = 3$, reference final sampling $n = 1$). Different small letters above boxes indicate significant differences between barriers at the initial sampling and capital letters indicate differences at the final sampling occasion (Tukey's HSD test, $\alpha = 0.05$, and the final sampling in the reference is not included in the test, denoted NA).

Pielou's indices (**Supplementary Figures 4B,C**). Overall, the water communities had a lower diversity based on Shannon's entropy than the barrier communities across time and among barrier types (**Supplementary Figure 4B**), but the phylogenetic diversity did not differ between water and barrier samples (**Supplementary Figure 4A**).

DISCUSSION

The overall N removal performance of the barriers was moderate, with only 29% of N removed on average across all the barrier types. During the period with less dissolved oxygen concentrations available in the water fed to the barriers, removal of ammonium decreased in all barriers except for CB1, which can likely be attributed to oxygen deficiency for the organisms involved in nitrification. We can only speculate why CB1 showed a more stable performance and functioned better than the other barriers under oxygen-limiting conditions. Compared to CB1-, CB1 had vegetation. The idea behind having vegetation in the barriers was to prevent clogging by facilitating the flow through small channels made by the roots. In addition, small channels might have helped in the advection and diffusion of oxygen, thereby favoring nitrification. However, this phenomenon should also have occurred in CB2. The higher proportion of compost, likely increasing heterotrophic respiration and thereby decreasing oxygen levels, is a more plausible explanation for the differences in ammonium removal. The significant removal of ammonium in the CB1 barrier with vegetation did not lead to a significantly higher net removal of reactive N in the barrier, since nitrate was formed. Nevertheless, decreasing the ammonium load is still advantageous, not only because of its toxicity, but also because it contributes to decreasing biological oxygen demand, thus preventing anoxic conditions in the recipient aquifer. Allowing plants to grow in the barriers could have several effects on the N dynamics, the most obvious being plant N uptake and accumulation in plant biomass. This could contribute to the lowered ammonium concentrations in the water from CB1 in comparison to the corresponding barrier without plants (CB1-). However, plants can also affect microbial activity, for example, resulting in immobilization of available ammonium (Skiba et al., 2011), and either increase or decrease nitrification depending on the plant species and soil (Skiba et al., 2011; Thion et al., 2016; Norton and Ouyang, 2019). Although our experimental design does not allow us to decipher the mechanisms, allowing plants to grow in the barriers makes the

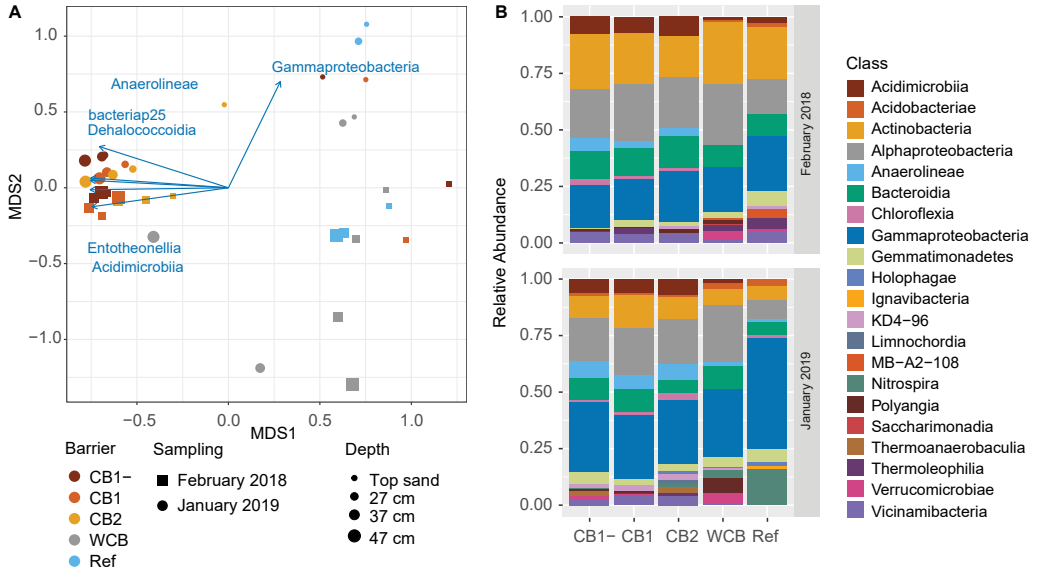

FIGURE 4 | Structure and taxonomic composition of microbial communities in the reactive barrier material. **(A)** Ordination is based on non-metric multidimensional scaling of Bray–Curtis dissimilarities of OTU abundances (stress = 0.13). Taxonomic classes that significantly correlated with the ordination ($p < 0.05$ and $r^2 > 0.7$) are shown as vectors. The lengths of the vectors are proportional to the strength of the correlation. **(B)** Mean relative abundances across the depths of microbial classes (>2% of the community) in the barriers at the initial and final sampling stages.

system resemble a vertical sub-surface flow constructed wetland or reedbed (Vymazal, 2007; Al-Ajalin et al., 2020), a design that has proven to be efficient in the removal of nutrients and organic material from domestic wastewater (e.g., Blankenberg et al., 2008). Further, in a full-scale SAT with more frequent alteration of wet and dry periods (Sharma and Kennedy, 2017), additional nitrification in the vadose zone, together with dilution when the recharged water reaches the aquifer, will contribute to lower ammonium levels in the aquifer than measured in our pilot system (Sopilniak et al., 2017).

The composition of the bacterial community differed and largely reflected the concentrations of DOC in the water after passage through the barrier, but in contrast to our hypothesis about diversity, there were no differences between the reactive barriers at the end of the first year of operation (reference barrier excluded). The reference showed a relative increase in Nitrospira, which is known to be involved in nitrification and is important in sand filters (Fowler et al., 2018), yet this was not reflected in the ammonium removal. The presence of compost in the barriers was the strongest driver of community structure, and hence strengthens the part of our first hypothesis about different communities developing in the barriers and supports the lab-scale study using the same compost material (Modrzyński et al., 2021). The type of available carbon is known to be an important factor that determines the development of soil bacterial communities (e.g., Cederlund et al., 2014), as well as their metabolic capacity and N removal rates in wastewater treatment plants (e.g., Hallin et al., 2006). One of the bacterial classes present in higher abundance in the compost barriers, which also increased in relative abundance over the year, was Anaerolineae, belonging to the phylum Chloroflexi. It has been retrieved from a wide range of habitats (Yamada and Sekiguchi, 2009), and members of this class have genes for cellulose hydrolyzation (Xia et al., 2016). The abundance of uncharacterized Chloroflexi KD4-96 also increased in the barriers with time and has previously been found in polluted soils (Gołębiewski et al., 2014; Wegner and Liesack, 2017). The origin of the compost used in our experiment was based on waste from gardens, and compost of a different origin could potentially promote a different community with other carbon degradation pathways or tolerance and capacity to degrade contaminants. Thus, when designing multipurpose reactive barriers, the origin of the compost could be a way of controlling which microorganisms proliferate and thrive in the barriers.

The differences in the genetic potentials for N-transforming processes that developed during the first year of operation were not reflected in the N removal activity among the barriers. The poor ammonium removal in the compost barriers could be due to the observed trend of increasing genetic potential for DNRA, even though we detected a high abundance and significant increase in ammonia-oxidizing bacteria and archaea in these barriers. A previous study has reported an increase in the DNRA

bacteria in the lower, anoxic layers in compost-based barriers, resulting in increased ammonium production despite efficient nitrification in the upper, oxic barrier layers (Modrzyński et al., 2021). The exception in our study was the increased ammonium removal in CB1, which had a lower ratio between *nrfA* (DNRA) and *amoA* (ammonia oxidation) in the barrier material at the end of the experimental period. Another aspect when comparing *amoA* abundances between the compost barriers *versus* the woodchips and reference is the possible effect of N mineralization. We speculate that N mineralization of organic matter in the compost continuously supplies the systems with ammonium (Habteselassie et al., 2006), and thereby supports the development of a larger ammonia-oxidizing community in the compost barriers. Hence, the resulting ammonium levels in the water after barrier passage is not lower in the compost barriers despite significantly higher *amoA* abundances. In other woodchip-based systems for N removal, it has been shown that changes in the microbial community composition appear within a few months (Grießmeier et al., 2017; Aalto et al., 2020; Hellman et al., 2021; Jéglot et al., 2021). Given that the increase in copy numbers of *nir* and *nosZ* genes in the woodchip barrier resulted in the same genetic potential for denitrification and nitrous oxide reduction between the compost and woodchip barriers, it is plausible that in the present systems, the potentials for denitrification and nitrous oxide reduction were similar among the barriers during a substantial part of the experimental period, which contributed to the equal overall removal of reactive N. A higher temporal resolution would be needed to better understand this phenomenon.

To conclude, our study found small or no differences in ammonium or overall N removal among the barriers, despite large differences in the composition of microbial community and genetic potential for N-transforming processes. The barrier with vegetation and the highest proportion of compost continued to remove approximately 50% of the ammonium even under conditions with low oxygen concentration in the water. The composition of the barrier material will be crucial to achieve sufficient N removal and avoid leakage of DOC. In this regard, a barrier based on woodchips is preferred over compost, but the removal of other pollutants must be considered as well, indicating that designing reactive barriers for multiple purposes is a challenge. In summary, a range of materials is likely necessary to achieve sustainable urban wastewater management using a soil aquifer treatment system in combination with barriers when recharging aquifers.

DATA AVAILABILITY STATEMENT

The raw sequence dataset is available under the BioProject accession number PRJNA773712 in the NCBI sequence read archive (SRA) at https://www.ncbi.nlm.nih.gov/. The other data used in the analyses are in the **Supplementary Table 1**.

AUTHOR CONTRIBUTIONS

LM-L, CV, JC, and SH designed the study. LM-L and CV conducted the fieldwork. MH performed the laboratory work. MH and JJ analyzed the data. MH, SH, and JJ prepared the manuscript, with input from the other authors. All authors approved the final version of the manuscript for publication.

FUNDING

This work was supported by the Water Joint Programming Initiative and financed *via* the Swedish Research Council Formas (grant nos 2016-00007 and 2018-02788) and the Spanish Ministry of Science, Innovation, and Universities through PCIN-2015-245. AGAUR-SGR2017-1485. IDAEA-CSIC is a Center of Excellence Severo Ochoa (Grant CEX2018-000794-S funded by MCIN/AEI/10.13039/501100011033). Sequencing was performed by the SNP&SEQ Technology Platform in Uppsala. The facility is part of the National Genomics Infrastructure (NGI), Sweden, and the Science for Life Laboratory. The SNP&SEQ Platform is also supported by the Swedish Research Council and the Knut and Alice Wallenberg Foundation.

ACKNOWLEDGMENTS

We thank Valerie Hubalek for help with sampling, Jakub Modrzynski for help with sampling and chemical analyses, and Consorci de la Costa Brava Girona (CCBGi) for help and unlimited access to the WWTP facility.

SUPPLEMENTARY MATERIAL

The Supplementary Material for this article can be found online at: https://www.frontiersin.org/articles/10.3389/fmicb.2022.877990/full#supplementary-material

REFERENCES

Aalto, S. L., Suurnäkki, S., von Ahnen, M., Siljanen, H. M. P., Pedersen, P. B., and Tiirola, M. (2020). Nitrate removal microbiology in woodchip bioreactors: a case-study with full-scale bioreactors treating aquaculture effluents. *Sci. Total Environ.* 723:138093. doi: 10.1016/j.scitotenv.2020.138093

Al-Ajalin, F. A. H., Idris, M., Abdullah, S. R. S., Kurniawan, S. B., and Imron, M. F. (2020). Evaluation of short-term pilot reed bed performance for real domestic wastewater treatment. *Environ. Technol. Innovat.* 20:101110. doi: 10.1016/j.eti.2020.101110

Battaglia, T. (2021). *A Suite of R Function for all Types of Microbial Diversity, version 0.0.1.*

Beganskas, S., Gorski, G., Weathers, T., Fisher, A. T., Schmidt, C., Saltikov, C., et al. (2018). A horizontal permeable reactive barrier stimulates nitrate removal and shifts microbial ecology during rapid infiltration for managed recharge. *Water Res.* 144, 274–284. doi: 10.1016/j.watres.2018.07.039

Bekele, E., Page, D., Vanderzalm, J., Kaksonen, A., and Gonzalez, D. (2018). Water recycling *via* aquifers for sustainable urban water quality management: current status, challenges and opportunities. *Water* 10:457. doi: 10.3390/w10040457

Blankenberg, A.-G. B., Haarstad, K., and Søvik, A.-K. (2008). Nitrogen retention in constructed wetland filters treating diffuse agriculture pollution. *Desalination* 226, 114–120. doi: 10.1016/j.desal.2007.01.237

Bouwer, H., Pyne, R., Brown, J., St. Germain, D., Morris, T. M., Brown, C. J., et al. (2008). *Design, Operation, and Maintenance for Sustainable Underground Storage FAcilities*. Jammu: AWWA Research Foundation.

Cederlund, H., Wessén, E., Enwall, K., Jones, C. M., Juhanson, J., Pell, M., et al. (2014). Soil carbon quality and nitrogen fertilization structure bacterial communities with predictable responses of major bacterial phyla. *Appl. Soil Ecol.* 84, 62–68. doi: 10.1016/j.apsoil.2014.06.003

Faith, D. P. (1992). Conservation evaluation and phylogenetic diversity. *Biol. Conservat.* 61, 1–10. doi: 10.1016/0006-3207(92)91201-3

Fowler, S. J., Palomo, A., Dechesne, A., Mines, P. D., and Smets, B. F. (2018). Comammox Nitrospira are abundant ammonia oxidizers in diverse groundwater-fed rapid sand filter communities. *Environ. Microbiol.* 20, 1002–1015. doi: 10.1111/1462-2920.14033

Gołębiewski, M., Deja-Sikora, E., Cichosz, M., Tretyn, A., and Wróbel, B. (2014). 16S rDNA pyrosequencing analysis of bacterial community in heavy metals polluted soils. *Microb. Ecol.* 67, 635–647. doi: 10.1007/s00248-013-0344-7

Grau-Martínez, A., Folch, A., Torrentó, C., Valhondo, C., Barba, C., Domènech, C., et al. (2018). Monitoring induced denitrification during managed aquifer recharge in an infiltration pond. *J. Hydrol.* 561, 123–135. doi: 10.1016/j.jhydrol.2018.03.044

Grießmeier, V., Bremges, A., McHardy, A. C., and Gescher, J. (2017). Investigation of different nitrogen reduction routes and their key microbial players in wood chip-driven denitrification beds. *Sci. Rep.* 7:17028. doi: 10.1038/s41598-017-17312-2

Habteselassie, M. Y., Stark, J. M., Miller, B. E., Thacker, S. G., and Norton, J. M. (2006). Gross nitrogen transformations in an agricultural soil after repeated dairy-waste application. *Soil Sci. Soc. Am. J.* 70, 1338–1348. doi: 10.2136/sssaj2005.0190

Hallin, S., Throbäck, I. N., Dicksved, J., and Pell, M. (2006). Metabolic profiles and genetic diversity of denitrifying communities in activated sludge after addition of methanol or ethanol. *Appl. Environ. Microbiol.* 72, 5445–5452. doi: 10.1128/aem.00809-06

Hellman, M., Bonilla-Rosso, G., Widerlund, A., Juhanson, J., and Hallin, S. (2019). External carbon addition for enhancing denitrification modifies bacterial community composition and affects CH4 and N2O production in sub-arctic mining pond sediments. *Water Res.* 158, 22–33. doi: 10.1016/j.watres.2019.04.007

Hellman, M., Hubalek, V., Juhanson, J., Almstrand, R., Peura, S., and Hallin, S. (2021). Substrate type determines microbial activity and community composition in bioreactors for nitrate removal by denitrification at low temperature. *Sci. Total Environ.* 755:143023. doi: 10.1016/j.scitotenv.2020.143023

Henry, S., Baudoin, E., López-Gutiérrez, J. C., Martin-Laurent, F., Brauman, A., and Philippot, L. (2004). Quantification of denitrifying bacteria in soils by nirK gene targeted real-time PCR. *J. Microbiol. Methods* 59, 327–335. doi: 10.1016/j.mimet.2004.07.002

Henry, S., Bru, D., Stres, B., Hallet, S., and Philippot, L. (2006). Quantitative detection of the nosZ gene, encoding nitrous oxide reductase, and comparison of the abundances of 16S rRNA, narG, nirK, and nosZ genes in soils. *Appl. Environ. Microbiol.* 72, 5181–5189. doi: 10.1128/aem.00231-06

Hervé, M. (2020). *"RVAideMemoire: Testing and Plotting Procedures for Biostatistics.", version 0.9-78*.

Jéglot, A., Sørensen, S. R., Schnorr, K. M., Plauborg, F., and Elsgaard, L. (2021). Temperature sensitivity and composition of nitrate-reducing microbiomes from a full-scale woodchip bioreactor treating agricultural drainage water. *Microorganisms* 9:1331. doi: 10.3390/microorganisms9061331

Jones, C. M., Graf, D. R. H., Bru, D., Philippot, L., and Hallin, S. (2013). The unaccounted yet abundant nitrous oxide-reducing microbial community: a potential nitrous oxide sink. *ISME J.* 7, 417–426. doi: 10.1038/ismej.2012.125

Jukes, T. H., and Cantor, C. R. (1969). "Evolution of protein molecules," in *Mammalian Protein Metabolism*, ed. H. N. Munro (New York, NY: Academic Press), 21–132. doi: 10.1016/b978-1-4832-3211-9.50009-7

Loos, R., Carvalho, R., António, D. C., Comero, S., Locoro, G., Tavazzi, S., et al. (2013). EU-wide monitoring survey on emerging polar organic contaminants in wastewater treatment plant effluents. *Water Res.* 47, 6475–6487. doi: 10.1016/j.watres.2013.08.024

Magurran, A. E., and Henderson, P. A. (2003). Explaining the excess of rare species in natural species abundance distributions. *Nature* 422, 714–716. doi: 10.1038/nature01547

McMurdie, P. J., and Holmes, S. (2013). phyloseq: an R package for reproducible interactive analysis and graphics of microbiome census data. *PLoS One* 8:e61217. doi: 10.1371/journal.pone.0061217

Modrzyński, J. J., Aamand, J., Wittorf, L., Badawi, N., Hubalek, V., Canelles, A., et al. (2021). Combined removal of organic micropollutants and ammonium in reactive barriers developed for managed aquifer recharge. *Water Res.* 190:116669. doi: 10.1016/j.watres.2020.116669

Mohan, S. B., Schmid, M., Jetten, M., and Cole, J. (2004). Detection and widespread distribution of the nrfA gene encoding nitrite reduction to ammonia, a short circuit in the biological nitrogen cycle that competes with denitrification. *FEMS Microbiol. Ecol.* 49, 433–443. doi: 10.1016/j.femsec.2004.04.012

Norton, J., and Ouyang, Y. (2019). Controls and adaptive management of nitrification in agricultural soils. *Front. Microbiol.* 10:1931. doi: 10.3389/fmicb.2019.01931

Oksanen, J., Blanchet, F. G., Friendly, M., Kindt, R., Legendre, P., McGlinn, D., et al. (2018). *vegan: Community Ecology Package*.

Page, D., Bekele, E., Vanderzalm, J., and Sidhu, J. (2018). Managed Aquifer Recharge (MAR) in sustainable urban water management. *Water* 10:239. doi: 10.3390/w10030239

Petrie, B., Barden, R., and Kasprzyk-Hordern, B. (2015). A review on emerging contaminants in wastewaters and the environment: current knowledge, understudied areas and recommendations for future monitoring. *Water Res.* 72, 3–27. doi: 10.1016/j.watres.2014.08.053

Price, M. N., Dehal, P. S., and Arkin, A. P. (2009). FastTree: computing large minimum evolution trees with profiles instead of a distance matrix. *Mol. Biol. Evol.* 26, 1641–1650. doi: 10.1093/molbev/msp077

Putz, M., Schleusner, P., Rütting, T., and Hallin, S. (2018). Relative abundance of denitrifying and DNRA bacteria and their activity determine nitrogen retention or loss in agricultural soil. *Soil Biol. Biochem.* 123, 97–104. doi: 10.1016/j.soilbio.2018.05.006

R Development Core Team (2016). *R: A Language and Environment for Statistical Computing*. Vienna: R Foundation for Statistical Computing.

Rognes, T., Flouri, T., Nichols, B., Quince, C., and Mahe, F. (2016). VSEARCH: a versatile open source tool for metagenomics. *PeerJ* 4:e2584. doi: 10.7717/peerj.2584

Rotthauwe, J. H., Witzel, K. P., and Liesack, W. (1997). The ammonia monooxygenase structural gene amoA as a functional marker: molecular fine-scale analysis of natural ammonia-oxidizing populations. *Appl. Environ. Microbiol.* 63, 4704–4712. doi: 10.1128/aem.63.12.4704-4712.1997

Saghaï, A., Banjeree, S., Degrune, F., Edlinger, A., Garcia-Palacios, P., Garland, G., et al. (2021). Diversity of archaea and niche preferences among putative ammonia-oxidizing Nitrososphaeria dominating across European arable soils. *Environ. Microbiol.* 24, 341–356. doi: 10.1111/1462-2920.15830

Schaffer, M., Kröger, K. F., Nödler, K., Ayora, C., Carrera, J., Hernández, M., et al. (2015). Influence of a compost layer on the attenuation of 28 selected organic micropollutants under realistic soil aquifer treatment conditions: insights from a large scale column experiment. *Water Res.* 74, 110–121. doi: 10.1016/j.watres.2015.02.010

Sharma, S. K., and Kennedy, M. D. (2017). Soil aquifer treatment for wastewater treatment and reuse. *Int. Biodeterior. Biodegradation* 119, 671–677. doi: 10.1016/j.ibiod.2016.09.013

Silver, M., Selke, S., Balsaa, P., Wefer-Roehl, A., Kübeck, C., and Schüth, C. (2018). Fate of five pharmaceuticals under different infiltration conditions for managed aquifer recharge. *Sci. Total Environ.* 642, 914–924. doi: 10.1016/j.scitotenv.2018.06.120

Skiba, M. W., George, T. S., Baggs, E. M., and Daniell, T. J. (2011). Plant influence on nitrification. *Biochem. Soc. Trans.* 39, 275–278. doi: 10.1042/bst0390275

Sopilniak, A., Elkayam, R., and Lev, O. (2017). Nitrification in a soil-aquifer treatment system: comparison of potential nitrification and concentration profiles in the vadose zone. *Environ. Sci. Processes Impacts* 19, 1571–1582. doi: 10.1039/C7EM00402H

Takahashi, S., Tomita, J., Nishioka, K., Hisada, T., and Nishijima, M. (2014). Development of a prokaryotic universal primer for simultaneous analysis of

Bacteria and Archaea using next-generation sequencing. *PLoS One* 9:e105592. doi: 10.1371/journal.pone.0105592

Thion, C. E., Poirel, J. D., Cornulier, T., De Vries, F. T., Bardgett, R. D., and Prosser, J. I. (2016). Plant nitrogen-use strategy as a driver of rhizosphere archaeal and bacterial ammonia oxidiser abundance. *FEMS Microbiol. Ecol.* 92:fiw091. doi: 10.1093/femsec/fiw091

Throbäck, I. N., Enwall, K., Jarvis, A., and Hallin, S. (2004). Reassessing PCR primers targeting nirS, nirK and nosZ genes for community surveys of denitrifying bacteria with DGGE. *FEMS Microbiol. Ecol.* 49, 401–417. doi: 10.1016/j.femsec.2004.04.011

Tourna, M., Freitag, T. E., Nicol, G. W., and Prosser, J. I. (2008). Growth, activity and temperature responses of ammonia-oxidizing archaea and bacteria in soil microcosms. *Environ. Microbiol.* 10, 1357–1364. doi: 10.1111/j.1462-2920.2007.01563.x

United Nations [UN] (2018). *68% of the World Population Projected to Live in Urban Areas by 2050, Says UN*. Available online at: https://www.un.org/development/desa/en/news/population/2018-revision-of-world-urbanization-prospects.html (accessed February 6, 2022).

Valhondo, C., and Carrera, J. (2019). "Chapter 1 - Water as a finite resource: from historical accomplishments to emerging challenges and artificial recharge," in *Sustainable Water and Wastewater Processing*, eds C. M. Galanakis and E. Agrafioti (Amsterdam: Elsevier), 1–17. doi: 10.1016/b978-0-12-816170-8.00001-6

Valhondo, C., Carrera, J., Ayora, C., Barbieri, M., Nödler, K., Licha, T., et al. (2014). Behavior of nine selected emerging trace organic contaminants in an artificial recharge system supplemented with a reactive barrier. *Environ. Sci. Pollut. Res.* 21, 11832–11843. doi: 10.1007/s11356-014-2834-7

Valhondo, C., Carrera, J., Martínez-Landa, L., Wang, J. J., Amalfitano, S., Levantesi, C., et al. (2020a). Reactive barriers for renaturalization of reclaimed water during soil aquifer treatment. *Water.* 12:1012. doi: 10.3390/w12041012

Valhondo, C., Martínez-Landa, L., Carrera, J., Díaz-Cruz, S. M., Amalfitano, S., and Levantesi, C. (2020b). Six artificial recharge pilot replicates to gain insight into water quality enhancement processes. *Chemosphere* 240:124826. doi: 10.1016/j.chemosphere.2019.124826

Valhondo, C., Martinez-Landa, L., Carrera, J., Ayora, C., Nödler, K., and Licha, T. (2018). Evaluation of EOC removal processes during artificial recharge through a reactive barrier. *Sci. Total Environ.* 612, 985–994. doi: 10.1016/j.scitotenv.2017.08.054

Vymazal, J. (2007). Removal of nutrients in various types of constructed wetlands. *Sci. Total Environ.* 380, 48–65. doi: 10.1016/j.scitotenv.2006.09.014

Wegner, C.-E., and Liesack, W. (2017). Unexpected dominance of elusive acidobacteria in early industrial soft coal slags. *Front. Microbiol.* 8:1023. doi: 10.3389/fmicb.2017.01023

Welsh, A., Chee-Sanford, J. C., Connor, L. M., Löffler, F. E., and Sanford, R. A. (2014). Refined NrfA phylogeny improves PCR-Based nrfA gene detection. *Appl. Environ. Microbiol.* 80, 2110–2119. doi: 10.1128/aem.03443-13

Wheeler, T., and von Braun, J. (2013). Climate change impacts on global food security. *Science* 341, 508–513. doi: 10.1126/science.1239402

Xia, Y., Wang, Y., Wang, Y., Chin, F. Y. L., and Zhang, T. (2016). Cellular adhesiveness and cellulolytic capacity in Anaerolineae revealed by omics-based genome interpretation. *Biotechnol. Biofuels* 9:111. doi: 10.1186/s13068-016-0524-z

Yamada, T., and Sekiguchi, Y. (2009). Cultivation of uncultured chloroflexi subphyla: significance and ecophysiology of formerly uncultured chloroflexi 'Subphylum I' with natural and biotechnological relevance. *Microbes Environ.* 24, 205–216. doi: 10.1264/jsme2.ME09151S

Yilmaz, P., Parfrey, L. W., Yarza, P., Gerken, J., Pruesse, E., Quast, C., et al. (2014). The SILVA and "All-species Living Tree Project (LTP)" taxonomic frameworks. *Nucleic Acids Res.* 42, D643–D648. doi: 10.1093/nar/gkt1209

Conflict of Interest: The authors declare that the research was conducted in the absence of any commercial or financial relationships that could be construed as a potential conflict of interest.

Publisher's Note: All claims expressed in this article are solely those of the authors and do not necessarily represent those of their affiliated organizations, or those of the publisher, the editors and the reviewers. Any product that may be evaluated in this article, or claim that may be made by its manufacturer, is not guaranteed or endorsed by the publisher.

Supplementary material for

Nitrogen removal capacity in microbial communities developing in compost- and woodchip-based multipurpose reactive barriers for aquifer recharge with wastewater

Maria Hellman[1]*, Cristina Valhondo[2,3], Lurdes Martínez-Landa[3,4], Jesús Carrera[2,3], Jaanis Juhanson[1], Sara Hallin[1]

[1]Department of Forest Mycology and Plant Pathology, SLU Uppsala, Sweden

[2]Institute of Environmental Assessment and Water Research (IDAEA), CSIC, Barcelona, Spain

[3]Hydrogeology Group (UPC-CSIC), Associate Unit, Barcelona, Spain

[4]Department of Civil and Environmental Engineering, Universitat Politecnica de Catalunya (UPC), Barcelona, Spain

Figures

Tables

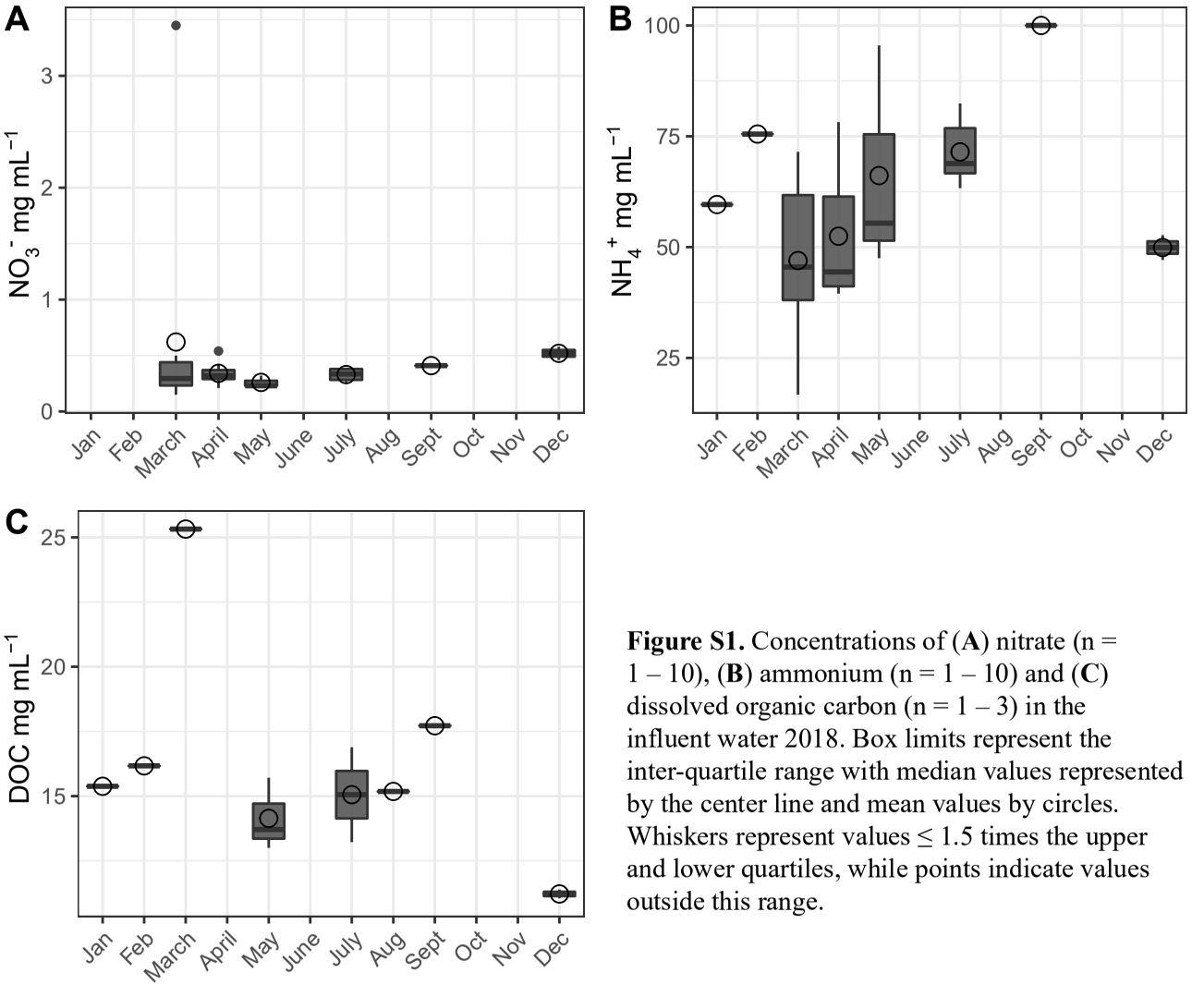

Figure S1. Concentrations of (**A**) nitrate (n = 1 – 10), (**B**) ammonium (n = 1 – 10) and (**C**) dissolved organic carbon (n = 1 – 3) in the influent water 2018. Box limits represent the inter-quartile range with median values represented by the center line and mean values by circles. Whiskers represent values ≤ 1.5 times the upper and lower quartiles, while points indicate values outside this range.

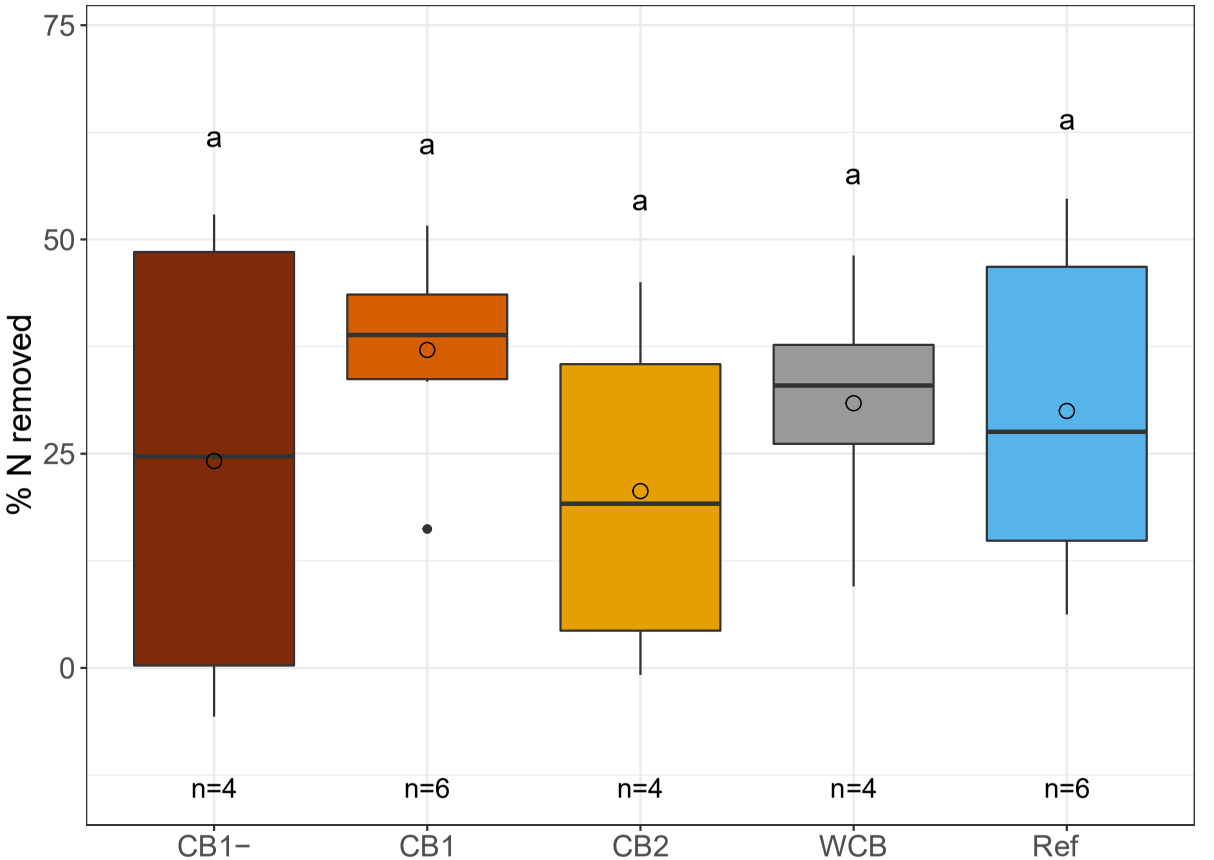

Figure S2. Reactive nitrogen removed in the water after passage through the reactive barriers and reference across all time points. Box limits represent the inter-quartile range with median values represented by the center line and mean values by circles. Whiskers represent values ≤ 1.5 times the upper and lower quartiles, while points indicate valuesoutside this range. Number of samples per barrier is indicated below the boxes.

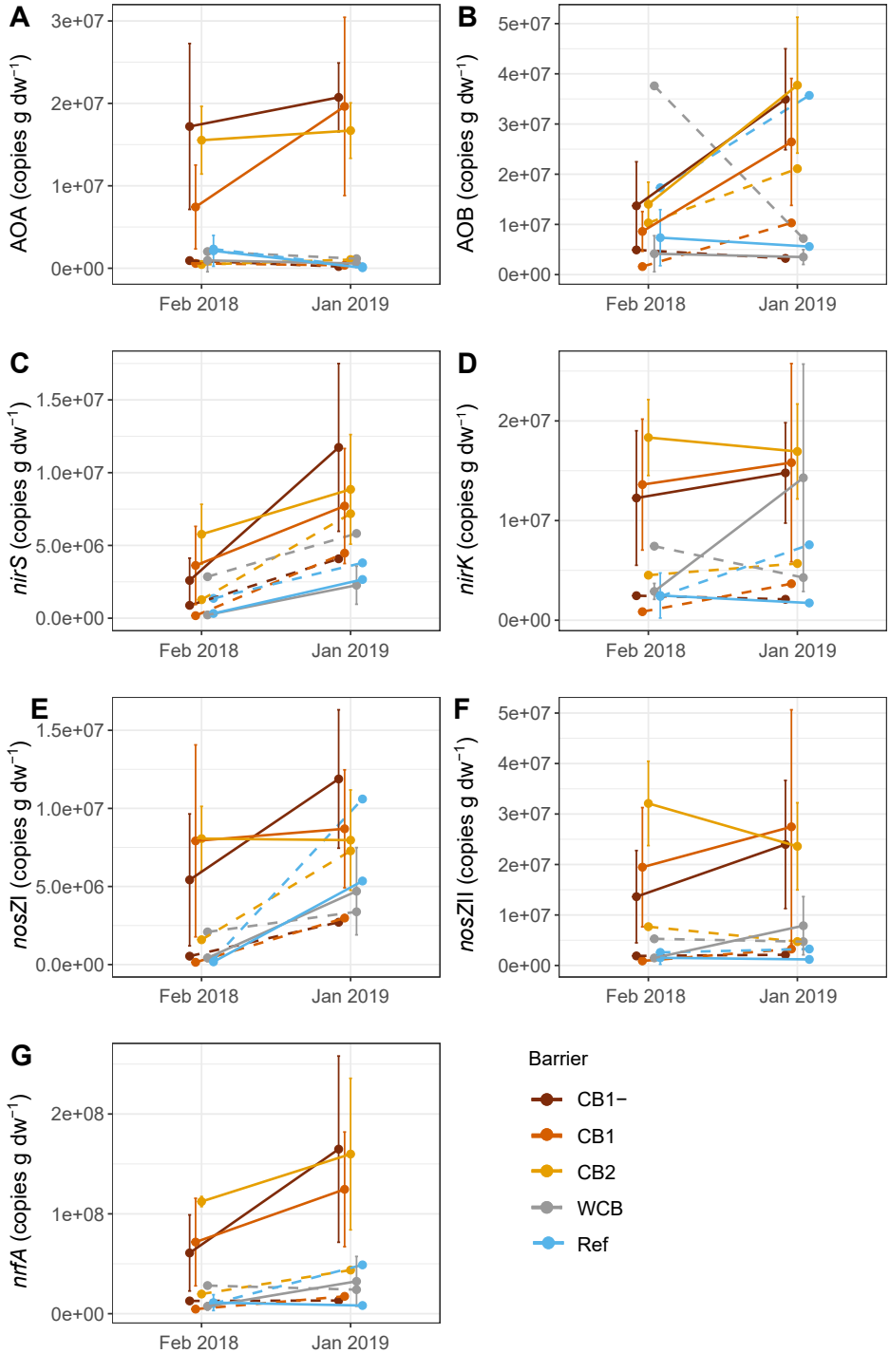

Fig. S3. Genetic potential for nitrogen transformation processes in top sand and barrier material shown as individual gene abundances at the initial (Feb 2018) and final (Jan 2019) sampling point. (**A**) *amoA* in ammonia oxidizing archaea, (**B**) *amoA* in ammonia oxidizing bacteria, (**C**) *nirS* in denitrifiers, (**D**) *nirK* in denitrifiers, (**E**) *nosZ*I in denitrifiers/nitrous oxide reducers, (**F**) *nosZ*II in denitrifiers/nitrous oxide reducers, (**G**) *nrfA* in DNRA bacteria. Dashed lines indicate gene abundances in the top sand and solid lines connect points representing the mean value of abundances at three depths (27, 37 and 47 cm) at each sampling occasion. Error bars show SD, n = 3 (Ref final sampling, n=1).

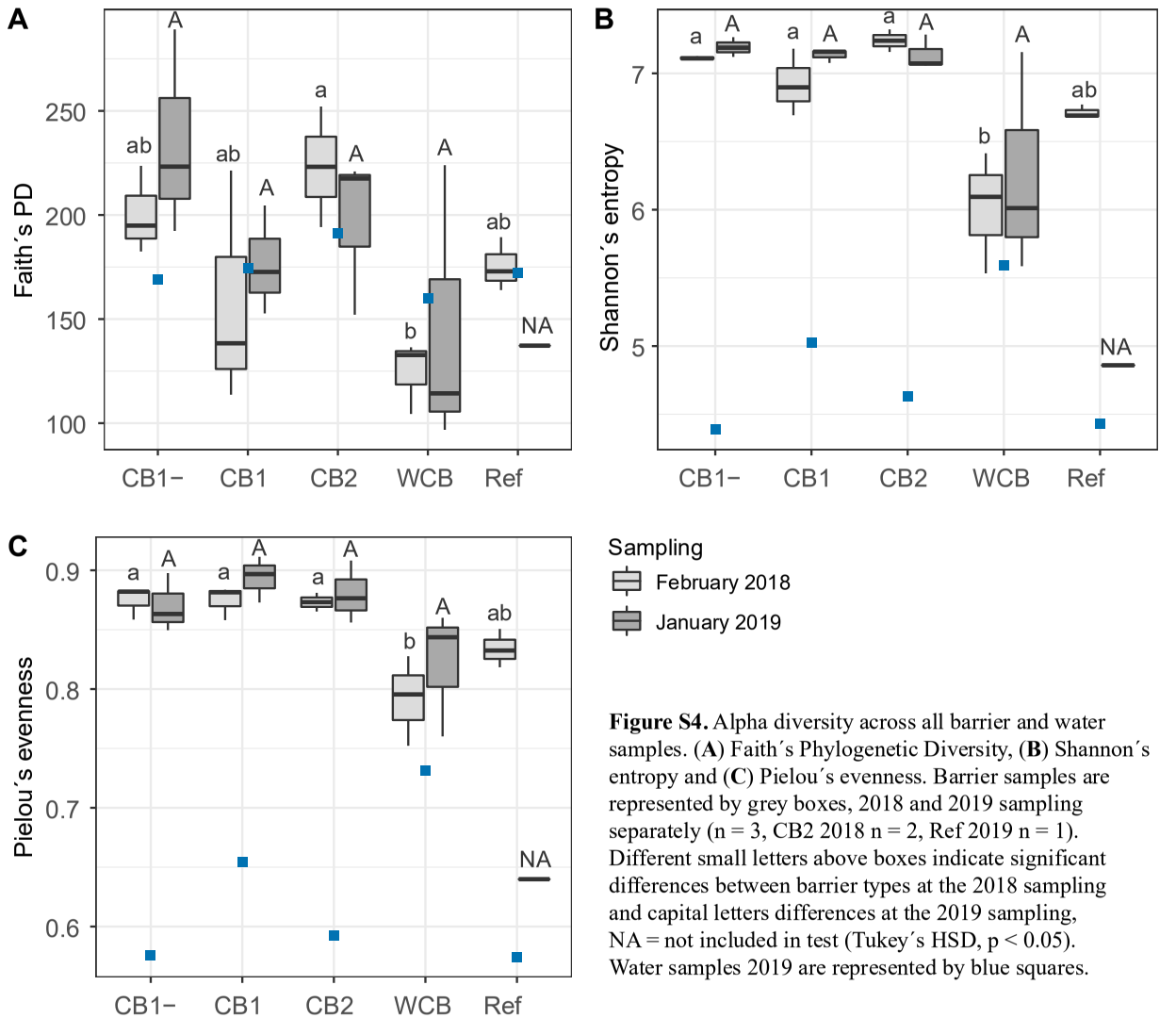

Figure S4. Alpha diversity across all barrier and water samples. (**A**) Faith´s Phylogenetic Diversity, (**B**) Shannon´s entropy and (**C**) Pielou´s evenness. Barrier samples are represented by grey boxes, 2018 and 2019 sampling separately (n = 3, CB2 2018 n = 2, Ref 2019 n = 1). Different small letters above boxes indicate significant differences between barrier types at the 2018 sampling and capital letters differences at the 2019 sampling, NA = not included in test (Tukey´s HSD, $p < 0.05$). Water samples 2019 are represented by blue squares.

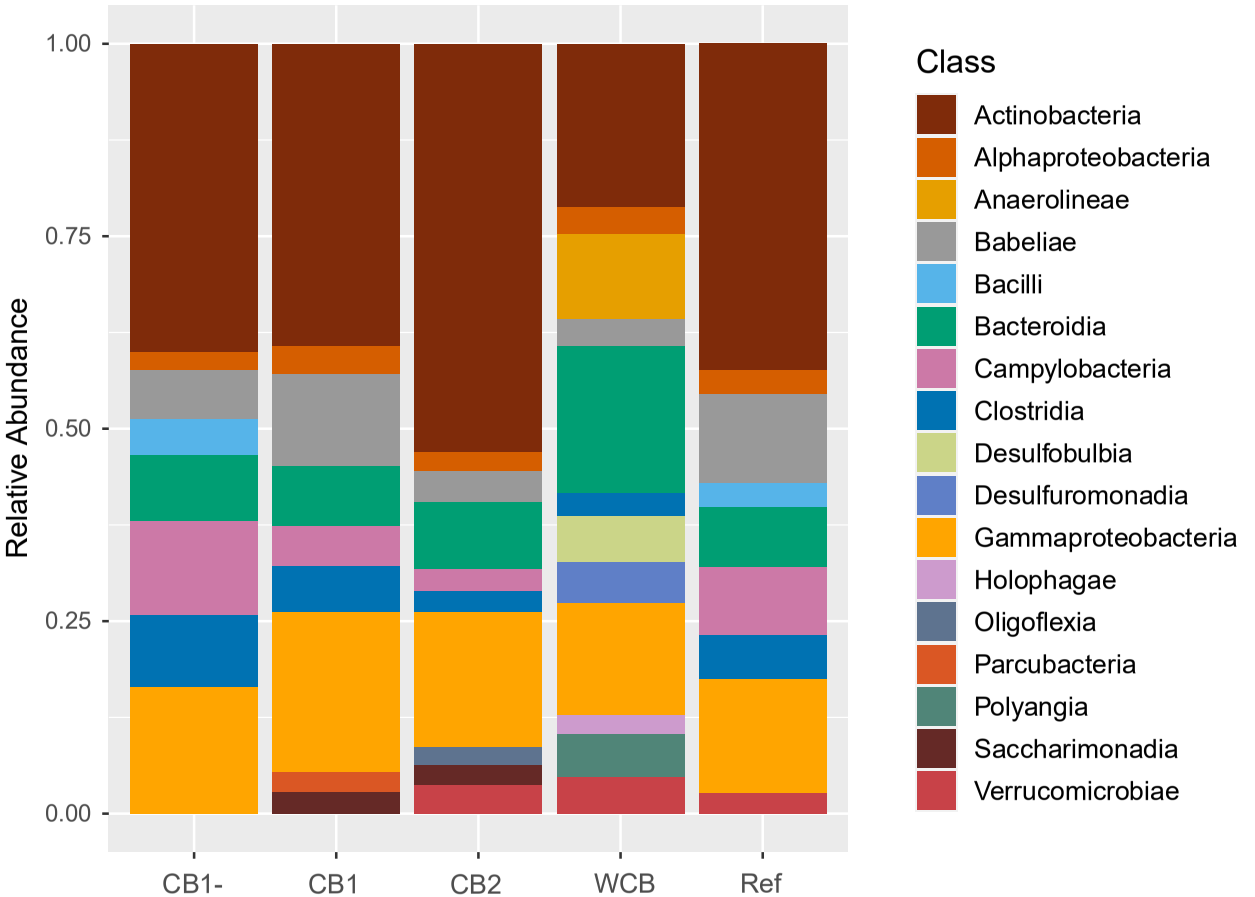

Figure S5. Relative contribution of microbial classes (> 2 % of the community) in the water samples (Dec 2018).

Table S1. Location, sampling date, chemical and microbial characterization of all samples.

Sample type	Barrier or Inflow	Date	Sampling	Depth cm	pH	LOI % of dw	NH4 mg L-1	NO3 mg L-1	DOC mg L-1	Oxygen mg L-1	Oxygen %	Faith PD	Shannon	Pielou	16S r RNA cop g dw-1	gAOA cop g dw-1	AOB cop g dw-1	*nirS* cop g dw-1	*nirK* cop g dw-1	*nosZ* I cop g dw-1	*nosZ* II cop g dw-1	*nrfA* cop g dw-1
															cop L-1	cop L-1	cop L-1	cop L-1	cop L-1	cop L-1	cop L-1	cop L-1
Water	INF	2018-01-25			7.9		59.6		15.38	6.2	61											
Water	INF	2018-02-20			7.9		75.5		16.17													
Water	INF	2018-03-06			7.9		46.7	0.5	25.32													
Water	INF	2018-03-07			7.4		40.9	0.44		3.7												
Water	INF	2018-03-23					71.5	0.33														
Water	INF	2018-03-25			7.1		16.7	3.45		4.4	40											
Water	INF	2018-03-26			7.3		27.1	0.44		4.5	43											
Water	INF	2018-03-27			7.3		37.1	0.23		2.4	23											
Water	INF	2018-03-28			7.3		44.3	0.26		1.2	13											
Water	INF	2018-03-29			7.3		59.4	0.24		1.0	10											
Water	INF	2018-03-30			7.5		63.4	0.15		5.5	56											
Water	INF	2018-03-31			7.5		62.5	0.17		5.6	58											
Water	INF	2018-04-01			7.6		44.4	0.42		5.4	54											
Water	INF	2018-04-02			7.9		42.0	0.3		7.8	80											
Water	INF	2018-04-03			7.7		46.3	0.28		6.0	64											
Water	INF	2018-04-04			7.6		40.3	0.54		5.3	55											
Water	INF	2018-04-05			7.6		39.5	0.21		6.3	64											
Water	INF	2018-04-06			7.7		78.2	0.32		6.4	68											
Water	INF	2018-04-07			7.6		76.5	0.32		5.9	60											
Water	INF	2018-05-11			7.7		95.5	0.23	13.00	5.9	69											
Water	INF	2018-05-23			7.7		55.4	0.23	13.71	0.8	9.3											
Water	INF	2018-05-25			7.7		47.5	0.32	15.71	0.6	7.1											
Water	INF	2018-07-20			7.6		63.3	0.32		1.3	16											
Water	INF	2018-07-24			7.6		82.4	0.26		1.5	18											
Water	INF	2018-07-25					69.7	0.39														
Water	INF	2018-07-27			7.7		68.0	0.39		1.4	18											
Water	INF	2018-07-30			7.7		66.2	0.35	13.22	1.0	13											
Water	INF	2018-07-31			7.6		79.2	0.27	16.89	1.2	15											
Water	INF	2018-08-29			7.7				15.18	1.9	24											
Water	INF	2018-09-05			7.2		100.0	0.41	17.72	5.2	65											
Water	INF	2018-12-10			7.3		47.1	0.58	11.05	3.0	30											
Water	INF	2018-12-11			7.3		52.7	0.46	11.39	3.8	38											
Water	CB1-	2018-01-25			7.7		50.2		34.69	0.2	1.6											
Water	CB1-	2018-02-01							29.34													
Water	CB1-	2018-02-01							28.46													
Water	CB1-	2018-02-20			7.4		54.7		31.42	1.6	15											
Water	CB1-	2018-03-27			7.2		39.0	0.97		0.1	0.8											
Water	CB1-	2018-07-30			7.2		63.3	5.13	33.43	0.8	10											
Water	CB1-	2018-09-05			7.2		46.7	1.52	20.89	0.8	10											
Water	CB1-	2018-12-10	final		6.8		23.0	6.92	10.15	1.9	18	169	4.386	0.576	3.78E+08	7.88E+06	4.08E+06	3.21E+06	2.77E+06	2.28E+06	4.34E+06	2.47E+07
Water	CB1	2018-01-25			7.3		34.8	12.43	56.34	0.2	1.9											
Water	CB1	2018-02-01							42.96													
Water	CB1	2018-02-01							43.16													
Water	CB1	2018-02-20			7.2		30.6		37.31	0.3	2.8											
Water	CB1	2018-03-27			6.7		16.8	49.25		0.4	3.8											
Water	CB1	2018-05-11			6.8		61.5	3.53	23.78	0.6	6.1											
Water	CB1	2018-05-25			6.8		23.3	11.97	25.85	0.3	3.7											
Water	CB1	2018-07-31			6.8		38.0	24.37	27.52	0.6	7.5											
Water	CB1	2018-09-05			7.4		48.4	0.18	19.65	0.4	5.3											
Water	CB1	2018-12-11	final		6.6		25.0	34.97	10.3	0.8	7.8	174	5.023	0.654	3.92E+08	3.84E+06	1.91E+06	4.00E+06	2.72E+06	1.77E+06	5.80E+06	2.39E+07
Water	CB2	2018-01-25			7.6		57.9	1.63	27.38	0.2	1.9											
Water	CB2	2018-02-01							28.22													
Water	CB2	2018-02-01							31.37													
Water	CB2	2018-02-20			7.0		46.2		40.34	0.6	5.8											
Water	CB2	2018-03-27			6.8		32.9	6.9		0.2	1.3											
Water	CB2	2018-07-30			7.3		66.7	0.51	22.63	0.6	7.0											
Water	CB2	2018-09-05			7.1		54.4	2.24	23.31	0.3	4.0											
Water	CB2	2018-12-10	final		7.0		30.0	6.94	9.65	0.9	9.1	191	4.631	0.592	3.21E+08	5.60E+06	6.38E+05	2.15E+06	3.50E+06	1.73E+06	6.32E+06	3.14E+07
Water	WCB	2018-01-25			7.6		52.3	5.99	16.96	0.2	1.9											
Water	WCB	2018-02-01							15.49													
Water	WCB	2018-02-01							19.94													
Water	WCB	2018-02-20			7.0		37.9		17.08	0.6	5.8											
Water	WCB	2018-03-27			6.8		13.8	36.56		0.2	1.3											
Water	WCB	2018-07-31			7.0		71.0	2.54	14.04	0.4	5.6											
Water	WCB	2018-09-05			7.1		51.6	1.14	17.5	0.3	4.0											
Water	WCB	2018-12-11	final		6.7		35.0	3.75	10.09	0.6	6.5	160	5.595	0.731	7.74E+08	4.22E+05	1.49E+06	4.93E+06	7.25E+06	3.31E+06	2.41E+07	8.93E+07
Water	Ref	2018-01-25			7.1		29.7	16.58	10.71	0.2	2.1											
Water	Ref	2018-02-01							9.21													
Water	Ref	2018-02-20			7.1		16.7		10.16	0.9	8.2											
Water	Ref	2018-03-27			6.5		9.99	26.54		0.4	4.0											
Water	Ref	2018-05-11			7.0		66.5	0.49	11.33	0.3	3.6											
Water	Ref	2018-05-25			7.0		41.8	1.09	11.66	0.3	3.6											
Water	Ref	2018-07-31			7.1		74.0	1.17	13.87	0.5	6.6											
Water	Ref	2018-09-05			7.3		45.2	0.32	12.69	0.7	8.3											
Water	Ref	2018-12-11	final		6.7		38.0	5.87	8.37	0.9	8.8	172	4.433	0.574	2.65E+08	2.14E+06	1.39E+06	1.77E+06	3.10E+06	2.07E+06	5.46E+06	3.31E+07
Barrier	CB1-	2018-02-08--09	initial	Top sand	7.8	0.39						118	5.384	0.72	2.24E+08	9.27E+05	4.92E+06	8.81E+05	2.46E+06	5.38E+05	1.89E+06	1.28E+07
Barrier	CB1-	2018-02-08--09	initial	27	7.6	4.84						195	7.125	0.883	4.04E+08	1.20E+07	1.80E+07	1.90E+06	1.14E+07	3.01E+06	1.01E+07	5.39E+07
Barrier	CB1-	2018-02-08--09	initial	37	7.6	5.70						182	7.102	0.882	1.12E+09	2.88E+07	1.95E+07	4.35E+06	1.94E+07	1.03E+07	2.40E+07	1.02E+08
Barrier	CB1-	2018-02-08--09	initial	47	7.9	4.71						224	7.11	0.858	2.82E+08	1.08E+07	3.61E+06	1.53E+06	5.99E+06	2.96E+06	6.78E+06	2.67E+07
Barrier	CB1	2018-02-08--09	initial	Top sand	7.7	0.34						118	6.079	0.791	4.70E+07	5.83E+05	1.60E+06	1.73E+05	8.55E+05	1.47E+05	8.98E+05	4.63E+06
Barrier	CB1	2018-02-08--09	initial	27	7.9	3.36						138	6.898	0.881	1.24E+09	1.33E+07	1.22E+07	6.67E+06	2.10E+07	1.50E+07	3.31E+07	1.22E+08
Barrier	CB1	2018-02-08--09	initial	37	7.5	4.45						114	6.693	0.884	4.74E+08	4.64E+06	9.24E+06	2.60E+06	1.14E+07	4.81E+06	1.26E+07	5.17E+07
Barrier	CB1	2018-02-08--09	initial	47	7.7	5.18						221	7.181	0.858	4.08E+08	4.36E+06	4.36E+06	1.60E+06	8.43E+06	3.95E+06	1.27E+07	4.15E+07
Barrier	CB2	2018-02-08--09	initial	Top sand	7.3	0.58						189	6.539	0.807	4.88E+08	4.53E+05	1.03E+07	1.27E+06	4.52E+06	1.59E+06	7.68E+06	1.97E+07
Barrier	CB2	2018-02-08--09	initial	27	7.5	3.62						252	7.322	0.865	9.81E+08	1.54E+07	1.52E+07	6.08E+06	1.66E+07	8.49E+06	3.00E+07	1.07E+08
Barrier	CB2	2018-02-08--09	initial	37	7.6	2.68						194	7.157	0.881	1.26E+09	1.97E+07	1.77E+07	7.65E+06	2.27E+07	9.88E+06	4.13E+07	1.17E+08
Barrier	CB2	2018-02-08--09	initial	47	7.6	4.80									8.49E+08	1.15E+07	9.15E+06	3.57E+06	1.57E+07	5.82E+06	2.50E+07	1.13E+08
Barrier	WCB	2018-02-08--09	initial	Top sand	7.3	0.62						143	5.976	0.763	3.87E+08	2.02E+06	3.76E+07	2.85E+06	7.43E+06	2.09E+06	5.28E+06	2.82E+07
Barrier	WCB	2018-02-08--09	initial	27	7.8	0.49						136	6.414	0.828	8.21E+07	2.54E+06	8.30E+06	4.70E+05	2.00E+06	1.95E+05	1.64E+06	1.16E+07
Barrier	WCB	2018-02-08--09	initial	37	7.8	7.80						133	6.094	0.795	6.18E+07	2.30E+05	1.90E+06	9.97E+04	3.14E+06	4.31E+05	1.27E+06	6.04E+06
Barrier	WCB	2018-02-08--09	initial	47	7.7	12.1						104	5.533	0.752	1.09E+08	7.96E+04	2.27E+06	1.02E+05	3.54E+06	6.49E+05	1.56E+06	4.55E+06
Barrier	Ref	2018-02-08--09	initial	Top sand	7.5	0.40						136	6.04	0.777	1.01E+08	2.33E+06	1.73E+07	1.36E+06	2.39E+06	3.38E+05	2.59E+06	1.01E+07
Barrier	Ref	2018-02-08--09	initial	27	7.8	0.40						173	6.69	0.832	1.22E+08	4.26E+06	1.38E+07	5.40E+05	5.09E+06	3.56E+05	2.98E+06	2.01E+07
Barrier	Ref	2018-02-08--09	initial	37	8.1	0.35						189	6.678	0.818	2.88E+07	8.15E+05	3.91E+06	1.60E+05	1.14E+06	6.86E+04	6.42E+05	5.10E+06
Barrier	Ref	2018-02-08--09	initial	47	8.1	0.38						164	6.772	0.851	4.13E+07	1.26E+06	4.36E+06	2.76E+05	1.21E+06	1.02E+05	9.15E+05	8.11E+06
Barrier	CB1-	2019-01-14	final	Top sand	7.4	0.50						170	6.269	0.794	8.88E+07	2.07E+05	3.23E+06	4.08E+06	2.10E+06	2.71E+06	2.12E+06	1.32E+07
Barrier	CB1-	2019-01-14	final	27	7.3	5.24						223	7.121	0.863	6.10E+08	1.61E+07	3.70E+07	7.51E+06	9.25E+06	7.35E+06	1.25E+07	9.64E+07
Barrier	CB1-	2019-01-14	final	37	7.6	4.33						289	7.266	0.85	8.19E+08	2.19E+07	4.38E+07	9.39E+06	1.60E+07	1.21E+07	2.18E+07	1.27E+08
Barrier	CB1-	2019-01-14	final	47	7.7	4.85						192	7.188	0.898	1.42E+09	2.42E+07	2.40E+07	1.83E+07	1.91E+07	1.62E+07	3.76E+07	2.71E+08
Barrier	CB1	2019-01-14	final	Top sand	7.1	0.67						137	6.039	0.792	1.91E+08	3.55E+05	1.03E+07	4.47E+06	3.66E+06	2.98E+06	3.26E+06	1.74E+07
Barrier	CB1	2019-01-14	final	27	7.0	5.06						173	7.166	0.897	7.38E+08	1.28E+07	3.49E+07	8.18E+06	1.20E+07	9.18E+06	1.52E+07	1.01E+08
Barrier	CB1	2019-01-14	final	37	7.0	4.34						205	7.159	0.873	1.39E+09	3.21E+07	3.25E+07	1.14E+07	2.71E+07	1.22E+07	5.42E+07	1.90E+08
Barrier	CB1	2019-01-14	final	47	7.2	4.77						153	7.076	0.911	4.91E+08	1.40E+07	1.19E+07	3.54E+06	8.34E+06	4.70E+06	1.30E+07	8.27E+07
Barrier	CB2	2019-01-14	final	Top sand	7.0	1.04						178	6.38	0.801	2.28E+08	1.05E+06	2.11E+07	7.18E+06	5.69E+06	7.28E+06	4.73E+06	4.37E+07
Barrier	CB2	2019-01-14	final	27	7.0	5.31						221	7.285	0.876	1.08E+09	1.64E+07	5.29E+07	1.32E+07	2.19E+07	1.10E+07	2.44E+07	2.10E+08
Barrier	CB2	2019-01-14	final	37	7.2	3.66						152	7.059	0.908	5.63E+08	1.35E+07	3.34E+07	6.62E+06	1.24E+07	4.60E+06	1.46E+07	7.26E+07
Barrier	CB2	2019-01-14	final	47	7.4	3.89						218	7.072	0.856	1.23E+09	2.02E+07	2.69E+07	6.74E+06	1.65E+07	8.30E+06	3.18E+07	1.97E+08
Barrier	WCB	2019-01-14	final	Top sand	7.1	0.64						169	6.333	0.798	2.00E+08	1.16E+06	7.19E+06	5.82E+06	4.28E+06	3.38E+06	4.72E+06	2.41E+07
Barrier	WCB	2019-01-14	final	27	7.2	0.69						114	5.586	0.76	1.41E+08	9.96E+05	3.98E+06	2.87E+06	2.98E+06	3.20E+06	2.55E+06	1.10E+07
Barrier	WCB	2019-01-14	final	37	7.2	4.40						96	6.012	0.844	4.75E+08	6.72E+05	4.68E+06	3.16E+06	2.58E+07	7.92E+06	1.40E+07	5.98E+07
Barrier	WCB	2019-01-14	final	47	7.2	8.10						224	7.156	0.86	2.28E+08	5.93E+04	1.84E+06	7.64E+05	1.41E+07	2.97E+06	7.07E+06	2.64E+07
Barrier	Ref	2019-01-14	final	Top sand	7.0	10.7						122	5.273	0.713	2.85E+08	1.84E+05	3.57E+07	3.80E+06	7.57E+06	1.06E+07	3.26E+06	4.89E+07
Barrier	Ref	2019-01-14	final	27	7.3	0.46						137	4.859	0.64	8.48E+07	6.06E+04	5.59E+06	2.66E+06	1.73E+06	5.35E+06	1.20E+06	8.22E+06

Table S2. Primers and reaction conditions for qPCR.

Gene	Primer pair	Primer sequence	Final conc	Melting		Annealing		Elongation		Data acquisition		Cycles[a]
Primer ref	Forw/Rev	5´- 3´	(µM)	T (°C)	t (s)	T (°C)	t (s)	T (°C)	t (s)	T (°C)	t (s)	
nirS (Throbäck et al., 2004)	Cd3a Fm	AACGYSAAGGARACSGG	0.50	95	15	65-60[b]	30	72	35	80	5	40
	R3cdm	GASTTCGGRTGSGTCTTSAYGAA	0.50									
nirK (Henry et al., 2004)	876F	ATCATGGTSCTGCCGCG	0.50	95	15	63-58[b]	30	72	30	80	5	40
	1040 R	GCCTCGATCAGRTTRTGGTT	0.50									
nosZI (Henry et al., 2006)	1840 F	CGCRACGGCAASAAGGTSMSSGT	0.50	95	15	65-60[b]	30	72	35	80	5	40
	2090 R	CAKRTGCAKSGCRTGGCAGAA	0.50									
nosZII (Jones et al., 2013)	nosZII F	CTIGGICCIYTKCAYAC	2.00	95	15	54	30	72	45	80	5	40
	nosZII R	GCIGARCARAAITCBGTRC	2.00									
nfrA (Welch et al., 2014/Mohan et al., 2004)	nrfAF2aw	CARTGYCAYGTBGARTA	0.50	95	15	57-52[b]	30	72	30	80	5	40
	nrfAR1	TWNGGCATRTGRCARTC	0.50									
amoA (AOA) (Tourna et al., 2008)	crenamoA 23F	ATGGTCTGGCTWAGACG	0.50	95	15	55	30	72	45	77	5	40
	crenamoA 616R	GCCATCCATCTGTATGTCCA	0.50									
amoA (AOB)	amoA 1F	GGGGTTTCTACTGGTGGT	0.50	95	15	55	30	72	45	77	5	40

amoA (AOB) (Rotthauwe et al., 1997)	amoA 1F	GGGGTTTCTACTGGTGGT	0.50	95	15	55	30	72	45	77	5	40
	amoA 2R	CCCCTCKGSAAAGCCTTCTTC	0.50									

a - Protocols start with an activation step, 95 °C for 5 minutes and are finished with a melt curve, 15 s at 95 °C followed by 65-95 °C in 0.5 °C increments for 5 s.
b - 1 °C decrease per cycle the first six cycles.

References

Henry, S., Baudoin, E., Lopez-Gutierrez, J.C., Martin-Laurent, F., Brauman, A., Philippot, L. 2004. Quantification of denitrifying bacteria in soils by nirK gene targeted real-time PCR. J. Microbiol. Methods 59, 327-335.

Henry, S., Bru, D., Stres, B., Hallet, S., Philippot, L., 2006. Quantitative detection of the nosZ gene, encoding nitrous oxide reductase, and comparison of the abundances of 16S rRNA, narG, nirK, and nosZ genes in soils. Appl. Environ. Microbiol. 72, 5181–5189.

Jones, C., Graf, D., Bru, D., Philippot, L., Hallin, S. 2013. The unaccounted yet abundant nitrous oxide-reducing microbial community: a potential nitrous oxide sink. ISME J. 7, 417-426.

Mohan, S.B., Schmid, M., Jetten, M., Cole, J., 2004. Detection and widespread distribution of the nrfA gene encoding nitrite reduction to ammonia, a short circuit in the biological nitrogen cycle that competes with denitrification. FEMS Microbiol. Ecol. 49, 433–443.

Muyzer, G., Dewaal, E.C., Uitterlinden, A. G. 1993. Profiling of Complex Microbial Populations by Denaturing Gradient Gel-Electroforesis Analysis of Polymerase Chain Reaction-Aplified Genes Coding for 16S Ribosomal RNA. Appl. Environ. Microbiol. 59, 695-700.

Rotthauwe, J.H., Witzel, K.P., Liesack, W. 1997. The ammonia monooxygenase structural gene amoA as a functional marker: molecular fine-scale analysis of natural ammonia-oxidizing populations. Appl. Environ. Microbio.l 63, 4704–4712.

Throbäck, I.N., Enwall, K., Jarvis, A., Hallin, S. 2004. Reassessing PCR primers targeting nirS, nirK and nosZ genes for community surveys of denitrifying bacteria with DGGE. FEMS Microbiol. Ecol. 49, 401-417.

Tourna, M., Freitag, T.E., Nicol, G.W., Prosser, J. I. 2008. Growth, activity and temperature responses of ammonia-oxidizing archaea and bacteria in soil microcosms. Environ. Microbiol. 10, 1357–1364.

Welsh, A., Chee-Sanford, J.C., Connor, L.M., Löffler, F.E., Sanford, R.A. 2014. Refined NrfA Phylogeny Improves PCR-Based nrfA Gene Detection. Appl. Environ. Microbiol. 80, 2110-2119.

Table S3. Correlations between Non-Metric Multidimensional Scaling based on Bray-Curtis distances of the frequent communities in the barrier samples and class level taxonomy, chemical and gene abundance data. Coordinates refer to main Figure 3A. Results from vegan function envfit.

	Variable	Coordinates		Strength	Significance[a]
		MDS1	MDS2	r^2	
Class	Nitrososphaeria	-1.000	0.016	0.189	*
	Methanobacteria	-0.919	0.395	0.037	
	Parcubacteria	0.060	0.998	0.094	
	Fimbriimonadia	0.637	-0.771	0.364	**
	Microgenomatia	0.000	1.000	0.017	
	Bacteroidia	0.823	-0.567	0.222	*
	Saccharimonadia	0.335	-0.942	0.326	**
	Spirochaetia	0.182	-0.983	0.429	**
	Lineage Iia[b]	0.345	0.939	0.208	*
	Blastocatellia	-0.289	-0.957	0.071	
	Thermoleophilia	0.394	-0.919	0.300	**
	Actinobacteria	0.562	-0.827	0.397	**
	Acidimicrobiia	-0.986	-0.165	0.841	**
	Rubrobacteria	-1.000	0.028	0.688	**
	Coriobacteriia	-0.706	0.708	0.206	*
	MB-A2-108	0.663	-0.749	0.141	.
	AKAU4049	0.887	0.462	0.050	
	Desulfitobacteriia	0.592	0.806	0.051	
	Clostridia	0.771	0.636	0.424	**
	Halanaerobiia	-0.993	-0.115	0.125	
	Limnochordia	-0.994	0.113	0.232	*
	Bacilli	-0.972	0.237	0.301	**
	Gitt-GS-136	-0.966	0.258	0.163	.
	KD4-96	-0.964	0.268	0.249	**
	P2-11E	0.795	-0.607	0.253	**
	Anaerolineae	-0.933	0.359	0.723	**
	Chloroflexia	-0.690	0.724	0.608	**
	Dehalococcoidia	-0.998	0.064	0.784	**
	OLB14	-0.735	0.678	0.399	**
	JG30-KF-CM66	-0.699	0.715	0.297	**
	TK10	0.912	-0.411	0.337	**
	Cyanobacteriia	0.800	-0.601	0.031	
	Nitrospira	0.346	0.938	0.460	**
	Fusobacteriia	0.037	0.999	0.132	
	S0134 terrestrial group	-0.865	0.502	0.531	**
	BD2-11terrestrial group	-0.927	0.375	0.692	**
	Longimicrobia	-0.711	-0.703	0.073	
	Gemmatimonadetes	0.623	0.782	0.268	*
	Vampirivibrionia	0.568	-0.823	0.228	*
	Sericytochromatia	0.761	0.649	0.224	*
	Dadabacteriia	0.336	-0.942	0.070	
	Bdellovibrionia	0.915	0.403	0.477	**
	bacteriap25[c]	-0.996	0.085	0.836	**
	uncultured[d]	-0.990	0.141	0.175	*
	Myxococcia	-0.844	0.536	0.137	.
	Desulfobacteria	-0.034	0.999	0.143	.
	Desulfobulbia	-0.797	0.603	0.291	**

	Desulfuromonadia	-0.541	0.841	0.425	**
	Polyangia	-0.301	-0.954	0.311	**
	Oligoflexia	0.985	-0.171	0.297	**
	Alphaproteobacteria	-0.302	-0.953	0.700	**
	Hydrogenedentia	0.682	0.731	0.489	**
	Gammaproteobacteria	0.376	0.927	0.738	**
	Desulfovibrionia	0.168	0.986	0.009	
	Planctomycetes	0.794	-0.608	0.152	.
	Phycisphaerae	-0.382	0.924	0.040	
	Sumerlaeia	0.131	0.991	0.089	
	Verrucomicrobiae	0.641	-0.768	0.439	**
	Subgroup 11[e]	0.816	-0.578	0.194	*
	Subgroup 5[e]	-0.990	0.140	0.379	**
	Acidobacteriae	0.509	0.861	0.102	
	Kapabacteria	0.999	0.038	0.349	**
	SJA-28	0.189	0.982	0.256	*
	Rhodothermia	-0.946	-0.325	0.177	.
	Ignavibacteria	0.244	0.970	0.504	**
	Kryptonia	-0.983	0.184	0.399	**
	Calditrichia	-0.981	0.196	0.271	*
	Methylomirabilia	-0.948	-0.319	0.339	**
	Vicinamibacteria	-0.841	-0.542	0.452	**
	Subgroup 25[e]	-1.000	-0.003	0.607	**
	Subgroup 22[e]	0.716	-0.698	0.073	
	Thermoanaerobaculia	-0.991	0.136	0.397	**
	Holophagae	0.306	0.952	0.373	**
	Entotheonellia	-1.000	-0.017	0.701	**
	Babeliae	0.133	-0.991	0.073	
	Campylobacteria	-0.181	0.983	0.162	.
	Gracilibacteria	-0.613	0.790	0.110	
Chemical	OrgC	-0.699	-0.715	0.209	*
	pH	0.189	-0.982	0.243	*
Gene abundance	16S rRNA	-0.996	0.089	0.559	**
	nrfA	-0.976	0.218	0.493	**
	Archaeal *amoA*	-0.992	0.127	0.578	**
	Bacterial *amoA*	-0.656	0.754	0.265	**
	nirS	-0.754	0.656	0.416	**
	nirK	-0.964	-0.266	0.519	**
	nosZI	-0.861	0.509	0.483	**
	*nosZ*II	-1.000	0.006	0.506	**

[a] p-values adjusted for multiple comparisons using false discovery rate. · p < 0.1, * p < 0.05, ** p < 0.01

[b] Phylum Elusimicrobiota

[c] Phylum Myxococcota

[d] Phylum Desulfobacterota

[e] Phylum Acidobacteriota

Acta Universitatis agriculturae Sueciae
Doctoral Thesis No. 2022:46

Water is a valuable resource at risk because of anthropogenic nitrogen (N) input to the environment. This thesis investigated how microorganisms in permeable reactive barriers remediate N-polluted water. The carbonaceous material in the barriers determined which microorganisms that established, and thereby the efficiency of the system. Woodchip-based barriers successfully removed nitrate from industrial wastewater and adverse side effects were found to be small.

Maria Hellman received her graduate degree at the Department of Forest Mycology and Plant Pathology at SLU, Uppsala. She received a licentiate degree in Biology from SLU (2020), a University Diploma in Education for Upper Secondary School (1994), and a BSc in Biology (1990) from Uppsala University.

Acta Universitatis agriculturae Sueciae presents doctoral theses from the Swedish University of Agricultural Sciences (SLU).

SLU generates knowledge for the sustainable use of biological natural resources. Research, education, extension, as well as environmental monitoring and assessment are used to achieve this goal.

ISSN 1652-6880
ISBN (print version) 978-91-7760- 967-4
ISBN (electronic version) 978-91-7760- 968-1